Dissertation

submitted to the

Combined Faculties for the Natural Sciences and for Mathematics

of the Ruperto-Carola University of Heidelberg, Germany

for the degree of

Doctor of Natural Sciences

presented by

Diplom. in Botany Anastasia Eskova

born in: Moscow, Russia

Oral examination: 07 June 2013

Systematic analysis of integrin α2β1 internalization

Referees:

Prof. Dr. Roland Eils

Dr. Vytaute Starkuviene-Erfle

Contents

List of publications

Eskova A., *B. Knapp, D. Matelska, T. Lisauskas, R. Pepperkok, R. Russell, R. Eils, L. Kaderali, H. Erfle, V. Starkuviene.* KIF15 emerges as a novel regulator of integrin endocytic trafficking (manuscript submitted)

Erfle, H., ***A. Eskova****, J. Reymann, V. Starkuviene.* Cell arrays and high content screening. 2011. Methods of Molecular Biology, 785, 277-87.

List of presentations

2011. "Dynamic Endosomes: Mechanisms Controlling Endocytosis" (24-29 September 2011, Chania, Grece) Poster presentation. *Eskova A., B. Knapp, D. Matelska, H. Demirdizen, H. Erfle, Eils, R. Pepperkok, L. Kaderali, R. Russell, R. V. Starkuviene.* High-content analysis of kinesins as regulators of integrin traffic.

2010. "International Conference on Systems Biology of Human Disease 2010" (16-18 June 2010, Boston, USA) Poster presentation. *Eskova A., B. Knapp, D. Matelska, H. Demirdizen, H. Erfle, Eils, R. Pepperkok, L. Kaderali, R. Russell, R. V. Starkuviene.* High-content analysis of kinesins as regulators of integrin traffic.

2010. 8th EMBO-Annaberg workshop “Protein and Lipid function in secretion and endocytosis”, Goldegg am See, Austria. Poster presentation. *Eskova A., Knapp B., Erfle H., Kaderali L., Pepperkok R., Starkuviene V.* Microscopy-based RNAi assay to identify regulators of integrin endocytosis.

Acknowledgements

I dedicate this work to my parents, my dear husband, and Prof. Regine Kahmann – the people who gave me the opportunity to become a scientist.

I am very grateful to my supervisor, Dr. Vytaute Starkuviene, who granted me an opportunity to work in her group in BioQuant, Heidelberg University and provided me with an exciting scientific project, inspiring supervision and advice. I would like to thank my co-workers from the "Screening of cellular networks" lab, who were a great support and lots of pleasure to work with all along: Dr. Christoph Claas, Dr. Andrius Serva, Tautvydas Lisauskas, Susanne Reusing, Sanchari Roy, Yueh-Tso Tsai.

I would like to thank Prof. Roland Eils and Prof. Ursula Klingmüller for fruitful discussions and support along the course of my studies. Many thanks to Prof. Ulrich Schwarz for joining to my doctoral examination committee.

Many thanks to Dr. Bettina Knapp, Dorota Matelska, and Philipp Albert, who helped me to shape this project in their areas of expertise and were so patient, explaining what is possible and what is not. Sincere gratitude for assistance with RNAi screening and automated imaging goes to Dr. Holger Erfle and the members of BioQuant RNAi screening facility: Nina Beil, Jürgen Beneke, Dr. Jürgen Reymann, Dr. Manuel Gunkel.

I would like to thank internship students Anna Reustle (Heidelberg University) and Gintare Garbenciute (Vilnus University) and former colleague Haydar Demirdizen, who provided me a helping hand on the micropatterns project and gave me a feeling of being a mentor.

Finally, I gratefully acknowledge being a member of Hartmut Hoffmann-Berling International Graduate School of Molecular and Cellular Biology (HBIGS) which was overall a wonderful environment and gave me so many opportunities to study the things which I would not otherwise encounter.

Abbreviations

CCP – clathrin coated pit

CIE – clathrin independent endocytosis

CLASP – clathrin-associated sorting protein

CME - clathrin-mediated endocytosis

ECL - enhanced chemiluminescence

ECM - extracellular matrix

FA – focal adhesion

EE – early endosomes

EEA1 – early endosome antigen 1

ER – endoplasmic reticulum

EGF – epidermal growth factor

GAP – GTPase activating protein

GEF – guanosine exchange factor

GFP- green fluorescent protein

MMP-matrix metalloproteinase

PAA – polyacrylamide

PRC – perinuclear recycling compartment

RGD – arginine-glycine-aspartic acid peptide

RT – room temperature

RNAi – RNA interference

siRNA – short interfering RNA

siCtrl – negative control siRNA

SNARE – soluble NSF attachment protein receptor

TGN - trans-Golgi network

Summary

Integrins are metazoan heterodimeric receptors for cell adhesion and interaction with extracellular matrix. Nowadays 18 integrin alpha chains and 8 beta chains are known in human cells, forming 24 different heterodimers specific for wide array of ligands, including collagens, laminins, and fibronectin. Dynamic assembly and disassembly of ligand-bound integrins as well as rearrangement of unengaged integrins on a cell surface depends on the intracellular trafficking. It is crucial for the processes related to cell adhesion, spreading, and migration, such as neutrophil migration or metastasis development in cancer.

Number of studies addressed endocytosis and recycling of integrins, yet, the comprehensive model of integrin trafficking is still missing as the pathways of integrin retrograde trafficking can differ depending on the integrin activation status, binding to the ligand, growth factors presence. An additional level of complexity dealt in the integrin trafficking studies is a certain promiscuity in integrin α and β chain interactions, therefore the knowledge on the specificity of a trafficking pathway for a certain heterodimer is often lacking.

This study focused on internalization regulators of integrin α2β1, which is a ubiquitously expressed receptor of collagens, mainly collagen I, one of the most abundant extracellular matrix proteins, which is known as a metastasis suppressor in human cancer. Studies on α2β1 endocytosis are sparse and mostly focused so far on the trafficking of α2β1 clustered by addition of virus or ligand.

To identify and characterize novel regulators of internalization of non-clustered integrin α2β1, we established a quantitative fluorescent-microscopy-based integrin α2 internalization assay. We demonstrated that bulk internalization of endogenously expressed non-clustered integrin α2 in HeLa cells is dependent on both clathrin and

caveolin1, and occurs via Rab5-, Rab4- and Rab11-positive endosomes. Next, we used RNAi to screen 386 cytoskeleton and cytoskeleton-associated genes for their involvement in integrin α2 internalization. We identified 122 primary screening hits as potential regulators of integrin α2 trafficking, number of which were previously known as regulators of endocytosis, focal adhesion formation, and cell migration, and as direct interactors of integrins. In the validation assays we could reproduce the results of the primary screening for 43% of expressed hits in the two groups of hits selected for validation (14 molecules that were targeted by multiple siRNAs in the primary screening, and 12 kinesin molecular motors).

Three validated kinesin hits have never previously been associated with endocytic trafficking events. To get an insight in the function of kinesins in integrin internalization, we further characterized the role of KIF15 in the trafficking of integrin α2. It was identified as a strong inhibitor of the early steps of integrin α2 endocytosis, but not transferrin or EGF. We demonstrated that knock-down of KIF15 lead in re-location of the integrin-specific clathrin adaptor Dab2 from the plasma membrane, which is likely to be the reason for the block of integrin α2 internalization.

Taken together, this study establishes the methods to address the internalization of non-clustered integrin α2β1, identifies the number of novel regulators of integrin trafficking, and provides insight into the role of KIF15 molecular motor in the integrin α2 internalization.

Zusammenfassung

Integrinen sind metazoische heterodimerische Rezeptoren für die Adhäsion der Zellen und ihre Wechselwirkung mit der Matrix. Zur Zeit sind 18 Alphaketten und 8 Betaketten der Integrinen in der humanen Zelle bekannt, die 24 unterschiedliche Heterodimeren bilden. Diese Heterodimeren sind für eine umfangreiche Reihe von Liganden spezifisch, wie zum Beispiel Kollagene, Laminine und Fibronektin. Dynamische Zusammenbildung und Zerlegung von Integrinen, die zu einem Ligand gebunden sind, sowie die Umstellung von ungebundenen Integrinen auf der Zellenoberfläche hängt von dem intrazellularen Traffiking ab. Das ist essentiel für die Prozesse, die mit Zellenadhäsion, Verbreitung und Migration verbunden sind, so wie Migration von Neutrophilen und das Entstehen von den Metastasen in Krebs.

Einige Studien gehen das Endozytosis und Recycling von Integrinen an, trotzdem fehlt es an einem umfassenden Model von Traffiking von Integrinen, weil der Verlauf von dem rückläufigen Traffiking von Integrinen je nach Aktivierungsstatus von Integrin, Ligandbindung, und die Präsenz von Wachstumsfaktoren sich unterscheiden kann. Ein zusätzliches Niveau der Komplexität, mit dem die Integrinstudien zu tun haben, bezieht sich auf eine gewisse Vermischtheit von Wechselwirkungen zwischen Alpha- und Betaketten; als Ergebnis davon fehlt es oft an Wissen über der Spezifität von den Traffikingverläufen von gewissen Heterodimeren.

Diese Studie ist auf die Internalisierungsregulatoren von Integrin α2β1 fokussiert, das ein allgegenwärtig exprimierter Kollagenrezeptor, hauptsächlich von dem Kollagen I, und ein der meist reichlichen extrazellularen Matrixproteinen ist. Studien über das Endozytosis von α2β1 sind knapp und hauptsächlich auf das Traffiking von α2β1 gesammelt durch eine Zufabe von Viren oder Liganden fokussiert.

Um die neuen Regulatoren von der Internalisierung von dem ungesammelten Integrin α2β1 zu identifizieren und zu beschreiben, wir haben ein Assay etabliert, das auf die quantitative Fluoriszenzmikroskopie basiert ist. Wir haben gezeigt, dass der Grossteil von der Internalisierung des endogen extremierten nicht gesammelten Integrins α2 in HeLa Zellen sowohl von Klathrin als auch von Kaveolin1 abhängt, und durch Rab5-, Rab4- und Rab11-positiven Endosomen stattfindet. Wir haben dann RNAi benutzt, um 386 Zytoskeleton- und zytoskeletonwerwandten Genen auf ihre Beteiligung an die Internalisierung von Integrin a2 zu screenen. Wir haben 122 primäre Screening-Hits als potentielle Regulatoren von dem Traffiking von Integrin α2 identifiziert, ein Anteil von denen bereits als Regulatoren von Endozytosis, Entstehen der fokale Adhäsion, Zellenmigration und direkte Interaktoren von Integrinen bekannt waren. In einem Validierungsassay konnten wir die Ergebnisse von dem primären Screening für 43% vom dem exprimierten Hits aus zwei Gruppen von für die Validierung ausgewählten Hits (14 Molekülen, die von mehreren siRNAs in dem primären Screening addressiert wurden, und 12 Kinesin-Molekularmotoren) nachvollziehen.

Drei validierte Kinesin-Hits wurden nie mit dem endozytotischen Traffiking früher assoziiert. Um einen Einblick in die Funktion von Kinesinen in der Integrininternalisierung zu erwerben, haben wir weiter die Rolle von KIF15 in dem Traffiking von Integrin α2 charakterisiert. Es wurde als ein starker Inhibitor von den frühen Schritten von Endozytosis von dem Integrin α2, aber nicht von Transferrin oder EGF identifiziert. Wir haben nachgewiesen, dass ein Knockdown von KIF15 zu einem Verlust von einem Integrin-spezifischen Klathrinadaptor Dab2 von der Plasmamembran führt, dass wahrscheinlich der Grund für die Blockierung von der Internalisierung dem Integrin α2 ist.

Also haben wir die Methoden für das Adressieren von der Internalisierung von dem nicht gesammelten Integrin α2 entwickelt, eine Reihe von neue Regulatoren von dem Trafficking des Integrins identifiziert, und einen Einblick auf die Rolle von dem Molekularmotor KIF15 in der Internalisierung das Integrin α2 geleistet.

1. Introduction

1.1. Integrins

Integrins are metazoan heterodimeric receptors involved in cell adhesion and interaction between cell and extracellular matrix (ECM). The first integrin heterodimers VLA-1 and VLA-2 (very late antigen-1 and -2, integrin α1β1 and α2β1 respectively) were identified in 1985 as protein complexes appearing on differentiated activated T-lymphocytes (Hemler, Jacobson, Brenner, Mann, & Strominger, 1985). Nowadays 18 integrin alpha chains and 8 beta chains are known in human cells, forming 24 different heterodimers specific for wide array of ligands, including collagens, laminins, and fibronectin (Takada, Ye, & Simon, 2007) (**Figure I.1**). Integrins provide physical attachment of cells to ECM and mediate outside-in and inside-out signaling on the adhesion status of the cell. On the cellular level, integrins control sensing of mechanistic properties of the substrate, cell proliferation and cell death, as proper attachment is crucial for cell division of adherent cells (Hynes, 2002; Pellinen et al., 2008; Schwarz, 2010), and loss of it leads to apopthosis (Taddei et al., 2012). On the level of organism they are involved in cell migration during development , differentiation, immunity, tumorigenesis and metastasis, haemostasis (Hynes, 2002). Integrin knock-out mouse models display a range of phenotypes, from embrionic lethality for knock-out of β1 integrin (Fässler and Meyer, 1995), defects in mesoderm development and vascularization and apoptosis of cranial neural crest cells upon knock-out α5 integrin (Yang et al., 1993; Goh et al., 1997) to abnormal platelet aggregation and osteosclerosis in mice lacking β3 integrin (Hodivala-Dilke et al., 1999; McHugh et al., 2000). Moreover, integrins can serve as co-receptors for viral entry (Stewart and Nemerow, 2007), i.e. integrin α2β1 is used for cell attachment and entry by rotavirus and EV1 (Bergelson et al., 1992; Fleming et al., 2010), whereas

αvβ3 is exploited by EV9, CA9, adenovirus, rotavirus and others (Roivainen et al., 1994)(Hamilton et al., 1997) (Nelsen-Salz et al., 1999) (Guerrero et al., 2000).

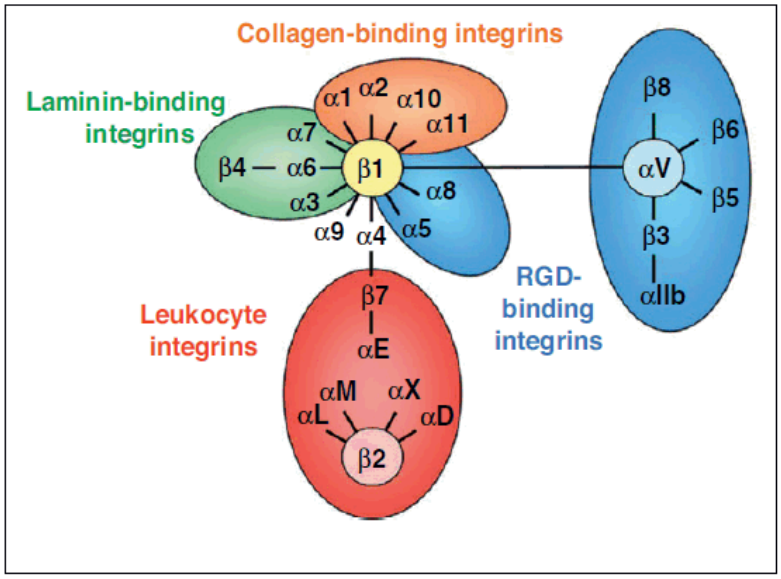

Figure I.1. Ligand specificity of mammalian integrin heterodimers. Adapted from (Margadant et al., 2011)

1.2. Integrin structure and function

Integrin receptors consist of two transmembrane non-covalently associated chains, which have large N-terminal extracellular region, responsible for interaction with ligand, single transmembrane domain, and short C-terminal cytoplasmic tail. Ligand-binding affinity of integrins depends on their conformation. Active conformation ("open" or extended) is characterized by stretched N-terminal head domain and spacial separation between tails and transmembrane domains of two chains. It has higher affinity to the ligand than inactive ("closed" or bent) or intermediate conformation (Kim et al., 2003).

Inside-out integrin signaling is supported by interactions of integrin cytoplasmic tails with number of effectors, aactivating or de-activating integrins. The key regulators of this process are known. Talins (Calderwood, 1999; Calderwood et al., 2002), and kindlins (Moser et al., 2008; Montanez et al., 2008; Harburger et al., 2009) activate integrins by

binding to the cytoplasmic tail of beta chains. Integrin activation can be attenuated by number of proteins sharing phosphotyrosine-binding (PTB) domain, that compete with talin for beta tail binding, as was shown for filamins (Kiema et al., 2006), ICAM1 (Millon-Frémillon et al., 2008) and Dok-1 (Calderwood et al., 2003).

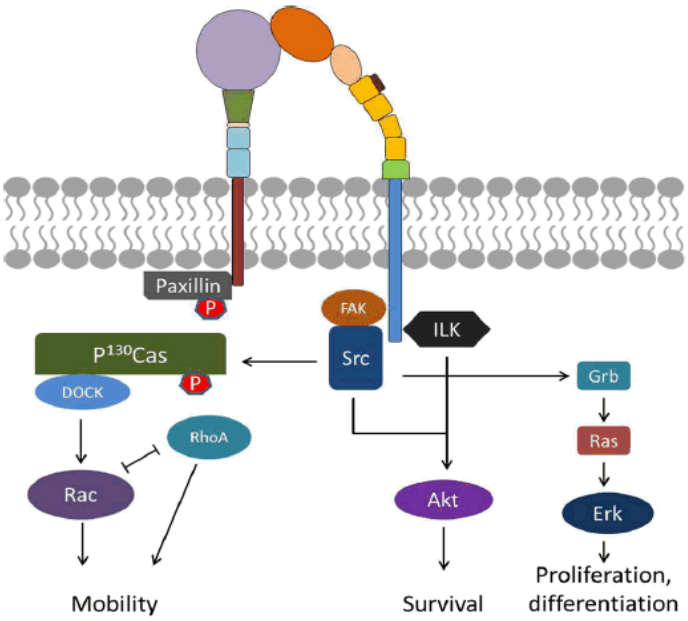

Figure I.2. Outside-in signaling of integrins elicits number of cellular responces. Ligand binding leads to separation of integrin tails and recruitment of FAK and Src, which phosphorylate scaffold protein paxillin and P130Cas. Phosphorylated P130Cas recruits guanine exchange factors DOCK, and leads to Rac activation. Rac and RhoA function oppositely during cell migration. ILK is recruited to b integrin cytoplasmic domain and promotes Akt activity. Src also activates Akt and can furthermore promote cell proliferation Adapted from (Hu and Luo, 2013)

Although most of existing evidence is for regulation of integrin inside-out activation through binding to its beta chains, recent data suggested, that interactors of α chains can also be involved, as this was demonstrated for integrin α chains-binding protein SHARPIN, that prevents talin and kindlin binding and thus maintains integrin in inactive state (Rantala et al., 2011).

Outside-in integrin signalling depends on integrin binding to to their ligands. There is no clear-cut answer, whether activation of integrin is a prerequisite of ligand-binding ("switchblade model" (Luo et al., 2007)) or inactive integrin can also bind ligand

and subsequently get activated ("deadbolt model" (Xiong et al., 2003). At any rate, ligand binding to integrin induces cascade of cellular responces (**Figure. I.2**) . Activated integrins cluster, recruit the signalling scaffolds paxillin, vinculin, CRK and integrin-linked kinase (ILK) (Schaller, 2001; Brown and Turner, 2004; Wickström et al., 2010; Carisey and Ballestrem, 2011), kinases focal adhesion kinase (FAK) and Src (Klinghoffer et al., 1999), and activate the small GTPases Rho and Rac, which serve as master regulators of actin cytoskeleton (Burridge and Wennerberg, 2004)**.** Rac is activated by complex of paxillin and focal adhesion protein pCas130 (Humphries et al., 2007). They stimulate the formation of lamellopodia at the leading edge of migrating cells by inducing actin polimerization through WAVE/Scar and Arp2/3 (Schaller and Parsons, 1995; Yeo and Song, 2008). Thus, initiation of cell adhesion co-incides with activation of Rac and Cdc42 signalling, which enhances actin-dependent protrusions, cell migration and cell spreading. Activity of RhoA and Rho-dependent actomyosin contractility is concomitantly down-regulated (Zaidel-Bar et al., 2005). On the contrary, Rho is responsible for stabilization of the adhesive sites, halting cell migration and formation of actin stress fibers. Increase of Rho activity and phophorylation of myosin light chain induces formation of stress fibers and prevents cell migration (Ridley et al., 1992; Miki et al., 1998, 2000; Eden et al., 2002).

Integrins organize in several kinds of complexes at the PM. Nascent adhesions form at the broad actin-rich edges of migrating cells called lamellopodia. Nascent adhesions are linked to actin cytoskeleton, but myosin independent. Actin crosslinking with myosin II allows them to mature to focal complexes (Choi et al., 2008). Focal complexes are small dot-like integrin complexes (about 2 μm in diameter) similar in composition to the mature focal adhesions (DePasquale, 1987; Rinnerthaler et al., 1988).

Focal complexes require on Cdc42 and Rac-GTPase activity, and can be matured to focal adhesions upon activation of Rho (Nobes and Hall, 1995; Rottner et al., 1999). The mature focal adhesions accommodate clustered ligand-bound integrins in the elongated structures sized and 3-10μm in length. At the cytosolic side of PM focal adhesions are connected to the acto-myosin stress fibers (reviewed in (Burridge and Fath, 1989; Rottner et al., 1999; Schwartz, 2010),

Focal adhesion complexes encompass number of proteins that directly and indirectly interact with integrin cytoplasmic tails, ensuring integrin signalling and physical association to the cytoskeleon. This dynamic complex of proteins is referred as an "integrin adhesome", and currently lists more than 150 proteins, including 24 cytoskeletal components, 25 adaptors, 18 kinases, 21 GTPases and their regulators (Zaidel-Bar et al., 2007). The main components of focal adhesion complexes, besides integrins and talins, are the polyvalent adaptors vinculin and paxillin that are able to directly recruit actin filaments, and serve as signalling platforms (Brown, 1996; Brown and Turner, 2004; Humphries et al., 2007)

Focal adhesions are dynamic structures, constantly formed, remodelled, and disassembled according to cellular needs. They persist at the PM for up to 40 min and then can be disassembled or matured into more stable fibrillar adhesions (Kaverina et al., 1999). Targeted delivery of integrins to the newly formed adhesion sites in migrating cells and disassembly of focal adhesions depends on the microtubules targeted to the focal adhesions and on the integrins endocytosis and recycling (Kaverina et al., 1999; Choi et al., 2008; Ezratti et al., 2005; Chao and Kunz, 2009; Theisen et al., 2012)

Integrin binding to ECM, signalling, and transduction of mechanical forces eventually results in the ECM remodeling by several mechanisms. First, integrin

signaling and attachment to substrate controls the levels of expression and extracellular assembly of ECM proteins such as fibronectin, collagen, and tenascin (Löer et al., 2008; Torgler et al., 2004; Clark et al., 2003; Zervas et al., 2001; Brown et al., 2002). Second, integrins can mediate ECM proteolytic degradation, as serve as receptors to several proteases, including matrix metalloproteases (MMP). By direct binding to the MMP, integrin can modulate activities of MMPs, and, thus, levels of substrate degradation (Pierini et al., 2000) (Maier et al., 2008; Lindahl et al., 2002; Liu et al., 2000; Chiquet et al., 2009; Tamariz and Grinnell, 2002; Ilić et al., 2004; Jülich et al., 2009; Pankov, 2000; Schiller et al., 2004; Canty et al., 2006). Induction of MMPs expression by integrins have was demonstrated for integrin α2β1 and MMP-1, a3b1 and MMP-2, aVb6 and MMP-2 and MMP-9 (Brooks et al., 1996) (Brooks et al., 1998) (Chintala et al., 1996; Parks, 1999; Thomas et al., 2001). And finally, integrins can directly mediate the internalization of ECM proteins from the extracellular space and target them to lysosomal degradation (Du et al., 2011; Dozynkiewicz et al., 2011; Shi and Sottile, 2008).

Besides their function in the cell attachment, spreading and migration, integrins are involved in the control of cell cycle and cell death and survival decisions. Integrin-dependent Rho- and ERK signalling via cyclin D results in cell cycle pogression (reviewed in (Assoian and Klein, 2008). Proper integrin-binding to the ECM protects the cells from apoptosis via activation of NFκB, ERK, and Akt/PI3K -dependent survival pathways by FAK and ILK. On the contrary, loss of attachment results in activation of several apoptotic mechnisms, including death receptor- and caspase 8-dependent apoptosis (reviewed in (Stupack, 2002; Taddei et al., 2012)).

Thus, integrins serve as both receptors for cellular environment, and the effectors for modulating of this environment and performing a range of crucial cellular functions,

such as regulation of cytoskeleton organization, cell motility, and cell cycle control. Integrins are regulated in number of ways, the principle of them are control of activation status, and modulation of integrin availability and distribution on the PM. The latter largely depends on the intracellular trafficking of integrins.

1.3. Intracellular trafficking pathways

Number of interconnected pathways link intracellular membrane compartments. The proteins destined to function at plasma membrane are generally synthesized in ER, then exported through ERGIC to Golgi, pass *cis*-, *medial*- and *trans*-Golgi, and trans-Golgi network (TGN), and finally are delivered to the cell surface (De Matteis and Luini, 2008; Gillon et al., 2012). Endocytosis, on contrary brings membranes and extracellular material from the surface to cell inside (Doherty and McMahon, 2009). The internalized cargo is sorted into the early endosomes (EE) and then can be driven to degradation in lysosomes via late endosomes and multivesicular bodies (MVB) or recycled back to the PM (Gruenberg and Stenmark, 2004; Grant and Donaldson, 2009) (**Figure I.3**). Due to the scope of this dissertation project, the further analysis will focus on the endocytosis and recycling pathways of the cell.

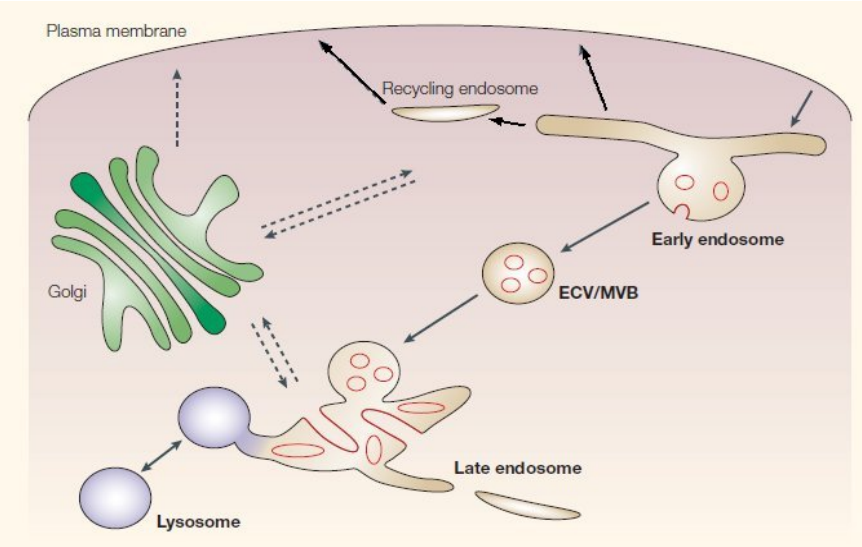

Figure I.3. The endomembrane compartments of the endocytic pathway in mammalian cells are outlined (solid arrows). Interconnections with the secretory pathway are shown with dashed arrows. Membrane invaginations and internal vesicles are shown in red, which highlights the tubular–cisternal and/or multivesicular regions of early and late endosomes. The outline indicates, using solid arrows, that recycling to the cell surface occurs through both an indirect (slow) route through recycling endosomes and a direct (rapid) route, and that trafficking routes also connect the Golgi apparatus to early and late endosomes and the plasma membrane. Modified from (Gruenberg and Stenmark, 2004)

There is number of entry pathways known by now, providing the endocytic flow of material, including (but not limited to) clathrin-mediated endocytosis (CME), caveolin-dependent, flotillin-dependent, Arf6-dependent, and macropinocytosis (Doherty & McMahon 2009). CME is the best studied endocytosis pathway. It is required for internalization of number of cellular receptors including transferrin receptor and G-protein coupled receptors. During CME, the endocytic cargo is packed into membrane pits coated with clathrin triskelions on cytoplasmic side of the membrane. This process is mediated by array of adaptor proteins, often cargo-specific, that can drive cargo proteins into clathrin-coated pits (CCP) (Traub, 2005; Kirchhausen, 2009). Upon assembly of clathrin on the cytosolic surface of growing pit, the large GTPase dynamin2 is recruited to the neck of the forming vesicle and performs a GTP-dependent scission of the vesicle

(Van der Bliek et al., 1993; Damke et al., 1994; Bashkirov et al., 2008; Pucadyil and Schmid, 2008).

Much more limited information on the clathrin-independent endocytosis (CIE) is available, if to compare to CME. One of the best studied CIE is caveolin-dependent endocytosis. Caveolae are flask-shaped invaginations on the plasma membrane. They are more stabile than CCP and provide the signalling plathform for number of pathways including integrin signalling (Parton and Simons, 2007). Formation of caveolae depends on scaffold protein caveolin1 (CAV1) and its orthologues CAV2 and CAV3 and mediates the internalization of so called lipid rafts or cholesterol enriched membrane microdomains (CEMMD) (Chidlow and Sessa, 2010).

After scission from the PM, the newly-formed vesicles lose their clathrin coat (Lemmon, 2001) and can further undergo homotypic fusion to form EE or fuse with existing EE (Nielsen et al., 1999). The formation of the early endosomes derived from clathrin-coated vesicles requires membrane recruitment of small GTPase Rab5 (Bucci et al., 1992; Zeigerer et al., 2012), but existing data suggests, that internalized caveolae and macropinosomes are targeted to Rab5 EE (Pelkmans et al., 2004; Zoncu et al., 2009)

Rab proteins have been long recognized as the master regulators of membrane trafficking They cycle between the active, GTP-bound and inactive GDP-bound form with help of accessory proteins that promote GTPase activity of Rabs (GTPase activating proteins, GAPs), displace GDP with GTP and thus activate Rabs (guanine nucleotide exchange factors, GEFs). Inactive Rabs can be retained in the GDP-bound form in the cytoplasm by guanine nucleotide dissociation inhibitors (GDI) (Zerial and McBride, 2001) (Mizuno-Yamasaki et al., 2012). GTP-bound Rab GTPase can be recruited to the cellular membranes, and, in turn, recruit specific effectors, altogether determining the

identity and function of membrane compartment **(Figure I.4**). The mechanism called "Rab conversion" was proposed to explain transformation of one compartment to another. It was initially described for maturation of Rab5-positive EE to Rab7-positive LE. With "Rab conversion" the Rab5-positive early endosomes, containing the cargo destined to degradation loose Rab5 and recruit Rab7 in a coordinated manner, which depends on Rab5 interaction with Vps/HOPS complex, working as Rab7 GEF (Rink et al., 2005). In *C. elegans* replacement of Rab5 with Rab7 is regulated by Rab7 GEF SAND-1, which is recruited by Rab5 GEF Rabex5, present on the EE in complex with Rab5, and, in turn, and physically recruits Rab7 to the endosomes via direct interaction with HOPS (Peralta et al., 2010; Poteryaev et al., 2010). Other small GTPases cascades are known, suggesting this is a general mechanism of membrane compartment identity acquisition (reviewed in (Mizuno-Yamasaki et al., 2012)).

The fate of internalized cargo is determined by the signals and post-translational modifications it is bearing. Whereas polyubiquitination with chains of at least four ubiquitin moieties is a signal for proteosomal degradation of ubiquitinated protein, monoubiquitination is sufficient to drive the membrane proteins for internalization, as was shown for receptor tyrosine kinases (Thrower et al., 2000). Ubiquitinated cargo is further sorted to the lysosomal pathway via ubiquitin-interacting ESCRT complex (Schields and Piper, 2011). Yet, for internalization and of number of proteins, including EGF receptor, ubiquitination is redundant or not required (Lombardi et al., 1993; Haglund et al., 2003; Huang et al., 2007).

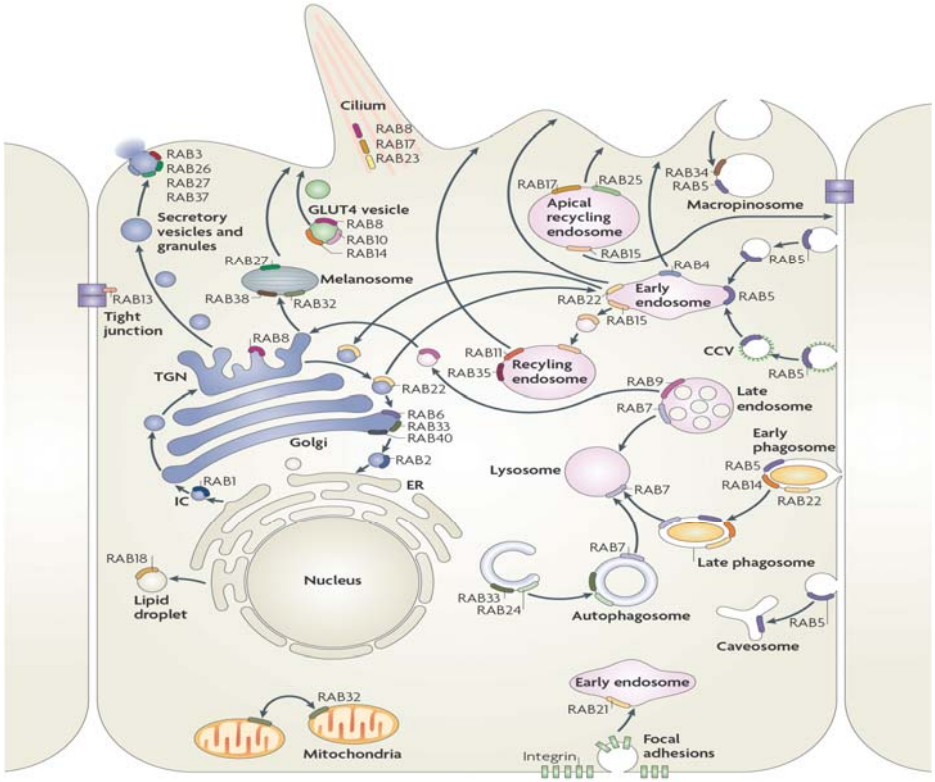

Figure I.4. Rab proteins determine the trafficking compartments identitiy. Adapted from (Stenmark, 2009)RAB1, located at endoplasmic reticulum (ER) exit sites and the pre-Golgi intermediate compartment (IC), mediates ER–Golgi trafficking. RAB2, located at the IC, might also regulate Golgi–ER trafficking. The Golgi-localized RAB6, RAB33 and RAB40 mediate intra-Golgi trafficking. RAB33, together with RAB24, also regulates the formation of autophagosomes. RAB8 mediates constitutive biosynthetic trafficking from the trans-Golgi network (TGN) to the plasma membrane and also participates in GLUT4 vesicle translocation (with RAB10 and RAB14) and ciliogenesis (with RAB17 and RAB23). RAB3, RAB26, RAB27 and RAB37 mediate various types of regulated exocytic events and RAB27 also mediates the translocation of melanosomes to the cell periphery. RAB32 and RAB38 are involved in the biogenesis of melanosomes and RAB32 also controls mitochondrial fission. RAB13 regulates the assembly of tight junctions between epithelial cells. RAB18 controls the formation of lipid droplets. RAB22 mediates trafficking between the TGN and early endosomes and vice versa. RAB5, which is localized to early endosomes, phagosomes, caveosomes and the plasma membrane, mediates endocytosis and endosome fusion of clathrin-coated vesicles (CCVs), macropinocytosis (with RAB34) and maturation of early phagosomes (with RAB14 and RAB22). RAB21 mediates integrin endocytosis. RAB11 and RAB35 mediate slow endocytic recycling through recycling endosomes, whereas RAB4 mediates fast endocytic recycling directly from early endosomes. RAB15 is involved in the trafficking from early endosomes to recycling endosomes and in the trafficking from apical recycling endosomes to the basolateral plasma membrane. RAB17 and RAB25 control trafficking through the apical recycling endosomes to the apical plasma membrane. The late endosome-associated RAB7 mediates maturation of late endosomes and phagosomes, and their fusion with lysosomes. Another late endosomal GTPase, RAB9, mediates trafficking from late endosomes to the TGN.

There are several main protein degradation pathways in the cell: proteosomal degradation, autophagosomal, and lysosomal degradation (Ciechanover, 2005; Wong and Cuervo, 2010). The chains of at least four ubiquitin Lysosomal degradation is the usual

route for the endocytic cargo destined for decay. Along this pathway, the internalized cargo, that is delivered into the EE, is sorted to the multivesicular bodies (MVB) and then delivered to the Rab7- and Rab9-positive late endosomes (LE) (Riederer et al., 1994; Feng et al., 1995). The cargo of late endosomes recruits ESCRT protein compex which induces inward invagination and leads to endosomes maturation into multivesicular bodies (MVB) which have characteristic appearance due to the vesicles enclosed into outer membrane (Gruenberg and Stenmark, 2004). Autophago-lysosomal degradation serves for removal of cell organelles and cytoplasm. The hallmark of this pathway is characteristic double membrane that appears from engulfing of the cell of its own content. In resemblance to MVB, the autophagosomes fuse to the lysosomes in order to degrade their cargo.

Variety of endocytic cargo, including number of receptors, is not degraded but recycle back to the PM. Two main pathways of recycling from endosomes to the PM are widely recognized in eukaryotic cells. One is so called “short-loop” recycling that occurs directly from the EE. This process is Rab4-dependent (Van der Sluijs et al., 1992). Alternatively, the recycled cargo is delivered to Rab11-positive recycling endosomes (Ullrich et al., 1996). The Rab4- and Rab11-positive membranes appear in the cell as the microdomains in the Rab5-positive EE (Sönnichsen et al., 2000), but Rab11 endosomes also form distinct compartments, localized in the perinuclear area (perinuclear recycling compartment, PRC) (Ullrich et al., 1996) or apical recycling endosomes in the polarized cells (Wang et al., 2000). Transferrin, being the cellular endocytic recycling cargo can pursue either recycling pathway, but with different dynamics. In HeLa cells, internalized transferrin accumulates in EE as early as in 5 min and is delivered to the RE 30 min after internalization (Peden et al., 2004).

The Rabs mentioned above are the main players in the organization of endocytosis and recycling pathways, which were discovered the earliest, characterized the best, and are conserved between different species, from yeast to human (Segev, 2001). Yet, as the family of Rabs is numerous, additional players of the trafficking pathways emerge. For instance, in human cells members of Rab5-subfamily Rab5a, b, c, Rab21, and Rab22 function in internalizaiton pathway at the level of early endosomes. The members of Rab11-subfamily Rab11a, b, and Rab25 are involved in recycling, and Rab 35 shares with Rab4 the function of short-loop recycling from EE (reviewed in (Scharwz et al., 2007)

The membrane fusion in all the trafficking steps is mediated by SNAREs (soluble N-ethylmaleimide-sensitive factor attachment protein receptors). They are the single transmembrane domain proteins, present on the donor and acceptor membranes, and are assembled into the tertiary complex of Q-SNAREs (Qa, Qb. And Qc) on one membrane and an R-SNARE at the opposing membrane (Jahn and Scheller, 2006). The energy required for the membrane fusion is released by assembly of SNAREs cytosolic domains into quaternary complex. There are 36 SNARE proteins present in humans mediating particular steps in the intracellular trafficking (reviewed in (Jahn and Scheller, 2006)).

1.4. Cytoskeleton in membrane trafficking

Cellular cytoskeleton consists of three types of structures: microtubules formed by tubulin polimers, actin microfilaments, and intermediate filaments. Cytoskeletal elements are crucial players in the intracellular trafficking, as they provide support and anchorage for individual compartments of the cell, and physical link between them, including tracks for vesicles and protein trafficking. Both actin and microtubular cytoskeleton are required for that, although their function is substantially different. Microtubules are crucial for

long-range traffic, chromosome organization in mitosis, and cell division (Vale, 2003; Manneville and Manneville, 2006; Meraldi, 2011). Actin filaments serve as tracks for short-range traffic, and organize the cortex of the cell – the dense meshwork of the actin fibers localized immediately beneath the PM, which plays the crucial role in the events of vesicle budding and fusion at the PM (Dominguez and Holmes, 2011). The physical movement of the cargo along the cytoskeleal tracks, and maintaining of cytoskeleton organization is provided by cytoplasmic molecular motors, that can convert chemical energy into mechanical, as they change conformation by hydrolyzing ATP. Microtubule-dependent molecular motors belong to kinesin and dynein families of molecular motors. The actin-dependent motors are myosins (Foth et al., 2006).

Microtubules are the polymers of α and β tubulins assembled as a hollow tube of 25 nm in diameter. For formation of microtubule, α- and β-tubulin dimerize, and then form linear protofilaments (Weisenberg, 1972). They posess an intrinsic polarity due to the polar organization of tubulin α and β dimers, so that one end of the protofilament exposes only one type of tubulin: α at the (-)-end of microtubules and β at the (+)-ends. The organization of microtubule arrays can differ dramatically depending on the cell type and cell state. In non-polarized animal interphase cells microtubules typically start nucleating at the microtubule organizing center (MTOC) in the perinuclear area and grow towards the PM, so that microtubular (+)-ends are found mostly at the cell periphery, and (-) ends in the perinuclear area (Manneville and Etienne-Manneville, 2006).

Kinesins superfamily of proteins performs numerous functions in organization of cytoskeleton, cell division, and intracellular transport of vesicles, protein complexes, and RNA. This variety of roles is provided by high diversification of kinesins in the evolution. Yeast genome encodes for 6 kinesins, which are involved in mitosis (Hildebrandt and

Hoyt, 2000). Yet mammalian cells encompass 45 members of this family, which can, in addition, produce multiple splice variants (Hirokawa et al., 2009). Mammalian kinesins are divided into 15 families, which can be grouped into three categories according to their structure: N-kinesins have the amino-terminal motor domain and, C-kinesins, that contain exclusively members of kinesin family 14A and 14B, have the motor domain at carboxy-terminus, and M-kinesins have the motor domain in the middle (**Figure I.5**). Kinesins, generally, move along the microtubules in the polarized manner. N-kinesins exhibit microtubule (+)-end directed movement, whereas C-kinesins drive microtubules (-)-end directed movememnt. M-kinesins act as microtubule depolymerases (reviewed in (Hirokawa et al., 2009). Yet, recent studies revealed that yeast mitotic kinesin Cin8 (member of kinesin-5 family of proteins), that belongs to kinesin-5 family of N-terminal kinesins, can switch directions, depending on whether it works alone or in the group of molecules (Roostalu et al., 2011).

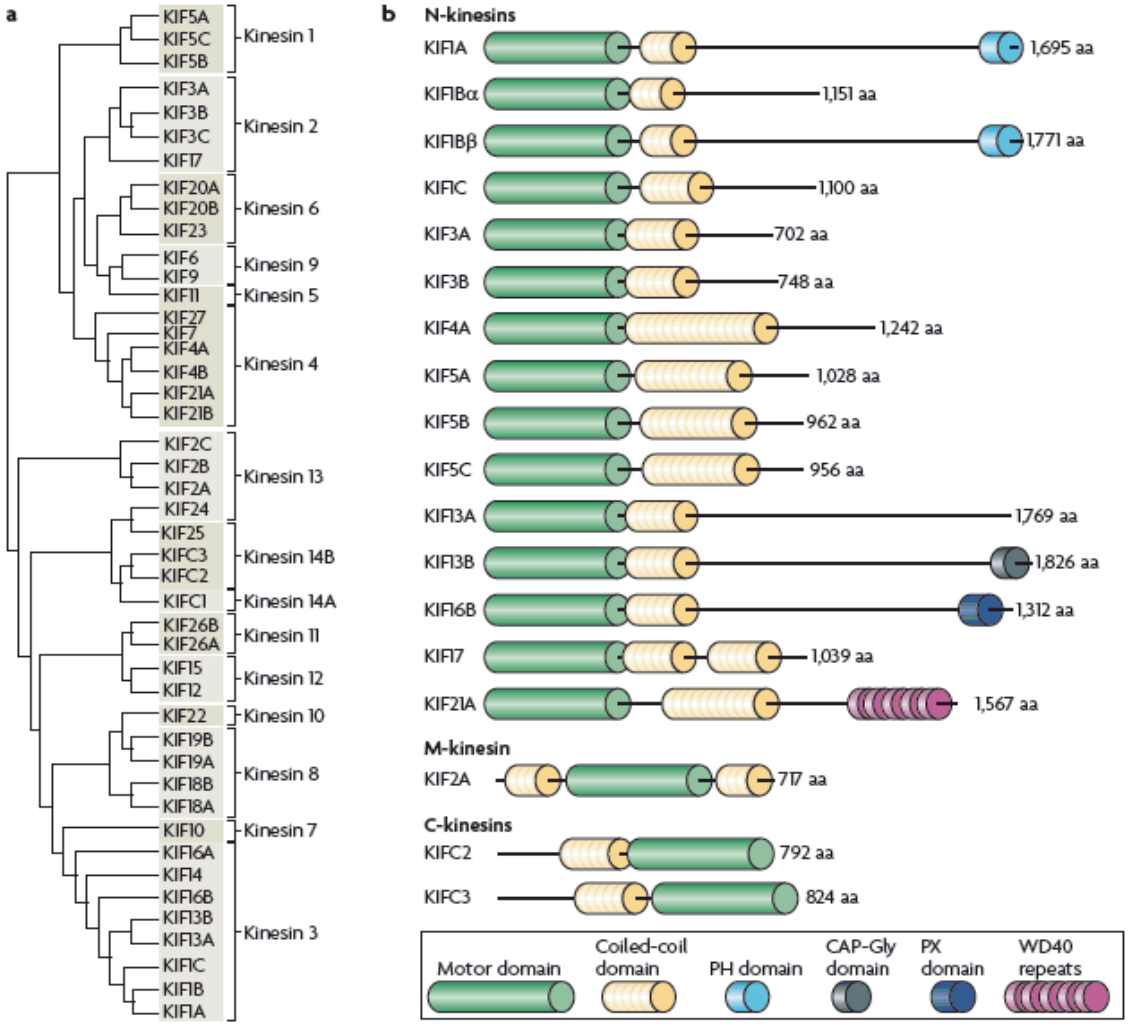

Figure I.5. The structure and phylogeny of major mouse kinesins. **(A)** A phylogenetic tree of all 45 kinesin superfamily (also known as KIF) genes in the mouse genome, which are classified into 15 families the major kinesins. In general, kinesins comprise a kinesin motor domain and a coiled-coil domain. **(B)** The 15 families of kinesins can be broadly grouped into N-kinesins, M-kinesins and C-kinesins, which contain their motor domain at the amino terminus, in the middle or at the carboxyl terminus, respectively. N-kinesins drive microtubule plus end-directed transport, C-kinesins drive minus end-directed transport and M-kinesins depolymerize microtubules. The three types of kinesin are grouped as indicated. Only the kinesin 13 family contains M-kinesins and only the kinesin 14A and kinesin 14B families contain C-kinesins. All other families consist of N-kinesins. aa, amino acids; PX, Phox homology. Adapted from (Hirokawa et al., 2009).

Dyneins are multimeric motors driving microtubule (-)-end directed transport. There are 14 dyneins encoded in human genome, but 13 of them (axonemal dyneins and cytoplasmic dynein-2) have specific function in motility of cilia and flagella and

intraflagellar transport. The bulk intracellular transport is carried out by cytoplasmic dynein-1, that is found in all microtubule-containing cells. Dynein-1 is a giant macromolecular complex consisting of heavy chains, that contain motor domains, required for microtubule-based motility, several intermediate chains, responsible for cargo binding, and at least three classes of light chains, thought to mediate dimerization of dyneins, and light intermediate chains binding to heavy chains independently (reviewed in (Sakakibara and Oiwa, 2011; Rapali et al., 2011; Allan, 2011). Cytoplasmic dynein-1 is crucial for the retrograde transport of numerous cellular cargoes, organization of intracellular compartments (i.e. Gogli, endosomes) and microtubule organization in the cell (Palmer et al., 2009; Allan, 2011; Hunt and Stephens, 2011).

Actin filaments consist of globular monomeric actin (G-actin), that can polymerize to form microfilaments (F-actin). Similar to microtubules, actin microfilaments are polar, with faster polymerization at the barbed ends and slower at the pointed end. F-actin can exist in the form of meshwork, that is typical for the cortex organization, or highly crosslinked anti-parallel bundles and stress fibers (Dominguez and Holmes, 2011)

Myosins are actin-dependent motors, providing short-range traffic along actin filaments, supporting cell shape, and organizing actin cytoskeleton. Myosins share the common strucural features: N-terminal actin-binding ATPase motor domain, a neck domain, containing light-chain-binding IQ motifs, and a C-terminal tail. Mammalian cells have up to 40 myosins belonging to ~20 different classes (Foth et al., 2006). Number of them are directly implicated in the transport of cargo along the actin filaments (i.e. myosin V, VI) (Desnos et al., 2007; Frank et al., 2004), and others can be required for reorganization of actin cortex during endocytosis and secretion to allow vesicles through

the dense network of actin fibers present below the PM (Bond et al., 2007). Most of the myosins are “plus”- (barbed) end directed, whereas myosin VI represents a single known exclusion so far, as it is “minus”- (pointed) end directed (Sweeney and Houdusse, 2010)

The role of intermediate filaments in the intracellular trafficking has been overlooked for a long time, yet, newly emerging data suggest they might directly interact with clathrin adaptor complex AP-3, mediate lysosomes positioning in the cells (Styers et al., 2004), and/or directly interact with kinesins (Helfand et al., 2004) or myosins (Rao et al., 2002).

1.5. Integrin trafficking

Integrins, being surface-resident receptors, have to be properly delivered to the PM, and their delivery, localization, and rearrangement depend on the intracellular vesicular trafficking.

There is very limited information available on the anterograde trafficking of integrins. Integrin heterodimers assemble in ER, and this is a prerequisite for correct chains folding (Huang et al. 1997) and integrin export from ER (Heino et al. 1989). There is evidence that other conponents of focal adhesions could regulate delivery of integrins to the PM, as talin associates with integrin complex already in ER and facilitates integrin complex exit from ER (Martel et al. 2000) Upon assembly alpha beta complex acquires inactive confirmation and is transported to Golgi and PM (Tiwari et al. 2011). In polarized cells integrins are sorted to the basolateral membranes, and this sorting requires protein kinases D 1 and 2 (PKD1 and PKD2) (Yeaman et al., 2004).

Being delivered to PM, integrins undergo rounds endocytosis and recycling and, to lesser extent can be driven into degradation pathway. Unlike the receptors internalized by

ligand-induced endocytosis (i.e. EGF or Tf), integrins do not require ligand-binding to trigger internalization, and can undergo endocytosis and recycling both in free and ligand-bound states (Sottile and Chandler, 2005; Shi and Sottile, 2008; Rintanen et al., 2011; Arjonen et al., 2012). Yet, the pathways of integrin retrograde trafficking can differ depending on the particular heterodimer, integrin activation status, binding to the ligand, growth factors presence. Although the comprehensive model of integrin trafficking in different conditions is still missing, a large number of regulators of different steps in integrin endocytosis and recycling are already known. The individual regulators are listed in the table I.1, and the outlines of the pathways of integrin trafficking they are organizing are discussed in more detail below.

Table I.1. Regulators of integrin trafficking.

Integrin trafficking regulator	**Integrin**	**Controlled process**	**References**
GTPases and their interactors			
Arf6	β1	Recycling of β1 integrin upon cells stimulation	(Powelka et al., 2004)
Arf5/BRAG2	α5β1	Internalization of β1, co-localizes with AP-2 and CCP at the PM	(Moravec et al., 2012)
Dnm2	β1	Required for focal adhesions disassembly but not for internalization of clustered α2	(Ezratty et al., 2005; Karjalainen et al., 2008)
Rab1/p115	β1	Required for anterograde trafficking of β1 to the lipid rafts	(Wang et al., 2010)
Rab5	β1, α5β1	Integrin internalization and trafficking in EE	(Pellinen et al., 2006; Valdembri et al., 2009; Arjonen et al., 2012)
Rab4	β1, αVβ3	Fast-loop recycling of αVβ3 integrin upon stimulation with PDGF; recycling of active β1	(Roberts et al., 2001) Woods et al., 2004; Arjonen et al., 2012)
Rab7	β1	Active β1 is found in the	Arjonen et al., 2012)

		Rab7-positive endosomes	
Rab11	β1, α5β1	Long-loop recycling of integrins	(Powelka et al., 2004; Woods et al., 2004; Veale et al., 2010; Arjonen et al., 2012))
Rab21/ p120RabsGAP	α1, α2, α5, α6, α11, β1	Rab21 binds a and b chains and regulates rapid internalization of integrins, but not transferrin. P120RabsGAP displaces Rab21 from tail of α integrin, promoting integrin recycling	(Pellinen et al., 2006) (Pellinen et al., 2008) (Mai et al., 2011)
Rab25	β1	Binds β1 tails and regulates recycling	(Caswell et al., 2007; Dozynkiewicz et al., 2011)
Kinases			
Akt/GSK3	αVβ3, α5β1	Promotes recycling of integrins, but not transferrin, by phosphorylation of glycogen synthase kinase 3	(Roberts et al., 2004)
PRKCα	β1, α5β1	Induces endocytosis and recycling of active β1; triggers caveolin-dependent endocytosis of α5β1 upon working in SDC4-RhoG pathway	(Ng et al., 1999; Bass et al., 2011)
PKD1	αVβ3, a3b1, β1	Required for Rab4-dependent recycling of αVβ3 and basolateral sorting of β1 integrins in TGN	(Woods et al., 2004; Yeaman et al., 2004; Onodera et al., 2012)
PKD2	β1	Together with PKD1 participates in sorting of β1 integrins to basalateral membranes in TGN	(Yeaman et al., 2004)
PAK1	Clustered α2β1	Required for sorting of clustered α2β1 to the caveolae	(Karjalainen et al., 2008)
aPKC	β1	Negatively regulates integrin internalization by phosphorylation of Numb	(Nishimura and Kaibuchi, 2007)
PKCε	β1	Phophorylates vimentin to promote integrin recycling	(Ivaska et al., 2005)
Integrin-binding proteins			

ACAP1	β1	Stimulation-dependent β1 recycling in migrating cells	(Li et al., 2005)
AP2	β1	Clathrin adaptor required for disassembly of FA	(Chao and Kunz, 2009)
ARH	β1	Adaptor protein required for β1 internalization in migrating cells	(Nishimura and Kaibuchi, 2007)
Dab2	α1, α2, α3, β1	Adaptor proteins required for disassembly of focal adhesions and bulk internalization of integrin β1	(Ezratty et ak., 2005; Teckchandani et al., 2009, 2012)
Numb	β1, b3, α5β1	Adaptor protein required for β1 internalization in migrating cells	(Nishimura and Kaibuchi, 2007; Teckchandani et al., 2009)
NRP/GIPC1	α5β1	Internalization at the endge of fibronectin-positive fibrillar structures	(Valdembri et al., 2009)
SNX17	β1	Promotes integrin recycling	(Böttcher et al., 2012)
Molecular motors			
KIF1C	α5β1	Supports the stabilization of trailing edge in migrating cells by targeted delivery of α5β1	(Theisen et al., 2012)
Myosin-X	β1	Relocalization of β1 integrin to phylopodia	(Zhang et al., 2004)
Myosin VI/GIPC	α5β1	Promotes internalization of active α5β1	(Valdembri et al., 2009)
SNAREs			
VAMP3/ SNX4/ SNAP23	α5β1	SNARE complex required for delivery of α5β1 integrin from RE to PM in the leading edge of migrating cells	(Veale et al., 2010)
SNAP29	β1	Regulates recycling of β1 integrin and transferrin	(Rapaport et al., 2010)
STX6/VAMP3	a3b1; α5β1	Recycling of α5β1; a3b1 recycling through TGN during chemotactic cell motility	(Tiwari et al., 2011; Riggs et al., 2012)
VAMP2	α5β1	Trafficking of α5β1 to the PM	(Hasan and Hu, 2010)

1.5.1. Early steps of integrin endocytosis

Cytoplasmic tail of β1 integrin contains 3 sequence stretches that are known to be involved in integrins localization to FA (Reszka et al., 1992). Two of them have a conserved NPXY motif, which is known to mediate internalization of low-density lipoprotein receptor (Chen et al., 1990), megalin (Takeda et al., 2003), insulin and insulin growth factor-like receptor (Rajagopalan et al., 1991; Hsu et al., 1994), EGF receptor, β-amyloid precursor protein (Perez et al., 1999), but not in transferrin receptor. NPXY works as a binding site for such endocytic adapters as Dab2, AP-2, Numb (Nishimura and Kaibuchi, 2007). However, the presence of this motif might not be sufficient to trigger cargo internalization, as introduction of it into the recombinant transferrin receptor did not promote NPXY-dependent internalization, but a longer amino acid stretch was required (Collawn et al., 1991). Moreover mutations of NPXY motifs present in β1 chain of α5β1 integrin did not block integrin internalization, as expected (Vignoud et al., 1994).

Number of adaptor proteins are known to be involved in CME of integrins. The role in internalization of integrins was shown for Dab2, ARH, Numb, AP2 (Ezratty et al., 2005; Nishimura and Kaibuchi, 2007; Chao and Kunz, 2009; Teckchandani et al., 2009, 2012) The described integrin internalization pathway mediated by Dab2 still has lots of controversies: it has been shown that in human fibrosarcoma HT1080 cells Dab2 mediates disassembly of integrin β1-containing FA (Chao & Kunz, 2009), which should normally accumulate active integrin. Yet Teckchandani et al (2009, 2012) demonstrated that in HeLa cells Dab2 preferentially co-localizes with the β1 integrin on the dorsal surface of the cell, which is not engaged in the interaction with ligand. The requirement for AP-2 adaptor complex was demostrated along with the requirement of Dab2 for β1 integrin internalization (Chao & Kunz, 2009; Teckchandani et al., 2009).

Despite the plethora of data on the clathrin-dependent internalizaiton of β1 integrin, alternative entry routes for integrins are also known. In myofibroblast cells siRNA experiments demonstrated that internalization of α5β1 integrin and its ligand fibronectin in fibroblasts depended on caveolin-1 (Sottile and Chandler, 2005; Shi and Sottile, 2008). It has been described recently, that internalization of αVβ3 integrin can occur via membrane ruffles at the dorsal surface of the cell (Gu et al., 2011). Intracellular trafficking regulators can take part in shifting of integrin towards one or another internalization pathway. over-expression of Rab21 in SAOS cells promotes clathrin-independent internalization of α5β1 and αVβ3, although normally they are internalized via CME in this cell line (Pellinen et al., 2008). Experiments on α2β1 integrin demonstrated that it can be clustered by its natural ligand collagen I, by EV1 virus binding or by incubation with primary anti-α2 chain antibodies followed by addition of appropriate secondary antibodies ,so that internalization of clustered α2β1 occurs via caveolae and is independent of clathrin in SAOS cells (Upla et al., 2004; Rintanen et al., 2012). Remarkably, the features of clustered α2β1 trafficking are clearly distinct from the constitutive internalization of non-clustered α2β1 and does not correspond to the conventional internalization pathway (see below).

Following internalization, integrins are delivered to the EE positive for Rab5 and its effectors (Pellinen et al., 2006; Valdembri et al., 2009; Arjonen et al., 2012) . From the EE they can be recycled back to PM via Rab21 and Rab4-dependent pathway (Roberts et al., 2001; Woods et al, 2004; Pellinen et al., 2008 ; Arjonen et al., 2012) or sorted into long-loop recycling (Powelka et al., 2004; Arjonen et al., 2012) or degradation pathways (Lobert et al., 2010). It has been shown that stimulation of the cells with PDGFβ results in fast Rab4-dependent recycling of αVβ3 integrin, but not of α5β1 (Roberts et al., 2001).

Integrin β1 was also efficiently recycled to the PM upon serum addition via Arf6 and Rab11 pathways (Powelka et al., 2004).

1.5.2. Integrin recycling

After internalization integrins are predominantly recycled back to the PM. The recycling pathway employed can differ depending on particular heterodimer, activation status of integrin or stimulation of the cell with growth factors. Rab4- (short-loop recycling) and Rab11-dependent (long-loop recycling) pathways are the best characterized, although the full understanding of the integrin recycling regulation is missing. Rab4-dependent pathway is used by integrin αVβ3, in contrast to α5β1, upon stimulation with PDGF (Roberts et al., 2001). Nevertheless, analysis of integrin β1 trafficking revealed that both active and inactive conformation of integrin β1 co-localized with Rab4, yet only recycling of inactive β1 was affected by expression of Rab4 dominant-negative mutant (Rab4S22N) (Arjonen et al., 2012). Both conformations could be found in the Rab11-positive PRC (Arjonen et al., 2012), and were recycled to the cell surface in Arf6 and Rab11-dependent manner upon the stimulation of cells with serum (Powelka et al., 2004).

In contrast to studies the report of Dozynkiewicz et al. (2011) which demonstrated involvement of member of Rab11 family, Rab25, in the recycling of ligand-occupied in A2780 from late endosomes, no co-localization of either active or inactive integrin β1 to Rab25 was found in MDA-MB-231 cells (Arjonen et al., 2012)

Recycling of integrins was shown to be driven by the competitive binding of regulators to the integrin tails. So, the efficient recycling of β1 depends on the displacement of Rab21 from the integrin heterodimer by p120RasGAP, and in the absence

of p120RasGAP the integrin is retained in the Rab21- and EEA1-positive endosomes (Mai et al., 2011). The re-routing of internalized β1 to the recycling compartment requires interaction of NXXY-motif in β1 tail with sorting nexin 17 (SNX17), and when SNX17 is depleted, α5β1 integrins are ubiquitilated and driven to ESCRT-mediated degradation (Böttcher et al., 2012).

Besides Rab proteins, several SNARE complexes were identified as regulators of integrin recycling. The first work indicating that SNAREs are involved in integrin recycling was done using the general inhibitor of SNARE function TeTx, application of which blocked cell spreading. This could be rescued by expression of toxin-insensitive VAMP3 (Skalski and Coppolino, 2005). Further insight in the role of VAMP3 in recycling of integrins was obtained from work of Veale and colleagues (2010), who demonstrated than the complex of R-SNARE VAMP3 and Q-SNAREs SNX4 and SNAP23 was required for delivery of α5β1 from the recycling compartment to newly forming lamellopodium in migrating cells. SNAP29 regulates recycling of β1 integrin through the recycling pathway shared by transferrin (Rappaport et al., 2010). In addition, the delivery of internalized α5β1, but not α2β1 or a3b1 integrin to the PM is dependent on VAMP2 (Hasan and Hu, 2010).

Regulation of integrin recycling depends on interaction of cytosolic proteins with integrins C-terminal domain. Interaction of catalytically-active protein kinase D (PKD1) with C-terminal b3 domain of αVβ3 integrin was required for Rab4-dependent recycling of internalized integrin to the nascent focal adhesions (Woods et al., 2004).

1.5.3. Integrin degradation

The degradation of integrins is by far less understood than their recycling.

Generally, the binding to the ligand can drive a fraction of internalized integrin-ligand complex to the lysosomal degradation. The degradation of integrins in the conventional lysosomal pathway is by far less efficient than their recycling: half-life of the α5β1 integrin in the lysosomal pathway is 18h (Lobert et al., 2010), whereas the cycle of endocytosis and recycling of the same heterodimer takes only 30 min (Roberts et al., 2001, 2004). The sorting of fibronectin-bound α5β1 into the MVBs and, subsequently, lysosomes depends on ubiquitination of a5 chain and requires the interaction of ESCRT complex with α5β1 (Lobert et al., 2010). In addition, the analysis of relation between integrin β1 activation state and the pursued trafficking pathway revealed that only active β1 is found in Rab7-positive endosomes, whereas EE and recycling compartments are occupied by both active and inactive forms (Arjonen et al., 2012).

However, different degradation pathway was recently described for clustered α2β1 integrin. There, the heterodimer clustered by EV1 virus, addition of collagen I, or sequential application of primary and secondary antibodies against α2 is efficiently internalized from the PM to the intracellular structures that does not co-localize neither to EE marker EEA1 (Rab5 effector, early endosome antigen 1) in the early steps of internalization (upon 5 and 15 min of internalization), nor to the conventional late-endosome-dependent degradation labeled by Rab7, CD63, LAMP1 at the later steps of internalization (30 min, 1h, 2h, 6h). The clustered integrin does not recycle to the PM, but is instead delivered to the integrin-specific MVBs and degraded by calpain proteases (Upla et al., 2004; Rintanen et al., 2012).

1.5.4. Cytoskeleton in integrin trafficking

Although integrin function is tightly interconnected with organization of

cytoskeleton, the role of cytoskeletal structural proteins like actin and tubulin, and cytoskeleton regulators in the integrin trafficking remains elusive. Several works identified the requirement for actin cytoskeleton in integrin recycling. Stimulation-dependent recycling of integrin β1 from the PRC requires intact actin and, presumably, Arf6-dependent actin rearrangments (Powelka et al., 2004). Treatment with actin-depolymerizing drug cytochalasin D specifically blocks recycling of inactive β1 integrin from PRC, but does not affect trafficking of active β1 (Arjonen et al., 2012). In addition, Q-SNARE complex SNX4/SNAP23, required for recycling of α5β1, was required for F-actin-rich lamellopodia formation in migrating macrophages, but causal relationship between F-actin enrichment in lamellopodia and delivery of α5β1 integrin to these locations was not investigated (Veale et al., 2010). Involvement of actin in the integrin trafficking implies the role for actin-based motors, and this was demonstrated for two of them. Myosin X (Myo10) was shown to directly interact with NPXY motifs in β1 integrin tail and to induce relocalization of integrins to extending filopodia (Zhang et al., 2004). Unconventional myosin VI (myo6) interacted with GIPC and Nrp to promote internalization of active α5β1 (Valdembti et al., 2009).

The requirement of microtubules for the directed migration of the cells has been demonstrated early (Vasiliev et al., 1970). Direct observations revealed link between microtubules and FA in goldfish fibroblasts (Kaverina et al., 1998) and indicated that mictotubules occurrence at FA site correlated with FA disassembly (Kaverina et al., 1999). Indeed, it has later been shown that dynamin-dependent dissassembly of FA is induced by regrowth of microtubules after their disruption with tubulin-depolymerizing drug nocodazole (Ezratty et al., 2005). In turn, microtubules reaching adhesion sites exhibit higher dynamics and multiple switching between growth and catastrophe, which

might depend on FA components paxillin and FAK (Palazzo et al., 2004; Schober et al., 2007; Efimov et al., 2008). One of the FAK downstream effectors which serve as factors of dynamic microtubule-dependent FA disassembly at the leading edge of migrating cells is a microtubule-associated kinase SLC (Wagner et al., 2008)

Kinesins were barely studied in the context of integrin trafficking. KIF1C was recently shown to mediate integrin α5β1 delivery to the rear adhesion site in the migrating epithelial cells and stabilization of the tail of migrating cells, which was required for maintenance of migration directionality (Theisen et al., 2012). Kinesins KIF5b and KIF3a/3b can indirectly mediate FA turnover by delivering an MT1-MMP (matrix metalloprotease) to the adhesion sites (Wiesner et al., 2010), where it is required for ECM degradation and integrin and fibronectin endocytosis (Takino et al., 2007; Shi and Sottile, 2011)

At last, sparse data indicate that there may also be a role for intermediate filaments in the integrin traffic. It has been shown that intermediate filaments are required for cell migration (Eckes et al., 1998). Moreover, phosphorylation of one of the intermediate filaments components vimentin promotes integrin β1 recycling (Ivaska et al, 2005).

1.6. Integrin α2β1

Integrin α2β1 is a receptor for collagens which are the most abundant ECM proteins in the human body (Myllyharju and Kivirikko, 2001). This heterodimer was initially identified as a surface glycoprotein complex on activated T-lymphocytes (Hemler et al. 1984; Hemler et al. 1985). Its main ligands are collagen I, and, to lesser extent, collagen IV (Kramer & Marks 1989). Suprisingly, although being the receptor for one of the most abundant ECM proteins, α2 integrin does not cause in major phenotype *in vivo*

when knocked out. Mice lacking α2β1 integrin were born, developed normally, and could reproduce. No gross abnormalities were recorded in most of the organ systems, but the mammary gland branching was diminished, and the platelet aggregation in response to collagen was delayed, although not completely blocked (Chen et al., 2002). In wound healing, α2β1 integrin was necessary for vascularization of the wound, but otherwise its role in the healing was dispensible. The reason for the lack of phenotype in integrin α2 knock-out is a matter of debate (Parks, 2007).

Integrin α2β1 is required for echovirus (EV1) and rotaviruses infection (Bergelson et al., 1992; Londrigan et al., 2003; Fleming et al., 2010). Both EV1 and rotaviruses utilize integrin α2 I-domain for binding, but, interestingly, their binding prefereces for activation state of integrin differ. Rotaviruses require for binding to α2 the residues similar to the ones exploited by collagen I, and more avidly bind to the active conformation of α2β1 (Londrigan et al., 2003; Fleming et al., 2010). Yet, EV1 preferentially binds to inactive α2 at the position distinct from the collagen-binding site and does not induce integrin activation (Jokinen et al., 2010).

So far little is known about intracellular trafficking pathways of α2β1. Recently a prominent pool of information emerged, characterizing the trafficking of α2 integrin clustered by addition of collagen I, EV1, or sequential treatment of living cells with primary anti-α2 antibodies and appropriate secondary antibody in SAOS cells (Upla et al., 2004; Karjalainen et al., 2008, 2011; Rintanen et al., 2012). Under these conditions, α2 gets internalized soon after clustering via caveolae, in 1h leaves the PM completely and is not recycled back upon internalization (Rintanen et al, 2012). Strikingly, pursuing this degradation pathway, internalized clustered α2 does not co-localize neither with markers of clathrin-dependent internalization pathway EEA1 nor with markers of late

endosomal/lysosomal pathway Rab7, LAMP1, and CD63, but is driven to the integrin-specific MVBs, and than degraded by calpains (Karjalainen et al., 2008, 2011; Rintanen et al., 2012).

The information on the trafficking of non-clustered is very sparse. In SAOS cells overexpressing α2β1, non-clustered α2 integrin upon internalization pursues recycling pathway (Rintanen et al., 2012). In HeLa and MDA-MB-231 cells α2 chain was shown to interact with Rab21, which is required for endocytosis and recycling of β1 integrins (Pellinen et al., 2006, 2008). Additionally, the involvement of Dab2 endocytic adaptor in the internalization of α2β1 heterodimer was suggested, as the surface levels of α2 and β1 integrins increased upon knock-down of Dab2 in HeLa cells, and Dab2 was further demostrate to play role in β1 internalization (Teckchandani et al., 2009, 2012)

Although plenty of data is available for the trafficking of non-clustered β1 integrin, the α2 binding partner, it can not be readily transferred to understand the trafficking of α2β1 integrin, as β1 forms heterodimers with 12 α chains, that can pursue different endocytosis pathways.

1.7. Integrin trafficking in disease

Abnormal integrin function has long been associated with diseases and integrins are successfully used as therapeutic targets. Over-expression of number of integrins, their ligands, and ECM-degrading MMPs is a cause for rheumatoid arthritis, although the primary reason for that seems to be the integrin signaling rather than trafficking (Lowin and Straub, 2011).

Integrin antagonists (i.e. RGD peptides) are used as therapeutics to prevent platelet aggregation and blood clot formation (Meyer et al., 2006). Antibodies against α4 integrin are used to block the leucocyte trafficking through the blood-brain barrier and

therefore control the inflammation in the multiple sclerosis (O'Connor, 2007). However, one of the most prominent medicine-related function of integrin is their association with cancer.

The development of solid cancers is often associates with dissemination of transformed cells which actively migrate from the primary tumor and invade to the adjacent tissues to form new tumor masses (Ramsay et al., 2007). Integrins can be involved in the cancer development through different mechanisms, e.g. by regulating cytokinesis of dividing cells (Pellinen et al., 2008), changing the MMPs expression profiles (Silletti et al., 2001) or altering migratory properties of the cells (Shin et al., 2012).

2. Objectives

Trafficking of integrins is of great relevance for understanding of normal and pathological cellular behaviour. The number of integrin heterodimers expressed in human cells, and the fact that integrins trafficking pathways can change according to integrins activity and ligand-binding status, introduces a vast complexity to the existing data on the subject. The current model of integrin trafficking is far from being comprehensive. Previous studies identified number of integrin-specific trafficking regulators, but many groups of proteins, known or expected to contribute to traffic specificity (i.e. molecular motors) have never been systematically explored in the context of integrin traffic.

For these reasons we decided to systematically search for the regulators of non-clustered α2 integrin retrograde trafficking.

To achieve this, the following goals were pursued:

1. establish a quantitative assay that could be applied to medium- or large-scale analysis of α2 integrin internalization;
2. perform RNAi screening for systematic analysis of α2 integrin internalization regulators;
3. validate the screening results and
4. characterize the role of selected hits in the α2 integrin traffic.

The following approaches were undertaken:

1. The quantitative fluorescent microscopy-based assay was established to measure the internalization of integrin α2 in a small- and medium scale. The quantification of the assay was developed to achieve an adequate representation of the observed experimental results and high dynamic range of the assay.

2. The library of 1084 siRNAs targeting 386 genes known or predicted to be involved in the cytoskeleton organization was used for RNAi screening for α2 integrin internalization regulators. The results were bioinformatically analyzed and compared to published relevant datasets to characterize the screening hits.

3. In order to verify the primary screening results, the reproducibility of the effect of the primary screening hits in the modified experimental conditions was assessed for selected group of hits. The presence of false-negatives among the screening results was tested. To eliminate the influence of secondary effects of hits knock-down, the changes in total α2 integrin expression were estimated for genes taken into validation, and the effect of local cell density changes on the α2 integrin endocytosis and expression.

4. To further dissect the role of novel α2 integrin endocytosis regulator KIF15 in intracellular trafficking, the effect of its knock-down on the trafficking of other endocytic cargoes and cellular distribution of integrin-specific clathrin adaptor Dab2 was tested. The specificity of hit effect was verified by Western Blotting and rescue by overe-expression of siRNA-resistant cDNA.

3. Materials and Methods

3.1 Materials, antibodies, plasmids, reagents

The following antibodies were used in this study: mouse monoclonal against human α2 integrin (clone P1E6, Merck-Millipore), mouse monoclonal against human α5 integrin (clone NKI-SAM1, Merck-Millipore), mouse monoclonal agains integrin β1 (clone TS2/16, BioLegend) rabbit monoclonal ant-Dab2 (H-110, Santa Cruz), mouse monoclonal antibody against Dab2 (clone 52/p96, BD Biosciences), anti-KIF15 antibodies reactive with human and mouse KIF15 (Tanenbaum et al., 2009) , anti-α-tubulin (Cell Signalling, clone DM1A), goat anti-mouse and anti-rabbit antibodies coupled to Alexa-488 and Alexa-647 (Invitrogen), anti-rabbit HRP-coupled (GE Healthcare), anti-mouse HRP-coupled (R&D). Lipofectamine^{TM}2000 (Invitrogen) was used for tranfection. Transferrin-Alexa568 and EGF-Alexa555 conjugates were purchased from Invitrogen. peGFP-C1 plasmid was purchased from Clontech. GFP-MmKIF15 plasmid was obtained from R. Medema (Tanenbaum et al., 2009). GFP-Rab5, GFP-Rab7a, mCherry-Rab11b, and mCherry-Rab4a were a kind gift of Dr. Brady.

Micropatterned coverglasses (Starter's CYTOOchips) with fibronectin-Alexa550 coating were obrained from Cytoo.

3.2 Cell culture

All experiments were performed in human epithelial carcinoma cells (HeLa, ATCC CCL-2). were grown in Minimum Essential Medium (Eagle) (MEM, Sigma-Aldrich) supplied with 10% (v/v) fetal calf serum (PAA Laboratories), 2mM L-glutamine (Invitrogen), 50g/ml streptomycin and 50U/ml penicillin (Invitrogen)., buffered with 30mM HEPES, pH 7,2-7,4. Cells were cultured in 10 cm cell-culture dishes in the

incubator maintaining 37 °C and humidified atmosphere with 5% CO_2, and split every 3 days in ratio 1:8 using 0.25% trypsin-EDTA (Invitrogen).

For serum-starvation the growth medium was replaced with MEM supplied with 2mM L-glutamine and 0,01% (w/v) BSA (Roth) (MEM-BSA). For transfection Opti-MEM (Invitrogen) without supplements was used for the first 4h of incubation of cells with transfection complexes (see ***Transection with siRNAs and cDNAs***) which was further replaced with MEM supplied with 10% fetal calf serum (PAA Laboratories) and 2mM L-glutamine (Invitrogen).

3.3 Transfection with siRNA and cDNA

For delivery of siRNAs or cDNAs in the HeLa cells we used liquid-phase direct transfection or reverse tranfection. For individual and small-scale experiments liquid-phase direct transfection with siRNAs or cDNA was performed using Lipofectamine 2000 reagent (Invitrogen) according to manufacturer's protocol. For single tranfection of cells growing in 24-well plate or in 8-well chambered coverslip 20 pmol of siRNA of was used. For cDNA tranfection amount of cDNA used was 800 ng per transfection in 24-well plate and 200 ng in 8-well chambered coverslip. Unless otherwise is stated, tranfection of the cells with siRNA occurred 48h before respective assay, and with cDNA – 24h before the assay. Reverse tranfection on cell arrays was used for delivery of siRNAs in large-scale screening format, as described (Erfle et al., 2007, 2011). In brief, 5 µl of siRNA from 30 µM stock was mixed with solution of 3,5 µl Lipofectamine 2000 and 3 µl Opti-MEM containing 0,4M sucrose and incubated for 20 min at RT. Thereafter it was mixed with 7,25 µl of 0,2% gelatine (w/v) in 0,01 % fibronectin (v/v), and transferred to contact printing on LabTek using eight solid pins PTS 600, which gives the spot size of approx.

400 µm. The spot-to-spot distance was set to 1125 µm, which allowed to fit on a single LabTek 384 spots organized in 12 columns and 32 rows. The whole library of 1084 siRNAs was spotted on 4 LabTeks, with 6-12 Scramble negative control spots distributed across each layout. Additional row of positive control siRNAs targeting DNM2 and CLTC was spotted on each LabTek several weeks prior the start of the screening. The printed cell arrays were dried for 24h at RT, and then stored at RT until cell plating on the spotted cell array 48h before performing the integrin endocytosis assay.

3.4 Western Blotting

For analysis of KIF15 knockdown and overexpression, HeLa cells were plated in 12-well plate, and tranfected with siRNA and cDNA for 48 and 24 h, respectively. Then cells were rinced with PBS and lysed with 80 µl of hot (95 °C) Laemmli buffer (Laemmli, 1970) supplemented with 100 mM DTT and Protease Inhibitor Coctail (Roche). The nucleic acids in lysate were sheared by adding to the sample 0,2 µl benzoase nuclease for 10 min at RT. The proteins were separated at 8% PAA gel. PVDF Immobilion-P membrane was used for protein blotting. The membrane was blocked with 5% non-fat dry milk in PBST (PBS-0,1% Tween). KIF15 was detected using anti-KIF15 antibodies reactive with human and mouse KIF15 (Tanenbaum et al., 2009) diluted 1:300, incubated at 4 °C ON. After short washes with PBST secondary HRP-coupled anti-rabbit antibody (Amersham, 1:20000 dilution in PBST) was added. The signal was detected by ECL system (GE Healthcare). Luminescence was recorded by Chemiluminescence Detection System (Intas) and quantified by ImageJ software (NIH, Abramoff et al., 2004). For analysis of changes of Dab2 amount upon KIF15 knockdown, the mouse p96/Dab2 (BD) antibodies were used in dilution 1:500 following detection with HRP-coupled anti-mouse

antibodies (R&D, 1:1000 dilution). Tubulin specific band at 55 kDa detected by anti-α-tubulin (clone DM1A9, Cell Signaling, 1:4000 dilution) was used for normalization of KIF15 or Dab2 signal.

3.5 RT-PCR

Preparation of total cellular RNA was made using TRIzol reagent (Invitrogen) according to manufacturer's protocol. cDNA was prepared with MMVL-reverse trancriptase (Ambion) and oligo-dT. The primer pairs used to assess the expression of genes of interest are listed in **Appendix IV**. Primer specificity was determined by nucleotide BLAST analysis against human genome and trancriptome. Primers were designed using Primer BLAST (NCBI) or the primer pairs published in (Jaulin et al., 2007) were used.

3.6. Non-clustered and clustered α2 integrin internalization assay

For α2 integrin internalization assays the cells were serum-starved for 14h before the assay, or, in case of cDNA tranfection, 6h before the assay. Internalization of non-clustered α2 integrin was previously published in (Erfle et al., 2011). For the assay, the primary antibody against α2 integrin (P1E6) was diluted in MEM-BSA to the final concentration 10 µg/ml and cooled on ice. The cells growing in multi-well plates were overlayed with 80-100 µl of antibody solution and placed on metal plate on ice. For the cells growing on coverslips, the antibody solution was pipeted in 50 µl droplets on parafilm-wrapped metal plate placed on ice, and the coverslips were flipped on them. The cells were kept on ice with antibody solution for 50 min, then shortly washed twice with ice-cold MEM-BSA to remove the excess of antibody, and then incubated with pre-

warmed MEM-BSA at 37 °C in humidified 5% CO_2 atmosphere for indicated time. After the incubation the cells were rinsed with PBS, stripped with acetic buffer (0,5% (v/v) acetic acid, 0,5M NaCl, pH 2,6) for 30-40 s, rinsed again with PBS and fixed with 2% PFA for 20 min at RT. The stripping step could be omitted, if indicated, for assessment of surface α2 integrin. After fixation the PFA was washed with PBS and quenched by incubation with 30mM glycin for 5 min. The cells were permeabilized with 0,2% (w/v) saponin in 10% (v/v) FCS in PBS and then were incubated for 1h with secondary anti-mouse antibodies (Alexa488 or Alexa647 coupled, Invitrogen) in permeabilisation solution. and the nuclei were counterstained with Hoechst 33342 dye (0,1 µg/ml). For experiments aiming for the surface α2 integrin visualization, 10% (v/v) FCS in PBS was used instead of permeabilisation solution.

Clustering and subsequent internalization of α2 integrin was induced as described in (Rintanen et al., 2012) by sequential incubation of living cells with primary anti-α2 (P1E6) antibodies and then with secondary anti-mouse antibodies coupled to Alexa647. Cells were incubated on ice with 10 µg/ml P1E6 as described for non-clustered integrin assay, then rinsed twice with ice-cold MEM-BSA, and then incubated for 50 min with secondary anti-mouse – Alexa647 antibodies on ice. Corresponding non-clustering control was incubated on ice with MEM-BSA without addition of secondary antibody. Then cells were shortly washed twice with ice-cold MEM-BSA and incubated with pre-warmed MEM-BSA at 37 °C in humidified 5% CO_2 atmosphere for indicated time. After the incubation the cells were rinsed with PBS and fixed with 2% PFA for 20 min at RT. The nuclei were counterstained with Hoechst 33342. Corresponding non-clustered control was subsequently stained with secondary anti-mouse antibody as previously described.

3.7. Non-clustered integrin α2 internalization on CYTOOchips

The cells were grown on plastic in multi-well plates and transfected with siRNAs (liquid phase transfection, as described earlier) 48 h before the integrin internalization assay. Next day after transfection the cells were trypsinized, counted, and 60000 cells were seeded on the Starter's CYTOOchip, that was beforehand briefly washed with 70% ethanol and kept in PBS. For seeding the cells were resuspended in the normal growth medium. The cells were allowed to sediment for 10 min at RT, then were gently transferred to 37 °C, 5% CO_2 for another 20 min to allow cell attachment. The the non-attached cells were washed by two-times partial replacement of the growth medium. 4h after seeding the cells on chip (which corresponds approx. 14H before the integrin α2 internalization assay), the growth medium was replaced by MEM-BSA. The integrin internalization was further performed as described previously.

3.8. EGF and Transferrin endocytosis assays

EGF endocytosis assay was performed as described in (Schmidt-Glenewinkel et al., 2009). Cells were serum-starved for 14 hours before the assay; then EGF-Alexa555 was added to the medium to final concentration of 100ng/ml and cells were incubated for indicated amount of time at 37 °C, stripped with acidic buffer (50 mM glycine, 150 mM NaCl, pH 3.0), and fixed with 3% PFA 20 min at RT.

For transferrin endocytosis assay cells were serum-starved for 1h, then tranferrin-Alexa568 was added to the medium to the final concentration of 25 µg/ml, and cells were incubated for indicated time at 37 °C, shortly rinsed with PBS and directly fixed with 3% PFA 20 min at RT.

3.9. Microscopy

Wide-field fluorescent microscopy was done with Olympus IX81 Scan^R automated inverted microscope (Olympus Biosystems) controlled by Scan^R acquisition software. Generally, imaging was made using 20x/0.75 NA air objective lens (UPlanSApo; Olympus Biosystems). For screening 10x/0.4 NA air objective lens (UPlanSApo; Olympus Biosystems) was used. Stabilised 150W Hg/Xe light source and combination of the following excitation/emission filters was used for the imaging of the fluorophores: excitation wavelength = 450-490 nm and emission wavelength 500 - 550 nm was used to to image integrin α2, excitation wavelength = 426-446 nm, emission wavelength = 460-500 nm - to image EGF-Alexa555, and 545-580 nm excitation and 610-700 emission wavelength - to image transferrin-Alexa568. Excitation wavelength = 325-375 nm, emission wavelength = 435-475 nm was used to image nuclei in all assays.

Confocal imaging was performed with confocal laser scanning microscope TCS SP5 (Leica Microsystems) using a 63x oil immersion objective lens. An argon (λ = 488nm) laser was used to excite GFP or Alexa-488 dye, diode laser (λ = 561 nm) was used to excite Alexa-568 dye or mCherry, and a helium/neon (λ = 633nm) laser was used to excite Alexa 647 dye.

TIRF was performed on Nikon Eclipse Ti TIRF microscope with Nikon Apo TIFR 60x NA 1.49 objective. 488 and 640 nm laser lines were used for excitation of Alexa488 and Alexa647, respectively, with following filters: excitation wavelength = 485-485nm, emission wavelength = 500-545 nm, and emission wavelength = 621-643, excitation wavelength = 672 - 712nm.

3.10. Image analysis and statistical data analysis for small-scale experiments

For experiments performed in 96-well plates, 8-chamber µ-slides, or on coverslips in 24-well plates, 30 to 42 images were analyzed. Images obtained by wide-field fluorescent automated screening microscopy were processed by Scan^R Analysis software (Olympus). The nuclei of individual cells were identified by intensity module of built-in Scan^R object finder using an intensity threshold to identify objects border. The threshold was set manually for each individual experiment. To measure the mean intensity of the perinuclear area, the outline of nuclei was expanded by 10 µm. Besides the mean intensity of imaged channels, the imaged position in which the cell was located, and the coordinates of nucleus center were recorded.

Quality control and statistical analysis of image analysis raw data were done using the following pipeline. First, all the images underwent visual control to exclude those of insufficient quality (i.e. out of focus, too little cells, scratches or other artefacts present); second, 2% of the cells with the highest fluorescence intensities were excluded to ensure that abnormal or apoptotic cells don't interfere with analysis. Further analysis depended on the assay.

For the integrin internalization assay in the multiwell plates a threshold, separating α2 integrin internalizing cells from non-internalizing was determined visually for each experiment. Percentage of internalizing cells was multiplied to the mean intensity of internalizing cells resulting in integrin endocytosis parameter per well (equation 1):

$$endocytosis = \frac{(mean\ intensity\ above\ threshold)\square(number\ of\ cells\ above\ threshold)}{(total\ number\ of\ cells)} \quad [1]$$

In the non-clustered α2 integrin endocytosis assay, for negative control siRNA-

transfected cells the number of internalizing cells was usually about 30%. The resulting "endocytosis" parameter was normalized to the corresponding negative control.

The similar calculation method was used for tranferrin, EGF, and clustered α2 integrin internalization assay. Due to the nature of these assays, the percentage of internalizing cells in the control experiments was usually close to 100%.

For quantification of rescue of human KIF15 knockdown with over-expression of GFP-mKIF15, the individual cells measurements were binned according to level of expression of GFP-mKIF15. The scale of binning was linear for low-level of expression (intensities from 0 to 100 A.U.), and logarithmic for high expression (higher then 100 A.U.). Three bins containing at least 20 cells/bin with highest GFP-mKIF15 signal were selected and mean intensity of internalized integrin was averaged.

For the assessment of α2 integrin expression, after removal of 2% of brightest cells, mean intensity of total cell population was calculated and then normalized to the corresponding negative control.

Statistical significance of difference between experiments mean was tested by Student's two-tailed t-test for samples with uneven variance. P-value less than 0,05 was considered significant.

3.11. Image analysis and statistical data analysis for RNAi screening on cell arrays

By imaging the cell arrays with 10x objective, each siRNA spot was fitted to an individual image. Central area of each image, corresponding to siRNA spot (represented with outline in Fig. 1), was selected by Scan^R software (Olympus) and the individual cells within it were detected by nuclear staining. One siRNA spot on cell arrays

accomodated 100-400 HeLa cells. Amount of internalized integrin represented by mean intensity of integrin staining in perinuclear region was measured for individual cells.

Statistical analysis of the primary screening raw data was done using the statistical language R (R Development Core Team. R: A language and environment for statistical computing, 2011) and the package cellHTS (Boutros et al., 2006) from Bioconductor http://www.bioconductor.org). Prior statistical analysis, all the images were subject to visual control to exclude those of insufficient quality, as described for smalle-scale experiments; then 2% of the cells with the highest fluorescence intensities were excluded for each imaged spot. The remaining cell intensities were averaged, and B-score normalization (Brideau et al., 2003) was applied to them, to calculate a correction factor for each well which would account for spatial effects and between-plate artifacts. In each well the computed correction factor was subtracted from the remaining cell intensities to obtain normalized single-cell data. The the normalized intensities of the whole cell population from the single cell array was pooled and Gaussian Mixture Model (Knapp et al., 2011) was fitted to it to automatically cluster the cells into two subpopulations that would correspond to internalizing and non-internalizing cells. The median signal intensitity and cell number of each of two clusters was calculated for single imaged positions (corresponding to single siRNA transfections). The median signal intensity of the internalizing cells was multiplied to the number of internalizing cells and divided by the total cell count in each well. This ratio was normalized against the median of the negative controls on each cell array by subtracting the median of the negative controls from each well and dividing the result through the median absolute deviation (MAD) of the negative controls (equation 2).

$$z = \frac{\text{median(well)} - \text{median(negative control)}}{\text{MAD(negative control)}} \quad [2]$$

Replicate measurements were summarized by taking the median. Z=±1 was selected as a threshold for determining hit siRNAs. The cell arrays, on which positive controls average did not reach the threshold were excluded from analysis. After all the quality control steps, 5 to 8 replicates remained for 95% of tested siRNAs. One-sided, one-sample Welch's t-test was used to compute significance values for each well where more than three replicates were available.

3.12. Co-localization analysis

Co-localization of the intracellular structures in the multi-channeled single confocal plane images was done in Image J (NIH, (Abramoff et al., 2004). For this, the images background was subtracted using rolling ball algorithm (radius 30px), the Gaussian Blur filter was appllied (σ = 0,75 – 1 μm), the channels were thresholded to detect individual vesicles and binarized. The resulting binary images were processed using "Image calculator" function ("AND" operator) for pairwise comparison of two images and creating the additional image on which only co-localizing pixels were present (co-localization image). The number and parameters of particles present in binarized channel images and co-localization image were analyzed by "Particle analysis" plugin. To exclude both the small stuctures and co-localization due to high density of vesicles (which is likely to occur in the perinuclear area) only particles of the size 10-100 μm^2 were taken into account. The number of particles in the co-localization image was divided by the number of particles of one of the channels of original image to get the percentage of co-localizing particles.

3.13. Bioinformatic analysis of screening results

Results of the screenings were compared to other high-throughput assays and gene annotations: genes from the adhesome (Zaidel-Bar et al., 2007), TFR and EGFR endocytosis (Collinet et al., 2010) (genes from phenotypic groups 1, 2, 12, 14 considered as affecting exclusively TFR endocytosis; groups 9, 10, 11, 13 as affecting exclusively EGFR endocytosis; groups 3, 4, 5, 6, 7, 8 as affecting both), MHC II antigen presentation machinery (Paul et al., 2011), focal adhesion formation (Winograd-Katz et al., 2009), mitosis (Neumann et al., 2010), epithelial cell migration (Simpson et al., 2009) (hits of medium and high confidence), integrin association (Humphries et al., 2009), β1-integrin activity (Pellinen et al, 2012) and binding to β1-integrin tail (Böttcher et al., 2012). Networks were prepared based on protein-protein interaction collected in SysBiomics (which contain data from the main PPI databases: DIP, BIND and HPRD). Network analysis was performed in Cytoscape 2.8.3.

4. Results

4.1. Fluorescent-microscopy-based α2 integrin internalization assay

To address the regulation of α2β1 integrin endocytosis, we developed the fluorescent-microscopy-based assay that would allow to visualize and quantify internalized integrin the individual cells and across the large cells population. Antibody-based assays are widely used to address internalization of various surface proteins, including different integrins and MHCII (Gao et al., 2000; Powelka et al., 2004; Ma et al., 2012). In such assays, antibodies targeting the extracellular epitope of the protein of interest are incubated with living cells (often upon block of internalization, i.e. by incubation at low temperature), then the excess of antibody is washed away, and the cells are returned to permissive conditions for internalization of protein-antibody complexes. The cells can be further subjected to immunostaining to visualize the internalized protein-antibody complex.

We have set such an experiment to to visualize and quantify α2β1 integrin endocytosis in human cells upon various conditions. For experimentation we selected HeLa cell line, that expresses high levels of endogenous α2β1 integrin (Fleming et al., 2010). Monoclonal antibody targeting extracellular I-domain of α2 chain of α2β1 heterodimer was used (Jokinen et al., 2010). As integrin α2 chain forms a unique heterodimer with β1 integrin (Hynes, 1992, 2002), we could follow a particular heterodimer by labeling the α2 chain only.

Integrin signalling and trafficking was shown to cross-talk with signalling of growth factors (Riikonen et al., 1995), therefore we performed the integrin internalization

assays in the cells after 14h of serum starvation to avoid interference of growth factors present in the full medium. To visualize α2 integrin endocytosis, live HeLa cells were incubated with P1E6 antibody for 50 min on ice **(Figure R.1A),** briefly washed with ice-cold medium, then supplied with pre-warmed serum-free medium and returned to 37°C for various periods of time **(Figure R.1B)**.

By staining of total and surface α2-integrin bound primary antibodies, we found that after 1h about 70% of antibody-bound integrin could be found on the PM, indicating only partial endocytosis and/or efficient recycling of α2 integrin. (**Figure R.1B, R.2B**). The assesment of α2 integrin endocytosis by parallel staining of surface and total integrin nevertheless presents a problem of dealing with two sets of samples per condition, and low dynamic range. Therefore we used short stripping with acidic buffer to remove the surface bound P1E6 antibodies after integrin internlization. This allowed to specifically visualize the pool of internalized α2 integrin (**Figure R.1C, R.2A**) by staining with secondary antibodies.

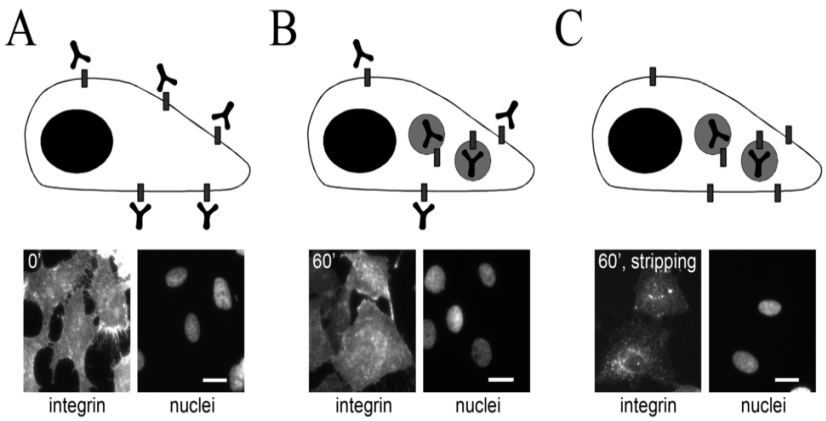

Figure R.1. Antibody-based integrin endocytosis assay. (A) Cells are incubated with antibodies against extracellular domain of integrin α2 on ice for 50 min. (B) The antibody-bound integrin α2 is allowed to get internalized over 60 min. (C) The surface-bound antibody is stripped and only internalized antibody-bound integrin is visualized. Scale bar = 20μm

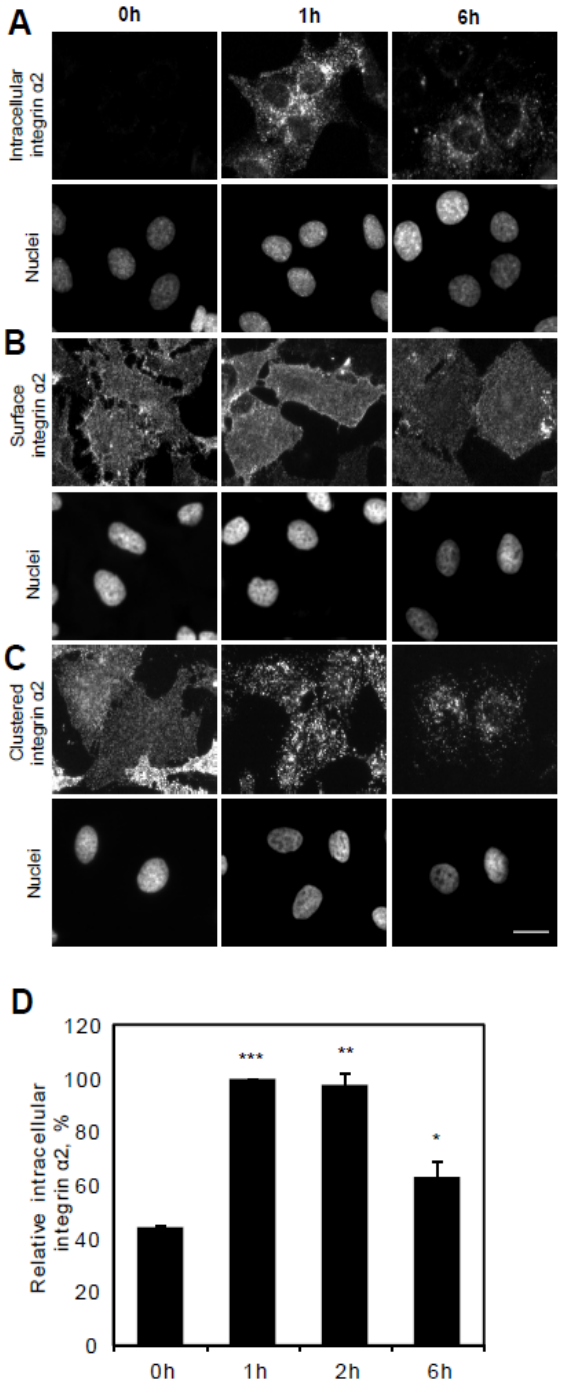

Figure R.2 Endogenous integrin α2 in HeLa cells changes internalization features when clustered by treatment with primary anti-integrin α2 and secondary antibodies. (A) Internalized non-clustered integrin α2. The integrin labelling was performed as described in (A), but prior fixation and staining the antibodies remaining on the surface were stripped, the cells were fixed, permeabilized, and stained with secondary Alexa647-coupled antibodies for internalized integrin alpha2. (B) Surface non-clustered integrin α2. Surface integrin alpha2 in HeLa cells was labeled on ice with primary anti-integrin alpha2 antibody (P1E6), left for internalization for 1h, and 6h, or fixed immediately after labelling (0h). Integrin alpha2 remaining on the cells surface was stained with secondary Alexa647-coupled antibodies. (C) Clustered integrin α2. Surface integrin alpha2 in HeLa cells was labeled on ice with primary anti-integrin alpha2 antibody (P1E6) followed by clustering with secondary Alexa647-coupled antibodies and left for internalization for 1h, and 6h, or fixed immediately after labelling (0h). Scale bar 20 µm (D) Quantification of the mean intensity of clustered integrin alpha2 after 6h of internalization. Bars represent mean intensity of clustered integrin (normalized to 1h of internalization) from three independent experiments ± SEM. (* $p < 0{,}05$, statistical significance measured with Student's t test, unpaired, unequal variance).

For assessment of the amount of internalized integrin, we used automated wide-field fluorescent microscopy, as it combines precise measurements of individual cell phenotypes with possibility of high-throughput experimentation and analysis (Tuckwell et al., 1995).

Allowing the cells to internalize antibody-bound α2 integrin, we saw that, after 1h

of internalization, intracellular pool of α2 integrin reached steady-state and persisted till two hours (**Figure R.2D**). At prolonged incubation of 6h and 24h integrin-specific fluorescence was strongly diminished (63% and 30% of 1h, correspondingly), most likely indicating degradation of antibody-bound integrin. Therefore, it was decided to perform futher measurements of intracellular α2 integrin after 1h of internalization. Additionally, attempts to establish comparable protocols for internalization of integrin β1 and integrin a5 chains were made. For this we used the stimulating anti-β1 antibodies (clone TS2/16) and anti-a5 antibodies (clone NKI-SAM1). However, application of different acidic stripping methods (30s stripping with acetic acid buffer at RT, stripping with glycine buffer for 30s at RT or 5 min on ice) did not result in complete removal of surface-bound antibodies (data not shown), therefore these protocols were not used.

4.1.1. Quantification of microscopy-based integrin internalization assay

The quantitative assessment of integrin α2 internalization was done by automated fluorescence microsopy and single cell-based analysis (Erfle et al., 2011). The individual cells were identified through the nuclei counterstaining, and the mean integrin-specific fluorescence was measured in the perinuclear area. We found high variety of internalization level of the endogenous α2 integrin in HeLa cells (**Figure R.3**), that is, most likely due to variability of integrin expression, which can have 10-folds difference between 10% of dimmest and brightest cells stained for total α2 integrin (data not shown). Comparable difference between the 10% of brightest and dimmest cells was observed for internalized integrin (**Figure R.3A**).

We found that about 60% of the cells contain low amount of intracellular integrin after 1h of internalization even in negative control siRNA

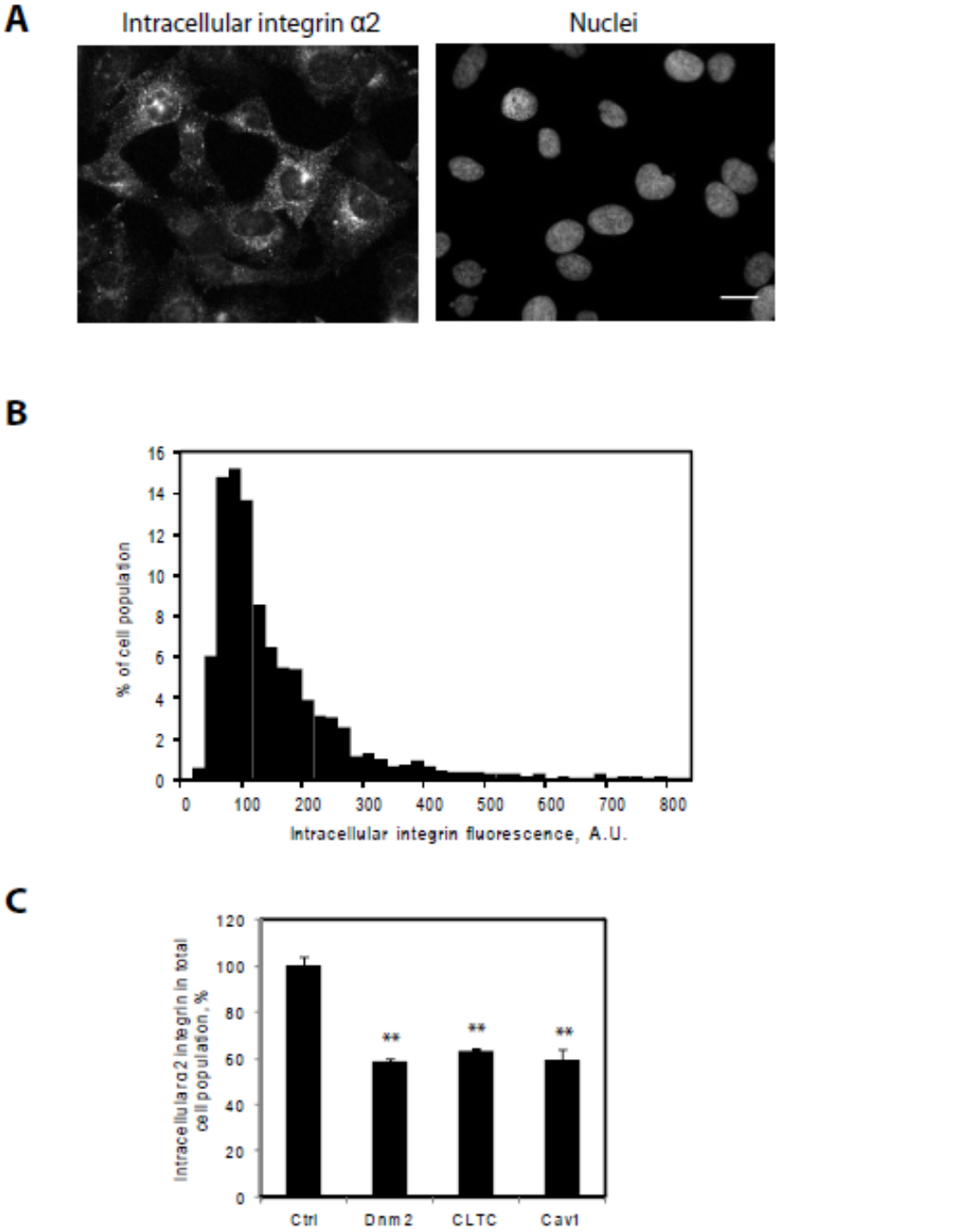

Figure R.3. Cell-to-cell variability in integrin internalization (A) Immunostaining of total integrin α2 chain in HeLa cells. Scale bar = 20 µm. (B) Distribution of integrin α2 staining intensity over the whole cell population in a single representative experiment. (C) Quantification of internalized integrin mean intensity after transfection with control siRNAs. Integrin internalization assay was performed 48 h after transfection with negative control (siCTRL) and integrin endocytosis effectors (CLTC, DNM2 and CAV1) siRNAs. Bars represent mean fluorescent intensity of intracellular integrin α2 after 1h of internalization from three independent experiments ± SEM. **p< 0,01; statistical significance measured with Student's t test, unpaired, unequal variance.

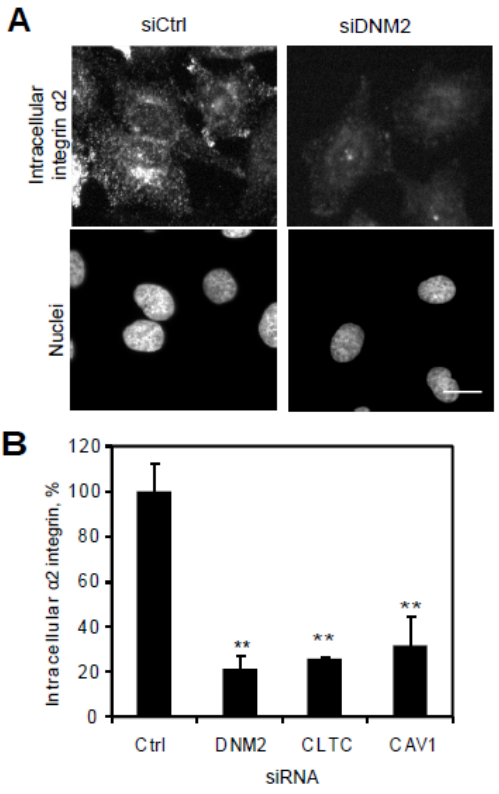

Figure R.4..Integrin α2 endocytosis in HeLa cells is inhibited by treatment by siRNAs targeting dynamin 2, clathrin heavy chain, and caveolin-1. (A) HeLa cells were transfected with corresponding siRNAs, and after 48h integrin internalization assay was performed. Treatment with siRNAs targeting dynamin2, CLTC and caveolin-1 led to strong reduction of integrin internalization (representative example of cells transfected with Dnm2 and negative control siRNAs downregulation is shown). Scale bar = 20 µm. (B) Quantification of the siRNA effect on integrin internalization. Bars represent mean endocytosis rate normalized to control siRNA-treated cells from two independent experiments ± SEM. (**p< 0,01; statistical significance measured with Student's t test, unpaired, unequal variance).

treatment (**Figure R3.B**) or no treatment (data not shown). Presence of a big unresponsive population of cells smooths the observed effects on integrin internalization. Having to deal with that, we have probed several quantification procedures to obtain a good dynamic range of our assay. By averaging the internalized α2 integrin intensity of all cells in a population, only 40% difference to control could be measured when dynamin-2, caveolin 1 and CLTC were down-regulated for 48h (**Figure** R3.**C**). Therefore we established the quantification procedure that would take into consideration a varying proportion of cells that demonstrate internalization of α2 integrin, defined by an experiment-dependent threshold (***see Methods***), Using this method, we could score the inhibition of α2 integrin internalization from 70% (upon down-regulation of caveolin-1) to 80% (down-regulation of dynamin-2) (**Figure R.4B**). As strong inhibition calculated by this method corresponds well to the little appearance of intracellular α2 integrin under

these conditions (**Figure R.4B**), we have used this method for the majority of experiments in this study unless stated otherwise.

4.2. Clustered and non-clustered integrin α2β1 pursues different internalization routes

We have initially tested whether endocytic trafficking of endogenous α2β1 in HeLa cells shares similar features as to SAOS cells over-expressing α2 (Rintanen et al., 2011; Karjalainen et al., 2008; Upla et al., 2004). At first, clustering of α2 integrin was induced by sequential addition of the primary and secondary antibodies (see Methods). Similar to the data obtained by Rintanen et al., 2011 in SAOS-α2β1 cells, an efficient accumulation of endogenous α2 integrin in cytoplasmic punctuate structures was observed after 1h of incubation (**Figure R.2C**). After longer incubation times α2 integrin was accumulated at a juxtanuclear area, and a reduction up to 70% of clustered α2 integrin was recorded after prolonged incubation times up to 6h (**Figure R.2C**). Hardly any PM localization of the clustered integrin α2 was observed already after 1h of incubation. In contrast, after internalization of non-clustered α2 integrin (Erfle et al., 2011), the larger fraction of α2 integrin was localized at PM even at longer incubation times (**Figure R2.B**). Thus, trafficking of clustered and non-clustered endogenous integrin α2 strongly resembles that of the over-expressed protein (Rintanen et al., 2012).

4.2.1. Non-clustered α2 integrin traffics through Rab5-Rab4-Rab11 positive pathway

To test, to which internalization pathway non-clustered α2 integrin is driven, we have co-localized it after 1h with Rab5, Rab4, Rab7, and Rab11, determinants of early,

late, and recycling endosomes, correspondigly (reviewed in (Stenmark., 2009)

It has previously been shown, that internalized β1 integrin, the binding partner of α2, is delivered to the Rab5- and EEA1-positive early endosomes, and then targeted to recycling via Rab4 or Rab11 endosomes (Powelka et al., 2004; Pellinen et al., 2006; Arjonen et al., 2012), or, in case of activated or ligand-bound β1, to Rab7-dependent pathway, from which it can be driven to degradation (Arjonen et al., 2012) or recycle back to PM .

After 1h of internalization we found substantial co-localization between integrin and overexpressed Rab5, Rab4 and Rab11 in the perinuclear area and peripheral vesicles (**Figure R.5A, B, C)**. The co-localization between α2 integrin and GFP-Rab7 was considerably less even in the perinuclear area and almost absent at the cell periphery (**Figure 5D, insert**). As the density of the vesicles in the perinuclear area of the cells is very high, we have used only peripheral vesicles to quantify co-localization and found 60% and 68 % of integrin-containing vesicles on the cell periphery co-localized with Rab5 and Rab11, correspondigly. Co-localization of internalized integrin with over-expressed Rab4 was 32%, but it is worthy to mention, that almost all the Rab4-positive vesicles (95% of them) contained internalized α2 integrin. Only 6% of peripheral integrin-containing vesicles were Rab7-positive. This would indicate that non-clustered α2 integrin following internalization via Rab5-dependent pathway, is driven to Rab11-positive recycling compartment. In contrary, clustered integrin α2 in SAOS-α2β1 cells bypassed conventional clathrin-dependent internalization route and did not co-localize with early endosomal marker EEA1 and Rab7 (Rintanen et al., 2012).

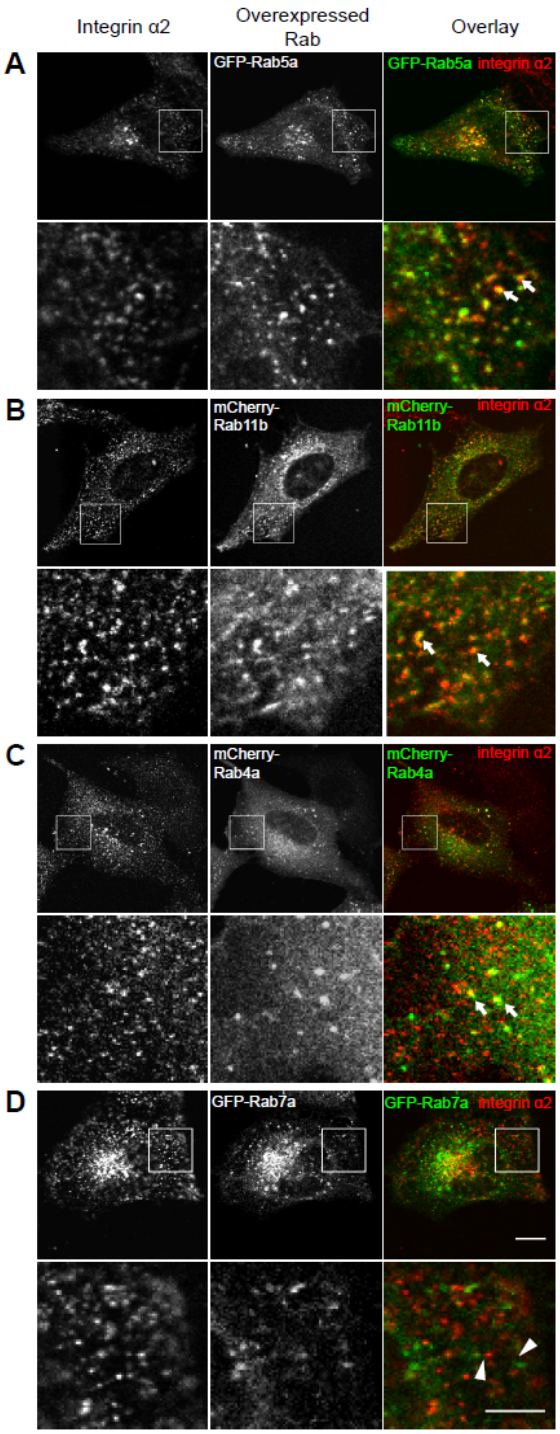

Figure R.5. Internalized integrin α2 co-localizes with Rab5a, Rab11b, and Rab4a but not Rab7a in HeLa cells. Co-localization with overexpressed GFP-Rab5 (A), mCherry-Rab11 (B), mCherry-Rab4a (C) and GFP-Rab7 (D) (green) and internalized integrin α2 (red) after 1h of internalization. Integrin α2 endocytosis assay was performed as described 30h after transfection of HeLa cells with corresponding plasmids. Confocal single sections are presented. Arrows point to internalized integrin co-localizing with corresponding Rab, arrowheads indicate the structures where no co-localization occures. Scale bar = 10 μm. Scale bar of inserts = 5 μm.

Thus, we demonstrate that, internalized non-clustered α2 integrin is driven to conventional Rab5-, Rab4- and Rab11-positive endocytic recycling route, and, to lesser

extent, to Rab7-positive late endocytic compartment, in contrast to published data on trafficking of clustered α2 integrin.

4.1.2. Endocytosis of non-clustered α2 integrin depends on clathrin and caveolin

Previous studies demonstrated by RNAi and proteomic analysis, that endocytosis of β1 integrin chain, the binding partner of α2 integrin, occurs via clathrin/Dab2-dependent (Chao and Kunz, 2009; Teckchandani et al., 2009, 2012) and caveolin-dependent pathways (Shi & Sottile, 2008). However, internalization of over-expressed clustered and ligand-bound α2 integrin was demostrated by fluorescence and electron microscopy to occur via caveolae (Upla et al., 2004; Rintanen et al., 2012). It was not inhibited by overexpression of clathrin adaptror AP180 C-terminus or dominant-negative EPS15, and did not co-localize with early endosomal maker EEA1 (Upla et al., 2004; Rintanen et al., 2012). Yet, hardly any data are available about the endocytic trafficking of non-clustered α2 integrin. Localization of internalized α2 integrin to Rab5-positive endosomes suggests that canonical clathrin-dependent (Bucci et al., 1992) or caveolin-dependent (Lucas et al., 2004) internalization pathways are involved. To test that, we have down-regulated the key components of clathrin-dependent and caveolae-dependent pathways (clathrin heavy chain (CLTC) and caveolin-1) and dynamin-2 which is required for both pathways (Hansen and Nichols, 2009, Doherty and McMahon, 2009, Parton and Simons, 2007, Caswell and Norman, 2006), and assessed integrin α2 endocytosis under these conditions (**Figure R.4**).

The siRNAs used for this experiment were previously published (Gregory, Hale, Perlmutter, & Houghton, 2012; Spoden et al., 2008) and were validated by manufacturer

(reported downregulation efficiency was more than 80% by qRT-PCR). We have confirmed downregulation of target transcripts by more than 50% by RT-PCR. Down-regulation of each of the the three components of endocytosis machinery resulted in strong reduction of intracellular integrin upon 1h of internalization compared to control, seemingly reflecting block in early steps of endocytosis (**Figure R.3**).

Thus we demonstrated that, in agreement to previously published data on trafficking of β1 integrin (Chao & Kunz, 2009; Teckchandani et al., 2009; Shi & Sottile, 2008), down-regulation of clathrin heavy chain, dynamin-2, and caveolin 1 strongly inhibits internalization of non-clustered α2 integrin, indicating that both clathrin-dependent and caveolae-dependent pathways are involved. Dependency on clathrin divercifies the internalization pathway of non-clustered α2 integrin from that of clustered α2.

4.3. Fluorescent microscopy-based RNAi screen identifies potential regulators of non-clustered α2 integrin endocytic trafficking

1084 siRNAs targeting 386 genes with known or predicted roles in cytoskeleton organization were chosen for the analysis (**Appendix 1,** RNAi library provided by R. Pepperkok, EMBL, Heidelberg**).** The gene set included 94 molecular motors (44 kinesins, 13 dynein subunits, and 37 myosins), 28 small Ras and Rho GTPases, 53 GAPs and 62 GEFs of these GTPases, 41 actin-associated and 14 microtubule-associated proteins, 34 kinases and 9 phosphatases, 5 different integrin β chains and, 23 scaffold and adaptor proteins as well as a number of proteins belonging to diverse functional groups. Products of 81 genes in this library were previously shown to constitute integrin adhesome (Zaidel-Bar et al., 2007).

For the primary screening we used format of reverse transfection in cell array

(Erfle et al., 2007) (see **Methods).** The cell arrays had a surface coating with fibronectin and gelatin. Unlike the collagen I (as demonstrated in (Ritanen et al., 2012), gelatine coating did not induce clustering of integrin and allowed us to follow the internalization of non-clustered α2 integrin. In agreement to our experiments with dynamin2 downregulation in cells grown on plastic, treatment with siRNAs targeting Dnm2 inhibited α2 integrin internalization by 80% in cells grown on mixture of gelatin and fibronectin (data not shown). Similar to the experiments in the conditions of the direct transfection, siRNAs targeting CLTC, dynamin-2 and caveolin-1 induced a strong inhibition of α2 integrin trafficking on cell arrays (**Appendix II**), therefore, they were used as the positive controls.

Data collection was made on a wide-field microscope and intracellular integrin α2-specific fluorescence was quantified for single cells. After a thorough quality control including manual image quality check, cell densities and performance of the controls, five to eight replicas were statistically analysed for 95% of all siRNAs. The statistical analysis was performed by B. Knapp (AG Kaderali, BioQuant, Heidelberg, currently TU Dresden, Dresden). As manual setting of the threshold to separate cells with high and low internalization levels of α2 integrin for every experiment could be biased depending on the experimenter, a mixture model has been applied to separate cells with the high and low internalization levels of α2 integrin automatically (see ***Methods***). For each siRNA spot the percentage of internalizing cells as well as amount of internalized integrin (as defined by mean intensity of the internalized integrin staining) was calculated.

Z-scores (see ***Methods***) of individual siRNAs on the labtek were normalized to the z-score of negative controls averaged across each labtek. Thus average z-score of scrambled negative control siRNA was 0 (**Figure R.6A**). CLTC siRNA had average z-

score -1,54 (p-value = 7,45E-29), and dynamin 2 siRNA had -1.49 (p-value = 2,24E-13) (**Figure R.6A, B**). Caveolin 1 siRNA had weaker effect (average z-score -1,14, p-value = 0,01). In our screen we have considered as primary hits those siRNAs, which had absolute z-scores > 1. Positive z-scores indicate acceleration and negative z-scores show inhibition of integrin α2 trafficking (Table 2). The gene was considered a primary hit in case one out of two tested siRNAs gave an effect on integrin internalization (for pool of genes tested with 2 siRNAs per gene), or if at least 2 siRNAs (for pool of genes tested with 4 or 6 siNRAs) or at least 3 siRNAs had consistent effect on integrin internalization. Altoghether we found 122 primary hits: 115 inhibitors and 7 accelerators of integrin internalization (**Appendix II**). Out of them, 28 were targeted by 2 or more siRNAs. In total, 31 primary hits had individual siRNAs absolute z-scores more than 1,5. Interestingly, the positive control siRNAs that in preliminary experiments in multi-well plates were blocking the integrin endocytosis by 70-80% (**Figure R.3**), in the screening have performed rather like mild inhibitors (z scores = -1,54; - 1,49; -1,14 for DNM2, CLTC, and caveolin 1 correspondingly) with number of hit siRNAs outperforming them (**Appendix II**).Among the screening hits we found molecules that could be expected to have an effect on integrin internalization: i.e. knockdown of integrin β1 (hit with 4 out of 12 siRNAs, z = -1.32), actin (1 out for 2 siRNAs, z = -1,11), β-tubulin (2 out of 2 siRNAs, z= -1,08) inhibited the α2 internalization, and ASAP1 (GAP for Arf6 involved in recycling of β1 integrin (Onodera et al., 2012) accelerated it (z = 2,26). The top scoring primary hits included trafficking regulator ARF1 (z= -1,62) (Gu, 2000), regulator of β1 integrin endocytosis syndecan 4 (Bass et al., 2011) (z=-1,78), actin-binding RhoA GAP ARHGAP6 (z=-2,11) (Prakash et al., 2000), kinesin molecular motor KIF18a (z = -1,76) (Mayr et al., 2007) (**Figure R.6B**).

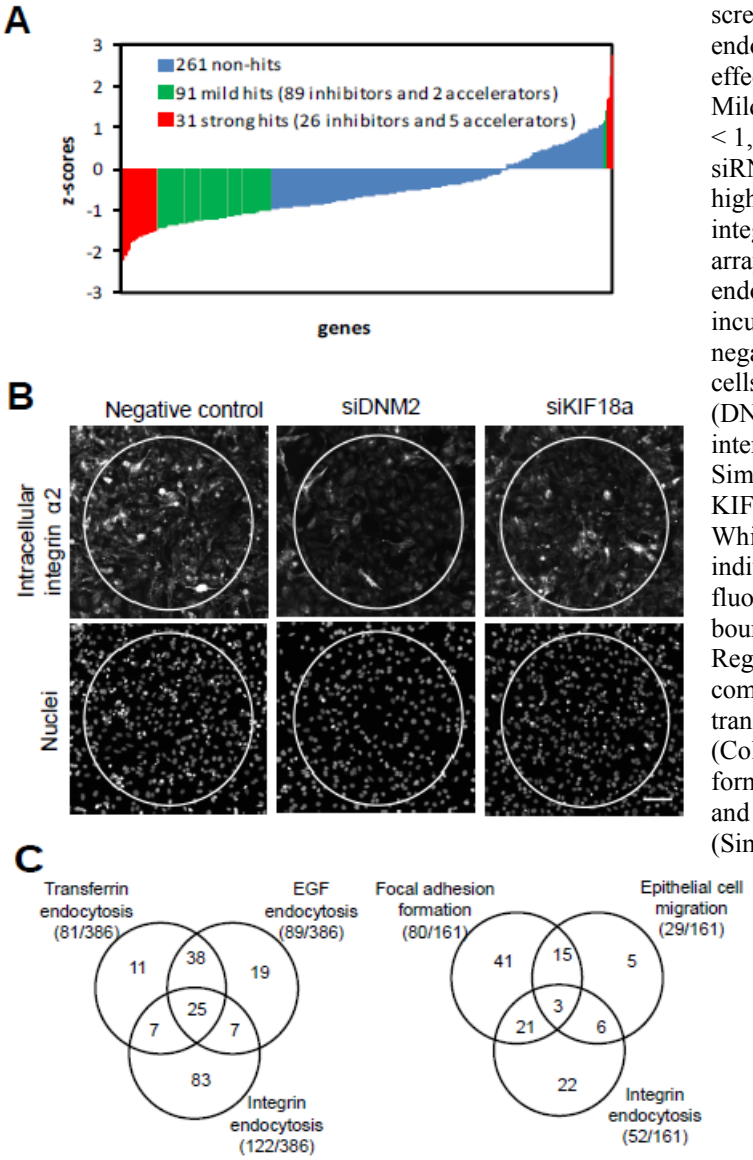

Figure R.6. Results of the primary screening for regulators of integrin α2 endocytosis (A) Hit z-scores of the most effective siRNAs tested in the screening. Mild hit siRNAs (1 < absolute z-scores < 1,5) are highlighted in green. Strong hit siRNAs (absolute z-scores > 1,5) are highlighted in red. (B) Examples of integrin α2 endocytosis assay on cell arrays. No changes in integrin α2 endocytosis was observed following incubation of HeLa cells with the negative control (left column). Treating cells with siRNA targeting dynamin2 (DNM2) induced a strong reduction of internalised integrin α2 (middle column). Similar effect was observed when KIF18a was down-regulated for 48h. White outlines represent spots containing individual siRNAs. Integrin α2 specific fluorescence was measured within spot boundaries. Scale bar = 100 µm. (C) Regulators of integrin endocytosis in comparison to known regulators of transferrin and EGF endocytosis (Collinet et al., 2010), focal adhesion formation (Winograd-Katz et al., 2009) and epithelial cell migration regulators (Simpson et al., 2008).

4.3.1. Bioinformatic analysis of the primary screening results

The following bioinformatic analysis was performed in collaboration with D. Matelska (AG Russell, BioQuant, Heidelberg).

Having classified the screening hits to functional classes according to Gene Ontology (GO) terms, we did not find enrichment of any functional groups among the screening hits compared to the screened library. This is likely a consequence of thorough preselection of genes included in the library.

We compared the results of our screening with other RNAi screening data. One of the most interesting datasets for us was the recent genome-wide screening for regulators of transferrin (Tf) and epidermal growth factor (EGF) endocytosis (Collinet et al., 2010). The list of our hits overlaps by 32% with the published endocytosis regulators (39 of our hits were found as the regulators of either Tf or EGF endocytosis). We have found that among the genes used in our screening, the hit rate was comparable with the screening of (Collinet et al., 2010). The latter collected 81 Tf endocytosis regualators (21%) and 89 EGF endocytosis regulators (23%) out of 386 cytoskeleton-associated genes, whereas our screening found 122 potential integrin endocytosis regulators (32%) (**Figure R6.C**). Majority of overlapping hits (25 of 39) regulated all three endocytic cargoes. Minority of hits was shared between integrin endocytosis and specific regulators of Tf or EGF endocytosis (7 regulators overlap with either Tf and EGF endocytosis). Hits overlapping with Tf endocytosis regulators (FARP2, PTPN1, MYH1, SDC4, VAV2, CAV1, DYNC1H1, ARHGEF2) include 2 integrin-interacting proteins (SDC4 and and 2 molecular motors. Regulators of EGF endocytosis include 4 kinases (LIMK2, PIK3CA, ROCK1, PRKCA) all of which, except LIMK2 are known as components of adhesome (as listed in (Zaidel-Bar et al., 2007)), GTPase-regulating protein CHN2, actin-binding protein LASP1, and integrin-interacting protein CIB. The observation that majority of integrin endocytosis regulators are specific for integrin, and the other big group overlaps with regulators of both Tf and EGF, suggests that regulators of integrin endocytosis either belong to general internalization machinery (shared by transferrin, EGF, integrin and, perhaps, other endocytic cargos) or integrin specific, but not more related to either transferrin or EGF internalization pathways.

Next, we have compared our results with the recent RNAi screenings for

regulators of focal adhesion formation (Winograd-Katz et al., 2009) and cell migration (Simpson et al., 2008), both using the same RNAi library (**Figure R6.C**). These screenings were not genome-wide, but covered three different libraries: kinases, phosphatases, and genes involved in cell adhesion and migration or suspected to play role in these processes. The gene set had a substantial overlap of 161 genes with our cytoskeleton-associated genes library. Out of these, 52 (33% of the libraries overlap subset) were found as primary hits in our integrin endocytosis screening. 80 (50% of the subset) genes were found as hits in the focal adhesion formation screening, and 24 of them were also found as integrin endocytosis regulators (including CDC42, PTEN, PTPN11). In the migration screening the hit rate was smaller: 29 of 161 tested genes (18%) were found as hits. Out of them 9 primary hits overlapped with the hits of integrin endocytosis screening (including CRK, ITGB1, LIMS1, ASAP1). Thus, both in case of focal adhesion formation screening and cell migration screening, the overlap with integrin endocytosis screening hits was about 30%. 3 hits were common between all the three screenings: ACTB, CRK, , and kinase PRKCA. Yet, 12 of these 26 proteins are known as components of integrin adhesome.

Recent biochemical screening for integrin α2 interactions (Uematsu et al., 2011) showed only minor overlap of 2 hits with our screening hits (MYH9 and GAPDH) This study was performed by nano-flow liquid chromatography/mass-spectrometry of the proteins co-precipitated with Flag-tagged α2 integrin chain over-expressed in HT1080 fibrosarcoma cells and identified in total 70 proteins only two of which were previously known as components of adhesome (Zaidel-Bar et al., 2007). Also, this study did not identify trafficking regulator Rab21 binding to integrin α2 (Pellinen et al., 2006), indicating that used methodology might not suit to detect trafficking-related interactions

which can be transient and or indirect. On the contrary, quantitative mass-spectrometry analysis of the protein complexes associated with ligand-bound integrins α5β1 and a4b1 in human leukemia K562 cell line stably expressing a4 integrin (Humphries et al., 2009), identified number of molecules that were subsequently found as regulators of integrin α2 endocytosis The total overlap between this hits study and the integrin endocytosis screening hits presented 19 proteins, including ARF1, dynamin 2, PTPN11 and molecular motors MYH9, KIF2C, and DYNC1H1.

Recent genome-wide RNAi screening for regulators of MHCII antigen presentation (Paul et al., 2011) had only a minor overlap with our screening results (3 hits in common). In the context of intracellular traffic, MHCII antigen presentation depends on the anterograde trafficking from ER to the PM (Bénaroch et al., 1995; Neefjes et al., 1990). High overlap of our screening results with the endocytotic regulators, and small overlap with the potential biosynthetic regulators indicates specificity of our screening to the endocytic pathway.

As no genome-wide or large-scale data are available for the cell entry of viruses using integrin α2 as a co-receptor (i.e. EV1 (Bergelson, Shepley, Chan, Hemler, & Finberg, 1992)or rotavirus (Fleming, Graham, Takada, & Coulson, 2010). Only negligible overlaps was obtained upon comparison of our screening with the genome-wide analyses of HIV (Brass et al., 2008) or HCV (Q. Li et al., 2009) replication, as neither of these viruses uses α2β1 integrin as a co-receptor.

The analysis of the primary screening results revealed a vast overlap of the screening hits with the published datasets of regulators of relevant processes: endocytosis, focal adhesion formation, and cell migration. On the contrary, the datasets on the processes not related directly to integrin endocytosis (i.e. anterograde trafficking or

MHCII or the entry of viruses which do not use integrin α2 as a co-receptor) was only minor. This indicates reliability of screening results even at the level of primary screening.

4.3.2. Validation

For the validation of primary screening results and further analysis we selected 26 primary hits (1/5 of primary hits).

Altogether 15 kinesins were identified as hits in the primary screening (KIF1B, KIF2A, KIF2C, KIF3B, KIF3C, KIF6, KIF15, KIF16B, KIF18A, KIF19, KIF22, KIF23, KIF24, KIF26A, KIF26B). For hit kinesins represented by two isoforms, one isoform was futher analyzed. Thus, in total 12 were tested in the validation assays (KIF1B, KIF2A, KIF3B, KIF6, KIF15, KIF16B, KIF18A, KIF19, KIF22, KIF23, KIF24, KIF26B). For 3 of them (KIF6, KIF19, KIF26b) we did not find evidence of expression in HeLa cells (**Appendix III**). Validation assays were performed using 2 siRNAs from Ambion similar to the ones used in the primary screening, and two additional siRNAs from Qiagen. In most cases siRNAs were functional and led to knockdown of target transcript by 40-90%. For KIF22 the knockdown induced by siRNAs was minimal (about 10%), and, therefore, the effect on integrin α2 endocytosis, induced by siRNA treatment, was considered unspecific. Hit genes were considered as effectors of α2 integrin endocytosis if knockdown of corresponding transcripts with at least two siRNAs consistently resulted in more than 40% difference in integrin endocytosis compared to negative control siRNA when measured in multiwell format. The summarized results of the validation assays are presented in **Table R.1**.

Table R.1. Validated screening hits

Gene name	Integrin endocytosis[1]	Integrin expression [1]	Cell count [1]
Negative control siRNA	100	100	100
DNM2	27,2 ± 6,63	82,45 ± 13,77	98,56 ± 6,88
ARF1[2]	49,17 ± 7,43	99,11 ± 17,67	99,16 ± 37,85
ABL2	52,78 ± 9,94	56,84 ± 4,49	72,05 ± 18,6
ARHGAP6	42,03 ± 6,35	43,14 ± 4,33	75,59 ± 7,24
ITGB1	7,38 ± 3,4	54,12 ± 7,1	99,93 ± 17,32
KIF15[2]	27,8 ± 4,45	96,5 ± 2,3	106,44 ± 7,75
KIF18A	51,12 ± 9,54	97,64 ± 16,74	98,64 ± 31,44
KIF23	25,4 ± 6,36	92,69 ± 33,23	49,11 ± 22,74
Myo1A	36.43 ± 17.79	64,72 ± 4.04	126,42 ± 46,71
NF2	35,59 ± 3,1	95,89 ± 13,64	85,77 ± 3,19
PTPN11	39,11 ± 5,19	76,83 ± 3,72	66,07 ± 28,1

Data show results of validation experiments for selected representative siRNA. for the whole set of data see Appendix V.
[1] Values show % of control ± SEM
[2] Hits affecting trafficking, but not total integrin expression are highlighted in green.

Among the 9 hit kinesins expression of which in HeLa cells we detected, 3 were validated as inhibitors of integrin α2 endocytosis: KIF15, KIF18a, KIF23. None of them was previously associated with endocytic trafficking, and only one recent screening for regulators of VSV-G secretion (Simpson et al., 2012) identified them as hits. Given that only few primary hit kinesins were previously associated with intracellular trafficking pathways, and many known traffic-regulating kinesins didn't show up in the screening, we additionally tested 17 known traffic-related kinesins in the validation screening together with the primary screening hits (listed in **Appendix IV**). For them, 2 Qiagen siRNAs per gene were tested, and, if one ot them had effect, 2 siRNAs from Ambion, same as used in

the primary screening. We have confirmed expression of 13 genes from this group in HeLa. From them, only KIF13a, that was previously known to organize endocytic recycling (Delevoye et al., 2009), showed effect on integrin endocytosis under conditions of validation screening (only with additional siRNAs but not with siRNAs used in the primary screening, therefore it couldn't be considered a hit).

As our library included variety of other molecules among which were 81 components of integrin adhesome, in the validation assays we also tested heterogenous group of 14 other hits, that were targeted by at least 2 different siRNAs in the primary screening. Among these were 8 adhesome components. For these genes 2 additional siRNAs from Qiagen were ordered, and hit was considered validated, if at least one of them gave effect on α2 integrin endocytosis, matching the primary screening effect. 7 genes of this group were validated,. Among these hits ARF1 was a general trafficking regulator known to recruit components of COPI coat on the transport vesicles in biosynthetic and endocytic pathways (Gu and Gruenberg, 2000; Kumari and Mayor, 2008). It was shown to mediate paxillin recruitment to the focal adesion sites and to potentiate RhoA-dependent actin stress fibers assembly (Norman et al., 1998). Another 5 molecules were known as integrin adhesome components or their interactors (ARF1, ABL2, ITGB1, NF2, PTPN11) (Zaidel-Bar, Itzkovitz, Ma'ayan, Iyengar, & Geiger, 2007). Neurofibromin 2 (NF2) directly interacts with integrin beta1 (Cabodi et al., 2010; Obremski et al., 1998). Non-receptor protein tyrosine phosphatase 11 (PTPN11) is a component of adhesome, where it dephosphorilates paxillin (Ren et al., 2004). Two validated hits regulates actin cytoskeleton organization via RhoA pathway: kinase ABL2, which was shown to be upstream mediator of RhoA (Shimizu et al., 2008) and and RhoA GAP ARHGAP6 (Prakash et al., 2000). Finally, MYO1A one is an actin-based molecular

motor involved in membrane movement along the actin cytoskeleton in enterocyte microvili and formation of lumenal vesicles in the interstine (Mooseker and Coleman, 1989; McConnell et al., 2009). Downregulation of all the listed hits, was inhibiting α2 integrin endocytosis by more than 40%.

Thus we could reproduce the primary screening result for 10 of the 23 expressed genes (43%) tested in the validation assays.

4.3.3. Expression of α2 integrin is affected by knockdown of number of hits

Given the fact, that knockdown of integrin β1 strongly inhibited integrin α2 endocytosis, and integrin α2 chain have previously been shown to be transcriptionally co-regulated with β1 integrin (Heino et al., 1989), we asked ourselves, if the decreased amount of internalised integrin can be due to downregulation of total α2 integrin resulting from knockdown of some genes selected for validation. To discriminate between the hits affecting integrin trafficking specifically and those influencing integrin expression, we stained for total α2 integrin upon hits knockdown**.** For 5 validated hits alterations in α2 integrin trafficking did not coincide with alterations in α2 expression: ARF1, NF2, KIF15, KIF18a, KIF23 (the difference was less than 25% compared to the negative control) (Table R.1, highlighted green). Yet, number of other genes tested in validation dramatically reduced or increased integrin expression in the cells, and in many cases it coincided with the effect on amount of internalized integrin (**Figure R.7, Appendix IV**). To resolve the other cases and show if the decrease of internalized integrin amount was due to blockage in trafficking machinery or only due to decrease of surface integrin, or both, more direct measurements of integrin endocytosis would be required.

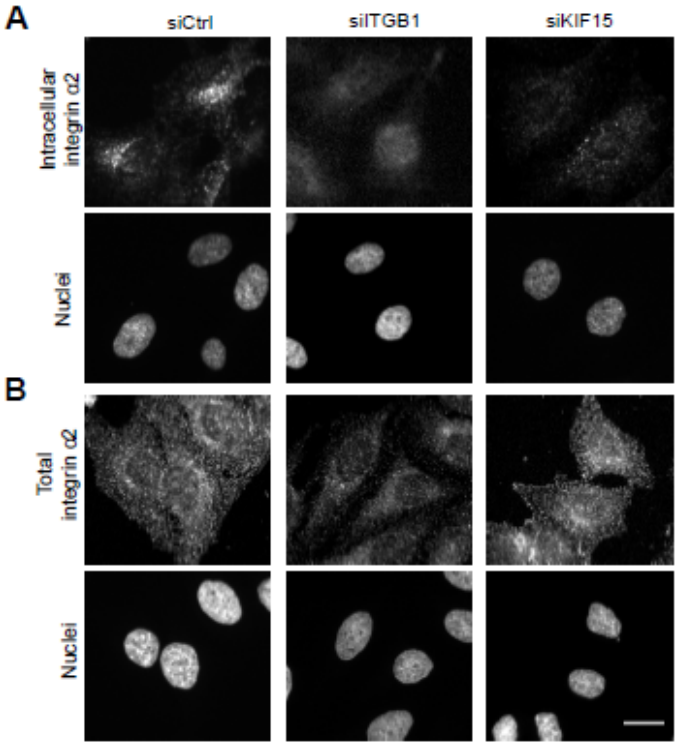

Figure R.7. Fig.5. Integrin endocytosis rate correlates with level of integrin expression for number of hits. Representative examples of siRNA effect of selected hits on integrin endocytosis and expression is shown: knockdown of KIF13a reduces both integrin internalization and expression, whereas knockdown of KIF15 inhibits only integrin α2 internalization, buut not expression. (A) Examples of integrin α2 endocytosis and expression stainings in HeLa cells. Cells were seeded on multiwell plates and transfected next day. 48h after transfection integrin endocytosis assay was performed. (B) Corresponding total integrin α2 expression staining examples. For measurement of integrin expression cells were fixed, permeabilized and stained for total integrin. SiRNAs affecting endocytosis but not expression were selected as trafficking hits. Bar 20 µm.

4.3.4. Endocytosis and expression of α2 integrin does not depend on local cell densities

All the three validated kinesin hits were known to play role in mitosis. KIF15 is involved in mitotic spindle organization (Tanenbaum et al., 2009; Vanneste et al., 2009) . KIF18a regulates chromosome congression in mitosis (Mayr et al., 2007). KIF23 is required for cytokinesis (Zhu et al., 2005). Two latter kinesins were also found as hits in the recent screening for mitosis regulators (Neumann et al., 2010). Question is, if this can be due to block in cell cycle progression, or a secondary effect resulting from lower cell

densities after knockdown of mitotic machinery, as, according to published data, local cell densities can influence internalization of other endocytic cargoes, namely tranferrin and EGF (Snijder et al., 2009).

To answer this question, we tested correlation of integrin α2 expression or integrin traffic with local cell densities to find out, it there could be a dependency (such as was shown for endocytosis of transferrin and EGF) (Snijder et al., 2009). Local cell densities were estimated from the coordinates of individual nuclei localizing to the same or neighbouring 15x15 μm position on the image (as described in (Knapp et al., 2011)). We could find no or little correlation neither of integrin expression nor integrin endocytosis with local cell densities (data not shown). Correlation coefficient between mean intensity of internalised α2 integrin per cell and the local cell density of the environment this cell belonged was -0,05± 0,03 for negative control siRNAs and -0,05± 0,02 for positive control siRNA targeting DNM2. For some individual siRNAs greater correlation was found, but it never exceeded 0,15. The same was true for integrin expression level of individual cells.

Selection of 15 kinesins, known or expected to be involved in traffic, included genes that have known mitotic function: KIF11 (Blangy et al., 1995; Kolluet al., 2009) and KIFC1 (Zhu et al., 2011). We have shown that KIF11 and KIFC1 had no effect on integrin internalization (101,8 ± 11,8 and 102,3 ± 25,4% of control, respectively), although knockdown of KIF11 led to dramatic decrease of cell counts per imaged position (50,8 ± 14,7% of control) (**Appendix IV**), as expected given its role in mitosis. This suggests that the inhibition of integrin endocytosis by hit kinesins involved in mitosis is independent of their mitotic function.

4.4. KIF15 is a novel regulator of membrane trafficking

In the validation screening KIF15 knockdown resulted in a strong inhibition of α2 integrin endocytosis. Unlike the other kinesin hits of our screening, KIF15 was not identified in the Mitocheck project (Neumann et al., 2010) as a master regulator of mitosis, which agrees with the knowledge that its function in maintenance of bipolar mitotic spindle is redundant with Eg5(KIF11) (Tanenbaum et al., 2009; Vanneste et al., 2009) .

However, it was also shown that rat KIF15 can have function beyond mitosis, as it is expressed in postmitotic neurons (Snijder et al., 2009), where it can contribute to the microtubule stability and microtubules-actin interactions (Neumann et al., 2010). We decided to further investigate the interphase role of KIF15 that could explain the strong inhibition of α2 integrin endocytosis upon its knockdown (**Table R.1**).

4.4.1. KIF15 specifically regulates α2 integrin internalization

To assess the specicity of KIF15 effect on integrin α2 endocytosis, we first confirmed KIF15 knockdown on the protein level and found that 48h after transfection with siRNAs KIF15 was downregulated by at least 75% (**Figure R.8A, C**).

Next, we attempted to rescue it by overexpression of siRNA-resistant murine KIF15 tagged with GFP (GFP-mKIF15) (Tanenbaum et al., 2009) in the background of control of KIF15 siRNAs transfection. Murine and KIF15 shares 86% identity at protein level. GFP-mKIF15 localized similar to the endogenous human KIF15 and could rescue the mitotic phenotype of human KIF15 knockdown, as demonstrated by (Tanenbaum et al., 2009).

According to our observations, GFP-mKIF15 localized mostly in the cytoplasm,

but, occasionally, to PM, cytoplasmic punctate structures and to the microtubules (although the latter two phenotypes were not predominant) (**Figure R. 9**).

The overexpression level of GFP-mKIF15 construct was reported to be close to endogenous (Tanenbaum et al., 2009), and the comparable -3,3-fold KIF15 overexpression we saw upon overexpression of GFP-mKIF15 (**Figure R.8B, D**).

To rescue the phenotype of KIF15 knockdown we have downregulated human KIF15 with siRNAs 48 hours before integrin endocytosis assay, and overexpressed GFP-mKIF15 or cytoplasmic eGFP 30h before the assay. To score the results of resque experiment, the total cells population was binned according to the GFP fluorescence intensity per cell. We found that overexpression of GFP-mKIF15 led to dose-dependent increase of internalized α2 integrin. Therefore only cells with high level of GFP-mKIF15 expression was taken for analysis. For overexpression of cytoplasmic eGFP, that was used as a negative control, the total cell population was taken into account, as it had no dose-dependent effect on integrin α2 internalization.

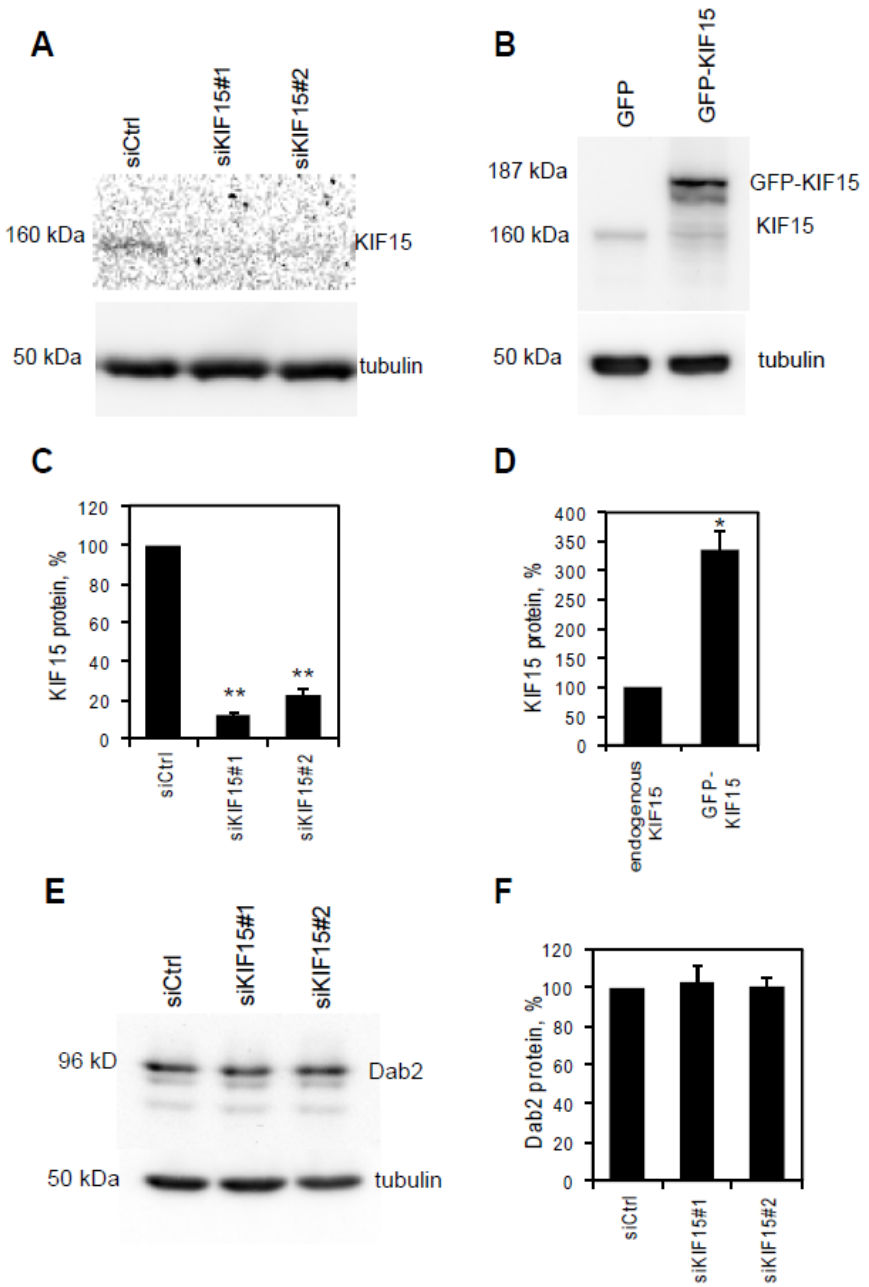

Figure R.8. Efiiciency of KIF15 knockdown and over-expression (A)HeLa cells were transfected with corresponding siRNAs for 48 hours and lysed. The amount of KIF15 in the whole-cell lysate was determined by protein gel blot. Efficiency of KIF15 down-regulation by RNAi (A, C) ectopic over-expression (B, D) , and effect of KIF15 down-regulation on Dab2 expression (E, F) in HeLa cells. Whole cell lysates were collected following 48h after siRNAs treatment and following 24h after transfection with cDNA encoding a full-length GFP-tagged KIF15. α-tubulin was used as a loading control for all experiments. The expression levels of endogenous KIF15 after treatment with the respective siRNAs (A, C) were normalized to the expression level of KIF15 when cells were treated with the negative control. The over-expression level of ectopic GFP-tagged KIF15 was normalized to the expression level of the endogenous KIF15 in cells expressing GFP (B, D). Expression level of Dab2 upon KIF15 knock-down was normalized to the negative control siRNA treatment (E, F). Bars represent means of normalized expression and the error bars indicate s.e.m. derived from at least 3 independent experiments. *, p≤0,05, **, p≤0,01.

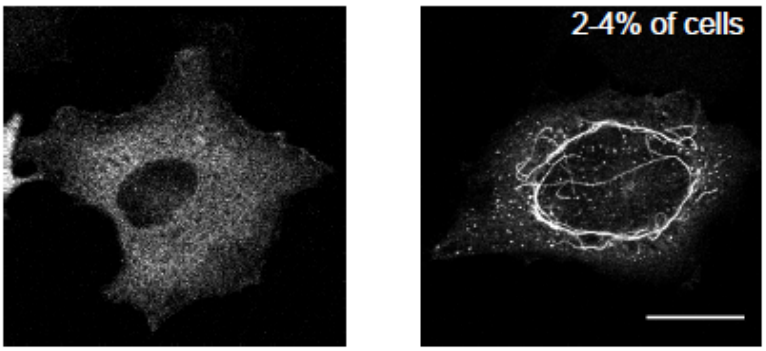

Figure R.9. Murine GFP-KIF15 localization in HeLa cells. Over-expressed KIF15 localizes predominantly in the cytoplasm (left), but also appears in speckles and microtubule-like pattern in 2-4% of cells (right).

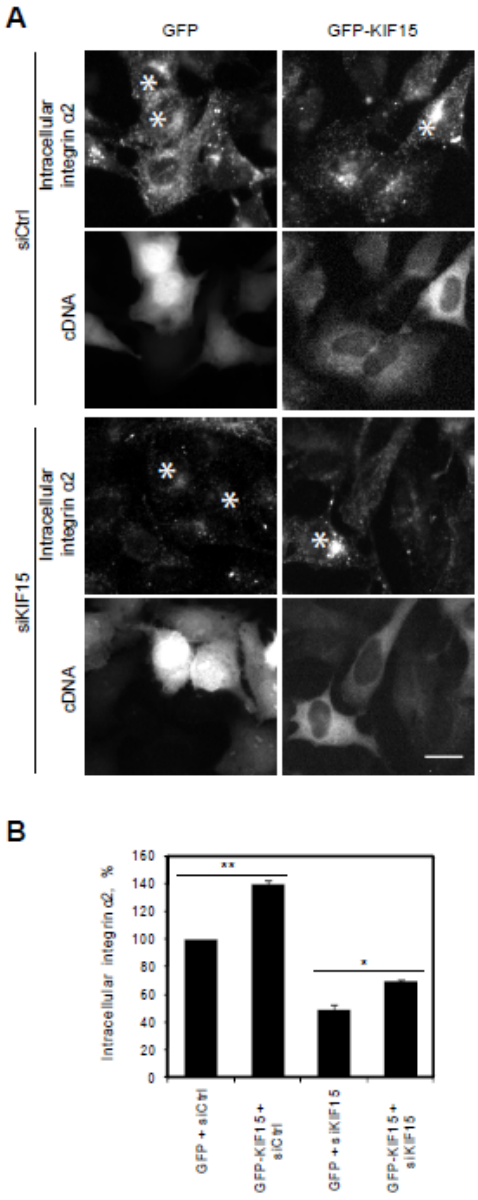

Figure R.10 Over-expression of murine GFP-KIF15 resques KIF15 knock-down in HeLa cells. (**A**) Knock-down of KIF15 prevents internalization of integrin α2 and this effect is lessened by the over-expression of GFP-tagged KIF15, but not GFP. Asterisks indicate cells expressing high levels of GFP and GFP-tagged KIF15. Scale bar = 20 µm. (**B**) Quantification of rescue of integrin α2 trafficking inhibition. Intracellular integrin α2 specific fluorescence is normalized to over-expression of GFP in the background of negative control transection Bars represent means of 3 endopendent experiments ±.SEM. *, p≤0,05.

We found that, comparable to the the KIF15 downregulation in the course of validation experiments, only 49,2 ± 3,1 % of α2 integrin endocytosis could be detected when cytoplasmic GFP was expressed upon KIF15 knockdown, compared to negative control siRNA. GFP-mKIF15 overexpression in the background of negative control siRNA treatment, on the contrary, increased amount of internalized α2 integrin to 139,3±3,1 %. Interestingly, internalized α2 integrin often tended to form accumulation in perinuclear area in the cells over-expressing GFP-mKIF15 (**Figure R.10A**). Over-exression of GFP-mKIF15 in the human KIF15 knockdown background restored internalization of α2 integrin to 69,5±1,0 % of control with similar integrin perinuclear accumulation in the strongly overexpressing cells (**Figure R.10A, B**).

To find out, which stage of α2 internalization was affected by KIF15 knock-down, we measured amount of internalized integrin at different timepoints upon KIF15 knock-down. In negative control treated cells the internalized α2 integrin could be detected as early as upon 5 min of internalization, and then was gradually increasing till reaching maximum after 60 min of internalization. On the other hand, KIF15 knockdown resulted in alsmost complete absence of internalized α2 integrin at 5 min of internalization. At 15, 30, and 45 min amount of internalized α2 integrin was at about 20% of coresponding time-point of the negative control (**Figure R.11A, D**). After 60 min, the amount of internlized integrin reached only 34% of control. In the cells internalizing α2 integrin upon KIF15 knock-down, the internalized integrin localized in similarly to the distribution in the negative control cells. Thus, lack of internalized α2 integrin in siKIF15-tranfected cells was due to block of early steps of integrin endocytosis.

Next, we have tested effect of KIF15 knock-down on the trafficking of other endocytic cargoes, namely tranferrin and EGF. In agreement to (Collinet et al., 2010),

knock-down of KIF15 did not affect early steps (5 and 10 min) of internalization of either cargo. Yet, the later steps of tranferrin endocytic trafficking were clearly affected by KIF15 knock-down. In contrast to internalized EGF, which is destined for degradation (Carpenter and Cohen, 1976), transferrin is recycled (Dickson et al., 1983). Re-appearance of fluorescently-bound transferrin on the plasma membrane of the control HeLa cells could be seen after 45 and 60 min of cells incubation with the ligand. KIF15 knock-down prevented transferrin from recycling (**Figure R.11B, E**). On the contrary, it induced a prominent clustering of internalized cargo in perinuclear region, presumably in recycling endosome. This is reflected by mean intensity of internalized cargo that is significantly increased by 25% after 60 min of internalization in siKIF15 treated cells compared to control.

For EGF, no difference could be observed also at all the measured time points (**Figure R.11C, F**).

4.4.2. KIF15 knock-down affects distribution of endocytic adaptor Dab2

The fact that KIF15 knock-down affects late steps of transferrin endocytic traffic, and the microtubule (+)-end directionality of the motor (Boleti et al., 1996), suggests, that KIF15 is involved in recycling of trafficking cargoes. Yet, its function is required for α2 integrin endocytosis at the very early steps. We hypothesized that KIF15 is required for membrane localization of some integrin entry factor. Several endocytosis adaptors required for entry of integrin, but not transferrin, are known. Dab2, Arh, and Numb have been shown to mediate β1 integrin recruitment to clathrin-coated pits (Teckchandani et al., 2009). It was demonstrated that among the numerous integrin β1 heterodimers, Dab2 regulates the endocytosis of integrins α2β1, α1β1, α3β1, but not α5 or αV (Teckchandani

et al., 2009, 2012).

Interestingly, it has already been demonstrated, that Dab2 is required for recycling of transferrin and other cargoes (Fu et al., 2012; Penheiter et al., 2010), and knock-down of Dab2 results in the intracellular accumulation of transferrin, similar as observed for knock-down of KIF15 **(Figure R.11B)**.

In HeLa cells Dab2 localizes predominantly to the PM in punctate structures, but also to the cytoplasmic structures **(Figure R12.A, D, negative control) .** First, we have tested, whether KIF15 would affect the PM localization of Dab2. For this we performed the TIRF imaging of the cells surface-labeled on ice with the antibody against α2 integrin (as in our regular integrin internalization assay), then fixed without integrin internalization and co-stained for Dab2 and surface α2. The samples were imaged by total internal reflection fluorescence (TIRF) microscopy and epifluorescence mode to discriminate between Dab2 localized directly below the PM (TIRF mode) and all the Dab2 below the PM, including the particles localizing to deeper in the cytoplasm. Co-localization of the imaged particles between TIRF and epifluorescence mode indicated that these particles localized to the PM. Alternatively, presence of the particle in the epifluorescence mode, but not in TIRF, would mean that the particle is located in the cytoplasm, but not at the PM. To ensure that the imaged cells were properly attached to the substrate, surface integrin α2 staining was also imaged in the TIRF mode and was used as a proof for the presence of PM in the focal plane.

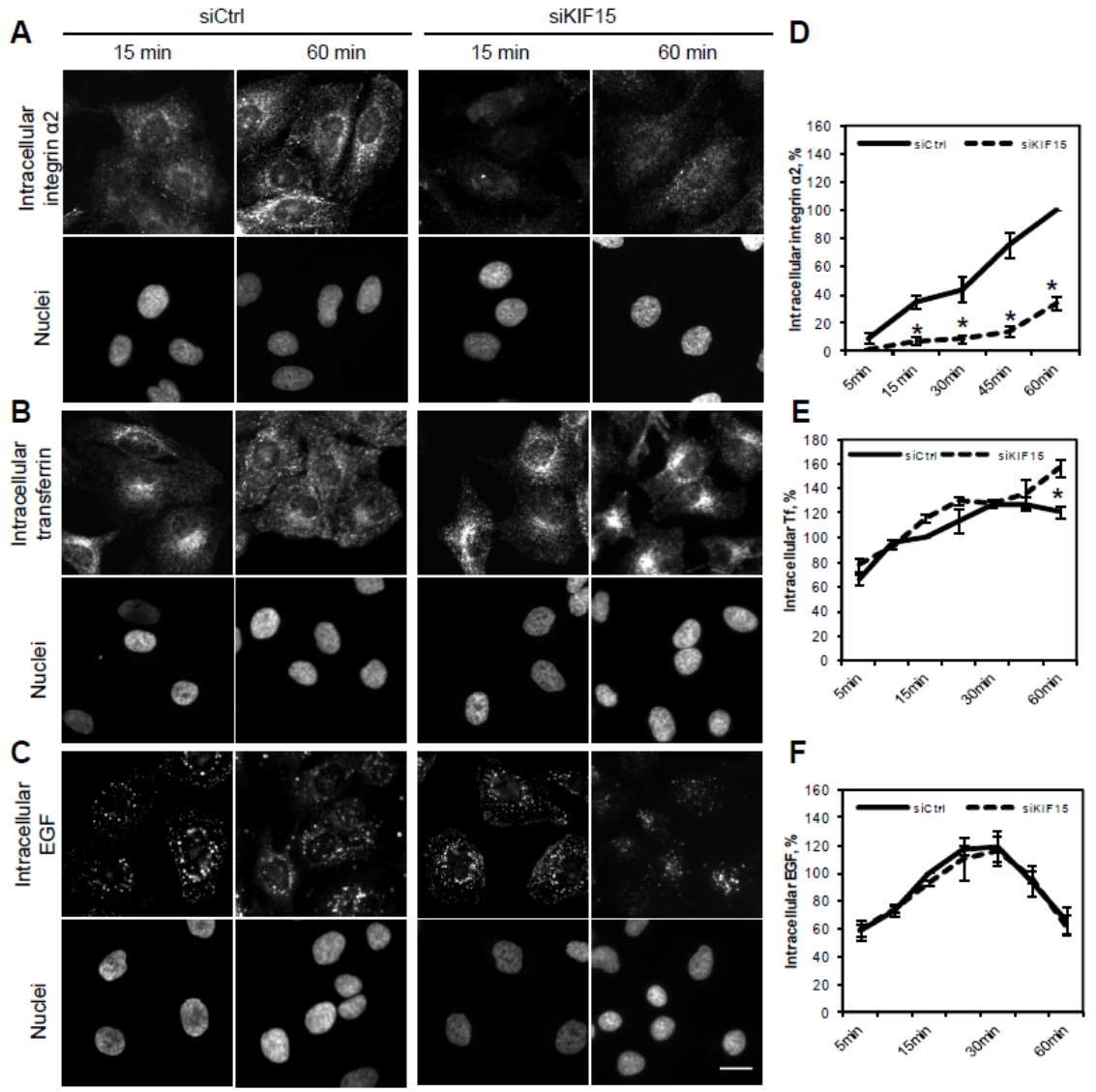

Fiure R.11. KIF15 is specifically required for internalization of non-clustered integrin α2. (A) Knockdown of KIF15 inhibits integrin internalization, but not transferrin (B, E) and EGF (C, F) internalization. HeLa cells were transfected with corresponding siRNAs for 48h, then the endocytosis assays were performed to asses tranferrin, EGF, and integrin internalization. Representative phenotypes resulting from transfection with of KIF15 siRNA and control siRNA are given. Scale bar = 20 μm. (D-F) Quantification of KIF15 knockdown effect on internalization of integrin, tranferrin, and EGF, correspondingly. Bars represent mean endocytosis rate (mean intensity of internalized ligand for transferrin and EGF) normalized to negative control siRNA at 60 min time-point (integrin) or 15 min time-point (transferrin and EGF) from three independent experiment ± SEM.

We found that knock-down of KIF15 led to partial loss of Dab2 from the PM (**Figure R.7, A-D**). In the negative control treated cells majority of the Dab2-structures detected in the epifluorescence mode, had a corresponding particle when imaged with TIRF, indicating it is PM associated. Yet, upon knock-down of KIF15, number of Dab2

particles that were seen only in the epifluorescence mode, but not in the TIRF mode, appeared (**Figure R.12, A, C** arrows), although the cells were arrached properly (data not shown). In agreement to that, the mean fluorescence of Dab2 imaged in TIRF mode was only 60% of the control in siKIF15-treated cells, whereas total Dab2-specific fluorescence (imaged in epifluorescence mode) was not changed significantly (**Figure R. 12B**). The latter was confirmed by the Western Blotting to detect total cellular Dab2 (**Figure R.8 E,F**), which showed that levels of Dab2 are unchanged by knock-down of KIF15. Interestingly, Dab2 and integrin α2 showed nearly no co-localization with each other at the PM.

Next, we asked ourselves, where the intracellular pool of Dab2 localized. As we assumed that Dab2 should be recycled in the KIF15-dependent manner, as tranferrin did, we expected to see it blocked in the perinuclear recycling compartment, as it was shown for transferrin after 60 min of internalization in KIF15 knockdown. In the negative control cells after 60 min of internalization transferrin was localized to the cytoplasm and the PM without any prominent accumulations. The same was true for Dab2 localization in the negative control. Interestingly, Dab2 and transferrin particles showed nearly no co-localization, indicating that the trafficking of Dab2 and transferrin occurs in the different carrier vesicles. KIF15 knock-down blocked transferrin in the perinuclear area, presumably corresponding to the perinuclear recycling compartment. The similar perinuclear accumulation of Dab2 could be observed in KIF15-depleted cells (**Figure R.12D**). It has to be mentioned, that, although all the cells reproducibly exhibited loss of the PM-associated Dab2, only fraction demonstrated clear perinuclear accumulation of Dab2. Most likely it indicates the dynamic association of Dab2 with the membrane, which can be lost upon internalization or when recycling to the PM is delayed.

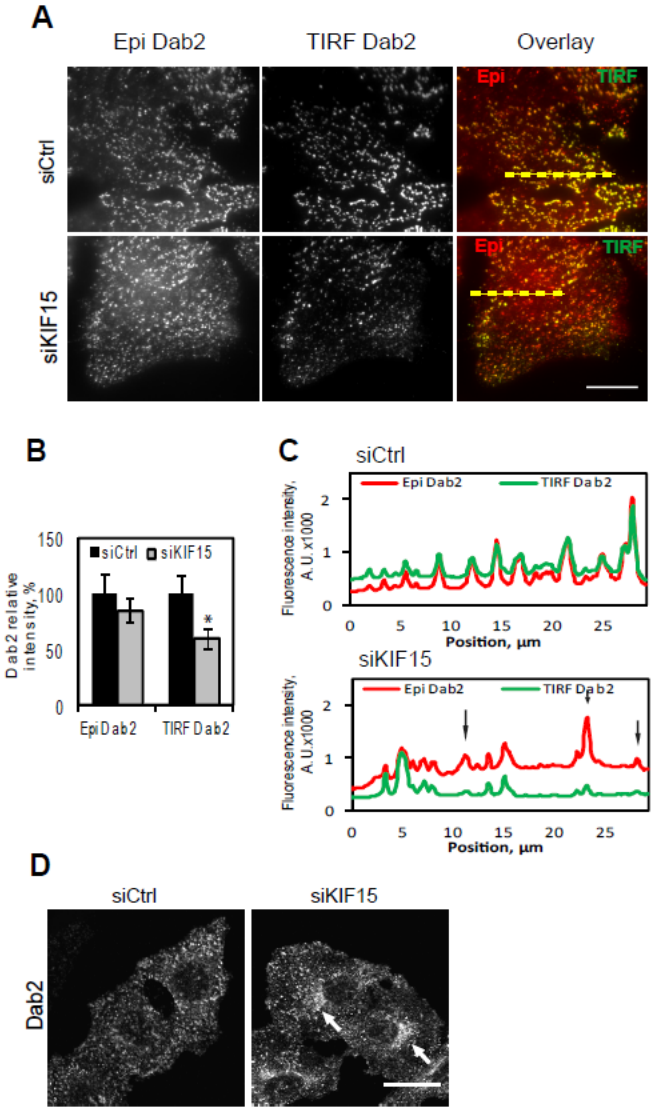

Figure R.12. Knock-down of KIF15 induces redistribution of Dab2. **(A)** Downregulation of KIF15 displaces Dab2 associated with the PM (TIRF imaging mode) to the intracellular space (epifluorescence imaging mode, Epi). Epifluorescence and TIRF images are overlaid and the position that was used for fluorescence intensity profile plotting is indicated by dashed line. **(B)** Fluorescence intensity profile plot, demonstrating strong correlation of the peaks, corresponding to Dab2 particles in the TIRF and Epi modes in control. Upon KIF15 knock-down number of Dab2 particles are displaced from the PM, as visulized by fluorescence peaks present in Epi mode only, but not in TIRF mode (arrows). **(C)** Quantification of mean fluorescent intensities of Dab2 staining imaged in epifluorescence and TIRF mode. N = 15 cells; error bars indicate SEM; *, p≤0,05. (D) KIF15 Knock-down leads to perinuclear accumulation of Dab2 (arrows). Single confocal sections taken 0,75 µm above the PM focal plane are shown. Scale bar = 20 µm.

4.4. Integrin endocytosis on micropatterned substrates

Integrin α2 internalization assay encounters of large cell-cell variability. To overcome this problem and improve the dynamic range of the assay, in each experiment we defined a population of strongly internalizing cells and disregard the others (see chapter **Quantification of integrin internalization assay**). This approach, although proved reliable, led to a gross loss of information, induced by omitting up to 70% of cells data. To improve the efficiency of the assay, we have attempted the biological normalization of cells by seeding them on micropatterns of certain shape and coating composition (Pitaval et al., 2011). The work on integrin internalization in the cells seeded on micropatterns was carried out in collaboration with Gintare Garbenciute (Vilnus University, Vilnus) and Philipp Albert (AG Schwarz, BioQuant, Heidelberg).

Indeed, seeding the cells on the micropatterned chips resulted in lower variability between cells. For the α2 integrin endocytosis assay performed in the cell culture the ratio between brightest and dimmest 10% of the cell population reached 10. Yet, after performing the similar assay on the micropatterned chips , the difference between the brightest and the dimmest cell was on average 4, varying negligibly across different shapes and conditions.

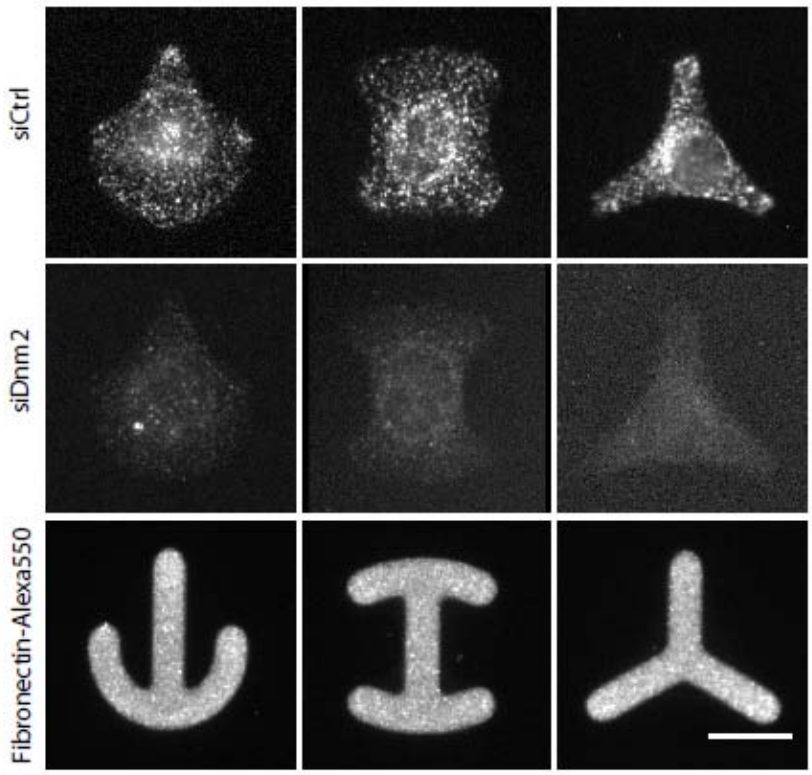

Figure R.13. Integrin α2 endocytosis on CYTOOchips is inhibited upon down-regulation of Dnm2 compared to control. HeLa cells were transfected 48h before the assay and seeded on micropatterned chip 16h before the assay. The integrin α2 endocytosis assay was performed as described in (***Methods***). The corresponding micropatterned coating is fibronectin-Alexa550 (lower panel). Representative cells are show. Scale bar = 20μm.

Next the effect of knock-down of DNM2 on integrin α2 internalization was tested in the cells seeded on the differently shaped and patterned fibronectin substrates. We could observe remarkable down-regulation of intracellular integrin α2 upon 1h of internalization, thereby reproducing the integrin internalization assay in the cell culture (**Figure R.13**). This method provides a possibility to address the intracellular distribution of internalized integrin in regard to cellular adhesion sites and elucidate the relation between the internalization of non-clustered integrin and cell motility (as the cells demonstrate different motility rates on the patterns of different sizes), however the methods for scoring of internalized integrin distribution and cell motility are yet to be developed.

5. Discussion

In this study we for the first time systematically address the regulation of non-clustered α2β1 integrin internalization. Although integrin α2β1 is a ubiquitously expressed receptor for collagen I, its intracellular traffic has barely been addressed. Here we describe the RNAi-based approach to identify novel regulators of integrin α2 internaliyation and further characterization of the novel trafficking regulator KIF15 in the context of integrin endocytosis.

5.1. Development of fluorescent-microscopy-based assay for analysis of non-clustered α2 integrin internalization

There are number of ways to address internalization of cellular cargo, that could be classified in two main groups: population-based methods (i.e. biotinylation or antibody-based assays followed by protein analysis, scoring the plate fluorescence in the assays quantifying internalization of the fluorescent ligands, or FACS) (exemplified in (Roberts et al., 2001)) or cell-based methods (direct imaging of internalizing cells) (Erfle et al., 2011). The cell-based methods provide numerous advantages, such as possibility to estimate cellular phenotypes and intracellular distribution of internalized protein of interest, cell-to-cell variability, possibility for high-throughput and high-content studies, even though they can be technically demanding.

In difference to the ligand-induced endocytosis, which is assayed in the transferrin, EGF or LDL internalization assays (Hanover et al., 1984; Dautry-Varsat, 1986; Li et al., 2001), integrins undergo internalization both in ligand-bound and ligand-free states. Several studies addressed the internalization of ligand-occupied integrins, and revealed that their trafficking follows the different pathways, predominantly degradative

(Lobert et al., 2010; Rintanen et al., 2011; Arjonen et al., 2012), compared to non-occupied integrins (Teckchandani et al., 2009; Arjonen et al., 2012). Nevertheless, endocytic and recycling trafficking of non-occupied integrins seem to be highly physiologically relevant in processes related to cell migration (Huttenlocher and Horwitz, 2011), and could even be a predominant mode of integrin trafficking, compared to integrin degradation (Lobert et al., 2010). It could be of particular importance for collagen I receptor integrin α2β1. Integrin α2β1 is ubiquitously expressed in different tissues. Although it is one of the most abundant integrins in keratinocytes (Watt, 2002), and is a prerequisite for keratinocytes binding to collagen I (Zhang et al., 2006), in the intact skin keratinocytes are never challenged with collagen I, which is a component of underlying dermal tissue, as they are separated from dermis by the basal membrane (Pilcher et al., 1998). Thus, trafficking of α2β1 when it is non-clustered and non-engaged with collagen I can be of higher physiological relevance, at least for epithelial cells, from which HeLa derived.

Therefore, this study focused on the ligand-independent trafficking of α2β1 integrin. The first step to address this was to establish appropriate quantitative cell-based integrin α2β1 internalization assay.

As α2 chain forms a unique heterodimer with β1 (Hynes, 1992), labeling α2 chain with the antibody targeting α2 extracellular domain, was enough to follow the fate of α2β1 integrin. This antibody labeled surface α2 integrin and could be internalized together with it similarly to other integrin internalization assays (Powelka et al., 2004; Gao et al., 2000). Yet, large fraction of α2 integrin remained at the cell surface even after long incubation time from 1 to 6h (**Figure R.1, R.2**). To readily visualize the integrin that was internalized, a short stripping (30-40s) with acidic buffer was used before fixation of

the cells, to remove the surface-bound antibodies (Erfle et al., 2011). After that the cells were permeabilized and the internalized antibody bound to integrin visualized with appropriate fluorescently-labeled secondary antibodies. When acidic surface stripping was applied in integrin α2 internalization assay performed with the primary antibodies MAB1950, it could completely prevent appearance of the integrin-specific surface fluorescence (**Figure R.2A, 0h**) , indicating that the surface-bound anti-integrin α2 antibody was properly removed. Yet, the acidic stripping, although used in several other published assays (Gao et al., 2000; Ma et al., 2012), was not a universal solution. Even at prolonged incubation time (up to 5 min on ice) it failed to completely remove the surface-bound anti-β1 integrin and anti-α5 integrin antibodies in the similar internalization assays. The reason for that could be the properties of the particular antibodies, but also the high abundance of the plasma membrane integrins β1 and α 5.

We demonstrate that trafficking of endogenous α2β1 in HeLa cells resembles the published data on the on α2β1 trafficking in Saos cells over-expressing α2, and endogenous β1 trafficking in various human cell lines. In Saos cells, over-expressing α2 integrin chain, α2β1 integrin, depending on clustering, can pursue distinct trafficking pathways. α2β1, clustered by binding to EV1 virus, antibodies, or its natural ligand collagen I, is redistributed to caveolae, internalized via clathrin-independent pathway, follows non-recycling route to integrin-specific MVBs, and then is degraded by calpains. In contrast, non-clustered α2β1 integrin is recycled to the PM (Rintanen et al., 2012). In agreement to that, trafficking of β1 not bound to ligand is also following recycling pathway through Rab11-positive compartment in HeLa cells (Powelka et al., 2004).

5.2. Internalization of non-clustered α2β1 requires clathrin and caveolin

The data on the entry routes of integrins in the endocytosis pathway are controversal. Number of studies have demonstrated that internalization of β1 integrins depends on clathrin and clathrin adaptors (Chao and Kunz, 2005; Teckchandani et al., 2009, 2012). However, there is also evidence of caveolin involvement in internalization of ligand-bound β1 (Shi and Sottile, 2008; Bass et al., 2011), and clustered α2 integrin (Upla et al., 2004; Karjalainen et al., 2008; Rintanen et al., 2012). Interestingly, it was also reported, that in the interstinal epithelial cells internalization of β1 integrin occurs through lipid rafts in clarhin-independent manner, but can be upregulated upon knock-down of caveolin1 or flotillins (Vassilieva et al., 2008).

To the best of our knowledge, the information about entry determinants of the non-clustered α2 is limited to the study of integrin-specific clathrin adaptor Dab2, knock-down of which resulted in entry block of β1 integrin and, consequently elevated surface level of β1 and several, but not all, corresponding a chains, α2 among them (Teckchandani et al., 2009). We tested the effect of knock-down of clathrin heavy chain (CLTC, the crucial component of clathrin-dependent endocytosis machinery), caveolin-1 (player of caveolin-dependent pathway), and dynamin-2 which is required for abscission of the newly formed endocytic vesicles in both clathrin-dependent and clathrin-independent pathways (Doherty and McMahon et al., 2009). To our surprise, both clathrin and caveolin were required for integrin endocytosis, as knock-down of either protein resulted in a strong inhibition (up to 75%) of integrin α2 internalization. Dynamin-2 knock-down, presumably blocking both pathways, resulted in integrin endocytosis inhibition of similar strength with but minor additive effect (up to 80% inhibition) (**Figure R.4**).

It is not clear, whether the requirement of both clathrin and caveolin for integrin internalization indicate redundancy of these pathways for integrin α2 endocytosis. There are data, suggesting that some endocytic cargoes can be rather promiscuous in the entry pathway, as was shown for EGF receptor, internalized via both clathrin- and caveolin-dependent pathways (Aguilar and Wendland, 2005; Schmidt-Glenewinkel et al., 2012). Yet, the nearly complete block of the integrin internalization upon either CLTC or caveolin-1 knock-down, suggests that the internplay of these pathways is more complicated and remains to be investigated. Although caveolin-1 have recently been identified as a transcriptional repressor of α5β1 integrin (Martin et al., 2009; Cosset et al., 2012), in our experiments it did not induce any prominent effect on the α2 cellular levels (**Appendix IV**). However, it cannot be excluded, that caveolin-dependent integrin signaling (Grande-García et al., 2007; Radel et al., 2007; Horiguchi et al., 2011) takes part in promoting clathrin-dependent integrin endocytosis.

5.3. Screening of cytoskeleton-associated proteins for involvement in integrin endocytosis

To find specific regulators of integrin α2β1 endocytosis, we performed RNAi screening of 386 genes predicted to regulate intracellular traffic and cytoskeleton organization (**Appendix I**). Number of them have previously been associated with intracellular traffic, i.e. were found as hits in the screenings for intracellular traffic regulators (Collinet et al., 2010; Paul et al., 2011, Simpson et al., 2012) or annotated with relevant GO terms (GO:0046907 intracellular transport; GO:0032386 regulation of intracellular transport; GO:0030705 cytoskeleton-dependent intracellular transport; GO:0030050 vesicle transport along actin filament; GO:0047496 vesicle transport along

microtubule; GO:0030139 endocytic vesicle; GO:0070382 exocytic vesicle). However, 197 of them have never been studied in this context.

By analyzing the amount of internalized integrin α2 in the cells, we identified 122 primary hits that were considered potential regulators of integrin α2 endocytosis. We deliberately set the threshold discriminating primary hits from non-hits relatively low (z=±1), as our aim was to identify the networks of regulators of α2 internalization, and not only few strongest hits. Another reason for high incidence of hits among the screened genes was the composition of screened library, which contained number of regulators of intracellular trafficking or integrin function, if to compare the number of hits across this set of genes in the screening for of endocytic regulators (Collinet et al., 2010) or focal adhesion formation regulators (Winograd-Katz et al., 2009) (**Figure R.6C**).

Comparing our hits with published relevant datasets (Collinet et al., 2010; Paul et al., 2011) we found that 39 (32%) of our our hits were also identified as regulators of Tf and EGF endocytosis (Collinet et al., 2010). Considerably less was the overlap with the screenings targeting for regulators of anterograde trafficking: 21 primary hits (17%) of the screening for VSV-G secretion regulators (Simpson et al., 2012), out of them 5 validated (4%), were in common with our primary screening, and only 3 (2%) of our hits were found as regulators of the MHCII presentation (Paul et al., 2011), This indicated that the trafficking regulators identified in our screening are specific for endocytic, but not secretory trafficking. Interestingly, the group of 83 hits that were identified as specific regulators of integrin α2 endocytosis, and did not affect transferrin or EGF endocytosis (according to Collinet et al., 2010) had no enrichment in the focal adhesion formation regulators (according to Winograd-Katz et al., 2009) and had impoverishment of the focal adhesion components compared to the whole screened

library (only 13% of α2 integrin-specific endocytic regulators were known as components of adhesome (Zaidel-Bar et al., 2007), while for the whole library the rate was 20%). This is well in agreement with the fact that our study addresses the endocytosis of integrin α2 that is non-clustered and not engaged in the focal adhesions under the experimental conditions (**Figure R.2**). Yet, number of proteins involved in the dynamics of focal adhesions (i.e. clustered and ligand-bound integrins) were also idenfied in our screening, as revealed by comparison with the screening for focal adhesion regulators (Winograd-Katz et al., 2009) (24 proteins in common) and epithelial cell migration regulators (Simpson et al., 2008) (9 proteins in common). This indicates a high level of cross-talk between regulation of clustered and non-clustered integrin.

Similarly, we found a prominent overlap with the hits of recent studies of interactors of ligand-bound a4b1 and α5β1, and non-ligand bound integrin β1 (Humphries et al., 2009; Böttcher et al., 2012). Nevertheless, mass-spectrometry of the proteins co-precipitated with Flag-tagged α2 integrin chain over-expressed in HT1080 fibrosarcoma cells (Uematsu et al., 2011) showed only minor overlap of 2 hits with our screening hits (MYH9 and GAPDH). This might indicate, that the interactions, regulating integrin trafficking are mostly transient or indirect. On the other hand, the study of Uematsu and colleagues identified only 70 proteins (compared to more than 400 identified in (Humphries et al., 2009) only two of which were previously known as components of adhesome (Zaidel-Bar et al., 2007).

In the screening we could identify not only individual hits, but the networks of proteins regulating integrin α2 endocytosis. For instance, NF2 was identified as a primary hit and validated as a strong inhibitors of integrin α2 internalization (**Appendix II, Table R.1**), and out of 7 proteins interacting with it, belonging to the screened library

(information from http://biomine.cigb.edu.cu/ sysbiomics/), 4 were found as hits in our screening. Out of them 3 were specific for integrin α2 endocytosis (ezrin, paxillin, and Ras GEF SOS1), and integrin β1 was also an effector of tranferrin and EGF endocytosis (Collinet et al., 2010). (**Figure D.1**)

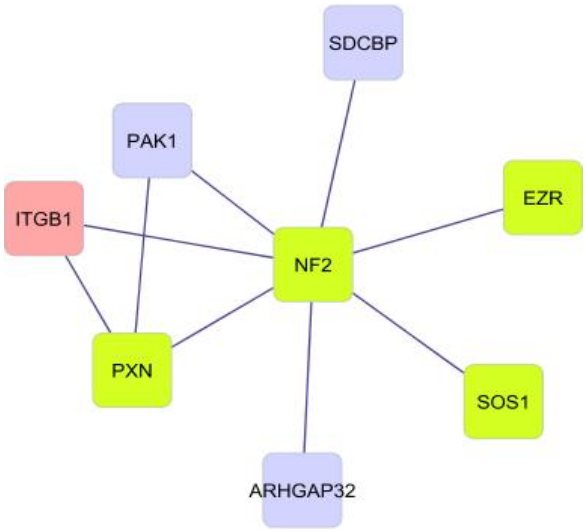

Figure D.1. Physical interactors of NF2 in the screened RNAi library. The proteins that were identified as integrin-specific regulators of integrin α2 endocytosis are highlighted in green; the regulators of both integrin α2, transferrin and EGF endocytosis in red; the proteins that did not regulate integrin α2 endocytosis are highlighted in blue. The network was based on the interaction data from SysBiomics database (http://biomine.cigb.edu.cu/sysbiomics/) and created by Cytoskape 2.8.3.

5.4. Validation of the primary screening results

To test the specificity of the primary screening results, we reproduced the results of the primary screening in the modified experimental conditions for three groups of proteins. One group comprised 14 functionally heterogeneous hits that were targeted by multiple siRNAs in the primary screening, the second one encompassed the 12 kinesin hits of the primary screening, additionally, we analyzed 17 traffic-related kinesins, that were not hits in the primary screening, which allowed us to estimate occurrence of false-negative results in the primary screening.

Altogether, the validation experiments verified the reliability of the screening results obtained with these cirteria: among the tested primary hits the validation rate was

43%, comparable to other RNAi screenings, using more stringent hit-calling criteria (51% in (Winograd-Katz et al., 2009) , 46% in (Neumann et al., 2010). Among 17 tested non-hits only one (KIF13A) had effect on integrin α2 endocytosis in the validation assays, and even this was with additional siRNAs, and not those used in the primary screening, and, most likely, this was due to down-regulation of total integrin α2 levels in the cell (**Appendix IV**). This indicates the reliability of the assignment of non-effector status as a screening result.

From the group of 14 hits, targeted by multiple siRNAs we could reproduce 7 in the validation assays. Yet, the testing of integrin α2 expression levels revealed that 5 hits from the first group of proteins can affect it. Among the effectors α2 of integrin expression, integrin β1 is long known to transcriptionally regulate corresponding alpha chains (Heino et al., 1989). The 3 other hits are involved in the regulation of RhoA-dependent actin organization and paxillin function: PTPN11 is required for paxillin dephosphorilation (Brown et al., 1998), kinase ABL2 is an upstream mediator of RhoA (Shimizu et al., 2008) and ARHGAP6 is a RhoA GAP (Prakash et al., 2000). The hits that affected integrin internalization but not expression were ARF1 (the regulator of COPI coat (Serafini et al., 1991), which was shown to mediate paxillin recruitment (Norman et al., 1998) and the component of the adhesome, integrin β1 binding protein NF2, which, has previously been implicated in the clearance of Notch, Patched, Smoothened and EGF receptor from the PM (McCartney and Fehon, 1996; Obremski et al., 1998; Stamenkovic and Yu, 2010). On the contrary, none of the validated kinesins had prominent effect on the integrin expression levels, indicating that their knock-down affects integrin trafficking only.

Next, we focused on kinesins because it is a prominent group of proteins which

contributes to specificity of intracellular trafficking, yet, the exhaustive analyzes of kinesins were mostly limited to their role in mitosis (Goshima and Vale, 2003, 2005; Tanenbaum et al., 2009; Zhu et al., 2005b; Neumann et al., 2010). On the contrary, there are only few datasets (coming from comprehensive genome-wide screenings) that could be used to analyze their traffic-related function(Collinet et al., 2010; (Paul et al., 2011; Simpson et al., 2012). So far only KIF1C is known to directly drive the integrin traffic (Theisen et al., 2012). Most of the tested hit kinesins (8 out of 12) in the primary screening were targeted by one out of two tested siRNAs, similar to most of our screening hits. Out of the 12 kinesin primary hits, that we took in the validation, for 9 we found evidence for expression in HeLa. From them, KIF15, KIF18A, and KIF23 had a profound inhibitory effect on integrin α2 internalization in the validation assays. The expression of integrin α2 remained unchanged in upon their knockdown.

Analysis of the primary hits that were not validated could provide an additional insight in the performance of the screening and particular hits. Several kinesin primary hits that were not validated, were represented by two isoforms (KIF26A, KIF26B, KIF3B, KIF3C , KIF2A, KIF2C). Having analyzed only one isoform of two, we might have encountered redundancy in their functions. The combinatorial knock-down of the isoforms would be required to resolve such cases. Why the primary screening conditions turned to be more sensitive for detection of these molecules, remains a question. One possible factor that could play a role was the presence of ECM coating in the primary screening. In this context especially interesting is the case of CRK, the integrin-interacting protein and component of integrin adhesome required for the formation of the focal adhesions (Wang et al., 1996; Winograd-Katz et al., 2009; Fathers et al., 2012), which was an α2 integrin internalization inhibitor under conditions of the primary

screening (**Appendix II**), but increased the integrin internalization in the validation assays (**Appendix IV**). Whether this was dependent on the availability of the ECM proteins is an open question.

All the three validated kinesin hits have never previously been associated with intracellular trafficking except of the recent report on the traffic of VSV-G protein (Simpson et al., 2012), in which KIF15 and KIF23 were validated as inhibitors of VSV-G secretion. On the contrary their mitotic function was well characterized. KIF18 and KIF23 were found as hits in the RNAi screening for mitotic regulators (Neumann et al., 2010). KIF18a is a crucial component in chromosome congression machinery (Mayr et al., 2007), and KIF23 is required for midbody formation and cytokinesis (Zhu et al., 2005a; Liu and Erikson, 2007). KIF15 was shown to cooperate with KIF11 (Eg5) in organization of bipolar mitotic spindles, although its function is dispensable when functional KIF11 is present (Tanenbaum et al., 2009; Vanneste et al., 2009). Yet, recently accumulated data indicate, that mitotic kinesins can have additional functions during interphase, as was demonstrated for KIF11 (Blangy et al., 1995; Bartoli et al., 2011; Falnikar et al., 2011; Collinet et al., 2010). Both KIF15 and KIF23, in addition to their roles in mitosis , function in postmitotic neurons. KIF23 supports dendrite formation (Sharp et al., 1997). KIF15 associates with microtubules in growing neurons and can contribute to the microtubule stability and microtubules-actin interactions and promote axonal branching (Buster et al., 2003; Liu et al., 2010).

KIF 15, KIF18a, and KIF23 all are microtubule (+)-end directed motors ((Nislow et al., 1992); Boleti et al., 1996; Mayr et al., 2007). The microtubular array in adherent non-polarized cells, including HeLa, is radial, with (-)-ends of the microtubules originating from cell center by centrosomes and (+)-ends growing towards cell periphery

(reviewed in Manneville and Manneville, 2006; Vinogradova et al., 2009). This suggests that (+)-end directed kinesins would be involved in the anterograde traffic and recycling of endocytic cargos towards PM, as was demonstrated for number of other kinesins i.e. for KIF16b or KIF5b (Hoepfner et al., 2005; Jaulin et al., 2007). Yet, for all the three validated hit kinesins we have observed strong inhibition of integrin endocytosis, which did not seem to result from the block in integrin recycling, but rather from perturbation of integrin internalization into the cell.

5.5. KIF15 is a novel regulator of membrane trafficking

To understand involvement of kinesins in integrin traffic, we have focused on KIF15, which was a strong inhibitor of integrin α2 endocytosis when downregulated, and, unlike KIF23, another strong inhibitor, did not affect cell proliferation. Human KIF15 belongs KIF15-subfamily of kinesin-12 family protein family (Miki et al., 2005), which is barely characterized. *Xenopus* ortholog of KIF15, that also has a role in maintanance of bipolar spindle in mitosis, was shown to be functional homodimeric microtubule (+)-end directed motor (Boleti, Karsenti, & Vernos, 1996; Wittmann, Boleti, Antony, Karsenti, & Vernos, 1998).

We confirmed the specificity of KIF15 effect on integrin α2 endocytosis by rescuing the knock-down phenotype with over-expression of siRNA-resistant murine KIF15 N-terminally fused to GFP, which was previously shown to completely rescue KIF15 mitotic phenotype (Tannenbaum et al., 2009). The over-expression of GFP-KIF15 in the background of endogenous KIF15 knock-down significantly increased the amount internalized integrin α2 endocytosis, although the rescue not complete (70% of control), which might possibly indicate the hindering of N-terminal motor domain function by

GFP-fusion (in contrast, the association of KIF15 to mitotic spindle depends on C-terminal leucine zipper (Tannenbaum et al., 2009).

Time-resolved integrin α2 endocytosis assay revealed that KIF15 knock-down results in inhibition of the early steps of integrin internalization. In agreement to that, upon over-expression of GFP-KIF15 we observed increase in intracellular integrin α2 after 5 min of internalizaition, and further accumulation of intracellular integrin after 60 min of internalization, which indicates that balance of integrin endocytosis and recycling is shifted towards endocytosis. However, directionality of the motor implies that its requirement in the early steps of integrin endocytosis is mediated by some additional factor.

KIF15 knock-down did not induce apparent alterations in either actin or microtubule cytoskeleton (our unpublished data), therefore it is unlikely that effect of KIF15 on integrin endocytosis is due to general cytoskeleton changes. Yet, testing of KIF15 impact on the other endocytic cargos, namely transferrin (recycled cargo (Dickson et al., 1983)) and EGF (degradable cargo (Carpenter and Cohen, 1976)), revealed that KIF15 is not for internalization of either transferrin or EGF, in agreement to the results of the screening of (Collinet et al., 2010), which measured intracellular EGF and transferrin after 10 min of internalization.

The possible explanation of specific requirement for KIF15 in integrin internalization, would be that KIF15 is involved in delivery of some integrin internalization factor to the plasma membrane. The data on the entry routes of integrins in the endocytosis pathway are controversal. Number of studies have demonstrated that internalization of β1 integrins depends on clathrin and clathrin adaptors (Chao and Kunz, 2005; Nishimura and Kaibuchi, 2007; Ezratty et al., 2009; Teckchandani et al., 2009,

2012). However, there is also evidence of caveolin involvement in internalization of integrin β1 (Shi and Sottile, 2008; Bass et al., 2011), clustered α2 integrin (Upla et al., 2004; Karjalainen et al., 2008; Rintanen et al., 2012), and α2 integrin internalized upon stimulation of the cells with EGF (Ning et al., 2007). Interestingly, it was also reported, that in the interstinal epithelial cells internalization of β1 integrin occurs through lipid rafts in clarhin-independent manner, but can be upregulated upon knock-down of caveolin1 or flotillins (Vassilieva et al., 2008).

To the best of our knowledge, the information about entry determinants specific for non-clustered α2 is limited to the study of integrin-specific clathrin adaptor Dab2, knock-down of which resulted in entry block of β1 integrin and, consequently elevated surface level of β1 and several, but not all, corresponding a chains, α2 among them (Teckchandani et al., 2009). Endocytic adaptors, such as AP2 or clathrin-associated sorting proteins (CLASPs) could be the factor affected by KIF15 knockdown. Insensitivity of early steps of transferrin and EGF endocytosis to KIF15 knock-down limits the range of suspects to the PTB-binding CLASPs Dab2, ARH, and Numb, which are known to regulate β1 integrin and LDLR, but not transferrin endocytosis (Keyel et al., 2006)(Ezratty et al., 2005; Chao and Kunz, 2009; Teckchandani et al., 2009; Nishimura and Kaibuchi, 2007; Teckchandani et al., 2012).

As shown by siRNA experiments, Dab2, ARH, and Numb are required for integrin β1 internalization in migrating cells (Nishimura and Kaibuchi, 2007; Ezratty et al., 2009) and disassembly of focal adhesions (Chao and Kunz, 2009), but only knock-down of Dab2 blocks bulk β1 internalization (Tackchandani et al., 2009, 2012). As neither KIF15 knock-down or over-expression had no effect on the focal adhesion abundance (our unpublished data), we selected Dab2 for testing whether KIF15 knock-down affects

integrin endocytic adaptors.

According to published studies, Dab2 in the interphase HeLa cells predominantly localizes to the PM, co-localizing with clathrin and AP2 adaptor (Keyel et al., 2006; Chetrit et al., 2011). Yet, for C. elegans orthologue (Ce-Dab-1) in addition to PM localization, partial localization to the perinuclear area was demonstrated. Perinuclear Dab2 co-localized with Golgi-markers, AP1 adaptor, and secretory cargos, but not with Rab11-positive perinuclear recycling compartment (Kamikura and Cooper, 2006).

In agreement to published data, we detected Dab2 predominantly at the PM of HeLa cells, and, to the lesser extent, in the cytoplasm. According to our observations, KIF15 knock-down induced remarkable displacement of Dab2 from the PM (**Figure R.12A-C**) with its partial re-location to perinuclear compartment (**Figure R.12D**), distinct from transferrin-positive recycling compartment. This relocation is likely to be the cause of entry block of integrin in the cells. However, effect of KIF15 knock-down on the other integrin-specific adaptors is yet to be tested and further studies are required to elucidate, whether KIF15 directly transports Dab2 to the PM or their association is indirect.

Moreover, interplay of KIF15 and Dab2 in the trafficking pathways can be more complicated. Dab2 is required for recycling of endocytic cargos, as was demonstrated for TGF-β, transferrin and cystic fibrosis transmembrane conductance receptor (Penheiter et al., 2010; Fu et al., 2012). Further experiments are required to clarify, whether recycling block of transferrin upon knock-down of KIF15 is a result of direct involvement of KIF15 in transferrin anterograde transport, perturbation of Dab2-dependent steps along the endocytic recycling pathway, or combination of both. Also, potential involvement of KIF15 and Dab2 in integrin recycling is yet to be investigated.

According GENT database, KIF15 is upregulated in numerous cancers (Shin et al., 2011). Alterations in integrin trafficking is a prominent cancer hallmark, primarily associated with the motility of transformed cells (Mosesson et al., 2008; Shin et al., 2012). Altogether our data demostrate that KIF15 over-expression can promote early steps of the integrin internalization, thus KIF15 can serve as a perspective therapeutic target in cancer treatment, and its implication in the the other steps of integrin trafficking, role in cell motility and cancer progression *in vivo* should be addressed.

5.6. Integrin α2 internalization of micropatterned surfaces

We have performed proof-of-principle experiments, demonstrating that non-clustered integrin α2 in absence of its ligand is efficiently internalized when cells are seeded onto micropatterned substrate that restricts the cell shape and motility (**Figure R.13**). Lesser difference of the integrin α2 internalization and expression in the cells grown on micropatterns indicates, that certain biological pre-selection of cells occurs, possibly, at the point of cell attachment to micropatterns. This would allow us to reach higher dynamic range of the integrin internalization assay, without having to disregard the majority of the cell population, as done in the experiments performed in cell culture (see ***Quantification of microscopy-based integrin internalization assay***). The use of both symmetric (Y- and H-shaped) and asymmetric (crossbow-shaped) patterns would allow us to directly compare the integrin internalization and intracellular distribution of internalized integrin in polarized and non-polarized cells, as the assymetric patterns were demonstrated to induce cell polarization (Thery et al., 2006) and focal adhesion re-distribution in a manner, similar to migrating cells (Theisen et al., 2012).

Yet, these experiments are still under development, and further optimization of

quantification of intracellular distribution of internalized integrin, as well as assessment of cell motility of the cells residing on micropatterns is needed.

6. Conclusions and outlook

In this study we aimed to characterize the endocytic trafficking of non-clustered integrin α2β1 in HeLa cells and discover the novel regulators of it. For this, a quantitative method to measure internalization of endogenously expressed non-clustered integrin α2 in the adherent cells was developed and the scoring pipeline was optimized. For the first time we demonstrated, that internalization of non-clustered integrin α2 in HeLa cells requires both clathrin and caveolin1 and proceeds through Rab4- Rab5- and Rab11-positive compartments.

We carried out an RNAi screening of 386 cytoskeleton-associated genes, and identified 122 hits as potential regulators of α2 integrin internalization, 83 of which have not previously been associated with endocytic trafficking . The reliability of the primary screening results we have verified by reproducing the primary screening results for 10 genes out of 26 taken into validation. Additionaly, we assessed effect of hits knock-down on the total integrin α2 expression and cell-counts, and identified 5 genes that affected α2 integrin at the expression level.

In our study we for the first time systematically addressed effect of kinesin molecular motors on integrin trafficking. Three kinesins (KIF15, KIF18a, and KIF23) were validated as inhibitors of integrin α2 internalization. We demonstrated that KIF15 is a novel trafficking regulator, that it is required at the early steps of α2 integrin endocytosis but not for endocytosis of transferrin or EGF. Strikingly, knock-down of KIF15 resulted in loss of integrin-specific clathrin adaptor Dab2 from the plasma membrane, which is likely to be the cause of integrin α2 internalization block. However, whether KIF15 directly transports Dab2 to the plasma membrane and whether its knock-down affects other integrin-specific endocytic adaptors remains to be investigated. Another question is whether KIF15 is required for the other steps of integrin tranficking,

i.e. recycling similarly to its requirement for tranferrin recycling.

Integrin trafficking is crucial for motility of cells, and deregulation of it, causing either to blockage or increase of integrin endocytic recycling, can lead to cancer development. Our results provide a link between integrin trafficking and KIF15, which is upregulated in numerous cancers, illuminating it as a potential therapeutic target. Further work is required to elucidate, whether KIF15 *in vivo* is involved in malignant transformation due to its interphase role in the integrin internalization.

7. Collaborations

In the course of this study the following collaborations were establishes:

Nina Beil, Jürgen Beneke, Dr. Jürgen Reymann and Dr. Holger Erfle (ViroQuant-CellNetworks RNAi Screening Facility, BioQuant, Heidelberg University, Heidelberg, Germany) and Dr. Rainer Pepperkok (EMBL, Heidelberg, Germany) provided of siRNA library for solid-phase transfection, automated image acquisition and analysis, and data storage;

Dr. Bettina Knapp[1] and Prof. Lars Kaderali[1] (BioQuant, Heidelberg University, Heidelberg, Germany) performed statistical data of the preliminary experiments and the primary screening;

Dorota Matelska[2] and Prof. Robert Russell (BioQuant, Heidelberg University, Heidelberg, Germany) performed bioinformatic analysis of the primary screening results;

Dr. Ulrike Engel and Nikon Imaging Center (Heidelberg, Germany) provided the training and facilities for TIRF imaging;

Cytoo (Grenoble, France) provided micropatterned substrates for study of integrin internalization in the constrained cells;

Gintare Garbenciute (Vilnus University, Vilnus, Lithuania) assisted with integrin internalization experiments on the micropatterned substrates.

1 Currently Technische Universität Dresden, Dresden, Germany
2 Currently International Institute of Molecular and Cell Biology in Warsaw, Warsaw, Poland

8. References

Abramoff, M.D.., P.J.. Magalhães, and S.J. Ram. 2004. Image processing with ImageJ. *Biophotonics international*. 11:36–42.

Aguilar, R.C., and B. Wendland. 2005. Endocytosis of membrane receptors: Two pathways are better than one. *PNAS*. 102:2679–2680.

Allan, V.J. 2011. Cytoplasmic dynein. *Biochemical Society transactions*. 39:1169–78.

Arjonen, A., J. Alanko, S. Veltel, and J. Ivaska. 2012. Distinct recycling of active and inactive β1 integrins. *Traffic (Copenhagen, Denmark)*.

Assoian, R.K., and E.A. Klein. 2008. Growth control by intracellular tension and extracellular stiffness. *Trends in cell biology*. 18:347–52.

Bashkirov, P. V, S.A. Akimov, A.I. Evseev, S.L. Schmid, J. Zimmerberg, and V.A. Frolov. 2008. GTPase cycle of dynamin is coupled to membrane squeeze and release, leading to spontaneous fission. *Cell*. 135:1276–86.

Bartoli, K.M., J. Jakovljevic, J.L. Woolford, and W.S. Saunders. 2011. Kinesin molecular motor Eg5 functions during polypeptide synthesis. *Molecular biology of the cell*. 22:3420–30.

Bass MD, Williamson RC, Nunan RD, Humphries JD, Byron A, Morgan MR, et al. A Syndecan-4 Hair Trigger Initiates Wound Healing through Caveolin- and RhoG-Regulated Integrin Endocytosis. Developmental cell. 2011 Oct 3

Bergelson, J.M., M.P. Shepley, B.M. Chan, M.E. Hemler, and R.W. Finberg. 1992. Identification of the integrin VLA-2 as a receptor for echovirus 1. *Science (New York, N.Y.)*. 255:1718–20.

Blangy, A., H.A. Lane, P. d'Hérin, M. Harper, M. Kress, and E.A. Nigg. 1995. Phosphorylation by p34cdc2 regulates spindle association of human Eg5, a kinesin-related motor essential for bipolar spindle formation in vivo. *Cell*. 83:1159–69.

Brideau, C., B. Gunter, B. Pikounis, and A. Liaw. 2003. Improved statistical methods for hit selection in high-throughput screening. *Journal of biomolecular screening*. 8:634–47.

Van der Bliek, A.M., T.E. Redelmeier, H. Damke, E.J. Tisdale, E.M. Meyerowitz, and S.L. Schmid. 1993. Mutations in human dynamin block an intermediate stage in coated vesicle formation. *The Journal of cell biology*. 122:553–63.

Boleti, H., E. Karsenti, and I. Vernos. 1996. Xklp2, a Novel Xenopus Centrosomal Kinesin-like Protein Required for Centrosome Separation during Mitosis. *Cell*. 84:49–59.

Bond, L.M., H. Brandstaetter, J.R. Sellers, J. Kendrick-Jones, and F. Buss. 2011. Myosin motor proteins are involved in the final stages of the secretory pathways. *Biochemical Society transactions*. 39:1115–9.

Böttcher, R.T., C. Stremmel, A. Meves, H. Meyer, M. Widmaier, H.-Y. Tseng, and R. Fässler. 2012. Sorting nexin 17 prevents lysosomal degradation of β1 integrins by binding to the β1-integrin tail. *Nature cell biology*. 14:584–92.

Boutros, M., L.P. Brás, and W. Huber. 2006. Analysis of cell-based RNAi screens. *Genome biology*. 7:R66.

Brooks, P.C., S. Silletti, T.L. von Schalscha, M. Friedlander, and D.A. Cheresh. 1998. Disruption of angiogenesis by PEX, a noncatalytic metalloproteinase fragment with integrin binding activity. *Cell*. 92:391–400.

Brooks, P.C., S. Strömblad, L.C. Sanders, T.L. von Schalscha, R.T. Aimes, W.G. Stetler-Stevenson, J.P. Quigley, and D.A. Cheresh. 1996. Localization of matrix

metalloproteinase MMP-2 to the surface of invasive cells by interaction with integrin alpha v beta 3. *Cell*. 85:683–93.

Brown, M.C. 1996. Identification of LIM3 as the principal determinant of paxillin focal adhesion localization and characterization of a novel motif on paxillin directing vinculin and focal adhesion kinase binding. *The Journal of Cell Biology*. 135:1109–1123.

Brown, M.C., J.A. Perrotta, and C.E. Turner. 1998. Serine and Threonine Phosphorylation of the Paxillin LIM Domains Regulates Paxillin Focal Adhesion Localization and Cell Adhesion to Fibronectin. *Mol. Biol. Cell*. 9:1803–1816.

Brown, M.C., and C.E. Turner. 2004. Paxillin: adapting to change. *Physiological reviews*. 84:1315–39.

Brown, N.H., S.L. Gregory, W.L. Rickoll, L.I. Fessler, M. Prout, R.A.H. White, and J.W. Fristrom. 2002. Talin is essential for integrin function in Drosophila. *Developmental cell*. 3:569–79.

Bucci, C., R.G. Parton, I.H. Mather, H. Stunnenberg, K. Simons, B. Hoflack, and M. Zerial. 1992. The small GTPase rab5 functions as a regulatory factor in the early endocytic pathway. *Cell*. 70:715–28.

Burridge, K., and K. Fath. 1989. Focal contacts: transmembrane links between the extracellular matrix and the cytoskeleton. *BioEssays□: news and reviews in molecular, cellular and developmental biology*. 10:104–8.

Burridge, K., and K. Wennerberg. 2004. Rho and Rac take center stage. *Cell*. 116:167–79.

Buster, D.W., D.H. Baird, W. Yu, J.M. Solowska, M. Chauvière, A. Mazurek, M. Kress, and P.W. Baas. 2003. Expression of the mitotic kinesin Kif15 in postmitotic neurons: implications for neuronal migration and development. *Journal of neurocytology*. 32:79–96.

Böttcher, R.T., C. Stremmel, A. Meves, H. Meyer, M. Widmaier, H.-Y. Tseng, and R. Fässler. 2012. Sorting nexin 17 prevents lysosomal degradation of β1 integrins by binding to the β1-integrin tail. *Nature cell biology*. 14:584–92.

Calderwood, D.A. 1999. The Talin Head Domain Binds to Integrin beta Subunit Cytoplasmic Tails and Regulates Integrin Activation. *Journal of Biological Chemistry*. 274:28071–28074.

Calderwood, D.A., Y. Fujioka, J.M. de Pereda, B. García-Alvarez, T. Nakamoto, B. Margolis, C.J. McGlade, R.C. Liddington, and M.H. Ginsberg. 2003. Integrin beta cytoplasmic domain interactions with phosphotyrosine-binding domains: a structural prototype for diversity in integrin signaling. *Proceedings of the National Academy of Sciences of the United States of America*. 100:2272–7.

Calderwood, D.A., B. Yan, J.M. de Pereda, B.G. Alvarez, Y. Fujioka, R.C. Liddington, and M.H. Ginsberg. 2002. The phosphotyrosine binding-like domain of talin activates integrins. *The Journal of biological chemistry*. 277:21749–58.

Canty, E.G., T. Starborg, Y. Lu, S.M. Humphries, D.F. Holmes, R.S. Meadows, A. Huffman, E.T. O'Toole, and K.E. Kadler. 2006. Actin filaments are required for fibripositor-mediated collagen fibril alignment in tendon. *The Journal of biological chemistry*. 281:38592–8.

Carisey, A., and C. Ballestrem. 2011. Vinculin, an adapter protein in control of cell adhesion signalling. *European journal of cell biology*. 90:157–63.

Caswell, P., and J. Norman. 2008. Endocytic transport of integrins during cell migration and invasion. *Trends in cell biology*. 18:257–63.

Caswell, P.T., H.J. Spence, M. Parsons, D.P. White, K. Clark, K.W. Cheng, G.B.

Mills, M.J. Humphries, A.J. Messent, K.I. Anderson, M.W. McCaffrey, B.W. Ozanne, and J.C. Norman. 2007. Rab25 associates with alpha5beta1 integrin to promote invasive migration in 3D microenvironments. *Developmental cell*. 13:496–510.

Chao, W.-T., and J. Kunz. 2009. Focal adhesion disassembly requires clathrin-dependent endocytosis of integrins. *FEBS Letters*. 583:1337–1343.

Chen, J., T.G. Diacovo, D.G. Grenache, S.A. Santoro, and M.M. Zutter. 2002. The alpha(2) integrin subunit-deficient mouse: a multifaceted phenotype including defects of branching morphogenesis and hemostasis. *The American journal of pathology*. 161:337–44.

Chen, W.J., J.L. Goldstein, and M.S. Brown. 1990. NPXY, a sequence often found in cytoplasmic tails, is required for coated pit-mediated internalization of the low density lipoprotein receptor. *The Journal of biological chemistry*. 265:3116–23.

Chetrit, D., L. Barzilay, and G. Horn. 2011. Negative regulation of the endocytic adaptor disabled-2 (Dab2) in mitosis. *Journal of Biological ….* 286:5392–5403.

Chidlow, J.H., and W.C. Sessa. 2010. Caveolae, caveolins, and cavins: complex control of cellular signalling and inflammation. *Cardiovascular research*. 86:219–25.

Ciechanover, A. 2005. Proteolysis: from the lysosome to ubiquitin and the proteasome. *Nature reviews. Molecular cell biology*. 6:79–87.

Chintala, S.K., R. Sawaya, Z.L. Gokaslan, and J.S. Rao. 1996. Modulation of matrix metalloprotease-2 and invasion in human glioma cells by alpha 3 beta 1 integrin. *Cancer letters*. 103:201–8.

Chiquet, M., L. Gelman, R. Lutz, and S. Maier. 2009. From mechanotransduction to extracellular matrix gene expression in fibroblasts. *Biochimica et biophysica acta*. 1793:911–20.

Choi, C.K., M. Vicente-Manzanares, J. Zareno, L.A. Whitmore, A. Mogilner, and A.R. Horwitz. 2008. Actin and alpha-actinin orchestrate the assembly and maturation of nascent adhesions in a myosin II motor-independent manner. *Nature cell biology*. 10:1039–50.

Clark, K.A., M. McGrail, and M.C. Beckerle. 2003. Analysis of PINCH function in Drosophila demonstrates its requirement in integrin-dependent cellular processes. *Development (Cambridge, England)*. 130:2611–21.

Collawn, J.F., L.A. Kuhn, L.F. Liu, J.A. Tainer, and I.S. Trowbridge. 1991. Transplanted LDL and mannose-6-phosphate receptor internalization signals promote high-efficiency endocytosis of the transferrin receptor. *The EMBO journal*. 10:3247–53.

Collinet, C., M. Stoter, C.R. Bradshaw, N. Samusik, J.C. Rink, D. Kenski, B. Habermann, F. Buchholz, R. Henschel, M.S. Mueller, W.E. Nagel, E. Fava, Y. Kalaidzidis, and M. Zerial. 2010. Systems survey of endocytosis by multiparametric image analysis. *Nature*. 464:243–249.

Cosset, E.C., J. Godet, N. Entz-Werlé, E. Guérin, D. Guenot, S. Froelich, D. Bonnet, S. Pinel, F. Plenat, P. Chastagner, M. Dontenwill, and S. Martin. 2012. Involvement of the TGFβ pathway in the regulation of α5 β1 integrins by caveolin-1 in human glioblastoma. *International journal of cancer. Journal international du cancer*. 131:601–11.

Damke, H., T. Baba, D.E. Warnock, and S.L. Schmid. 1994. Induction of mutant dynamin specifically blocks endocytic coated vesicle formation. *The Journal of cell biology*. 127:915–34.

Dautry-Varsat, A. 1986. Receptor-mediated endocytosis: the intracellular journey of transferrin and its receptor. *Biochimie*. 68:375–81.

Day, P., K.A. Riggs, N. Hasan, D. Corbin, D. Humphrey, and C. Hu. 2011. Syntaxins 3 and 4 mediate vesicular trafficking of α5β1 and α3β1 integrins and cancer cell migration. *International journal of oncology*. 39:863–71.

Delevoye, C., I. Hurbain, D. Tenza, J.-B. Sibarita, S. Uzan-Gafsou, H. Ohno, W.J.C. Geerts, A.J. Verkleij, J. Salamero, M.S. Marks, and G. Raposo. 2009. AP-1 and KIF13A coordinate endosomal sorting and positioning during melanosome biogenesis. *The Journal of cell biology*. 187:247–64.

DePasquale, J.A. 1987. Evidence for an actin-containing cytoplasmic precursor of the focal contact and the timing of incorporation of vinculin at the focal contact. *The Journal of Cell Biology*. 105:2803–2809.

Desnos, C., S. Huet, and F. Darchen. 2007. "Should I stay or should I go?": myosin V function in organelle trafficking. *Biology of the cell / under the auspices of the European Cell Biology Organization*. 99:411–23.

Dominguez, R., and K.C. Holmes. 2011. Actin structure and function. *Annual review of biophysics*. 40:169–86.

Doherty GJ, McMahon HT. Mechanisms of endocytosis. Annual review of biochemistry. 2009 Jan;78:857-902.

Dozynkiewicz, M. a, N.B. Jamieson, I. Macpherson, J. Grindlay, P.V.E. van den Berghe, A. von Thun, J.P. Morton, C. Gourley, P. Timpson, C. Nixon, C.J. McKay, R. Carter, D. Strachan, K. Anderson, O.J. Sansom, P.T. Caswell, and J.C. Norman. 2011. Rab25 and CLIC3 Collaborate to Promote Integrin Recycling from Late Endosomes/Lysosomes and Drive Cancer Progression. *Developmental cell*. 3:1–15.

Du, J., X. Chen, X. Liang, G. Zhang, J. Xu, L. He, Q. Zhan, X.-Q. Feng, S. Chien, and C. Yang. 2011. Integrin activation and internalization on soft ECM as a mechanism of induction of stem cell differentiation by ECM elasticity. *Proceedings of the National Academy of Sciences of the United States of America*. 108:9466–71.

Eckes, B., D. Dogic, E. Colucci-Guyon, N. Wang, A. Maniotis, D. Ingber, A. Merckling, F. Langa, M. Aumailley, A. Delouvée, V. Koteliansky, C. Babinet, and T. Krieg. 1998. Impaired mechanical stability, migration and contractile capacity in vimentin-deficient fibroblasts. *Journal of cell science*. 111 (Pt 1:1897–907.

Eden, S., R. Rohatgi, A. V Podtelejnikov, M. Mann, and M.W. Kirschner. 2002. Mechanism of regulation of WAVE1-induced actin nucleation by Rac1 and Nck. *Nature*. 418:790–3.

Efimov, A., N. Schiefermeier, I. Grigoriev, R. Ohi, M.C. Brown, C.E. Turner, J.V. Small, and I. Kaverina. 2008. Paxillin-dependent stimulation of microtubule catastrophes at focal adhesion sites. *Journal of cell science*. 121:196–204.

Erfle, H., A. Eskova, J. Reymann, and V. Starkuviene. 2011. Cell arrays and high-content screening. *Methods in molecular biology*. 785:277–87.

Erfle, H., B. Neumann, U. Liebel, P. Rogers, M. Held, T. Walter, J. Ellenberg, and R. Pepperkok. 2007. Reverse transfection on cell arrays for high content screening microscopy. *Nat. Protocols*. 2:392–399.

Ezratty, E.J., M.A. Partridge, and G.G. Gundersen. 2005. Microtubule-induced focal adhesion disassembly is mediated by dynamin and focal adhesion kinase. *Nature cell biology*. 7:581–90.

Ezratty, E.J., C. Bertaux, E.E. Marcantonio, and G.G. Gundersen. 2009. Clathrin mediates integrin endocytosis for focal adhesion disassembly in migrating cells. *The Journal of cell biology*. 187:733–47.

Falnikar, A., S. Tole, and P.W. Baas. 2011. Kinesin-5, a mitotic microtubule-

associated motor protein, modulates neuronal migration. *Molecular biology of the cell*. 22:1561–74.

Feng, Y., B. Press, and A. Wandinger-Ness. 1995. Rab 7: an important regulator of late endocytic membrane traffic. *The Journal of cell biology*. 131:1435–52.

Fleming, F.E., K.L. Graham, Y. Takada, and B.S. Coulson. 2010. Determinants of the specificity of rotavirus interactions with the {alpha}2{beta}1 integrin. *The Journal of biological chemistry*. 286:6165–74.

Fässler, R., and M. Meyer. 1995. Consequences of lack of beta 1 integrin gene expression in mice. *Genes & development*. 9:1896–908.

Fathers, K.E., E.S. Bell, C. V Rajadurai, S. Cory, H. Zhao, A. Mourskaia, D. Zuo, J. Madore, A. Monast, A.-M. Mes-Masson, A.-A. Grosset, L. Gaboury, M. Hallett, P. Siegel, and M. Park. 2012. Crk adaptor proteins act as key signaling integrators for breast tumorigenesis. *Breast cancer research□: BCR*. 14:R74.

Foth, B.J., M.C. Goedecke, and D. Soldati. 2006. New insights into myosin evolution and classification. *Proceedings of the National Academy of Sciences of the United States of America*. 103:3681–6.

Frank, D.J., T. Noguchi, and K.G. Miller. 2004. Myosin VI: a structural role in actin organization important for protein and organelle localization and trafficking. *Current opinion in cell biology*. 16:189–94.

Fu, L., A. Rab, L.P. Tang, S.M. Rowe, Z. Bebok, and J.F. Collawn. 2012. Dab2 is a key regulator of endocytosis and post-endocytic trafficking of the cystic fibrosis transmembrane conductance regulator. *The Biochemical journal*. 441:633–43.

Gao, B., T.M. Curtis, F.A. Blumenstock, F.L. Minnear, and T.M. Saba. 2000. Increased recycling of (alpha)5(beta)1 integrins by lung endothelial cells in response to tumor necrosis factor. *Journal of cell science*. 113 Pt 2:247–57.

Gillon, A.D., C.F. Latham, and E.A. Miller. 2012. Vesicle-mediated ER export of proteins and lipids. *Biochimica et biophysica acta*. 1821:1040–9.

Goh, K.L., J.T. Yang, and R.O. Hynes. 1997. Mesodermal defects and cranial neural crest apoptosis in alpha5 integrin-null embryos. *Development (Cambridge, England)*. 124:4309–19.

Goshima, G., and R.D. Vale. 2003. The roles of microtubule-based motor proteins in mitosis: comprehensive RNAi analysis in the Drosophila S2 cell line. *The Journal of cell biology*. 162:1003–16.

Goshima, G., and R.D. Vale. 2005. Cell cycle-dependent dynamics and regulation of mitotic kinesins in Drosophila S2 cells. *Molecular biology of the cell*. 16:3896–907.

Grande-García, A., A. Echarri, J. de Rooij, N.B. Alderson, C.M. Waterman-Storer, J.M. Valdivielso, and M.A. del Pozo. 2007. Caveolin-1 regulates cell polarization and directional migration through Src kinase and Rho GTPases. *The Journal of cell biology*. 177:683–94.

Grant, B.D., and J.G. Donaldson. 2009. Pathways and mechanisms of endocytic recycling. *Nature reviews. Molecular cell biology*. 10:597–608.

Gruenberg, J., and H. Stenmark. 2004. The biogenesis of multivesicular endosomes. *Nature reviews. Molecular cell biology*. 5:317–23.

Gu, F., and J. Gruenberg. 2000. ARF1 regulates pH-dependent COP functions in the early endocytic pathway. *The Journal of biological chemistry*. 275:8154–60.

Gu, Z., E.H. Noss, V.W. Hsu, and M.B. Brenner. 2011. Integrins traffic rapidly via circular dorsal ruffles and macropinocytosis during stimulated cell migration. *The Journal of cell biology*. 193:61–70.

Guerrero, C.A., E. Méndez, S. Zárate, P. Isa, S. López, and C.F. Arias. 2000. Integrin alpha(v)beta(3) mediates rotavirus cell entry. *Proceedings of the National Academy of Sciences of the United States of America*. 97:14644–9.

Haglund, K., S. Sigismund, S. Polo, I. Szymkiewicz, P.P. Di Fiore, and I. Dikic. 2003. Multiple monoubiquitination of RTKs is sufficient for their endocytosis and degradation. *Nature cell biology*. 5:461–6.

Hamilton, T.E., S.J. McClane, S. Baldwin, C. Burke, H. Patel, J.L. Rombeau, and S.E. Raper. 1997. Efficient adenoviral-mediated murine neonatal small intestinal gene transfer is dependent on alpha(v) integrin expression. *Journal of pediatric surgery*. 32:1695–703.

Hanover, J.A., M.C. Willingham, and I. Pastan. 1984. Kinetics of transit of transferrin and epidermal growth factor through clathrin-coated membranes. *Cell*. 39:283–93.

Harburger, D.S., M. Bouaouina, and D.A. Calderwood. 2009. Kindlin-1 and -2 directly bind the C-terminal region of beta integrin cytoplasmic tails and exert integrin-specific activation effects. *The Journal of biological chemistry*. 284:11485–97.

Heino J, Ignotz RA, Hemler ME, Crouse C, Massague J. Regulation of cell adhesion receptors by transforming growth factor- beta. Concomitant regulation of integrins that share a common beta 1 subunit. J. Biol. Chem. 1989;264(1):380-388.

Helfand, B.T., L. Chang, and R.D. Goldman. 2004. Intermediate filaments are dynamic and motile elements of cellular architecture. *Journal of cell science*. 117:133–41.

Hemler ME, Sanchez-Madrid F, Flotte TJ, Krensky AM, Burakoff SJ, Bhan AK, et al. Glycoproteins of 210,000 and 130,000 m.w. on activated T cells: cell distribution and antigenic relation to components on resting cells and T cell lines. Journal of immunology (Baltimore, Md.□: 1950). 1984 Jun;132(6):3011-3018.

Hemler ME, Jacobson JG, Strominger JL. Biochemical characterization of VLA-1 and VLA-2. Cell surface heterodimers on activated T cells. The Journal of biological chemistry. 1985 Dec 5;260(28):15246-52.

Hildebrandt, E.R., and M.A. Hoyt. 2000. Mitotic motors in Saccharomyces cerevisiae. *Biochimica et biophysica acta*. 1496:99–116.

Hirokawa, N., Y. Noda, Y. Tanaka, and S. Niwa. 2009. Kinesin superfamily motor proteins and intracellular transport. *Nat Rev Mol Cell Biol*. 10:682–696.

Horiguchi, K., K. Fujiwara, C. Ilmiawati, M. Kikuchi, T. Tsukada, T. Kouki, and T. Yashiro. 2011. Caveolin 3-mediated integrin β1 signaling is required for the proliferation of folliculostellate cells in rat anterior pituitary gland under the influence of extracellular matrix. *The Journal of endocrinology*. 210:29–36.

Hodivala-Dilke, K.M., K.P. McHugh, D.A. Tsakiris, H. Rayburn, D. Crowley, M. Ullman-Culleré, F.P. Ross, B.S. Coller, S. Teitelbaum, and R.O. Hynes. 1999. Beta3-integrin-deficient mice are a model for Glanzmann thrombasthenia showing placental defects and reduced survival. *The Journal of clinical investigation*. 103:229–38.

Hoepfner, S., F. Severin, A. Cabezas, B. Habermann, A. Runge, D. Gillooly, H. Stenmark, and M. Zerial. 2005. Modulation of receptor recycling and degradation by the endosomal kinesin KIF16B. *Cell*. 121:437–50.

Hsu, D., P.E. Knudson, A. Zapf, G.C. Rolband, and J.M. Olefsky. 1994. NPXY motif in the insulin-like growth factor-I receptor is required for efficient ligand-mediated receptor internalization and biological signaling. *Endocrinology*. 134:744–50.

Hu, P., and B.-H. Luo. 2013. Integrin bi-directional signaling across the plasma membrane. *Journal of cellular physiology*. 228:306–12.

Huang, F., L.K. Goh, and A. Sorkin. 2007. EGF receptor ubiquitination is not necessary for its internalization. *Proceedings of the National Academy of Sciences of the United States of America*. 104:16904–9.

Huang C, Lu C, Springer TA. Folding of the conserved domain but not of flanking regions in the integrin beta2 subunit requires association with the alpha subunit. Proceedings of the National Academy of Sciences of the United States of America. 1997 Apr 1;94(7):3156-61.

Humphries, J.D., P. Wang, C. Streuli, B. Geiger, M.J. Humphries, and C. Ballestrem. 2007. Vinculin controls focal adhesion formation by direct interactions with talin and actin. *The Journal of cell biology*. 179:1043–57.

Humphries, J.D., A. Byron, M.D. Bass, S.E. Craig, J.W. Pinney, D. Knight, and M.J. Humphries. 2009. Proteomic analysis of integrin-associated complexes identifies RCC2 as a dual regulator of Rac1 and Arf6. *Science signaling*. 2:ra51.

Hunt, S.D., and D.J. Stephens. 2011. The role of motor proteins in endosomal sorting. *Biochemical Society transactions*. 39:1179–84.

Hynes, R.O. 1992. Integrins: versatility, modulation, and signaling in cell adhesion. *Cell*. 69:11–25.

Ilić, D., B. Kovacic, K. Johkura, D.D. Schlaepfer, N. Tomasević, Q. Han, J.-B. Kim, K. Howerton, C. Baumbusch, N. Ogiwara, D.N. Streblow, J.A. Nelson, P. Dazin, Y. Shino, K. Sasaki, and C.H. Damsky. 2004. FAK promotes organization of fibronectin matrix and fibrillar adhesions. *Journal of cell science*. 117:177–87.

Ivaska, J., and J. Heino. 2010. Interplay between cell adhesion and growth factor receptors: from the plasma membrane to the endosomes. *Cell and tissue research*. 339:111–20.

Ivaska, J., K. Vuoriluoto, T. Huovinen, I. Izawa, M. Inagaki, and P.J. Parker. 2005. PKCepsilon-mediated phosphorylation of vimentin controls integrin recycling and motility. *The EMBO journal*. 24:3834–45.

Jahn, R., and R.H. Scheller. 2006. SNAREs--engines for membrane fusion. *Nature reviews. Molecular cell biology*. 7:631–43.

Jaulin, F., X. Xue, E. Rodriguez-Boulan, and G. Kreitzer. 2007. Polarization-dependent selective transport to the apical membrane by KIF5B in MDCK cells. *Developmental cell*. 13:511–22.

Jokinen, J., D.J. White, M. Salmela, M. Huhtala, J. Käpylä, K. Sipilä, J.S. Puranen, L. Nissinen, P. Kankaanpää, V. Marjomäki, T. Hyypiä, M.S. Johnson, and J. Heino. 2010. Molecular mechanism of alpha2beta1 integrin interaction with human echovirus 1. *The EMBO journal*. 29:196–208.

Jülich, D., A.P. Mould, E. Koper, and S.A. Holley. 2009. Control of extracellular matrix assembly along tissue boundaries via Integrin and Eph/Ephrin signaling. *Development (Cambridge, England)*. 136:2913–21.

Kamikura, D., and J. Cooper. 2006. Clathrin Interaction and Subcellular Localization of Ce-□DAB-□1, an Adaptor for Protein Secretion in Caenorhabditis elegans. *Traffic*. 7:324–336.

Kapoor, T.M., and T.J. Mitchison. 2001. Eg5 is static in bipolar spindles relative to tubulin: evidence for a static spindle matrix. *The Journal of cell biology*. 154:1125–33.

Karjalainen, M., E. Kakkonen, P. Upla, H. Paloranta, P. Kankaanpää, P. Liberali, G.H. Renkema, T. Hyypiä, J. Heino, and V. Marjomäki. 2008. A Raft-derived, Pak1-regulated entry participates in alpha2beta1 integrin-dependent sorting to caveosomes. *Molecular biology of the cell*. 19:2857–69.

Karjalainen, M., N. Rintanen, M. Lehkonen, K. Kallio, A. Mäki, K. Hellström, V. Siljamäki, P. Upla, and V. Marjomäki. 2011. Echovirus 1 infection depends on biogenesis of novel multivesicular bodies. *Cellular microbiology*. 13:1975–95.

Kaverina, I., O. Krylyshkina, and J. V Small. 1999. Microtubule targeting of substrate contacts promotes their relaxation and dissociation. *The Journal of cell biology*. 146:1033–44.

Kaverina, I., K. Rottner, and J. V Small. 1998. Targeting, capture, and stabilization of microtubules at early focal adhesions. *The Journal of cell biology*. 142:181–90.

Keyel, P.A., S.K. Mishra, R. Roth, J.E. Heuser, S.C. Watkins, and L.M. Traub. 2006. A single common portal for clathrin-mediated endocytosis of distinct cargo governed by cargo-selective adaptors. *Molecular biology of the cell*. 17:4300–17.

Kirchhausen, T. 2009. Imaging endocytic clathrin structures in living cells. *Trends in cell biology*. 19:596–605.

Knapp, B., I. Rebhan, A. Kumar, P. Matula, N.A. Kiani, M. Binder, H. Erfle, K. Rohr, R. Eils, R. Bartenschlager, and L. Kaderali. 2011. Normalizing for Individual Cell Population Context in the Analysis of high-content Cellular Screens. *BMC bioinformatics*. 12:485.

Kramer RH, Marks N. Identification of integrin collagen receptors on human melanoma cells. The Journal of biological chemistry. 1989 Mar 15;264(8):4684-8.

Krauss K, Altevogt P. Integrin leukocyte function-associated antigen-1-mediated cell binding can be activated by clustering of membrane rafts. The Journal of biological chemistry. 1999 Dec 24;274(52):36921-7.

Kiema, T., Y. Lad, P. Jiang, C.L. Oxley, M. Baldassarre, K.L. Wegener, I.D. Campbell, J. Ylänne, and D.A. Calderwood. 2006. The molecular basis of filamin binding to integrins and competition with talin. *Molecular cell*. 21:337–47.

Kim, M., C. V Carman, and T.A. Springer. 2003. Bidirectional transmembrane signaling by cytoplasmic domain separation in integrins. *Science (New York, N.Y.)*. 301:1720–5.

Klinghoffer, R.A., C. Sachsenmaier, J.A. Cooper, and P. Soriano. 1999. Src family kinases are required for integrin but not PDGFR signal transduction. *The EMBO journal*. 18:2459–71.

Kumari, S., and S. Mayor. 2008. ARF1 is directly involved in dynamin-independent endocytosis. *Nature cell biology*. 10:30–41.

Laemmli, U.K. 1970. Cleavage of structural proteins during the assembly of the head of bacteriophage T4. *Nature*. 227:680–5.

Leitinger B, Hogg N. The involvement of lipid rafts in the regulation of integrin function. Journal of cell science. 2002 Mar 1;115(Pt 5):963-72.

Lemmon, S.K. 2001. Clathrin uncoating: Auxilin comes to life. *Current biology : CB*. 11:R49–52.

Li, J., B.A. Ballif, A.M. Powelka, J. Dai, S.P. Gygi, and V.W. Hsu. 2005. Phosphorylation of ACAP1 by Akt regulates the stimulation-dependent recycling of integrin beta1 to control cell migration. *Developmental cell*. 9:663–73.

Li, Y., J. Cam, and G. Bu. 2001. Low-density lipoprotein receptor family: endocytosis and signal transduction. *Molecular neurobiology*. 23:53–67.

Lindahl, G.E., R.C. Chambers, J. Papakrivopoulou, S.J. Dawson, M.C. Jacobsen, J.E. Bishop, and G.J. Laurent. 2002. Activation of fibroblast procollagen alpha 1(I) transcription by mechanical strain is transforming growth factor-beta-dependent and involves increased binding of CCAAT-binding factor (CBF/NF-Y) at the proximal

promoter. *The Journal of biological chemistry*. 277:6153–61.

Liu, C., J. Yao, D. Mercola, and E. Adamson. 2000. The transcription factor EGR-1 directly transactivates the fibronectin gene and enhances attachment of human glioblastoma cell line U251. *The Journal of biological chemistry*. 275:20315–23.

Liu, X., and R.L. Erikson. 2007. The nuclear localization signal of mitotic kinesin-like protein Mklp-1: effect on Mklp-1 function during cytokinesis. *Biochemical and biophysical research communications*. 353:960–4.

Liu, M., V.C. Nadar, F. Kozielski, M. Kozlowska, W. Yu, and P.W. Baas. 2010. Kinesin-12, a mitotic microtubule-associated motor protein, impacts axonal growth, navigation, and branching. *The Journal of neuroscience*. 30:14896–906.

Lobert, V.H., A. Brech, N.M. Pedersen, J. Wesche, A. Oppelt, L. Malerød, and H. Stenmark. 2010. Ubiquitination of alpha 5 beta 1 integrin controls fibroblast migration through lysosomal degradation of fibronectin-integrin complexes. *Developmental cell*. 19:148–59.

Lombardi, D., T. Soldati, M.A. Riederer, Y. Goda, M. Zerial, and S.R. Pfeffer. 1993. Rab9 functions in transport between late endosomes and the trans Golgi network. *The EMBO journal*. 12:677–82.

Londrigan, S.L., K.L. Graham, Y. Takada, P. Halasz, and B.S. Coulson. 2003. Monkey rotavirus binding to alpha2beta1 integrin requires the alpha2 I domain and is facilitated by the homologous beta1 subunit. *Journal of virology*. 77:9486–501.

Lowin, T., and R.H. Straub. 2011. Integrins and their ligands in rheumatoid arthritis. *Arthritis research & therapy*. 13:244.

Luo, B.-H., C. V Carman, and T.A. Springer. 2007. Structural basis of integrin regulation and signaling. *Annual review of immunology*. 25:619–47.

Löer, B., R. Bauer, R. Bornheim, J. Grell, E. Kremmer, W. Kolanus, and M. Hoch. 2008. The NHL-domain protein Wech is crucial for the integrin-cytoskeleton link. *Nature cell biology*. 10:422–8.

Ma, J.K., M.Y. Platt, J. Eastham-Anderson, J.-S. Shin, and I. Mellman. 2012. MHC class II distribution in dendritic cells and B cells is determined by ubiquitin chain length. *Proceedings of the National Academy of Sciences of the United States of America*. 109:8820–7.

Mai, A., S. Veltel, T. Pellinen, A. Padzik, E. Coffey, V. Marjomäki, and J. Ivaska. 2011. Competitive binding of Rab21 and p120RasGAP to integrins regulates receptor traffic and migration. *The Journal of cell biology*.

Maier, S., R. Lutz, L. Gelman, A. Sarasa-Renedo, S. Schenk, C. Grashoff, and M. Chiquet. 2008. Tenascin-C induction by cyclic strain requires integrin-linked kinase. *Biochimica et biophysica acta*. 1783:1150–62.

Manneville, J.-B., and S. Etienne-Manneville. 2006. Positioning centrosomes and spindle poles: looking at the periphery to find the centre. *Biology of the cell / under the auspices of the European Cell Biology Organization*. 98:557–65.

Margadant, C., H.N. Monsuur, J.C. Norman, and A. Sonnenberg. 2011. Mechanisms of integrin activation and trafficking. *Current opinion in cell biology*. 23:607–614.

Margadant, C., M. Kreft, D.-J. de Groot, J.C. Norman, and A. Sonnenberg. 2012. Distinct Roles of Talin and Kindlin in Regulating Integrin α5β1 Function and Trafficking. *Current biology : CB*. 22:1554–63.

Martel V, Vignoud L, Dupé S, Frachet P, Block MR, Albigès-Rizo C. Talin controls the exit of the integrin alpha 5 beta 1 from an early compartment of the secretory

pathway. Journal of cell science. 2000 Jun;113(Pt 11):1951-61.

Martin, S., E.C. Cosset, J. Terrand, A. Maglott, K. Takeda, and M. Dontenwill. 2009. Caveolin-1 regulates glioblastoma aggressiveness through the control of alpha(5)beta(1) integrin expression and modulates glioblastoma responsiveness to SJ749, an alpha(5)beta(1) integrin antagonist. *Biochimica et biophysica acta*. 1793:354–67.

Martin, T.D., N. Mitin, A.D. Cox, J.J. Yeh, and C.J. Der. 2012. Phosphorylation by protein kinase Cα regulates RalB small GTPase protein activation, subcellular localization, and effector utilization. *The Journal of biological chemistry*. 287:14827–36.

De Matteis, M.A., and A. Luini. 2008. Exiting the Golgi complex. *Nature reviews. Molecular cell biology*. 9:273–84.McHugh, K.P., K. Hodivala-Dilke, M.H. Zheng, N. Namba, J. Lam, D. Novack, X. Feng, F.P. Ross, R.O. Hynes, and S.L. Teitelbaum. 2000. Mice lacking beta3 integrins are osteosclerotic because of dysfunctional osteoclasts. *The Journal of clinical investigation*. 105:433–40.

McCartney, B.M., and R.G. Fehon. 1996. Distinct cellular and subcellular patterns of expression imply distinct functions for the Drosophila homologues of moesin and the neurofibromatosis 2 tumor suppressor, merlin. *The Journal of cell biology*. 133:843–52.

Meraldi, P. 2012. Keeping kinetochores on track. *European journal of cell biology*. 91:103–6.

Meyer, A., J. Auernheimer, A. Modlinger, and H. Kessler. 2006. Targeting RGD recognizing integrins: drug development, biomaterial research, tumor imaging and targeting. *Current pharmaceutical design*. 12:2723–47.

Miki, H., Y. Okada, and N. Hirokawa. 2005. Analysis of the kinesin superfamily: insights into structure and function. *Trends in cell biology*. 15:467–76.

Miki, H., S. Suetsugu, and T. Takenawa. 1998. WAVE, a novel WASP-family protein involved in actin reorganization induced by Rac. *The EMBO journal*. 17:6932–41.

Miki, H., H. Yamaguchi, S. Suetsugu, and T. Takenawa. 2000. IRSp53 is an essential intermediate between Rac and WAVE in the regulation of membrane ruffling. *Nature*. 408:732–5.

Millon-Frémillon, A., D. Bouvard, A. Grichine, S. Manet-Dupé, M.R. Block, and C. Albiges-Rizo. 2008. Cell adaptive response to extracellular matrix density is controlled by ICAP-1-dependent beta1-integrin affinity. *The Journal of cell biology*. 180:427–41.

Mizuno-Yamasaki, E., F. Rivera-Molina, and P. Novick. 2012. GTPase networks in membrane traffic. *Annual review of biochemistry*. 81:637–59.

Montanez, E., S. Ussar, M. Schifferer, M. Bösl, R. Zent, M. Moser, and R. Fässler. 2008. Kindlin-2 controls bidirectional signaling of integrins. *Genes & development*. 22:1325–30.

Moravec, R., K.K. Conger, R. D'Souza, A.B. Allison, and J.E. Casanova. 2012. BRAG2/GEP100/IQSec1 interacts with clathrin and regulates α5β1 integrin endocytosis through activation of ADP ribosylation factor 5 (Arf5). *The Journal of biological chemistry*. 287:31138–47.

Moser, M., B. Nieswandt, S. Ussar, M. Pozgajova, and R. Fässler. 2008. Kindlin-3 is essential for integrin activation and platelet aggregation. *Nature medicine*. 14:325–30.

Mosesson, Y., G.B. Mills, and Y. Yarden. 2008. Derailed endocytosis: an emerging feature of cancer. *Nature reviews. Cancer*. 8:835–50.

Myllyharju, J., and K.I. Kivirikko. 2001. Collagens and collagen-related diseases. *Annals of medicine*. 33:7–21.

Nakagawa, T., M. Setou, D. Seog, K. Ogasawara, N. Dohmae, K. Takio, and N. Hirokawa. 2000. A novel motor, KIF13A, transports mannose-6-phosphate receptor to

plasma membrane through direct interaction with AP-1 complex. *Cell*. 103:569–81.

Nelsen-Salz, B., H.J. Eggers, and H. Zimmermann. 1999. Integrin alpha(v)beta3 (vitronectin receptor) is a candidate receptor for the virulent echovirus 9 strain Barty. *The Journal of general virology*. 80 (Pt 9):2311–3.

Neumann, B., T. Walter, J.-K. Heriche, J. Bulkescher, H. Erfle, C. Conrad, P. Rogers, I. Poser, M. Held, U. Liebel, C. Cetin, F. Sieckmann, G. Pau, R. Kabbe, A. WÃ¼nsche, V. Satagopam, M.H.A. Schmitz, C. Chapuis, D.W. Gerlich, R. Schneider, R. Eils, W. Huber, J.-M. Peters, A.A. Hyman, R. Durbin, R. Pepperkok, and J. Ellenberg. 2010. Phenotypic profiling of the human genome by time-lapse microscopy reveals cell division genes. *Nature*. 464:721–727.

Ng, T., D. Shima, A. Squire, P.I.H. Bastiaens, S. Gschmeissner, M.J. Humphries, and P.J. Parker. 1999. PKCalpha regulates beta1 integrin-dependent cell motility through association and control of integrin traffic. *EMBO J*. 18:3909–3929.

Nielsen, E., F. Severin, J.M. Backer, A.A. Hyman, and M. Zerial. 1999. Rab5 regulates motility of early endosomes on microtubules. *Nature cell biology*. 1:376–82.

Ning, Y., T. Buranda, and L.G. Hudson. 2007. Activated epidermal growth factor receptor induces integrin alpha2 internalization via caveolae/raft-dependent endocytic pathway. *The Journal of biological chemistry*. 282:6380–7.

Nislow, C., V.A. Lombillo, R. Kuriyama, and J.R. McIntosh. 1992. A plus-end-directed motor enzyme that moves antiparallel microtubules in vitro localizes to the interzone of mitotic spindles. *Nature*. 359:543–7.

Nishimura, T., and K. Kaibuchi. 2007. Numb controls integrin endocytosis for directional cell migration with aPKC and PAR-3. *Developmental cell*. 13:15–28.

Nobes, C.D., and A. Hall. 1995. Rho, rac, and cdc42 GTPases regulate the assembly of multimolecular focal complexes associated with actin stress fibers, lamellipodia, and filopodia. *Cell*. 81:53–62.

Norman, J.C., D. Jones, S.T. Barry, M.R. Holt, S. Cockcroft, and D.R. Critchley. 1998. ARF1 mediates paxillin recruitment to focal adhesions and potentiates Rho-stimulated stress fiber formation in intact and permeabilized Swiss 3T3 fibroblasts. *The Journal of cell biology*. 143:1981–95.

Obremski, V.J., A.M. Hall, and C. Fernandez-Valle. 1998. Merlin, the neurofibromatosis type 2 gene product, and beta1 integrin associate in isolated and differentiating Schwann cells. *Journal of neurobiology*. 37:487–501.

O'Connor, P. 2007. Natalizumab and the role of alpha 4-integrin antagonism in the treatment of multiple sclerosis. *Expert opinion on biological therapy*. 7:123–36.

Onodera, Y., J.-M. Nam, A. Hashimoto, J.C. Norman, H. Shirato, S. Hashimoto, and H. Sabe. 2012. Rab5c promotes AMAP1-PRKD2 complex formation to enhance β1 integrin recycling in EGF-induced cancer invasion. *The Journal of cell biology*. 197:983–96.

Palazzo, A.F., C.H. Eng, D.D. Schlaepfer, E.E. Marcantonio, and G.G. Gundersen. 2004. Localized stabilization of microtubules by integrin- and FAK-facilitated Rho signaling. *Science (New York, N.Y.)*. 303:836–9.

Palmer, K.J., H. Hughes, and D.J. Stephens. 2009. Specificity of cytoplasmic dynein subunits in discrete membrane-trafficking steps. *Molecular biology of the cell*. 20:2885–99.

Pankov, R. 2000. Integrin Dynamics and Matrix Assembly: Tensin-dependent Translocation of alpha5beta1 Integrins Promotes Early Fibronectin Fibrillogenesis. *The Journal of Cell Biology*. 148:1075–1090.

Parks, W.C. 1999. Matrix metalloproteinases in repair. *Wound repair and regeneration□: official publication of the Wound Healing Society [and] the European Tissue Repair Society*. 7:423–32.

Parks, W.C. 2007. What is the alpha2beta1 integrin doing in the epidermis? *The Journal of investigative dermatology*. 127:264–6.

Peden, A.A., E. Schonteich, J. Chun, J.R. Junutula, R.H. Scheller, and R. Prekeris. 2004. The RCP-Rab11 complex regulates endocytic protein sorting. *Molecular biology of the cell*. 15:3530–41.

Pelkmans, L., T. Bürli, M. Zerial, A. Helenius, and P. Lucas. 2004. Caveolin-stabilized membrane domains as multifunctional transport and sorting devices in endocytic membrane traffic. *Cell*. 118:767–780.

Pellinen, T., and J. Ivaska. 2006. Integrin traffic. *J Cell Sci*. 119:3723–3731.

Pellinen, T., A. Arjonen, K. Vuoriluoto, K. Kallio, J.A.M. Fransen, and J. Ivaska. 2006. Small GTPase Rab21 regulates cell adhesion and controls endosomal traffic of {beta}1-integrins. *J. Cell Biol.* 173:767–780.

Pellinen, T., S. Tuomi, A. Arjonen, M. Wolf, H. Edgren, H. Meyer, R. Grosse, T. Kitzing, J.K. Rantala, O. Kallioniemi, R. Fässler, M. Kallio, and J. Ivaska. 2008. Integrin trafficking regulated by Rab21 is necessary for cytokinesis. *Developmental cell*. 15:371–85.

Penheiter, S.G., R.D. Singh, C.E. Repellin, M.C. Wilkes, M. Edens, P.H. Howe, R.E. Pagano, and E.B. Leof. 2010. Type II transforming growth factor-beta receptor recycling is dependent upon the clathrin adaptor protein Dab2. *Molecular biology of the cell*. 21:4009–19.

Peralta, E.R., B.C. Martin, and A.L. Edinger. 2010. Differential effects of TBC1D15 and mammalian Vps39 on Rab7 activation state, lysosomal morphology, and growth factor dependence. *The Journal of biological chemistry*. 285:16814–21.

Perez, R.G., S. Soriano, J.D. Hayes, B. Ostaszewski, W. Xia, D.J. Selkoe, X. Chen, G.B. Stokin, and E.H. Koo. 1999. Mutagenesis identifies new signals for beta-amyloid precursor protein endocytosis, turnover, and the generation of secreted fragments, including Abeta42. *The Journal of biological chemistry*. 274:18851–6.

Pierini, L.M., M.A. Lawson, R.J. Eddy, B. Hendey, and F.R. Maxfield. 2000. Oriented endocytic recycling of alpha 5beta 1 in motile neutrophils. *Blood*. 95:2471–2480.

Pilcher, B.K., B.D. Sudbeck, J.A. Dumin, H.G. Welgus, and W.C. Parks. 1998. Collagenase-1 and collagen in epidermal repair. *Archives of dermatological research*. 290 Suppl:S37–46.

Pitaval, A., Q. Tseng, M. Bornens, and M. Théry. 2010. Cell shape and contractility regulate ciliogenesis in cell cycle–arrested cells. *The Journal of Cell Biology*. 191:303–312.

Poteryaev, D., S. Datta, K. Ackema, M. Zerial, and A. Spang. 2010. Identification of the switch in early-to-late endosome transition. *Cell*. 141:497–508.

Powelka, A.M., J. Sun, J. Li, M. Gao, L.M. Shaw, A. Sonnenberg, and V.W. Hsu. 2004. Stimulation-Dependent Recycling of Integrin β1 Regulated by ARF6 and Rab11. *Traffic*. 5:20–36.

Pucadyil, T.J., and S.L. Schmid. 2008. Real-time visualization of dynamin-catalyzed membrane fission and vesicle release. *Cell*. 135:1263–75.

R Development Core Team. R: A language and environment for statistical computing. 2011. R Foundation for Statistical Computing, Vienna, Austria.

Radel, C., M. Carlile-Klusacek, and V. Rizzo. 2007. Participation of caveolae in beta1 integrin-mediated mechanotransduction. *Biochemical and biophysical research communications*. 358:626–31.

Rajagopalan, M., J.L. Neidigh, and D.A. McClain. 1991. Amino acid sequences Gly-Pro-Leu-Tyr and Asn-Pro-Glu-Tyr in the submembranous domain of the insulin receptor are required for normal endocytosis. *The Journal of biological chemistry*. 266:23068–73.

Ramamurthy, B., W. Cao, E.M. De la Cruz, and M.S. Mooseker. 2012. Plus-end directed myosins accelerate actin filament sliding by single-headed myosin VI. *Cytoskeleton (Hoboken, N.J.)*. 69:59–69.

Rantala, J.K., J. Pouwels, T. Pellinen, S. Veltel, P. Laasola, E. Mattila, C.S. Potter, T. Duffy, J.P. Sundberg, O. Kallioniemi, J.A. Askari, M.J. Humphries, M. Parsons, M. Salmi, and J. Ivaska. 2011. SHARPIN is an endogenous inhibitor of β1-integrin activation. *Nature cell biology*. 13:1315–24.

Ramsay, A., J. Marshall, and I. Hart. 2007. Integrin trafficking and its role in cancer metastasis. *Cancer and Metastasis Reviews*. 26:567–578.

Rao, M. V, L.J. Engle, P.S. Mohan, A. Yuan, D. Qiu, A. Cataldo, L. Hassinger, S. Jacobsen, V.M.-Y. Lee, A. Andreadis, J.-P. Julien, P.C. Bridgman, and R.A. Nixon. 2002. Myosin Va binding to neurofilaments is essential for correct myosin Va distribution and transport and neurofilament density. *The Journal of cell biology*. 159:279–90.

Rapali, P., Á. Szenes, L. Radnai, A. Bakos, G. Pál, and L. Nyitray. 2011. DYNLL/LC8: a light chain subunit of the dynein motor complex and beyond. *The FEBS journal*. 278:2980–96.

Rapaport, D., Y. Lugassy, E. Sprecher, and M. Horowitz. 2010. Loss of SNAP29 impairs endocytic recycling and cell motility. *PloS one*. 5:e9759.

Reszka, A.A., Y. Hayashi, and A.F. Horwitz. 1992. Identification of amino acid sequences in the integrin beta 1 cytoplasmic domain implicated in cytoskeletal association. *The Journal of cell biology*. 117:1321–30.

Ridley, A.J., H.F. Paterson, C.L. Johnston, D. Diekmann, and A. Hall. 1992. The small GTP-binding protein rac regulates growth factor-induced membrane ruffling. *Cell*. 70:401–10.

Riederer, M.A., T. Soldati, A.D. Shapiro, J. Lin, and S.R. Pfeffer. 1994. Lysosome biogenesis requires Rab9 function and receptor recycling from endosomes to the trans-Golgi network. *The Journal of cell biology*. 125:573–82.

Riggs, K.A., N. Hasan, D. Humphrey, C. Raleigh, C. Nevitt, D. Corbin, and C. Hu. 2012. Regulation of Integrin Endocytic Recycling and Chemotactic Cell Migration by Syntaxin 6 and VAMP3 Interaction. *Journal of cell science*.

Riikonen, T., P. Vihinen, M. Potila, W. Rettig, and J. Heino. 1995. Antibody against human alpha 1 beta 1 integrin inhibits HeLa cell adhesion to laminin and to type I, IV, and V collagens. *Biochemical and biophysical research communications*. 209:205–12.

Rink, J., E. Ghigo, Y. Kalaidzidis, and M. Zerial. 2005. Rab conversion as a mechanism of progression from early to late endosomes. *Cell*. 122:735–49.

Rinnerthaler, G., B. Geiger, and J. V Small. 1988. Contact formation during fibroblast locomotion: involvement of membrane ruffles and microtubules. *The Journal of cell biology*. 106:747–60.

Rintanen, N., M. Karjalainen, J. Alanko, L. Paavolainen, A. Mäki, L. Nissinen, M. Lehkonen, K. Kallio, R.H. Cheng, P. Upla, J. Ivaska, and V. Marjomäki. 2012. Calpains promote α2β1 integrin turnover in nonrecycling integrin pathway. *Molecular biology of*

the cell. 23:448–63.

Roberts, M., S. Barry, A. Woods, P. van der Sluijs, J. Norman, and G. Dev. 2001. PDGF-regulated rab4-dependent recycling of alphavbeta3 integrin from early endosomes is necessary for cell adhesion and spreading. *Current biology□: CB*. 11:1392–402.

Roberts, M.S., A.J. Woods, T.C. Dale, P. Van Der Sluijs, and J.C. Norman. 2004. Protein kinase B/Akt acts via glycogen synthase kinase 3 to regulate recycling of alpha v beta 3 and alpha 5 beta 1 integrins. *Molecular and cellular biology*. 24:1505–15.

Roivainen, M., L. Piirainen, T. Hovi, I. Virtanen, T. Riikonen, J. Heino, and T. Hyypiä. 1994. Entry of coxsackievirus A9 into host cells: specific interactions with alpha v beta 3 integrin, the vitronectin receptor. *Virology*. 203:357–65.

Roostalu, J., C. Hentrich, P. Bieling, I.A. Telley, E. Schiebel, and T. Surrey. 2011. Directional switching of the kinesin Cin8 through motor coupling. *Science (New York, N.Y.)*. 332:94–9.

Rottner, K., A. Hall, and J. V Small. 1999. Interplay between Rac and Rho in the control of substrate contact dynamics. *Current biology□: CB*. 9:640–8.

Sakakibara, H., and K. Oiwa. 2011. Molecular organization and force-generating mechanism of dynein. *The FEBS journal*. 278:2964–79.

Schaller, M., and J. Parsons. 1995. pp125FAK-dependent tyrosine phosphorylation of paxillin creates a high- affinity binding site for Crk. *Mol. Cell. Biol.* 15:2635–2645.

Schaller, M.D. 2001. Paxillin: a focal adhesion-associated adaptor protein. *Oncogene*. 20:6459–72.

Schiller, M., D. Javelaud, and A. Mauviel. 2004. TGF-beta-induced SMAD signaling and gene regulation: consequences for extracellular matrix remodeling and wound healing. *Journal of dermatological science*. 35:83–92.

Schmidt-Glenewinkel, H., E. Reinz, R. Eils, and N.R. Brady. 2009. Systems Biological Analysis of Epidermal Growth Factor Receptor Internalization Dynamics for Altered Receptor Levels. *The Journal of Biological Chemistry*. 284:17243–17252.

Schmidt-Glenewinkel, H., E. Reinz, S. Bulashevska, J. Beaudouin, S. Legewie, A. Alonso, and R. Eils. 2012. Multiparametric image analysis reveals role of Caveolin1 in endosomal progression rather than internalization of EGFR. *FEBS letters*. 586:1179–89.

Schober, M., S. Raghavan, M. Nikolova, L. Polak, H.A. Pasolli, H.E. Beggs, L.F. Reichardt, and E. Fuchs. 2007. Focal adhesion kinase modulates tension signaling to control actin and focal adhesion dynamics. *The Journal of cell biology*. 176:667–80.

Schwartz, M.A. 2010. Integrins and extracellular matrix in mechanotransduction. *Cold Spring Harbor perspectives in biology*. 2:a005066.

Schwartz, S.L., C. Cao, O. Pylypenko, A. Rak, and A. Wandinger-Ness. 2007. Rab GTPases at a glance. *J Cell Sci*. 120:3905–10.

Segev, N. 2001. Ypt/rab gtpases: regulators of protein trafficking. *Science's STKE□: signal transduction knowledge environment*. 2001:re11.

Serafini, T., L. Orci, M. Amherdt, M. Brunner, R.A. Kahn, and J.E. Rothman. 1991. ADP-ribosylation factor is a subunit of the coat of Golgi-derived COP-coated vesicles: a novel role for a GTP-binding protein. *Cell*. 67:239–53.

Shi, F., and J. Sottile. 2008. Caveolin-1-dependent beta1 integrin endocytosis is a critical regulator of fibronectin turnover. *Journal of cell science*. 121:2360–71.

Shields, S.B., and R.C. Piper. 2011. How ubiquitin functions with ESCRTs. *Traffic (Copenhagen, Denmark)*. 12:1306–17.

Shin, G., T.-W. Kang, S. Yang, S.-J. Baek, Y.-S. Jeong, and S.-Y. Kim. 2011.

GENT: gene expression database of normal and tumor tissues. *Cancer informatics*. 10:149–57.

Shin, S., L. Wolgamott, and S.-O. Yoon. 2012. Integrin trafficking and tumor progression. *International journal of cell biology*. 2012:516789.

Sigismund, S., T. Woelk, C. Puri, E. Maspero, C. Tacchetti, P. Transidico, P.P. Di Fiore, and S. Polo. 2005. Clathrin-independent endocytosis of ubiquitinated cargos. *Proceedings of the National Academy of Sciences of the United States of America*. 102:2760–5.

Silletti, S., T. Kessler, J. Goldberg, D.L. Boger, and D.A. Cheresh. 2001. Disruption of matrix metalloproteinase 2 binding to integrin alpha vbeta 3 by an organic molecule inhibits angiogenesis and tumor growth in vivo. *Proceedings of the National Academy of Sciences of the United States of America*. 98:119–24.

Simpson, K.J., L.M. Selfors, J. Bui, A. Reynolds, D. Leake, A. Khvorova, and J.S. Brugge. 2008. Identification of genes that regulate epithelial cell migration using an siRNA screening approach. *Nature cell biology*. 10:1027–38.

Simpson, J.C., B. Joggerst, V. Laketa, F. Verissimo, C. Cetin, H. Erfle, M.G. Bexiga, V.R. Singan, J.-K. Hériché, B. Neumann, A. Mateos, J. Blake, S. Bechtel, V. Benes, S. Wiemann, J. Ellenberg, and R. Pepperkok. 2012. Genome-wide RNAi screening identifies human proteins with a regulatory function in the early secretory pathway. *Nature cell biology*. 14:764–74.

Skalski, M., and M.G. Coppolino. 2005. SNARE-mediated trafficking of alpha5beta1 integrin is required for spreading in CHO cells. *Biochemical and biophysical research communications*. 335:1199–210.

Van der Sluijs, P., M. Hull, P. Webster, P. Mâle, B. Goud, and I. Mellman. 1992. The small GTP-binding protein rab4 controls an early sorting event on the endocytic pathway. *Cell*. 70:729–40.

Smoot, M.E., K. Ono, J. Ruscheinski, P.-L. Wang, and T. Ideker. 2011. Cytoscape 2.8: new features for data integration and network visualization. *Bioinformatics (Oxford, England)*. 27:431–2.

Snijder, B., R. Sacher, P. Ramo, E.-M. Damm, P. Liberali, and L. Pelkmans. 2009. Population context determines cell-to-cell variability in endocytosis and virus infection. *Nature*. 461:520–523.

Sottile, J., and J. Chandler. 2005. Fibronectin matrix turnover occurs through a caveolin-1-dependent process. *Molecular biology of the cell*. 16:757–68.

Stamenkovic, I., and Q. Yu. 2010. Merlin, a "magic" linker between extracellular cues and intracellular signaling pathways that regulate cell motility, proliferation, and survival. *Current protein & peptide science*. 11:471–84.

Starkuviene, V., U. Liebel, J.C. Simpson, H. Erfle, A. Poustka, S. Wiemann, and R. Pepperkok. 2004. High-content screening microscopy identifies novel proteins with a putative role in secretory membrane traffic. *Genome research*. 14:1948–1956.

Stenmark, H. 2009. Rab GTPases as coordinators of vesicle traffic. *Nature reviews. Molecular cell biology*. 10:513–25.

Stewart PL, Nemerow GR. Cell integrins: commonly used receptors for diverse viral pathogens. Trends in microbiology. 2007 Nov;15(11):500-7.

Stupack, D.G. 2002. Get a ligand, get a life: integrins, signaling and cell survival. *Journal of Cell Science*. 115:3729–3738.

Styers, M.L., G. Salazar, R. Love, A.A. Peden, A.P. Kowalczyk, and V. Faundez. 2004. The endo-lysosomal sorting machinery interacts with the intermediate filament

cytoskeleton. *Molecular biology of the cell*. 15:5369–82.

Sweeney, H.L., and A. Houdusse. 2010. Myosin VI rewrites the rules for myosin motors. *Cell*. 141:573–82.

Sönnichsen, B., S. De Renzis, E. Nielsen, J. Rietdorf, and M. Zerial. 2000. Distinct membrane domains on endosomes in the recycling pathway visualized by multicolor imaging of Rab4, Rab5, and Rab11. *The Journal of cell biology*. 149:901–14.

Taddei, M.L., E. Giannoni, T. Fiaschi, and P. Chiarugi. 2012. Anoikis: an emerging hallmark in health and diseases. *The Journal of pathology*. 226:380–93.

Takeda, T., H. Yamazaki, and M.G. Farquhar. 2003. Identification of an apical sorting determinant in the cytoplasmic tail of megalin. *American journal of physiology. Cell physiology*. 284:C1105–13.

Takino, T., H. Saeki, H. Miyamori, T. Kudo, and H. Sato. 2007. Inhibition of membrane-type 1 matrix metalloproteinase at cell-matrix adhesions. *Cancer research*. 67:11621–9.

Tamariz, E., and F. Grinnell. 2002. Modulation of fibroblast morphology and adhesion during collagen matrix remodeling. *Molecular biology of the cell*. 13:3915–29.

Tanenbaum, M.E., L. Macůrek, A. Janssen, E.F. Geers, M. Alvarez-Fernández, and R.H. Medema. 2009. Kif15 cooperates with eg5 to promote bipolar spindle assembly. *Current biology□: CB*. 19:1703–11.

Teckchandani, A., N. Toida, J. Goodchild, C. Henderson, J. Watts, B. Wollscheid, and J.A. Cooper. 2009. Quantitative proteomics identifies a Dab2/integrin module regulating cell migration. *The Journal of cell biology*. 186:99–111.

Teckchandani, A., E.E. Mulkearns, T.W. Randolph, N. Toida, and J.A. Cooper. 2012. The clathrin adaptor Dab2 recruits EH domain scaffold proteins to regulate integrin β1 endocytosis. *Molecular biology of the cell*. 23:2905–16.

Theisen, U., E. Straube, and A. Straube. 2012. Directional Persistence of Migrating Cells Requires Kif1C-Mediated Stabilization of Trailing Adhesions. *Developmental Cell*. 23:1153–1166.

Théry, M., V. Racine, M. Piel, A. Pépin, A. Dimitrov, Y. Chen, J.-B. Sibarita, and M. Bornens. 2006. Anisotropy of cell adhesive microenvironment governs cell internal organization and orientation of polarity. *Proceedings of the National Academy of Sciences of the United States of America*. 103:19771–6.

Thomas, G.J., M.P. Lewis, I.R. Hart, J.F. Marshall, and P.M. Speight. 2001. AlphaVbeta6 integrin promotes invasion of squamous carcinoma cells through up-regulation of matrix metalloproteinase-9. *International journal of cancer. Journal international du cancer*. 92:641–50.

Thrower, J.S., L. Hoffman, M. Rechsteiner, and C.M. Pickart. 2000. Recognition of the polyubiquitin proteolytic signal. *The EMBO journal*. 19:94–102.

Tiwari S, Askari JA, Humphries MJ, Bulleid NJ. Divalent cations regulate the folding and activation status of integrins during their intracellular trafficking. Journal of cell science. 2011 Apr;:jcs.084483-.

Tiwari, A., J.-J. Jung, S.M. Inamdar, C.O. Brown, A. Goel, and A. Choudhury. 2011. Endothelial cell migration on fibronectin is regulated by syntaxin 6-mediated alpha5beta1 integrin recycling. *The Journal of biological chemistry*. 286:36749–61.

Torgler, C.N., M. Narasimha, A.L. Knox, C.G. Zervas, M.C. Vernon, and N.H. Brown. 2004. Tensin stabilizes integrin adhesive contacts in Drosophila. *Developmental cell*. 6:357–69.

Traub, L.M. 2005. Common principles in clathrin-mediated sorting at the Golgi

and the plasma membrane. *Biochimica et biophysica acta*. 1744:415–37.

Tringali, C., B. Lupo, I. Silvestri, N. Papini, L. Anastasia, G. Tettamanti, and B. Venerando. 2012. The plasma membrane sialidase NEU3 regulates the malignancy of renal carcinoma cells by controlling β1 integrin internalization and recycling. *The Journal of biological chemistry*. 287:42835–45.

Tuckwell, D., D.A. Calderwood, L.J. Green, and M.J. Humphries. 1995. Integrin alpha 2 I-domain is a binding site for collagens. *Journal of cell science*. 108 (Pt 4:1629–37.

Ullrich, O., S. Reinsch, S. Urbé, M. Zerial, and R.G. Parton. 1996. Rab11 regulates recycling through the pericentriolar recycling endosome. *The Journal of cell biology*. 135:913–24.

Upla, P., V. Marjomaki, P. Kankaanpaa, J. Ivaska, T. Hyypia, F.G. van der Goot, and J. Heino. 2004. Clustering Induces a Lateral Redistribution of {alpha}2{beta}1 Integrin from Membrane Rafts to Caveolae and Subsequent Protein Kinase C-dependent Internalization. *Mol. Biol. Cell*. 15:625–636.

Valdembri, D., P.T. Caswell, K.I. Anderson, J.P. Schwarz, I. König, E. Astanina, F. Caccavari, J.C. Norman, M.J. Humphries, F. Bussolino, and G. Serini. 2009. Neuropilin-1/GIPC1 signaling regulates alpha5beta1 integrin traffic and function in endothelial cells. *PLoS biology*. 7:e25.

Vale, R.D. 2003. The Molecular Motor Toolbox for Intracellular Transport. *Cell*. 112:467–480.

Vassilieva, E. V, K. Gerner-Smidt, A.I. Ivanov, and A. Nusrat. 2008. Lipid rafts mediate internalization of beta1-integrin in migrating intestinal epithelial cells. *American journal of physiology. Gastrointestinal and liver physiology*. 295:G965–76.

Vasiliev, J.M., I.M. Gelfand, L. V Domnina, O.Y. Ivanova, S.G. Komm, and L. V Olshevskaja. 1970. Effect of colcemid on the locomotory behaviour of fibroblasts. *Journal of embryology and experimental morphology*. 24:625–40.

Veale, K.J., C. Offenhäuser, S.P. Whittaker, R.P. Estrella, and R.Z. Murray. 2010. Recycling endosome membrane incorporation into the leading edge regulates lamellipodia formation and macrophage migration. *Traffic (Copenhagen, Denmark)*. 1370–1379.

Vignoud, L., Y. Usson, F. Balzac, G. Tarone, and M.R. Block. 1994. Internalization of the alpha 5 beta 1 integrin does not depend on “NPXY” signals. *Biochemical and biophysical research communications*. 199:603–11.

Wagner, S., C.J. Storbeck, K. Roovers, Z.Y. Chaar, P. Kolodziej, M. McKay, and L.A. Sabourin. 2008. FAK/src-family dependent activation of the Ste20-like kinase SLK is required for microtubule-dependent focal adhesion turnover and cell migration. *PloS one*. 3:e1868.

Wang, B., T. Mysliwiec, S.M. Feller, B. Knudsen, H. Hanafusa, and G.D. Kruh. 1996. Proline-rich sequences mediate the interaction of the Arg protein tyrosine kinase with Crk. *Oncogene*. 13:1379–85.

Wang, C., Y. Yoo, H. Fan, E. Kim, K.-L. Guan, and J.-L. Guan. 2010. Regulation of Integrin β 1 recycling to lipid rafts by Rab1a to promote cell migration. *The Journal of biological chemistry*. 285:29398–405.

Wang, X., R. Kumar, J. Navarre, J.E. Casanova, and J.R. Goldenring. 2000. Regulation of vesicle trafficking in madin-darby canine kidney cells by Rab11a and Rab25. *The Journal of biological chemistry*. 275:29138–46.

Wang, Z., J.G. Edwards, N. Riley, D.W. Provance, R. Karcher, X.-D. Li, I.G.

Davison, M. Ikebe, J.A. Mercer, J.A. Kauer, and M.D. Ehlers. 2008. Myosin Vb mobilizes recycling endosomes and AMPA receptors for postsynaptic plasticity. *Cell*. 135:535–48.

Watanabe, S., K. Mabuchi, R. Ikebe, and M. Ikebe. 2006. Mechanoenzymatic characterization of human myosin Vb. *Biochemistry*. 45:2729–38.

Watt, F.M. 2002. Role of integrins in regulating epidermal adhesion, growth and differentiation. *The EMBO journal*. 21:3919–26.

Weisenberg, R.C. 1972. Microtubule Formation in vitro in Solutions Containing Low Calcium Concentrations. *Science*. 177:1104–1105.

Wickström, S.A., A. Lange, E. Montanez, and R. Fässler. 2010. The ILK/PINCH/parvin complex: the kinase is dead, long live the pseudokinase! *The EMBO journal*. 29:281–91.

Wiesner, C., J. Faix, M. Himmel, F. Bentzien, and S. Linder. 2010. KIF5B and KIF3A/KIF3B kinesins drive MT1-MMP surface exposure, CD44 shedding, and extracellular matrix degradation in primary macrophages. *Blood*. 116:1559–69.

Winograd-Katz, S.E., S. Itzkovitz, Z. Kam, and B. Geiger. 2009. Multiparametric analysis of focal adhesion formation by RNAi-mediated gene knockdown. *The Journal of cell biology*. 186:423–36.

Wittmann, T., H. Boleti, C. Antony, E. Karsenti, and I. Vernos. 1998. Localization of the kinesin-like protein Xklp2 to spindle poles requires a leucine zipper, a microtubule-associated protein, and dynein. *The Journal of cell biology*. 143:673–85.

Wong, E., and A.M. Cuervo. 2010. Integration of clearance mechanisms: the proteasome and autophagy. *Cold Spring Harbor perspectives in biology*. 2:a006734.

Woods, A.J., D.P. White, P.T. Caswell, and J.C. Norman. 2004. PKD1/PKCmu promotes alphavbeta3 integrin recycling and delivery to nascent focal adhesions. *The EMBO journal*. 23:2531–43.

Xiong, J.-P., T. Stehle, S.L. Goodman, and M.A. Arnaout. 2003. New insights into the structural basis of integrin activation. *Blood*. 102:1155–9.

Yang, J.T., H. Rayburn, and R.O. Hynes. 1993. Embryonic mesodermal defects in alpha 5 integrin-deficient mice. *Development (Cambridge, England)*. 119:1093–105.

Yeaman, C., M.I. Ayala, J.R. Wright, F. Bard, C. Bossard, A. Ang, Y. Maeda, T. Seufferlein, I. Mellman, W.J. Nelson, and V. Malhotra. 2004. Protein kinase D regulates basolateral membrane protein exit from trans-Golgi network. *Nature cell biology*. 6:106–12.

Yeo, M.G., and W.K. Song. 2008. v-Crk regulates membrane dynamics and Rac activation. *Cell adhesion & migration*. 2:174–6.

Zaidel-Bar, R., S. Itzkovitz, A. Ma'ayan, R. Iyengar, and B. Geiger. 2007. Functional atlas of the integrin adhesome. *Nat Cell Biol*. 9:858–867.

Zaidel-Bar, R., Z. Kam, and B. Geiger. 2005. Polarized downregulation of the paxillin-p130CAS-Rac1 pathway induced by shear flow. *Journal of cell science*. 118:3997–4007.

Zeigerer, A., J. Gilleron, R.L. Bogorad, G. Marsico, H. Nonaka, S. Seifert, H. Epstein-Barash, S. Kuchimanchi, C.G. Peng, V.M. Ruda, P. Del Conte-Zerial, J.G. Hengstler, Y. Kalaidzidis, V. Koteliansky, and M. Zerial. 2012. Rab5 is necessary for the biogenesis of the endolysosomal system in vivo. *Nature*. 485:465–70.

Zerial, M., and H. McBride. 2001. Rab proteins as membrane organizers. *Nat Rev Mol Cell Biol*. 2:107–117.

Zervas, C.G., S.L. Gregory, and N.H. Brown. 2001. Drosophila integrin-linked

kinase is required at sites of integrin adhesion to link the cytoskeleton to the plasma membrane. *The Journal of cell biology*. 152:1007–18.

Zhang, Z.-G., I. Bothe, F. Hirche, M. Zweers, D. Gullberg, G. Pfitzer, T. Krieg, B. Eckes, and M. Aumailley. 2006. Interactions of primary fibroblasts and keratinocytes with extracellular matrix proteins: contribution of {alpha}2{beta}1 integrin. *J Cell Sci*. 119:1886–1895.

Zhang, H., J.S. Berg, Z. Li, Y. Wang, P. Lång, A.D. Sousa, A. Bhaskar, R.E. Cheney, and S. Strömblad. 2004. Myosin-X provides a motor-based link between integrins and the cytoskeleton. *Nature cell biology*. 6:523–31.

Zhu, C., E. Bossy-Wetzel, and W. Jiang. 2005a. Recruitment of MKLP1 to the spindle midzone/midbody by INCENP is essential for midbody formation and completion of cytokinesis in human cells. *The Biochemical journal*. 389:373–81.

Zhu, C., J. Zhao, M. Bibikova, J.D. Leverson, E. Bossy-Wetzel, J.-B. Fan, R.T. Abraham, and W. Jiang. 2005b. Functional analysis of human microtubule-based motor proteins, the kinesins and dyneins, in mitosis/cytokinesis using RNA interference. *Molecular biology of the cell*. 16:3187–99.

Zhu, J.-X., S. Goldoni, G. Bix, R.T. Owens, D.J. McQuillan, C.C. Reed, and R. V Iozzo. 2005c. Decorin evokes protracted internalization and degradation of the epidermal growth factor receptor via caveolar endocytosis. *The Journal of biological chemistry*. 280:32468–79.

Zoncu, R., R.M. Perera, D.M. Balkin, M. Pirruccello, D. Toomre, and P. De Camilli. 2009. A Phosphoinositide Switch Controls the Maturation and Signaling Properties of APPL Endosomes. *Cell*. 136:1110–1121.

Appendix

Appendix I. List of genes tested in the primary screening for regulators of integrin α2 internalization

Gene ID and gene information is given according to http://www.ncbi.nlm.nih.gov/gene/

Gene ontology annotations (GO) are given according to http://www.ebi.ac.uk/GOA/

Gene ID	Gene symbol	Gene description	GO, Molecular Function
25	**ABL1**	c-abl oncogene 1, receptor tyrosine kinase	magnesium ion binding, protein kinase activity, adenyl ribonucleotide binding, transition metal ion binding
27	**ABL2**	v-abl Abelson murine leukemia viral oncogene homolog 2 (arg, Abelson-related gene)	magnesium ion binding, protein kinase activity, adenyl ribonucleotide binding, transition metal ion binding
29	**ABR**	active BCR-related gene	Ras guanyl-nucleotide exchange factor activity
60	**ACTB**	actin, beta	protein kinase binding, adenyl ribonucleotide binding
87	**ACTN1**	actinin, alpha 1	calcium ion binding, actin filament binding
81	**ACTN4**	actinin, alpha 4	calcium ion binding, actin filament binding
11214	**AKAP13**	A kinase (PRKA) anchor protein 13	protein kinase activity, Ras guanyl-nucleotide exchange factor activity, transition metal ion binding
57679	**ALS2**	amyotrophic lateral sclerosis 2 (juvenile)	Ras guanyl-nucleotide exchange factor activity, Rab GTPase binding, small GTPase binding, protein serine/threonine kinase activator activity
302	**ANXA2**	annexin A2 pseudogene 3; annexin A2; annexin A2 pseudogene 1	
162	**AP1B1**	adaptor-related protein complex 1, beta 1 subunit	
324	**APC**	adenomatous polyposis coli	microtubule binding, protein kinase binding

Gene ID	Gene symbol	Gene description	GO, Molecular Function
10297	**APC2**	adenomatosis polyposis coli 2	microtubule binding
116985	**ARAP1**	ArfGAP with RhoGAP domain, ankyrin repeat and PH domain 1	
116984	**ARAP2**	ArfGAP with RhoGAP domain, ankyrin repeat and PH domain 2	
64411	**ARAP3**	ArfGAP with RhoGAP domain, ankyrin repeat and PH domain 3	
375	**ARF1**	ADP-ribosylation factor 1	pyrophosphatase activity, guanyl ribonucleotide binding
392	**ARHGAP1**	Rho GTPase activating protein 1	Ras GTPase activator activity, Rho GTPase activator activity
79658	**ARHGAP10**	Rho GTPase activating protein 10	Ras GTPase activator activity, Rho GTPase activator activity
9824	**ARHGAP11**	Rho GTPase activating protein 11B; Rho GTPase activating protein 11A	
94134	**ARHGAP12**	Rho GTPase activating protein 12	
55843	**ARHGAP15**	Rho GTPase activating protein 15	
55114	**ARHGAP17**	Rho GTPase activating protein 17	
93663	**ARHGAP18**	Rho GTPase activating protein 18	
84986	**ARHGAP19**	Rho GTPase activating protein 19	
57569	**ARHGAP20**	Rho GTPase activating protein 20	
58504	**ARHGAP22**	Rho GTPase activating protein 22	
57636	**ARHGAP23**	Rho GTPase activating protein 23	
83478	**ARHGAP24**	Rho GTPase activating protein 24	
9938	**ARHGAP25**	Rho GTPase activating protein 25	
23092	**ARHGAP26**	Rho GTPase activating protein 26	Ras GTPase activator activity, Rho GTPase activator activity

Gene ID	Gene symbol	Gene description	GO, Molecular Function
201176	**ARHGAP27**	Rho GTPase activating protein 27	Ras GTPase activator activity, Rho GTPase activator activity
79822	**ARHGAP28**	Rho GTPase activating protein 28	
9411	**ARHGAP29**	Rho GTPase activating protein 29	Ras GTPase activator activity, Rho GTPase activator activity, transition metal ion binding
57514	**ARHGAP31**	Cdc42 GTPase-activating protein	
9743	**ARHGAP32**	Rho GTPase-activating protein	
115703	**ARHGAP33**	sorting nexin 26	Ras GTPase activator activity, Rho GTPase activator activity
80728	**ARHGAP39**	Rho GTPase activating protein 39	
393	**ARHGAP4**	Rho GTPase activating protein 4	Ras GTPase activator activity, Rho GTPase activator activity
394	**ARHGAP5**	Rho GTPase activating protein 5	Ras GTPase activator activity, Rho GTPase activator activity, pyrophosphatase activity, guanyl ribonucleotide binding
395	**ARHGAP6**	Rho GTPase activating protein 6	Ras GTPase activator activity, Rho GTPase activator activity
23779	**ARHGAP8**	Rho GTPase activating protein 8; proline rich 5 (renal); PRR5-ARHGAP8 fusion	
64333	**ARHGAP9**	Rho GTPase activating protein 9	
396	**ARHGDIA**	Rho GDP dissociation inhibitor (GDI) alpha	GDP-dissociation inhibitor activity
397	**ARHGDIB**	Rho GDP dissociation inhibitor (GDI) beta	GDP-dissociation inhibitor activity
398	**ARHGDIG**	Rho GDP dissociation inhibitor (GDI) gamma	GDP-dissociation inhibitor activity
9138	**ARHGEF1**	Rho guanine nucleotide exchange factor (GEF) 1	Ras guanyl-nucleotide exchange factor activity
9639	**ARHGEF10**	Rho guanine nucleotide exchange factor (GEF) 10	Ras guanyl-nucleotide exchange factor activity
55160	**ARHGEF10L**	Rho guanine nucleotide exchange factor (GEF) 10-like	Ras guanyl-nucleotide exchange factor activity, Ras GTPase activator activity, Rho GTPase activator activity

Gene ID	Gene symbol	Gene description	GO, Molecular Function
9826	**ARHGEF11**	Rho guanine nucleotide exchange factor (GEF) 11	Ras guanyl-nucleotide exchange factor activity
23365	**ARHGEF12**	Rho guanine nucleotide exchange factor (GEF) 12	Ras guanyl-nucleotide exchange factor activity
22899	**ARHGEF15**	Rho guanine nucleotide exchange factor (GEF) 15	Ras guanyl-nucleotide exchange factor activity
27237	**ARHGEF16**	Rho guanine exchange factor (GEF) 16	Ras guanyl-nucleotide exchange factor activity
9828	**ARHGEF17**	Rho guanine nucleotide exchange factor (GEF) 17	Ras guanyl-nucleotide exchange factor activity
23370	**ARHGEF18**	Rho/Rac guanine nucleotide exchange factor (GEF) 18	Ras guanyl-nucleotide exchange factor activity
9181	**ARHGEF2**	Rho/Rac guanine nucleotide exchange factor (GEF) 2	Ras guanyl-nucleotide exchange factor activity, microtubule binding, small GTPase binding, transition metal ion binding
115557	**ARHGEF25**	Rho guanine nucleotide exchange factor (GEF) 25	Ras guanyl-nucleotide exchange factor activity
50650	**ARHGEF3**	Rho guanine nucleotide exchange factor (GEF) 3	Ras guanyl-nucleotide exchange factor activity
50649	**ARHGEF4**	Rho guanine nucleotide exchange factor (GEF) 4	Ras guanyl-nucleotide exchange factor activity
7984	**ARHGEF5**	Rho guanine nucleotide exchange factor (GEF) 5	Ras guanyl-nucleotide exchange factor activity, guanyl ribonucleotide binding
9459	**ARHGEF6**	Rac/Cdc42 guanine nucleotide exchange factor (GEF) 6	Ras guanyl-nucleotide exchange factor activity
8874	**ARHGEF7**	Rho guanine nucleotide exchange factor (GEF) 7	Ras guanyl-nucleotide exchange factor activity

Gene ID	Gene symbol	Gene description	GO, Molecular Function
23229	**ARHGEF9**	Cdc42 guanine nucleotide exchange factor (GEF) 9; hypothetical protein LOC100134381	Ras guanyl-nucleotide exchange factor activity
50807	**ASAP1**	ArfGAP with SH3 domain, ankyrin repeat and PH domain 1	ARF GTPase activator activity, transition metal ion binding
9564	**BCAR1**	similar to breast cancer anti-estrogen resistance 1; breast cancer anti-estrogen resistance 1	protein kinase binding, protein phosphatase binding
613	**BCR**	breakpoint cluster region	protein kinase activity, Ras guanyl-nucleotide exchange factor activity, adenyl ribonucleotide binding
811	**CALR**	calreticulin	calcium ion binding, nuclear hormone receptor binding, transition metal ion binding
821	**CANX**	calnexin	calcium ion binding
823	**CAPN1**	calpain 1, (mu/I) large subunit	endopeptidase activity, calcium ion binding, cysteine-type peptidase activity
824	**CAPN2**	calpain 2, (m/II) large subunit	endopeptidase activity, calcium ion binding, cysteine-type peptidase activity
826	**CAPNS1**	calpain, small subunit 1	endopeptidase activity, calcium ion binding, cysteine-type peptidase activity
857	**CAV1**	caveolin 1, caveolae protein, 22kDa	cholesterol binding
858	**CAV2**	caveolin 2	protein kinase activity, dopamine receptor binding
867	**CBL**	Cas-Br-M (murine) ecotropic retroviral transforming sequence	calcium ion binding, small conjugating protein ligase activity, transition metal ion binding
977	**CD151**	CD151 molecule (Raph blood group)	
975	**CD81**	CD81 molecule	
998	**CDC42**	cell division cycle 42 (GTP binding protein, 25kDa); cell division cycle 42 pseudogene 2	pyrophosphatase activity, guanyl ribonucleotide binding
1062	**CENPE**	centromere protein E, 312kDa	pyrophosphatase activity, protein kinase binding, adenyl ribonucleotide binding

Gene ID	Gene symbol	Gene description	GO, Molecular Function
1072	**CFL1**	cofilin 1 (non-muscle)	
1123	**CHN1**	chimerin (chimaerin) 1	transition metal ion binding
1124	**CHN2**	chimerin (chimaerin) 2	transition metal ion binding
10519	**CIB1**	calcium and integrin binding 1 (calmyrin)	calcium ion binding
9793	**CKAP5**	cytoskeleton associated protein 5	
23332	**CLASP1**	cytoplasmic linker associated protein 1	microtubule binding
23122	**CLASP2**	cytoplasmic linker associated protein 2	microtubule binding, fucosyltransferase activity
6249	**CLIP1**	CAP-GLY domain containing linker protein 1	microtubule binding, transition metal ion binding
7461	**CLIP2**	CAP-GLY domain containing linker protein 2	microtubule binding
1213	**CLTC**	clathrin, heavy chain (Hc)	
1398	**CRK**	v-crk sarcoma virus CT10 oncogene homolog (avian)	
1399	**CRKL**	v-crk sarcoma virus CT10 oncogene homolog (avian)-like	protein kinase activity
1445	**CSK**	c-src tyrosine kinase	protein kinase activity, adenyl ribonucleotide binding
1465	**CSRP1**	cysteine and glycine-rich protein 1	transition metal ion binding
1639	**DCTN1**	dynactin 1 (p150, glued homolog, Drosophila)	pyrophosphatase activity
1729	**DIAPH1**	diaphanous homolog 1 (Drosophila)	small GTPase binding
1730	**DIAPH2**	diaphanous homolog 2 (Drosophila)	small GTPase binding
81624	**DIAPH3**	diaphanous homolog 3 (Drosophila)	small GTPase binding
10395	**DLC1**	deleted in liver cancer 1	Ras GTPase activator activity, Rho GTPase activator activity
1759	**DNM1**	dynamin 1	pyrophosphatase activity, guanyl ribonucleotide binding

Gene ID	Gene symbol	Gene description	GO, Molecular Function
1785	**DNM2**	dynamin 2	microtubule binding, pyrophosphatase activity, guanyl ribonucleotide binding
23268	**DNMBP**	dynamin binding protein	Ras guanyl-nucleotide exchange factor activity
1793	**DOCK1**	dedicator of cytokinesis 1	
55619	**DOCK10**	dedicator of cytokinesis 10	Ras guanyl-nucleotide exchange factor activity, small GTPase binding, guanyl ribonucleotide binding
139818	**DOCK11**	dedicator of cytokinesis 11	guanyl ribonucleotide binding
1794	**DOCK2**	dedicator of cytokinesis 2	Ras guanyl-nucleotide exchange factor activity, Ras GTPase activator activity, Rho GTPase activator activity, transition metal ion binding
1795	**DOCK3**	dedicator of cytokinesis 3	guanyl ribonucleotide binding
9732	**DOCK4**	dedicator of cytokinesis 4	Ras GTPase activator activity, Rho GTPase activator activity, small GTPase binding
80005	**DOCK5**	dedicator of cytokinesis 5	
57572	**DOCK6**	dedicator of cytokinesis 6	guanyl ribonucleotide binding
85440	**DOCK7**	dedicator of cytokinesis 7	small GTPase binding, guanyl ribonucleotide binding
81704	**DOCK8**	dedicator of cytokinesis 8	guanyl ribonucleotide binding
23348	**DOCK9**	dedicator of cytokinesis 9	Ras guanyl-nucleotide exchange factor activity, small GTPase binding, guanyl ribonucleotide binding
1778	**DYNC1H1**	dynein, cytoplasmic 1, heavy chain 1	pyrophosphatase activity, adenyl ribonucleotide binding
1780	**DYNC1I1**	dynein, cytoplasmic 1, intermediate chain 1	microtubule binding, pyrophosphatase activity
1781	**DYNC1I2**	similar to dynein cytoplasmic 1 intermediate chain 2; dynein, cytoplasmic 1, intermediate chain 2	pyrophosphatase activity
51143	**DYNC1LI1**	dynein, cytoplasmic 1, light intermediate chain 1	pyrophosphatase activity, adenyl ribonucleotide binding

Gene ID	Gene symbol	Gene description	GO, Molecular Function
1783	**DYNC1LI2**	dynein, cytoplasmic 1, light intermediate chain 2	pyrophosphatase activity, adenyl ribonucleotide binding
79659	**DYNC2H1**	dynein, cytoplasmic 2, heavy chain 1	pyrophosphatase activity, adenyl ribonucleotide binding
51626	**DYNC2LI1**	dynein, cytoplasmic 2, light intermediate chain 1	pyrophosphatase activity
8655	**DYNLL1**	dynein, light chain, LC8-type 1	pyrophosphatase activity
140735	**DYNLL2**	dynein, light chain, LC8-type 2	pyrophosphatase activity
83658	**DYNLRB1**	dynein, light chain, roadblock-type 1	pyrophosphatase activity
83657	**DYNLRB2**	dynein, light chain, roadblock-type 2	pyrophosphatase activity
6993	**DYNLT1**	dynein, light chain, Tctex-type 1	pyrophosphatase activity
6990	**DYNLT3**	dynein, light chain, Tctex-type 3	pyrophosphatase activity
1894	**ECT2**	epithelial cell transforming sequence 2 oncogene	Ras guanyl-nucleotide exchange factor activity, small GTPase binding
55740	**ENAH**	enabled homolog (Drosophila)	
51466	**EVL**	Enah/Vasp-like	
7430	**EZR**	hypothetical protein LOC100129652; ezrin	actin filament binding
51306	**FAM13B**	family with sequence similarity 13, member B	
10160	**FARP1**	FERM, RhoGEF (ARHGEF) and pleckstrin domain protein 1 (chondrocyte-derived)	Ras guanyl-nucleotide exchange factor activity
9855	**FARP2**	FERM, RhoGEF and pleckstrin domain protein 2	Ras guanyl-nucleotide exchange factor activity
54751	**FBLIM1**	filamin binding LIM protein 1	transition metal ion binding
10979	**FERMT2**	fermitin family homolog 2 (Drosophila)	

Gene ID	Gene symbol	Gene description	GO, Molecular Function
2245	**FGD1**	FYVE, RhoGEF and PH domain containing 1	Ras guanyl-nucleotide exchange factor activity, small GTPase binding, transition metal ion binding
221472	**FGD2**	FYVE, RhoGEF and PH domain containing 2	Ras guanyl-nucleotide exchange factor activity, small GTPase binding, transition metal ion binding
89846	**FGD3**	FYVE, RhoGEF and PH domain containing 3	Ras guanyl-nucleotide exchange factor activity, small GTPase binding, transition metal ion binding
121512	**FGD4**	FYVE, RhoGEF and PH domain containing 4	Ras guanyl-nucleotide exchange factor activity, small GTPase binding, transition metal ion binding, actin filament binding
55785	**FGD6**	FYVE, RhoGEF and PH domain containing 6	Ras guanyl-nucleotide exchange factor activity, small GTPase binding, transition metal ion binding
54848	**FLJ20184**	hypothetical protein FLJ20184	Ras guanyl-nucleotide exchange factor activity
2316	**FLNA**	filamin A, alpha (actin binding protein 280)	protein kinase binding, small GTPase binding, Fc-gamma receptor I complex binding, actin filament binding
2317	**FLNB**	filamin B, beta (actin binding protein 278)	
2318	**FLNC**	filamin C, gamma (actin binding protein 280)	
2534	**FYN**	FYN oncogene related to SRC, FGR, YES	protein kinase activity, adenyl ribonucleotide binding, transition metal ion binding
2597	**GAPDH**	glyceraldehyde-3-phosphate dehydrogenase-like 6; hypothetical protein LOC100133042; glyceraldehyde-3-phosphate dehydrogenase	glyceraldehyde-3-phosphate dehydrogenase activity
28964	**GIT1**	G protein-coupled receptor kinase interacting ArfGAP 1	ARF GTPase activator activity, transition metal ion binding
9815	**GIT2**	G protein-coupled receptor kinase interacting ArfGAP 2	ARF GTPase activator activity, transition metal ion binding
51291	**GMIP**	GEM interacting protein	Ras GTPase activator activity, Rho GTPase activator activity, transition metal ion binding

Gene ID	Gene symbol	Gene description	GO, Molecular Function
10399	**GNB2L1**	guanine nucleotide binding protein (G protein), beta polypeptide 2-like 1	protein phosphatase binding
2885	**GRB2**	growth factor receptor-bound protein 2	phosphotyrosine binding
2886	**GRB7**	growth factor receptor-bound protein 7	
2909	**GRLF1**	glucocorticoid receptor DNA binding factor 1	transcription corepressor activity, Ras GTPase activator activity, Rho GTPase activator activity
2934	**GSN**	gelsolin (amyloidosis, Finnish type)	calcium ion binding
23526	**HMHA1**	histocompatibility (minor) HA-1	transition metal ion binding
3611	**ILK**	integrin-linked kinase	protein kinase activity, adenyl ribonucleotide binding
3619	**INCENP**	inner centromere protein antigens 135/155kDa	
8826	**IQGAP1**	IQ motif containing GTPase activating protein 1	Ras GTPase activator activity, protein phosphatase binding
3688	**ITGB1**	integrin, beta 1 (fibronectin receptor, beta polypeptide, antigen CD29 includes MDF2, MSK12)	
9270	**ITGB1BP1**	integrin beta 1 binding protein 1	
3690	**ITGB3**	integrin, beta 3 (platelet glycoprotein IIIa, antigen CD61)	
23421	**ITGB3BP**	integrin beta 3 binding protein (beta3-endonexin)	
3691	**ITGB4**	integrin, beta 4	
3693	**ITGB5**	integrin, beta 5	
3694	**ITGB6**	integrin, beta 6	
6453	**ITSN1**	intersectin 1 (SH3 domain protein)	Ras guanyl-nucleotide exchange factor activity, calcium ion binding

Gene ID	Gene symbol	Gene description	GO, Molecular Function
50618	**ITSN2**	intersectin 2	Ras guanyl-nucleotide exchange factor activity, calcium ion binding
8997	**KALRN**	kalirin, RhoGEF kinase	magnesium ion binding, protein kinase activity, Ras guanyl-nucleotide exchange factor activity, adenyl ribonucleotide binding
3832	**KIF11**	kinesin family member 11	pyrophosphatase activity, adenyl ribonucleotide binding
113220	**KIF12**	kinesin family member 12	pyrophosphatase activity, adenyl ribonucleotide binding
63971	**KIF13A**	kinesin family member 13A	pyrophosphatase activity, adenyl ribonucleotide binding
23303	**KIF13B**	kinesin family member 13B	pyrophosphatase activity, protein kinase binding, adenyl ribonucleotide binding
9928	**KIF14**	kinesin family member 14	pyrophosphatase activity, adenyl ribonucleotide binding
56992	**KIF15**	kinesin family member 15	pyrophosphatase activity, adenyl ribonucleotide binding
55614	**KIF16B**	kinesin family member 16B	pyrophosphatase activity, adenyl ribonucleotide binding
57576	**KIF17**	kinesin family member 17	pyrophosphatase activity, adenyl ribonucleotide binding
81930	**KIF18A**	kinesin family member 18A	microtubule binding, pyrophosphatase activity, adenyl ribonucleotide binding
146909	**KIF18B**	kinesin family member 18B	pyrophosphatase activity, adenyl ribonucleotide binding
124602	**KIF19**	kinesin family member 19	pyrophosphatase activity, adenyl ribonucleotide binding
547	**KIF1A**	kinesin family member 1A	pyrophosphatase activity, adenyl ribonucleotide binding
23095	**KIF1B**	kinesin family member 1B	pyrophosphatase activity, adenyl ribonucleotide binding
10749	**KIF1C**	kinesin family member 1C	pyrophosphatase activity, adenyl ribonucleotide binding
10112	**KIF20A**	kinesin family member 20A	pyrophosphatase activity, adenyl ribonucleotide binding
9585	**KIF20B**	kinesin family member 20B	pyrophosphatase activity, adenyl ribonucleotide binding
55605	**KIF21A**	kinesin family member 21A	pyrophosphatase activity, adenyl ribonucleotide binding
23046	**KIF21B**	kinesin family member 21B	pyrophosphatase activity, adenyl ribonucleotide binding
3835	**KIF22**	kinesin family member 22	pyrophosphatase activity, adenyl ribonucleotide binding

Gene ID	Gene symbol	Gene description	GO, Molecular Function
9493	**KIF23**	kinesin family member 23	pyrophosphatase activity, adenyl ribonucleotide binding
347240	**KIF24**	kinesin family member 24	pyrophosphatase activity, adenyl ribonucleotide binding
3834	**KIF25**	kinesin family member 25	pyrophosphatase activity, adenyl ribonucleotide binding
26153	**KIF26A**	kinesin family member 26A	pyrophosphatase activity, adenyl ribonucleotide binding
55083	**KIF26B**	kinesin family member 26B	pyrophosphatase activity, adenyl ribonucleotide binding
55582	**KIF27**	kinesin family member 27	pyrophosphatase activity, adenyl ribonucleotide binding
3796	**KIF2A**	kinesin heavy chain member 2A	pyrophosphatase activity, adenyl ribonucleotide binding
84643	**KIF2B**	kinesin family member 2B	pyrophosphatase activity, adenyl ribonucleotide binding
11004	**KIF2C**	kinesin family member 2C	pyrophosphatase activity, centromeric DNA binding, adenyl ribonucleotide binding
11127	**KIF3A**	kinesin family member 3A	pyrophosphatase activity, adenyl ribonucleotide binding
9371	**KIF3B**	kinesin family member 3B	pyrophosphatase activity, adenyl ribonucleotide binding
3797	**KIF3C**	kinesin family member 3C	pyrophosphatase activity, adenyl ribonucleotide binding
24137	**KIF4A**	kinesin family member 4B; kinesin family member 4A	pyrophosphatase activity, adenyl ribonucleotide binding
285643	**KIF4B**	kinesin family member 4B	pyrophosphatase activity, adenyl ribonucleotide binding
3798	**KIF5A**	kinesin family member 5A	pyrophosphatase activity, adenyl ribonucleotide binding
3799	**KIF5B**	kinesin family member 5B	microtubule binding, pyrophosphatase activity, adenyl ribonucleotide binding
3800	**KIF5C**	kinesin family member 5C	pyrophosphatase activity, adenyl ribonucleotide binding
221458	**KIF6**	kinesin family member 6	pyrophosphatase activity, adenyl ribonucleotide binding
374654	**KIF7**	kinesin family member 7	pyrophosphatase activity, adenyl ribonucleotide binding
64147	**KIF9**	kinesin family member 9	pyrophosphatase activity, adenyl ribonucleotide binding
22920	**KIFAP3**	kinesin-associated protein 3	

Gene ID	Gene symbol	Gene description	GO, Molecular Function
3833	**KIFC1**	kinesin family member C1	pyrophosphatase activity, adenyl ribonucleotide binding
90990	**KIFC2**	kinesin family member C2	pyrophosphatase activity, adenyl ribonucleotide binding
3801	**KIFC3**	kinesin family member C3	pyrophosphatase activity, adenyl ribonucleotide binding
3927	**LASP1**	LIM and SH3 protein 1	transition metal ion binding, actin filament binding
3984	**LIMK1**	LIM domain kinase 1	protein kinase activity, adenyl ribonucleotide binding, transition metal ion binding
3985	**LIMK2**	LIM domain kinase 2	protein kinase activity, adenyl ribonucleotide binding, transition metal ion binding
3987	**LIMS1**	LIM and senescent cell antigen-like domains 1	transition metal ion binding
55679	**LIMS2**	LIM and senescent cell antigen-like domains 2	transition metal ion binding
441930	**LOC441930**	similar to kinesin-like protein (103.5 kD) (klp-6)	
4035	**LRP1**	low density lipoprotein-related protein 1 (alpha-2-macroglobulin receptor)	calcium ion binding
23499	**MACF1**	microtubule-actin crosslinking factor 1	calcium ion binding, microtubule binding, actin filament binding
4214	**MAP3K1**	mitogen-activated protein kinase kinase kinase 1	magnesium ion binding, protein kinase activity, MAP kinase kinase kinase activity, small conjugating protein ligase activity, protein kinase binding, adenyl ribonucleotide binding, transition metal ion binding
5594	**MAPK1**	mitogen-activated protein kinase 1	phosphotyrosine binding, protein kinase activity, MAP kinase activity, protein kinase binding, adenyl ribonucleotide binding
5595	**MAPK3**	hypothetical LOC100271831; mitogen-activated protein kinase 3	protein kinase activity, MAP kinase activity, adenyl ribonucleotide binding
9479	**MAPK8IP1**	mitogen-activated protein kinase 8 interacting protein 1	MAP-kinase scaffold activity, protein kinase binding
23542	**MAPK8IP2**	mitogen-activated protein kinase 8 interacting	MAP-kinase scaffold activity, protein kinase binding

Gene ID	Gene symbol	Gene description	GO, Molecular Function
		protein 2	
23162	**MAPK8IP3**	mitogen-activated protein kinase 8 interacting protein 3	MAP-kinase scaffold activity, protein kinase binding
22919	**MAPRE1**	microtubule-associated protein, RP/EB family, member 1	microtubule binding
10982	**MAPRE2**	microtubule-associated protein, RP/EB family, member 2	microtubule binding
22924	**MAPRE3**	microtubule-associated protein, RP/EB family, member 3	microtubule binding
4168	**MCF2**	MCF.2 cell line derived transforming sequence	Ras guanyl-nucleotide exchange factor activity
23263	**MCF2L**	MCF.2 cell line derived transforming sequence-like	Ras guanyl-nucleotide exchange factor activity
23101	**MCF2L2**	MCF.2 cell line derived transforming sequence-like 2	Ras guanyl-nucleotide exchange factor activity
79083	**MLPH**	melanophilin	microtubule binding, Rab GTPase binding, small GTPase binding, myosin V binding, transition metal ion binding
4478	**MSN**	moesin	
4619	**MYH1**	myosin, heavy chain 1, skeletal muscle, adult	pyrophosphatase activity, adenyl ribonucleotide binding
4628	**MYH10**	myosin, heavy chain 10, non-muscle	pyrophosphatase activity, adenyl ribonucleotide binding, actin filament binding
4629	**MYH11**	myosin, heavy chain 11, smooth muscle	pyrophosphatase activity, adenyl ribonucleotide binding
8735	**MYH13**	myosin, heavy chain 13, skeletal muscle	pyrophosphatase activity, adenyl ribonucleotide binding
22989	**MYH15**	myosin, heavy chain 15	pyrophosphatase activity, adenyl ribonucleotide binding
4620	**MYH2**	myosin, heavy chain 2, skeletal muscle, adult	pyrophosphatase activity, adenyl ribonucleotide binding

Gene ID	Gene symbol	Gene description	GO, Molecular Function
4621	**MYH3**	myosin, heavy chain 3, skeletal muscle, embryonic	pyrophosphatase activity, adenyl ribonucleotide binding
4622	**MYH4**	myosin, heavy chain 4, skeletal muscle	pyrophosphatase activity, adenyl ribonucleotide binding
4624	**MYH6**	myosin, heavy chain 6, cardiac muscle, alpha	pyrophosphatase activity, adenyl ribonucleotide binding
4625	**MYH7**	myosin, heavy chain 7, cardiac muscle, beta	pyrophosphatase activity, adenyl ribonucleotide binding
57644	**MYH7B**	myosin, heavy chain 7B, cardiac muscle, beta	pyrophosphatase activity, adenyl ribonucleotide binding
4626	**MYH8**	myosin, heavy chain 8, skeletal muscle, perinatal	pyrophosphatase activity, adenyl ribonucleotide binding
4627	**MYH9**	myosin, heavy chain 9, non-muscle	pyrophosphatase activity, adenyl ribonucleotide binding, actin filament binding
29116	**MYLIP**	myosin regulatory light chain interacting protein	small conjugating protein ligase activity, transition metal ion binding
4638	**MYLK**	myosin light chain kinase	magnesium ion binding, protein kinase activity, calcium ion binding, adenyl ribonucleotide binding
4651	**MYO10**	myosin X	pyrophosphatase activity, adenyl ribonucleotide binding
51168	**MYO15A**	myosin XVA	pyrophosphatase activity, adenyl ribonucleotide binding
80022	**MYO15B**	myosin XVB pseudogene	
23026	**MYO16**	myosin XVI	pyrophosphatase activity, adenyl ribonucleotide binding, actin filament binding
399687	**MYO18A**	myosin XVIIIA	pyrophosphatase activity, adenyl ribonucleotide binding
84700	**MYO18B**	myosin XVIIIB	pyrophosphatase activity, adenyl ribonucleotide binding
4640	**MYO1A**	myosin IA	pyrophosphatase activity, adenyl ribonucleotide binding
4430	**MYO1B**	myosin IB	pyrophosphatase activity, adenyl ribonucleotide binding
4641	**MYO1C**	myosin IC	pyrophosphatase activity, adenyl ribonucleotide binding
4642	**MYO1D**	myosin ID	pyrophosphatase activity, adenyl ribonucleotide binding

Gene ID	Gene symbol	Gene description	GO, Molecular Function
4643	**MYO1E**	myosin IE	pyrophosphatase activity, adenyl ribonucleotide binding
4542	**MYO1F**	myosin IF	pyrophosphatase activity, adenyl ribonucleotide binding
64005	**MYO1G**	myosin IG	pyrophosphatase activity, adenyl ribonucleotide binding
53904	**MYO3A**	myosin IIIA	protein kinase activity, pyrophosphatase activity, adenyl ribonucleotide binding
140469	**MYO3B**	myosin IIIB	protein kinase activity, pyrophosphatase activity, adenyl ribonucleotide binding
4644	**MYO5A**	myosin VA (heavy chain 12, myoxin)	pyrophosphatase activity, adenyl ribonucleotide binding, actin filament binding
4645	**MYO5B**	similar to acetyl-Coenzyme A acyltransferase 2 (mitochondrial 3-oxoacyl-Coenzyme A thiolase); similar to KIAA1119 protein; myosin VB	pyrophosphatase activity, adenyl ribonucleotide binding, actin filament binding
55930	**MYO5C**	myosin VC	pyrophosphatase activity, adenyl ribonucleotide binding, actin filament binding
4646	**MYO6**	myosin VI	pyrophosphatase activity, adenyl ribonucleotide binding, actin filament binding
4647	**MYO7A**	myosin VIIA	pyrophosphatase activity, adenyl ribonucleotide binding
4648	**MYO7B**	myosin VIIB	pyrophosphatase activity, adenyl ribonucleotide binding
4649	**MYO9A**	myosin IXA	pyrophosphatase activity, adenyl ribonucleotide binding, transition metal ion binding
4650	**MYO9B**	myosin IXB	Ras GTPase activator activity, Rho GTPase activator activity, pyrophosphatase activity, small GTPase binding, adenyl ribonucleotide binding, transition metal ion binding, actin filament binding
4690	**NCK1**	NCK adaptor protein 1	
8440	**NCK2**	NCK adaptor protein 2	
10276	**NET1**	neuroepithelial cell transforming 1	Ras guanyl-nucleotide exchange factor activity
91624	**NEXN**	nexilin (F actin binding protein)	actin filament binding
4771	**NF2**	neurofibromin 2 (merlin)	

Gene ID	Gene symbol	Gene description	GO, Molecular Function
25791	**NGEF**	neuronal guanine nucleotide exchange factor	Ras guanyl-nucleotide exchange factor activity
84309	**NUDT16L1**	nudix (nucleoside diphosphate linked moiety X)-type motif 16-like 1	
84033	**OBSCN**	obscurin, cytoskeletal calmodulin and titin-interacting RhoGEF	magnesium ion binding, protein kinase activity, Ras guanyl-nucleotide exchange factor activity, adenyl ribonucleotide binding
4952	**OCRL**	oculocerebrorenal syndrome of Lowe	phosphatase activity
4983	**OPHN1**	oligophrenin 1	Ras GTPase activator activity, Rho GTPase activator activity
5048	**PAFAH1B1**	platelet-activating factor acetylhydrolase, isoform Ib, subunit 1 (45kDa)	microtubule binding, heparin binding
5058	**PAK1**	p21 protein (Cdc42/Rac)-activated kinase 1	protein kinase activity, small GTPase binding, adenyl ribonucleotide binding
5062	**PAK2**	p21 protein (Cdc42/Rac)-activated kinase 2	protein kinase activity, adenyl ribonucleotide binding
10298	**PAK4**	p21 protein (Cdc42/Rac)-activated kinase 4	protein kinase activity, adenyl ribonucleotide binding
23022	**PALLD**	palladin, cytoskeletal associated protein	alpha-actinin binding
55742	**PARVA**	parvin, alpha	
29780	**PARVB**	parvin, beta	
5216	**PFN1**	profilin 1	small GTPase binding
5217	**PFN2**	profilin 2	
5290	**PIK3CA**	phosphoinositide-3-kinase, catalytic, alpha polypeptide	lipid kinase activity, inositol or phosphatidylinositol kinase activity, adenyl ribonucleotide binding, phosphoinositide 3-kinase activity
5291	**PIK3CB**	phosphoinositide-3-kinase, catalytic, beta polypeptide	lipid kinase activity, inositol or phosphatidylinositol kinase activity, adenyl ribonucleotide binding, phosphoinositide 3-kinase activity
5294	**PIK3CG**	phosphoinositide-3-kinase, catalytic, gamma polypeptide	lipid kinase activity, inositol or phosphatidylinositol kinase activity, adenyl ribonucleotide binding, phosphoinositide 3-kinase activity
5295	**PIK3R1**	phosphoinositide-3-kinase, regulatory subunit	phosphatidylinositol binding, protein phosphatase binding

Gene ID	Gene symbol	Gene description	GO, Molecular Function
		1 (alpha)	
5296	**PIK3R2**	phosphoinositide-3-kinase, regulatory subunit 2 (beta)	lipid kinase activity, inositol or phosphatidylinositol kinase activity, phosphoinositide 3-kinase activity
23396	**PIP5K1C**	phosphatidylinositol-4-phosphate 5-kinase, type I, gamma	lipid kinase activity, inositol or phosphatidylinositol kinase activity, phosphatidylinositol phosphate kinase activity, adenyl ribonucleotide binding
64857	**PLEKHG2**	pleckstrin homology domain containing, family G (with RhoGef domain) member 2	Ras guanyl-nucleotide exchange factor activity
25894	**PLEKHG4**	pleckstrin homology domain containing, family G (with RhoGef domain) member 4	Ras guanyl-nucleotide exchange factor activity
57449	**PLEKHG5**	pleckstrin homology domain containing, family G (with RhoGef domain) member 5	Ras guanyl-nucleotide exchange factor activity
55200	**PLEKHG6**	pleckstrin homology domain containing, family G (with RhoGef domain) member 6	Ras guanyl-nucleotide exchange factor activity
8500	**PPFIA1**	protein tyrosine phosphatase, receptor type, f polypeptide (PTPRF), interacting protein (liprin), alpha 1	
5478	**PPIA**	similar to TRIMCyp; peptidylprolyl isomerase A (cyclophilin A); peptidylprolyl isomerase A (cyclophilin A)-like 3	
57580	**PREX1**	phosphatidylinositol-3,4,5-trisphosphate-dependent Rac exchange factor 1	Ras guanyl-nucleotide exchange factor activity, Ras GTPase activator activity, Rho GTPase activator activity
5578	**PRKCA**	protein kinase C, alpha	protein kinase activity, calcium ion binding, adenyl ribonucleotide binding, transition metal ion binding
5581	**PRKCE**	protein kinase C, epsilon	protein kinase activity, adenyl ribonucleotide binding, transition metal ion binding
5587	**PRKD1**	protein kinase D1	protein kinase activity, adenyl ribonucleotide binding, transition metal ion binding

Gene ID	Gene symbol	Gene description	GO, Molecular Function
5728	**PTEN**	phosphatase and tensin homolog; phosphatase and tensin homolog pseudogene 1	magnesium ion binding, phosphatase activity
5747	**PTK2**	PTK2 protein tyrosine kinase 2	protein kinase activity, adenyl ribonucleotide binding
5770	**PTPN1**	protein tyrosine phosphatase, non-receptor type 1	phosphatase activity, transition metal ion binding
5781	**PTPN11**	protein tyrosine phosphatase, non-receptor type 11; similar to protein tyrosine phosphatase, non-receptor type 11	phosphatase activity, peptide hormone receptor binding
5782	**PTPN12**	protein tyrosine phosphatase, non-receptor type 12	phosphatase activity
5786	**PTPRA**	protein tyrosine phosphatase, receptor type, A	phosphatase activity, transmembrane receptor protein phosphatase activity
5792	**PTPRF**	protein tyrosine phosphatase, receptor type, F	phosphatase activity, transmembrane receptor protein phosphatase activity
5829	**PXN**	paxillin	transition metal ion binding
5879	**RAC1**	ras-related C3 botulinum toxin substrate 1 (rho family, small GTP binding protein Rac1)	pyrophosphatase activity, guanyl ribonucleotide binding
5880	**RAC2**	ras-related C3 botulinum toxin substrate 2 (rho family, small GTP binding protein Rac2)	pyrophosphatase activity, guanyl ribonucleotide binding
5881	**RAC3**	ras-related C3 botulinum toxin substrate 3 (rho family, small GTP binding protein Rac3)	pyrophosphatase activity, guanyl ribonucleotide binding
29127	**RACGAP1**	Rac GTPase activating protein 1 pseudogene; Rac GTPase activating protein 1	alpha-tubulin binding, gamma-tubulin binding, transition metal ion binding, beta-tubulin binding
10928	**RALBP1**	hypothetical LOC100129773; ralA binding protein 1	Ras GTPase activator activity, Rho GTPase activator activity, pyrophosphatase activity, small GTPase binding
5923	**RASGRF1**	Ras protein-specific guanine nucleotide-releasing factor 1	Ras guanyl-nucleotide exchange factor activity

Gene ID	Gene symbol	Gene description	GO, Molecular Function
5924	**RASGRF2**	Ras protein-specific guanine nucleotide-releasing factor 2	Ras guanyl-nucleotide exchange factor activity, calcium ion binding
5962	**RDX**	radixin	
64283	**RGNEF**	Rho-guanine nucleotide exchange factor	Ras guanyl-nucleotide exchange factor activity, transition metal ion binding
387	**RHOA**	ras homolog gene family, member A	magnesium ion binding, pyrophosphatase activity, guanyl ribonucleotide binding
388	**RHOB**	ras homolog gene family, member B	pyrophosphatase activity, guanyl ribonucleotide binding
9886	**RHOBTB1**	Rho-related BTB domain containing 1	guanyl ribonucleotide binding
23221	**RHOBTB2**	Rho-related BTB domain containing 2	guanyl ribonucleotide binding
389	**RHOC**	ras homolog gene family, member C	pyrophosphatase activity, guanyl ribonucleotide binding
29984	**RHOD**	ras homolog gene family, member D	pyrophosphatase activity, guanyl ribonucleotide binding
54509	**RHOF**	ras homolog gene family, member F (in filopodia)	pyrophosphatase activity, guanyl ribonucleotide binding
391	**RHOG**	ras homolog gene family, member G (rho G)	pyrophosphatase activity, guanyl ribonucleotide binding
399	**RHOH**	ras homolog gene family, member H	small GTPase binding, guanyl ribonucleotide binding
57381	**RHOJ**	ras homolog gene family, member J	pyrophosphatase activity, guanyl ribonucleotide binding
23433	**RHOQ**	ras homolog gene family, member Q; similar to small GTP binding protein TC10	pyrophosphatase activity, guanyl ribonucleotide binding
58480	**RHOU**	ras homolog gene family, member U	magnesium ion binding, pyrophosphatase activity, guanyl ribonucleotide binding
171177	**RHOV**	ras homolog gene family, member V	magnesium ion binding, guanyl ribonucleotide binding
9912	**RICH2**	Rho-type GTPase-activating protein RICH2	
27289	**RND1**	Rho family GTPase 1	pyrophosphatase activity, guanyl ribonucleotide binding
8153	**RND2**	Rho family GTPase 2	pyrophosphatase activity, guanyl ribonucleotide binding
390	**RND3**	Rho family GTPase 3	pyrophosphatase activity, guanyl ribonucleotide binding

Gene ID	Gene symbol	Gene description	GO, Molecular Function
6048	**RNF5**	ring finger protein 5; ring finger protein 5 pseudogene 1	transition metal ion binding
6093	**ROCK1**	similar to Rho-associated, coiled-coil containing protein kinase 1; Rho-associated, coiled-coil containing protein kinase 1	protein kinase activity, small GTPase binding, adenyl ribonucleotide binding, transition metal ion binding
9475	**ROCK2**	Rho-associated, coiled-coil containing protein kinase 2	protein kinase activity, adenyl ribonucleotide binding, transition metal ion binding
6385	**SDC4**	syndecan 4	alpha-actinin binding
6386	**SDCBP**	syndecan binding protein (syntenin)	interleukin-5 receptor binding
26084	**SGEF**	Src homology 3 domain-containing guanine nucleotide exchange factor	Ras guanyl-nucleotide exchange factor activity
23616	**SH3BP1**	SH3-domain binding protein 1	
140885	**SIRPA**	signal-regulatory protein alpha	
65012	**SLC26A10**	RhoA/RAC/CDC42 exchange factor; solute carrier family 26, member 10	Ras guanyl-nucleotide exchange factor activity, antiporter activity
10580	**SORBS1**	sorbin and SH3 domain containing 1	protein kinase binding
10174	**SORBS3**	sorbin and SH3 domain containing 3	
6654	**SOS1**	son of sevenless homolog 1 (Drosophila)	Ras guanyl-nucleotide exchange factor activity, Ras GTPase activator activity, Rho GTPase activator activity
6655	**SOS2**	son of sevenless homolog 2 (Drosophila)	Ras guanyl-nucleotide exchange factor activity
221178	**SPATA13**	spermatogenesis associated 13	Ras guanyl-nucleotide exchange factor activity
6714	**SRC**	v-src sarcoma (Schmidt-Ruppin A-2) viral oncogene homolog (avian)	protein kinase activity, adenyl ribonucleotide binding
57522	**SRGAP1**	SLIT-ROBO Rho GTPase activating protein 1	

Gene ID	Gene symbol	Gene description	GO, Molecular Function
23380	**SRGAP2**	SLIT-ROBO Rho GTPase activating protein 2	
9901	**SRGAP3**	SLIT-ROBO Rho GTPase activating protein 3	
90627	**STARD13**	StAR-related lipid transfer (START) domain containing 13	
9754	**STARD8**	StAR-related lipid transfer (START) domain containing 8	
57519	**STARD9**	StAR-related lipid transfer (START) domain containing 9	pyrophosphatase activity, adenyl ribonucleotide binding
85360	**SYDE1**	synapse defective 1, Rho GTPase, homolog 1 (C. elegans)	Ras GTPase activator activity, Rho GTPase activator activity
23371	**TENC1**	tensin like C1 domain containing phosphatase (tensin 2)	phosphatase activity, transition metal ion binding
26136	**TES**	testis derived transcript (3 LIM domains)	transition metal ion binding
7041	**TGFB1I1**	transforming growth factor beta 1 induced transcript 1	transcription coactivator activity, nuclear hormone receptor binding, transition metal ion binding
7074	**TIAM1**	T-cell lymphoma invasion and metastasis 1	Ras guanyl-nucleotide exchange factor activity
26230	**TIAM2**	T-cell lymphoma invasion and metastasis 2	Ras guanyl-nucleotide exchange factor activity
7094	**TLN1**	talin 1	
83660	**TLN2**	talin 2	
7145	**TNS1**	tensin 1	
7168	**TPM1**	tropomyosin 1 (alpha)	
7169	**TPM2**	tropomyosin 2 (beta)	
7170	**TPM3**	tropomyosin 3	
7171	**TPM4**	tropomyosin 4	calcium ion binding

Gene ID	Gene symbol	Gene description	GO, Molecular Function
7204	**TRIO**	triple functional domain (PTPRF interacting)	protein kinase activity, Ras guanyl-nucleotide exchange factor activity, adenyl ribonucleotide binding
7205	**TRIP6**	thyroid hormone receptor interactor 6	interleukin-1 receptor binding, nuclear hormone receptor binding, transition metal ion binding
54822	**TRPM7**	transient receptor potential cation channel, subfamily M, member 7	protein kinase activity, ion channel activity, calcium ion binding, cation transmembrane transporter activity, substrate specific channel activity, adenyl ribonucleotide binding, transition metal ion binding
7106	**TSPAN4**	tetraspanin 4	
7105	**TSPAN6**	tetraspanin 6	
10376	**TUBA1B**	hypothetical gene supported by AF081484; NM_006082; tubulin, alpha 1b	pyrophosphatase activity, guanyl ribonucleotide binding
203068	**TUBB**	tubulin, beta; similar to tubulin, beta 5; tubulin, beta pseudogene 2; tubulin, beta pseudogene 1	pyrophosphatase activity, guanyl ribonucleotide binding, MHC class I protein binding
7408	**VASP**	vasodilator-stimulated phosphoprotein	
7409	**VAV1**	vav 1 guanine nucleotide exchange factor	Ras guanyl-nucleotide exchange factor activity, transition metal ion binding
7410	**VAV2**	vav 2 guanine nucleotide exchange factor	Ras guanyl-nucleotide exchange factor activity, transition metal ion binding
10451	**VAV3**	vav 3 guanine nucleotide exchange factor	Ras guanyl-nucleotide exchange factor activity, transition metal ion binding
7414	**VCL**	vinculin	
7431	**VIM**	vimentin	protein kinase binding
7525	**YES1**	v-yes-1 Yamaguchi sarcoma viral oncogene homolog 1	protein kinase activity, adenyl ribonucleotide binding
7791	**ZYX**	zyxin	transition metal ion binding

Appendix II. Results of the primary screening for regulators of integrin α2 internalization for individual tested siRNAs

1 Gene name and Gene ID according to http://www.ncbi.nlm.nih.gov/gene/

2 Target mRNA accession number according to http://www.ncbi.nlm.nih.gov/nuccore/

3 SiRNA target sequence and siRNA ID according to manufacturer's information

4 Gene summary according to performance of all tested siRNAs

5 Performance of individual siRNAs in the screening (see ***Methods*** for explanation of Z-scores and p-values calculation)

Gene Symbol[1]	Gene ID[1]	RefSeq Accession Number[2]	siRNA ID[3]	Antisense (target) siRNA Sequence[3]	Hit gene[4]	Z-score[5]	P-value[5]
Scramble			251283	ACGUGACACGUUCGGAGAAtt	Negative control	0	0,913
CLTC	1213	NM_004859	SI00299880	*TAATCCAATTCGAAGACCAAT	Positive control	-1,54	7,45E-29
DNM2	1785	NM_001005360 NM_001005361 NM_001005362 NM_004945	SI02654687	*CTGCAGCTCATCTTCTCAAAA	Positive control	-1,49	2,24E-13
ABL1	25	NM_007313	1241	UAUCUCAGCGAGAUGGACCtc	Non-hit	-0,874	0,066

Gene Symbol [1]	Gene ID[1]	RefSeq Accession Number[2]	siRNA ID[3]	Antisense (target) siRNA Sequence[3]	Hit gene[4]	Z-score [5]	P-value [5]
ABL1	25	NM_007313	147447	AUAGCCUAAGACCCGGAGCtt	Non-hit	-0,843	0,056
ABL2	27	NM_007314	1478	GAUAGCCUCAUUUAGUGCCtg	Mild hit	-1,043	0,016
ABL2	27	NM_005158	103346	GUAGUGAUACACACGUCCCtc	Mild hit	-1,452	0,088
ABL2	27	NM_007314	103430	CUCAGCAGUCACAUACACCtt	Mild hit	-0,350	0,826
ABL2	27	NM_007314	147450	GUAACCAAGGACUCGUAGCtt	Mild hit	-1,292	0,000
ABR	29	NM_021962	29582	GUGGAUCUCAUAGAUGUCCtg	Mild hit	-1,235	0,143
ABR	29	NM_021962	29678	CAGGUUGUCAUAGAACUCCtt	Mild hit	-0,442	0,553
ABR	29	NM_021962	29772	AUUGUUGUCCUUGUUGACCtt	Mild hit	-1,392	0,013
ABR	29	NM_021962	147813	UUAAUGUAGAUCUCUUCGCtg	Mild hit	-1,112	0,003
ABR	29	NM_021962	147814	ACAGUCAUACUGCUGGUGCtt	Mild hit	-0,570	0,092
ABR	29	NM_021962	147815	GUGCAUCAUGCAGUUUUCCtt	Mild hit	-0,171	0,870
ABR	29	NM_001092	288548	UUCUUAGCCUGACUCCUGCtg	Mild hit	-0,774	0,028
ABR	29	NM_021962	288549	GCAUCAAACAGACCACUGCtg	Mild hit	-0,620	0,243
ACTB	60	NM_001101	9415	GUCGCCCACAUAGGAAUCCtt	Mild hit	-1,106	0,153
ACTB	60	NM_001101	9511	CGUUCCAGUUUUUAAAUCCtg	Mild hit	-0,546	0,334
ACTN1	87	NM_001102	9416	UGUGCACUCUCAUCUUGCCtc	Strong hit	-1,529	0,168
ACTN1	87	NM_001102	9512	GGCUAUGAAAUCCAGGGCCtt	Strong hit	0,241	0,421
ACTN4	81	NM_004924	15476	AUUGAAGGCAAGACCAUCCtt	Non-hit	-0,915	0,040

Gene Symbol [1]	Gene ID[1]	RefSeq Accession Number[2]	siRNA ID[3]	Antisense (target) siRNA Sequence[3]	Hit gene[4]	Z-score [5]	P-value [5]
ACTN4	81	NM_004924	15570	UUGGUUGACAGCCAGCACCtt	Non-hit	-0,967	0,671
AKAP13	11214	NM_006738	1475	AGAAUCUUUCUCCUUCUCCtt	Non-hit	0,417	0,643
AKAP13	11214	NM_007200	1569	GUCUUUAGAAUCUUUCUCCtt	Non-hit	-1,263	0,028
AKAP13	11214	NM_007200	103341	CUAGACUUUCUCGGCAGCCtt	Non-hit	-0,391	0,432
AKAP13	11214	NM_144767	103506	UUUUCAUUAAAGGUCCUCCtt	Non-hit	-0,746	0,015
AKAP13	11214	NM_144767	136052	GUAUAGGCAUCUUUGUUGGtg	Non-hit	-0,444	0,466
AKAP13	11214	NM_144767	136053	UCCGACUCCAAGACUCUGCtt	Non-hit	-0,359	0,346
ALS2	57679	NM_020919	28809	UAUGGGAAAGGAUCCUGCCtg	Mild hit	-1,300	0,045
ALS2	57679	NM_020919	133298	CAUUGUACAAGGGCUAAGCtg	Mild hit	-0,509	0,643
ANXA2	302	NM_004039	147285	GUAGGCGAAGGCAAUAUCCtg	Non-hit	-0,003	0,334
ANXA2	302	NM_004039	147286	AUAAGGCUGACUUCAGUGCtg	Non-hit	0,049	0,824
ANXA2	302	NM_004039	147287	UGUGUCCGAAAUAAUGUCCtt	Non-hit	-0,404	0,829
ANXA2	302	NM_004039	288566	ACUGUUAUUCGCAAGCUGGtt	Non-hit	-0,239	0,842
ANXA2	302	NM_001002858	288567	AUGAGAGAGUCCUCGUCGGtt	Non-hit	-1,050	0,067
ANXA2	302	NM_001002858	288568	AAUGUUCAAAGCAUCCCGCtc	Non-hit	0,279	0,246
AP1B1	162	NM_145730	9431	UGCCUCCUUCUUCUUCUCCtt	Mild hit	-1,382	0,149
AP1B1	162	NM_145730	9527	CACAUAUGGAUCCUCGUCCtt	Mild hit	-0,510	0,011
APC	324	NM_000038	42812	CUUCAUCUUCAAUACUUCCtt	Non-hit	-0,769	0,719

Gene Symbol [1]	Gene ID[1]	RefSeq Accession Number[2]	siRNA ID[3]	Antisense (target) siRNA Sequence[3]	Hit gene[4]	Z-score [5]	P-value [5]
APC	324	NM_000038	44755	UGGAAUUAUCUUCUAGCUCtt	Non-hit	-0,951	0,092
APC2	10297	NM_005883	16896	UAGGUGCUUCAGGACCUCCtt	Mild hit	0,055	0,318
APC2	10297	NM_005883	16991	GAUGUCCAUCUGUAGGGCCtt	Mild hit	-1,230	0,035
ARAP1	116985	NM_139181	22844	GCAUUUCAUUUUCACUACCtc	Non-hit	-0,916	0,221
ARAP1	116985	NM_139181	128706	ACGCUCAUGUCGAUGAAGGtg	Non-hit	-0,282	0,912
ARAP1	116985	NM_139181	128707	CAGGACAACUGAGUAGUGCtt	Non-hit	0,128	0,625
ARAP1	116985	NM_139181	128708	GAACUUCAUCAUGCCAUGCtt	Non-hit	-1,359	0,002
ARAP2	116984	NM_015230	22649	CUCUUGACUUAAUACACCCtc	Non-hit	-0,709	0,757
ARAP2	116984	NM_139182	22745	AGUAACUCAAGAAGCCUCCtt	Non-hit	-0,654	0,223
ARAP2	116984	NM_139182	22840	UUUAAAGCUUCUUGCAUCCtt	Non-hit	-0,823	0,130
ARAP2	116984	NM_139182	128701	UGUCCAUAGCAAACCAGCCtt	Non-hit	0,185	0,753
ARAP3	64411	NM_022481	29944	CUGGAAGACAUAGUUUCCCtg	Non-hit	-0,006	0,546
ARAP3	64411	NM_022481	30036	CCAAAGUACAUCAGACUCCtc	Non-hit	-0,128	0,825
ARF1	375	NM_001024227	10237	GCCUGAAUGUACCAGUUCCtg	Strong hit	-0,673	0,481
ARF1	375	NM_001024228	10333	AGGAGUACCAGAAACUGCCtc	Strong hit	0,554	0,081
ARF1	375	NM_001658	10426	UCGAUGGCAAAUCGGACCCtt	Strong hit	0,385	0,184
ARF1	375	NM_001658	147188	GUACUCCACGGUUUCCACGtt	Strong hit	-1,420	0,196
ARF1	375	NM_001658	147189	ACACGCUCUCUGUCAUUGCtg	Strong hit	0,431	0,903

Gene Symbol [1]	Gene ID[1]	RefSeq Accession Number[2]	siRNA ID[3]	Antisense (target) siRNA Sequence[3]	Hit gene[4]	Z-score [5]	P-value [5]
ARF1	375	NM_001024228	214733	AACAGUUGAUUACUAAUCGtg	Strong hit	-0,562	0,171
ARF1	375	NM_001658	288550	UAAAUUUAACAGCUCCAGCtt	Strong hit	-1,623	0,001
ARF1	375	NM_001024227	288551	AAAUAGACCAGUUCUGAGGtt	Strong hit	-1,252	0,261
ARHGAP1	392	NM_004308	14383	GCCCAUACUUGUCAUCUCCtg	Non-hit	-0,828	0,658
ARHGAP1	392	NM_004308	14477	AUGCACGAUGUACAAGGCCtt	Non-hit	0,053	0,995
ARHGAP10	79658	NM_024605	31229	UGCGAGUAGUACAGUUCCCtt	Non-hit	-0,903	0,540
ARHGAP10	79658	NM_024605	127413	UCUCCAUGUAACUCAUAGGtc	Non-hit	-0,288	0,649
ARHGAP11A	9824	NM_199357	21847	GCUGCUGUUUCAUGUCUCCtg	Non-hit	-1,444	0,023
ARHGAP11A	9824	NM_199357	21943	CUGAUUUCCGAAAAAGCCCtt	Non-hit	-0,552	0,012
ARHGAP11A	9824	NM_199357	140197	UUAGGCGAAUCACAGAUCCtg	Non-hit	0,211	0,399
ARHGAP11A	9824	NM_199357	140198	GUGCAGAAGAUAGGCAACCtt	Non-hit	1,210	0,333
ARHGAP12	94134	NM_018287	26692	UUUUUCACCAAGAUGUACCtc	Non-hit	-0,771	0,047
ARHGAP12	94134	NM_018287	128737	UAACAGGUGGCAUGAGAGCtt	Non-hit	-0,359	0,770
ARHGAP15	55843	NM_018460	26915	UUCUCAUUUGCACAGCUCCtg	Non-hit	-0,328	0,847
ARHGAP15	55843	NM_018460	132552	UUCUGUGUCUGGAUAUAGGtt	Non-hit	-0,228	0,719
ARHGAP17	55114	NM_018054	26031	GGCAGUUUUUUGUGUCUCCtc	Non-hit	0,104	0,795

Gene Symbol [1]	Gene ID[1]	RefSeq Accession Number[2]	siRNA ID[3]	Antisense (target) siRNA Sequence[3]	Hit gene[4]	Z-score [5]	P-value [5]
ARHGAP17	55114	NM_018054	132261	CUUCCAGCUGAGUCGAUGCtt	Non-hit	-0,208	0,759
ARHGAP17	55114	NM_001006634	132262	UAAAGUUGUACAUGUCUGCtg	Non-hit	0,082	0,539
ARHGAP17	55114	NM_018054	132263	AAUAGGAUUUUAAAGCACCtg	Non-hit	-1,306	0,018
ARHGAP18	93663	NM_033515	35378	UAGUUCAUCCAAAGAAUCCtg	Mild hit	-1,326	0,606
ARHGAP18	93663	NM_033515	128827	UGAUCGAUCAAAUGGAGGCtt	Mild hit	-1,054	0,125
ARHGAP19	84986	NM_032900	34874	GUAUAUUGGUCUUGUUUCCtt	Non-hit	-0,603	0,159
ARHGAP19	84986	NM_032900	35051	UAACUUUGUGAUAUUCUCCtg	Non-hit	0,009	0,757
ARHGAP20	57569	NM_020809	148781	UAGGAAAAGAUGCCGCUCCtg	Mild hit	-0,803	0,032
ARHGAP20	57569	NM_020809	148782	AAUGCUCUUCGGGUAGUCCtt	Mild hit	-1,224	0,029
ARHGAP22	58504	NM_021226	29210	UUCUCAGGUCAGCACUCCCtt	Non-hit	-0,204	0,546
ARHGAP22	58504	NM_021226	147798	GAGCAGGUUGUAAUUUGCCtg	Non-hit	-0,265	0,605
ARHGAP23	57636	XM_290799	272050	UAGGUCUUCCCAAUGACGCtt	Non-hit	-0,101	0,395
ARHGAP23	57636	XM_290799	272051	CUUGGGCAUGAUAGACAGCtc	Non-hit	-0,433	0,713
ARHGAP24	83478	NM_031305	33188	GUUUCUGUCCAAAAAUGCCtt	Non-hit	-0,238	0,637
ARHGAP24	83478	NM_031305	33369	AUCAUUGUGAACUUUUUCCtc	Non-hit	0,322	0,360
ARHGAP24	83478	NM_031305	148939	CUCCUUAACAAGAUUAGCCtg	Non-hit	-0,019	0,678
ARHGAP24	83478	NM_031305	148941	GCAAAUAUACUUGAGGAGGtt	Non-hit	0,176	0,511
ARHGAP25	9938	NM_014882	22105	CAGUUCUUCACGAUGGACCtc	Non-hit	-0,335	0,458

Gene Symbol [1]	Gene ID[1]	RefSeq Accession Number[2]	siRNA ID[3]	Antisense (target) siRNA Sequence[3]	Hit gene[4]	Z-score [5]	P-value [5]
ARHGAP25	9938	NM_014882	22201	CUUCGUGUCCUCUUCAUCCtt	Non-hit	-0,230	0,526
ARHGAP25	9938	NM_001007231	22297	AAGGUUUUUAAUCUGUUCCtc	Non-hit	0,143	0,401
ARHGAP25	9938	NM_014882	288610	UGAAUACAGCGAUGGAUGGtc	Non-hit	-0,530	0,315
ARHGAP26	23092	NM_015071	22398	UAUGAGUGACUUCCCGUCCtt	Non-hit	-0,707	0,534
ARHGAP26	23092	NM_015071	22590	AUUCUUAAUUCUCAUUCCCtg	Non-hit	-0,130	0,891
ARHGAP27	201176	NM_199282	142018	GUCCACCUUAUAGCGUAGCtt	Non-hit	-0,181	0,681
ARHGAP27	201176	NM_199282	142019	AAGCCCUCCAUCAAACUCCtc	Non-hit	0,527	0,154
ARHGAP28	79822	NM_030672	32666	ACUUUCUCUGUUUUGUUCCtt	Non-hit	0,134	0,308
ARHGAP28	79822	NM_030672	32759	AAAUCCCAUUGUCUCGUCCtt	Non-hit	0,057	0,229
ARHGAP28	79822	NM_001010000	32847	CUGAAAGUCGAAAAAUUCCtt	Non-hit	-0,736	0,050
ARHGAP28	79822	NM_030672	288619	GUUCCACAGACUCAUUCGGtt	Non-hit	0,320	0,960
ARHGAP29	9411	NM_004815	122573	UAAAACACGGAGCAGUUCCtc	Mild hit	-1,148	0,079
ARHGAP29	9411	NM_004815	122574	AUUUGUUAGCCUGGAGAGCtg	Mild hit	-0,691	0,093
ARHGAP31	57514	NM_020754	219541	GUAUGUUUGAGGUGACUCCtg	Non-hit	0,068	0,313
ARHGAP31	57514	NM_020754	219542	UUCUUUAGACCUGAGGAGGtt	Non-hit	-0,285	0,617
ARHGAP32	9743	NM_014715	21792	UGUGCAGCUUUGAAGAACCtg	Non-hit	-0,076	0,501
ARHGAP32	9743	NM_014715	21983	UCGUGGAUUUUUAUCAGCCtt	Non-hit	-0,562	NA
ARHGAP33	115703	NM_052948	35730	CAUUUCUGUACAAGGACCCtc	Non-hit	-0,260	0,088

Gene Symbol [1]	Gene ID[1]	RefSeq Accession Number[2]	siRNA ID[3]	Antisense (target) siRNA Sequence[3]	Hit gene[4]	Z-score [5]	P-value [5]
ARHGAP33	115703	NM_052948	35819	AGUUACAAAGUUAGAAACCtg	Non-hit	0,573	0,840
ARHGAP39	80728	NM_025251	261264	CAGUACUUGGCAUACGUGCtt	Strong hit	0,586	0,443
ARHGAP39	80728	NM_025251	288618	GGUAGAGCUUGGUUUUUGGtc	Strong hit	-1,740	0,028
ARHGAP4	393	NM_001666	10244	GCUCUCCAUGUGAUAUGCCtg	Non-hit	0,220	0,802
ARHGAP4	393	NM_001666	10340	AGCAUGCACCUCGAGAACCtt	Non-hit	-0,572	0,774
ARHGAP44	9912	NM_014859	22182	AAUAUUUGGGAUUUCCACCtc	Non-hit	-0,201	0,879
ARHGAP44	9912	NM_014859	22278	UCAUCUCUGUAAUGUUCCCtt	Non-hit	0,016	0,381
ARHGAP5	394	NM_001173	9456	UUCCAACUCCACAGUUACCtt	Non-hit	-0,460	0,051
ARHGAP5	394	NM_001030055	9551	CAUUGUUUACUACUCGUCCtc	Non-hit	0,199	0,589
ARHGAP5	394	NM_001030055	147081	GCUAAGCACAGAAGUAUGCtc	Non-hit	0,427	0,151
ARHGAP5	394	NM_001173	147082	GUCUUGUUCUAAGCCUAGCtg	Non-hit	-0,137	0,792
ARHGAP6	395	NM_006125	20636	UUCCUUUUUACUUUGAGCCtc	Strong hit	-1,067	0,336
ARHGAP6	395	NM_013427	121662	AGAUGCAUCUUUCUGCUCGtc	Strong hit	-0,395	0,595
ARHGAP6	395	NM_013423	288604	UGAUUGUCAUCAAGAUCGGtg	Strong hit	-1,505	0,016
ARHGAP6	395	NM_013423	288605	AAUCCCACGGUCAAAUUCCtc	Strong hit	-0,787	0,009
ARHGAP6	395	NM_013423	288606	AGGUUGGGUCCAAAUAUGGtg	Strong hit	-0,754	0,005
ARHGAP6	395	NM_013427	288607	CAGGCUGAUCAGCACUUCGtt	Strong hit	0,082	0,827
ARHGAP6	395	NM_001174	20459	UAAGGGCAUUCCAAAUGCCtg	Strong hit	-0,067	0,628

Gene Symbol [1]	Gene ID[1]	RefSeq Accession Number[2]	siRNA ID[3]	Antisense (target) siRNA Sequence[3]	Hit gene[4]	Z-score [5]	P-value [5]
ARHGAP6	395	NM_001174	20550	UGCUUGAGUUUAUAGGCCCtg	Strong hit	-2,109	0,001
ARHGAP6	395	NM_001174	121663	CUGAGAGAUGAGUUACUGCtt	Strong hit	-0,659	0,013
ARHGAP6	395	NM_001174	121664	UCAUUCGGUGUUUCUGAGGtt	Strong hit	0,813	0,222
ARHGAP9	64333	NM_032496	34278	UUCUGACGGCAAGUCUUCCtg	Non-hit	0,386	0,665
ARHGAP9	64333	NM_032496	34374	UGCAGGACAUCAUUGUUCCtc	Non-hit	-0,675	0,772
ARHGDIA	396	NM_004309	14384	UUGGUCCCUUGUUUGUUCCtg	Non-hit	-0,238	0,258
ARHGDIA	396	NM_004309	119907	CUUCAGCACAAACGACUGCtt	Non-hit	-0,079	0,569
ARHGDIB	397	NM_001175	9457	AUCAUCUUUGUCCAUUUCCtg	Non-hit	0,293	0,283
ARHGDIB	397	NM_001175	9552	CUUUAACACAAUGGUUUCCtt	Non-hit	0,221	0,626
ARHGDIG	398	NM_001176	9458	AUCUCCAAGAGGCUCUUCCtc	Non-hit	-0,637	0,944
ARHGDIG	398	NM_001176	9553	CAGGACAAACACCUGGUCCtt	Non-hit	-0,381	0,527
ARHGEF1	9138	NM_004706	5309	GUUCUCAAAAUCCUCAUCCtc	Mild hit	-0,558	0,105
ARHGEF1	9138	NM_199002	5491	UUUUUCCGGAAGAAGUUCCtc	Mild hit	-1,387	0,047
ARHGEF1	9138	NM_199002	119420	UUCUUGUCUCCACUCUUGGtc	Mild hit	0,580	0,206
ARHGEF1	9138	NM_199002	119421	AGCACACCAGUUUUUCCGCtc	Mild hit	0,155	0,943
ARHGEF1	9138	NM_199002	119422	UAGAAGGCUUUGUGAUCGGtg	Mild hit	0,395	0,900
ARHGEF1	9138	NM_004706	214561	UAAAAAGGACGUAGAAGGCtt	Mild hit	-1,299	0,070
ARHGEF10	9639	NM_014629	21727	AAAUAAGCCUUUGUAAACCtg	Non-hit	-0,477	0,247

Gene Symbol [1]	Gene ID[1]	RefSeq Accession Number[2]	siRNA ID[3]	Antisense (target) siRNA Sequence[3]	Hit gene[4]	Z-score [5]	P-value [5]
ARHGEF10	9639	NM_014629	138290	UAGGUCAUGAGAAAGUUGCtt	Non-hit	-0,349	0,594
ARHGEF10L	55160	NM_001011722	26281	CUGGAUGAGCACAUUGUCCtt	Non-hit	-0,346	0,126
ARHGEF10L	55160	NM_018125	26377	GUACACCUUAUUCUGAGCCtg	Non-hit	-0,244	0,902
ARHGEF10L	55160	NM_018125	123057	CAAACAAGUGAUACUGGGCtt	Non-hit	-0,713	0,251
ARHGEF10L	55160	NM_018125	123058	GGCACAGACAAGCAUGUCGtt	Non-hit	-0,102	0,914
ARHGEF11	9826	NM_198236	21848	UUUUUGAACUUCGGGAUCCtg	Non-hit	-0,962	0,542
ARHGEF11	9826	NM_198236	119417	AGAUGCCCAUGGAUGAAGGtg	Non-hit	-0,501	0,127
ARHGEF11	9826	NM_198236	119418	UGGGCUUUGAUCUACACCCtg	Non-hit	-0,271	0,585
ARHGEF11	9826	NM_014784	214646	GUUGUUGAAAUAACCCGGGtc	Non-hit	-1,221	0,052
ARHGEF12	23365	NM_015313	22673	UAUCUCGGAUCUACUCUCCtc	Mild hit	-0,590	0,424
ARHGEF12	23365	NM_015313	119311	AUCUGUUGGUGACUCUCGGtt	Mild hit	-1,066	0,939
ARHGEF15	22899	NM_173728	122079	CAUUCACAUCUGCUCUCGCtt	Non-hit	-0,017	0,185
ARHGEF15	22899	NM_173728	122080	AGACAGGACCAGUCAUUGCtg	Non-hit	-0,674	0,874
ARHGEF16	27237	NM_014448	42188	UCCUCGAAGAACCUCUGACtg	Non-hit	-0,680	0,644
ARHGEF16	27237	NM_014448	42260	GCUCUCCUCGCUCUUCUUCtt	Non-hit	-0,139	0,591
ARHGEF17	9828	NM_014786	21850	GUACGAGGGAAAGCUCACCtt	Non-hit	-0,515	0,019
ARHGEF17	9828	NM_014786	21946	AGACCAUAGGUCGUCGUCCtt	Non-hit	0,292	0,776
ARHGEF18	23370	NM_015318	43400	AAUCGGCUUCAUCCAUCUCtc	Non-hit	-0,095	0,997

Gene Symbol [1]	Gene ID[1]	RefSeq Accession Number[2]	siRNA ID[3]	Antisense (target) siRNA Sequence[3]	Hit gene[4]	Z-score [5]	P-value [5]
ARHGEF18	23370	NM_015318	43583	ACUUGUAAUGACUAACAGCtt	Non-hit	-0,276	0,884
ARHGEF2	9181	NM_004723	15160	CAUAGCACAUGGUCAUGCCtg	Mild hit	-1,081	0,294
ARHGEF2	9181	NM_004723	15256	CUGUUGCUUCUGCUUGACCtt	Mild hit	-0,178	0,606
ARHGEF25	115557	NM_182947	36435	CUUCUUCUUCUGUUCCUCCtc	Non-hit	-1,305	0,009
ARHGEF25	115557	NM_182947	141956	GUUCUCAUAUGGUCCUGCCtg	Non-hit	-0,411	0,443
ARHGEF26	26084	NM_015595	22998	AGUCAACCCAGUAAGGUCCtc	Non-hit	-0,627	0,065
ARHGEF26	26084	NM_015595	121751	AUCCGUAAUUAGUAACCCGtt	Non-hit	-0,248	0,691
ARHGEF3	50650	NM_019555	27760	CCGUUUAUUACUAGGCUCCtc	Non-hit	-0,761	0,065
ARHGEF3	50650	NM_019555	135243	GACCCGUUUAUUACUAGGCtc	Non-hit	0,744	0,202
ARHGEF38	54848	NM_017700	25195	AGCAUAUAGAGUCUAGACCtc	Strong hit	-0,024	0,984
ARHGEF38	54848	NM_017700	25387	AUAGGAUUUAUGUGAGACCtt	Strong hit	1,702	0,005
ARHGEF4	50649	NM_015320	22774	CAGGUCAUCAUACAGGUCCtc	Non-hit	-0,380	0,390
ARHGEF4	50649	NM_032995	22869	UCAACAUCCUUGAAGUCCCtg	Non-hit	-1,161	0,211
ARHGEF4	50649	NM_032995	119317	AGUAGAUCUGGAAGUCGGCtt	Non-hit	-0,527	0,807
ARHGEF4	50649	NM_032995	119318	CAAGGCGGCUUCAACAUCCtt	Non-hit	0,373	0,065
ARHGEF5	7984	NM_005435	2841	AAUCAGCUCAAAUUUGACCtc	Non-hit	-0,184	0,658
ARHGEF5	7984	NM_005435	3027	UUCUAGGUUAGAAGAUACCtt	Non-hit	-0,389	0,510
ARHGEF5	7984	NM_005435	121538	ACGAGAGAAGAGCCAUUGGtg	Non-hit	-1,434	0,164

Gene Symbol [1]	Gene ID[1]	RefSeq Accession Number[2]	siRNA ID[3]	Antisense (target) siRNA Sequence[3]	Hit gene[4]	Z-score [5]	P-value [5]
ARHGEF5	7984	NM_005435	288577	CUGGAUUUUGUCCUUGAGCtt	Non-hit	0,112	0,240
ARHGEF6	9459	NM_004840	5326	CGAGGACUUUAAAAACUCCtc	Non-hit	-0,692	0,393
ARHGEF6	9459	NM_004840	119232	UUUCAAAUCCUUUGACGGCtt	Non-hit	-0,309	0,665
ARHGEF7	8874	NM_145735	38124	UGAGAAGGAAAGCUCGUCCtc	Non-hit	-0,588	0,156
ARHGEF7	8874	NM_145735	38215	UGGCAGUCGUAUCAAAUCCtt	Non-hit	-0,962	0,032
ARHGEF7	8874	NM_145735	38295	UCUAUCUGUAUGAUAAUCCtc	Non-hit	-0,483	0,899
ARHGEF7	8874	NM_145735	119396	UGCAAUGGCCGUAGGUACGtt	Non-hit	-0,014	0,865
ARHGEF9	23229	NM_015185	22731	UCGUCACUGAACAUGUCCCtt	Non-hit	0,263	0,818
ARHGEF9	23229	NM_015185	22826	AAUGUUCCCAAAGAUUACCtt	Non-hit	-0,765	0,616
ASAP1	50807	NM_018482	42901	AACUGUGUGAAGGGUUGACtt	Strong hit	0,369	0,494
ASAP1	50807	NM_018482	43082	AGCAUGGGAAAAGAAACACtt	Strong hit	2,265	0,111
BCAR1	9564	NM_014567	21515	CACCGUCAUGAUGUCACCCtt	Non-hit	-0,147	0,343
BCAR1	9564	NM_014567	21608	UGGCACCUGGUAAAUAUCCtg	Non-hit	0,066	0,578
BCR	613	NM_004327	1237	GUCAUAGCUCUUCUUUUCCtt	Non-hit	0,576	0,851
BCR	613	NM_021574	1332	CACCUCUUUGUCGUUGACCtt	Non-hit	-0,423	0,661
BCR	613	NM_004327	1427	UUUUCAUAGCACAGUAUCCtc	Non-hit	-0,871	0,183
BCR	613	NM_021574	110844	GUUCUUGGUCGUUGGAUCCtt	Non-hit	-0,960	0,048
BCR	613	NM_021574	147329	GUCCGACACCUCUUUGUCGtt	Non-hit	-0,146	0,734

Gene Symbol [1]	Gene ID[1]	RefSeq Accession Number[2]	siRNA ID[3]	Antisense (target) siRNA Sequence[3]	Hit gene[4]	Z-score [5]	P-value [5]
BCR	613	NM_021574	147330	UCCAGAGAGUUCUUGGUCGtt	Non-hit	-0,412	0,673
BCR	613	NM_021574	147331	UCAGAGGAGAUCAGGAACGtg	Non-hit	-0,514	0,259
BCR	613	NM_021574	214833	UGGGACCUUUAGACUUCGGtg	Non-hit	1,061	0,075
CALR	811	NM_004343	14400	UCCGUCCAGAAACUGCUCCtt	Mild hit	-1,024	0,280
CALR	811	NM_004343	14494	CAAACCUUUAUCUUUCUCCtc	Mild hit	-0,521	0,676
CANX	821	NM_001746	10290	GACAUCGUCAAGGUCAUCCtc	Non-hit	-1,489	0,002
CANX	821	NM_001746	10385	UGGUUUUGAGUCUUCUACCtc	Non-hit	-0,168	0,963
CANX	821	NM_001024649	10472	UCCAUUUUGGAAAUUAACCtc	Non-hit	-0,966	0,061
CANX	821	NM_001746	145945	CUAGUGUUCAACUGGAGCCtg	Non-hit	-0,045	0,069
CAPN1	823	NM_005186	15805	AUUUACCUUGGCAUAGGCCtt	Strong hit	-1,754	0,169
CAPN1	823	NM_005186	15898	GAAGUUCUCGUCAAUCUCCtc	Strong hit	-0,759	0,037
CAPN2	824	NM_001748	10292	UUGAGGUACUUGAUGGCCCtc	Non-hit	0,215	0,266
CAPN2	824	NM_001748	10387	GAUCCCUGCAUAGUUUUCCtg	Non-hit	0,455	0,429
CAPNS1	826	NM_001003962	10293	AGGGUGUCGUGUCACAACCtt	Non-hit	-1,128	0,010
CAPNS1	826	NM_001749	10388	CCACAAGUACUUGAAUUCCtc	Non-hit	-0,323	0,119
CAPNS1	826	NM_001003962	10475	GAACUGUUUGUAUAUGGCCtg	Non-hit	1,245	0,097
CAPNS1	826	NM_001003962	105571	UGAUCGGUCAGUGUCGAACtg	Non-hit	-0,121	0,539
CAV1	857	NM_001753	10297	GUUGACCAGGUCGAUCUCCtt	Mild hit	-0,976	0,133

Gene Symbol [1]	Gene ID[1]	RefSeq Accession Number[2]	siRNA ID[3]	Antisense (target) siRNA Sequence[3]	Hit gene[4]	Z-score [5]	P-value [5]
CAV1	857	NM_001753	145951	CGGUAAAACCAGUAUUUCGtc	Mild hit	-1,140	0,010
CAV2	858	NM_198212	9481	GGGUCCAAGUAUUCAAUCCtg	Non-hit	-0,147	0,354
CAV2	858	NM_001233	9575	GUAUCCCAAUCUCCAGACCtg	Non-hit	-0,757	0,540
CAV2	858	NM_198212	145680	CCAAGUAUUCAAUCCUGGCtc	Non-hit	0,850	0,002
CAV2	858	NM_198212	145681	UACUAUAAUCGUUGUGUGCtt	Non-hit	-0,712	0,635
CBL	867	NM_005188	2827	CAUUCUUUCUUUUCCCUCCtt	Non-hit	-0,478	0,277
CBL	867	NM_005188	2921	AUACAUUCUUUCUUUUCCCtc	Non-hit	0,248	0,913
CD151	977	NM_139030	43352	CAGGCUGAUGUAGUCACUCtt	Non-hit	-0,166	0,778
CD151	977	NM_004357	43447	AGCAGGCUGAUGUAGUCACtc	Non-hit	0,204	0,774
CD151	977	NM_139030	43538	CUGGAUGAAGGUCUCCAACtt	Non-hit	-0,265	0,795
CD151	977	NM_139030	288629	GGUCAUGGUGUCCUUCAGGtt	Non-hit	-0,874	0,243
CD81	975	NM_004356	14407	AUCCUUGGCGAUCUGGUCCtt	Non-hit	0,016	0,340
CD81	975	NM_004356	14501	AUAGAACUGCUUCACAUCCtt	Non-hit	-0,990	0,072
CDC42	998	NM_001791	10324	UGUCAUAAUCCUCUUGCCCtg	Non-hit	-0,392	0,778
CDC42	998	NM_044472	10418	UCGUAAUCUGUCAUAAUCCtc	Non-hit	-0,580	0,601
CDC42	998	NM_001791	242554	ACAUCUGUUUGUGGAUAACtc	Non-hit	-1,089	0,010
CDC42	998	NM_044472	242555	AGGAGUCUUUGGACAGUGGtg	Non-hit	-0,704	0,824
CENPE	1062	NM_001813	10520	AUAUAGUACCAUUGUAGCCtt	Mild hit	-1,011	0,212

Gene Symbol [1]	Gene ID[1]	RefSeq Accession Number[2]	siRNA ID[3]	Antisense (target) siRNA Sequence[3]	Hit gene[4]	Z-score [5]	P-value [5]
CENPE	1062	NM_001813	121337	UGGCAGAAUCGAUGAUUGGtg	Mild hit	0,251	0,942
CFL1	1072	NM_005507	5366	GAUGAUGUUCUUCUUGUCCtc	Non-hit	-0,640	0,794
CFL1	1072	NM_005507	5455	AUCCUCCUUCUUGCUCUCCtt	Non-hit	-0,133	0,507
CHN1	1123	NM_001025201	10528	AAGCCAAAGUGUAGGUCCCtg	Strong hit	-0,147	0,655
CHN1	1123	NM_001025201	10622	UUGCCAUCGUAGUAGAGCCtg	Strong hit	2,737	0,000
CHN1	1123	NM_001025201	146034	AGCCACAAUCAAGAGCUGGtc	Strong hit	0,165	0,756
CHN1	1123	NM_001025201	146035	GGUUGUGUAUCCUACGUGCtc	Strong hit	1,323	0,098
CHN2	1124	NM_004067	14167	AAGGUCUGGUUUCCAAACCtg	Mild hit	0,828	0,411
CHN2	1124	NM_004067	146298	CACAAAGUGUUUCCCGUCGtg	Mild hit	-1,194	0,006
CIB1	10519	NM_006384	17715	CCUGUCAAUGUCAGACUCCtc	Mild hit	-1,100	0,008
CIB1	10519	NM_006384	17808	AGGUUGAUGGUUCCAUCCCtg	Mild hit	-0,506	0,977
CKAP5	9793	NM_001008938	21827	UCUUCAUACCCACUUAACCtt	Non-hit	-0,177	0,958
CKAP5	9793	NM_001008938	21923	CAAGUGCAGCUUCUAAUCCtt	Non-hit	-1,102	0,093
CKAP5	9793	NM_001008938	22017	UAUGUGAACAGCUAUUUCCtt	Non-hit	-0,162	0,707
CKAP5	9793	NM_014756	122703	CAUACCCACUUAACCUUGCtt	Non-hit	0,143	0,817
CLASP1	23332	NM_015282	136866	ACAAGUUUAUCUAACAUGGtc	Non-hit	0,024	0,391
CLASP1	23332	NM_015282	136867	UUAGUGUUAAAGUCUGUGCtc	Non-hit	-0,348	0,828
CLASP2	23122	NM_015097	261144	UAGUUUCAACCAAGACGGCtg	Non-hit	-0,394	0,174

Gene Symbol [1]	Gene ID[1]	RefSeq Accession Number[2]	siRNA ID[3]	Antisense (target) siRNA Sequence[3]	Hit gene[4]	Z-score [5]	P-value [5]
CLASP2	23122	NM_015097	261145	UGGUAAUUUUUGAGUCGGCtg	Non-hit	-0,202	0,226
CLIP1	6249	NM_002956	12224	GUCAUCCACAAAUUCCUCCtg	Mild hit	-0,082	0,767
CLIP1	6249	NM_198240	12317	AAAGUCAUCCACAAAUUCCtc	Mild hit	-0,450	0,567
CLIP1	6249	NM_198240	142516	UCCAUUCACCCAAACUCGCtc	Mild hit	-1,218	0,132
CLIP1	6249	NM_002956	142517	ACUGGAAAUACCGAACUCCtg	Mild hit	-1,049	0,184
CLIP2	7461	NM_032421	43346	CGAAUGCAAUGACAGGUUCtg	Non-hit	-0,317	0,745
CLIP2	7461	NM_032421	43442	GGAAGCCGAUACGGAUCACtt	Non-hit	0,163	0,476
CLIP2	7461	NM_003388	43533	CUCGUAGUCCAACAUCUUCtt	Non-hit	-0,735	0,120
CLIP2	7461	NM_032421	139011	UCGCCUGACUUACACUUGCtc	Non-hit	0,833	0,121
COPB1	1315	NA		AUUAGGAUGUUGAAGAUCCtt	Non-hit	-0,660	0,027
CRK	1398	NM_005206	6472	GAGAAUCACUCCACUACCCtg	Mild hit	-0,631	0,232
CRK	1398	NM_016823	146743	GAGGCAAGAUACCUAUCCCtt	Mild hit	-1,137	0,146
CRK	1398	NM_016823	146744	AGUUAGGACUCUAGUUAGCtg	Mild hit	-0,053	0,964
CRK	1398	NM_005206	146745	UCGCCAUUUGAUAGUAUGGtt	Mild hit	-1,433	0,042
CRKL	1399	NM_005207	2828	CGGCAAAUGGUCAAAUUCCtg	Non-hit	0,195	0,648
CRKL	1399	NM_005207	2922	AUUGGUGGGCUUGGAUACCtg	Non-hit	-0,934	0,116
CSK	1445	NM_004383	146413	GGCCCACCUUGUUUUUGGCtt	Mild hit	-1,344	0,036
CSK	1445	NM_004383	146414	GUACAUGAUGCGGUAGUGCtc	Mild hit	0,299	0,965

Gene Symbol [1]	Gene ID[1]	RefSeq Accession Number[2]	siRNA ID[3]	Antisense (target) siRNA Sequence[3]	Hit gene[4]	Z-score [5]	P-value [5]
CSRP1	1465	NM_004078	14079	AUUUAUGGAAGCUGUUGCCtt	Mild hit	-1,322	0,275
CSRP1	1465	NM_004078	14172	CUUCCCAGCACCAAUCACCtt	Mild hit	-0,023	0,971
DCTN1	1639	NM_023019	14081	CAGGGUCUCUAGUUUCUCCtc	Non-hit	-0,826	0,118
DCTN1	1639	NM_023019	146317	CAGCUGCAUAGUACAGUCCtc	Non-hit	0,654	0,796
DCTN1	1639	NM_023019	146318	UAGGAGCGUGUCAGAUACCtg	Non-hit	-1,007	0,077
DCTN1	1639	NM_023019	242560	AUCAAUGGUGCUCUCUGCCtg	Non-hit	-0,346	0,169
DIAPH1	1729	NM_005219	15997	AUUUCUUUUCUUCUCCACCtt	Mild hit	-1,239	0,632
DIAPH1	1729	NM_005219	242566	AUAGUACUGAGGUCUGGCCtc	Mild hit	-0,733	0,747
DIAPH2	1730	NM_007309	18467	GGGUUUGUUUUUCGUUUCCtc	Non-hit	0,123	0,802
DIAPH2	1730	NM_006729	18657	CUUCCUGAUUUUCUAAACCtt	Non-hit	0,033	0,667
DIAPH2	1730	NM_007309	146689	UCGUUCAUCAUAUAAUGGCtg	Non-hit	0,890	0,019
DIAPH2	1730	NM_007309	146690	UUCGUUAAGGUUCAUGUCCtc	Non-hit	-0,942	0,019
DIAPH3	81624	NM_030932	32930	UCAUUUCUGAUGUGAAGCCtg	Non-hit	-0,896	0,196
DIAPH3	81624	NM_030932	33026	AAGCUCAUUAAUCUUUGCCtc	Non-hit	0,141	0,532
DLC1	10395	NM_182643	17367	CGAAAGAGUCGUCAUUGCCtg	Mild hit	0,705	0,085
DLC1	10395	NM_024767	31555	GUUGGAAAAAUUGGAUCCCtt	Mild hit	0,104	0,415
DLC1	10395	NM_024767	31650	CCAGCAACAUGGAAAAGCCtc	Mild hit	0,773	0,105
DLC1	10395	NM_024767	46352	CAUCCACUUCCAACUUUACtg	Mild hit	-0,152	0,499

Gene Symbol [1]	Gene ID[1]	RefSeq Accession Number[2]	siRNA ID[3]	Antisense (target) siRNA Sequence[3]	Hit gene[4]	Z-score [5]	P-value [5]
DLC1	10395	NM_182643	202494	CUAGUCCAUGAUGACAUGCtg	Mild hit	1,415	0,272
DLC1	10395	NM_182643	213191	GUCAGGUUUCCUUCGUUGCtg	Mild hit	1,053	0,036
DNM1	1759	NM_001005336	14616	GUCGGUGAAUUUCUUUCCCtt	Non-hit	0,958	0,412
DNM1	1759	NM_001005336	14711	CAGGAUGAGGCAGUUCUCCtt	Non-hit	-0,904	0,027
DNM1	1759	NM_004408	14804	UAAUCCUUGUAGACAUUCCtc	Non-hit	0,535	0,085
DNM1	1759	NM_004408	146449	AGGUGUCGAUCUGAUCUCCtg	Non-hit	-0,594	0,020
DNMBP	23268	NM_015221	136834	AAAAAUGCCUCUUCGGCCCtc	Non-hit	-0,033	0,212
DNMBP	23268	NM_015221	136835	ACUGUAGAAUAAUACUGGCtt	Non-hit	0,371	0,273
DOCK1	1793	NM_001380	145822	UUAGACUUUUUUCGUAACGtg	Mild hit	-1,110	0,002
DOCK1	1793	NM_001380	145823	ACACUUCGAAACAUCUCCCtg	Mild hit	0,577	0,411
DOCK10	55619	NM_014689	258559	CUUGAGUCGAUUCUGAAGGtg	Non-hit	0,498	0,343
DOCK10	55619	NM_014689	258560	UCCAUUGUGACAAGAGACCtg	Non-hit	-0,868	0,031
DOCK11	139818	NM_144658	37496	UGAAAUUUGACUUUAGCCCtt	Mild hit	-1,257	0,351
DOCK11	139818	NM_144658	129250	UAGACUGCACCGUUCUGCGtt	Mild hit	-0,763	0,606
DOCK2	1794	NM_004946	146561	CUAUACCAGUCUCCACACGtc	Non-hit	-0,937	0,092
DOCK2	1794	NM_004946	146562	UCUGACAAUCAAAUCAAGCtc	Non-hit	-0,644	0,374
DOCK3	1795	NM_004947	146564	UGACCAGACAGUAGCUGCCtt	Non-hit	-0,488	0,396
DOCK3	1795	NM_004947	146565	UGGGCGCAUUGUAUCUACCtg	Non-hit	-0,869	0,523

Gene Symbol [1]	Gene ID[1]	RefSeq Accession Number[2]	siRNA ID[3]	Antisense (target) siRNA Sequence[3]	Hit gene[4]	Z-score [5]	P-value [5]
DOCK4	9732	NM_014705	21785	GCGUAUAUACAUCUCCUCCtt	Non-hit	-0,978	0,017
DOCK4	9732	NM_014705	21881	GUAGCGUAUAUACAUCUCCtc	Non-hit	-0,357	0,538
DOCK5	80005	NM_024940	31982	ACUGAGGUGAUGGACAACCtc	Strong hit	-0,928	0,052
DOCK5	80005	NM_024940	130801	CUUGUUGUUCACGUAGAGCtt	Strong hit	-2,022	0,243
DOCK6	57572	NM_020812	133244	AGACACUUGACCAAGAUCCtt	Non-hit	-0,330	0,782
DOCK6	57572	NM_020812	133245	GGGCUUGAUAUGAAGCAGCtc	Non-hit	0,629	0,328
DOCK7	85440	NM_033407	147974	AUACUACGGCUGUAUAGGCtt	Non-hit	-0,761	0,716
DOCK7	85440	NM_033407	147975	AGUUAAAGUAGCAGGAAGCtt	Non-hit	-0,837	0,359
DOCK8	81704	NM_203447	149461	GUCCUACAUUCCUUUGGCGtg	Non-hit	-0,646	0,545
DOCK8	81704	NM_203447	149462	CAGGAGGUUUUCUAGCCGCtt	Non-hit	0,240	0,527
DOCK9	23348	NM_015296	22669	UGAGCAUAUGUAUCGACCCtg	Non-hit	-0,147	0,918
DOCK9	23348	NM_015296	22765	AAACAAGCUCUGUGCUUCCtc	Non-hit	-0,087	0,222
DYNC1H1	1778	NM_001376	118309	CAUCAAUCACGGGAGUACGtt	Mild hit	-1,241	0,064
DYNC1H1	1778	NM_001376	118310	CGGAAUUUCAAUAUUUUGCtg	Mild hit	-0,064	0,658
DYNC1I1	1780	NM_004411	14617	CUUUUUCCUCUCCUCUUCCtt	Non-hit	-0,103	0,833
DYNC1I1	1780	NM_004411	14712	UCAGCCUCUUUCUUUUUCCtc	Non-hit	-0,280	0,616
DYNC1I2	1781	NM_001378	9741	CACAGGAGCAACAGCUUCCtt	Non-hit	-0,183	0,278
DYNC1I2	1781	NM_001378	9836	UUCCAAGUUUAAUAGGUCCtc	Non-hit	-0,745	0,144

Gene Symbol [1]	Gene ID[1]	RefSeq Accession Number[2]	siRNA ID[3]	Antisense (target) siRNA Sequence[3]	Hit gene[4]	Z-score [5]	P-value [5]
DYNC1LI1	51143	NM_016141	23822	CUUAUACUCCUCUAUUCCCtg	Non-hit	0,466	0,546
DYNC1LI1	51143	NM_016141	24008	AAUAUUCCAAUCCUCUUCCtt	Non-hit	0,261	0,580
DYNC1LI2	1783	NM_006141	17395	UUUUGCCAUGCUCAGCUCCtt	Non-hit	1,178	0,084
DYNC1LI2	1783	NM_006141	118326	UCCAUCCAGAAUCCACACGtt	Non-hit	-1,480	0,240
DYNC2H1	79659	HSU53531	288695	UGGCAAUCAUCAACCAGCUtt	Non-hit	-0,366	0,123
DYNC2H1	79659	HSU53531	288696	AAAUUAGGCUCUUCCAGUCta	Non-hit	0,084	0,566
DYNC2LI1	51626	NM_016008	124933	AGUGAGCGAUAUCUUUUGGtg	Non-hit	-0,941	0,185
DYNC2LI1	51626	NM_001012665	215817	AAGCUAAGGUUGGUUUUGGtg	Non-hit	-0,623	0,274
DYNLL1	8655	NM_001037495	13539	GUACUUCUUGUCAAAUUCCtt	Non-hit	-0,331	0,486
DYNLL1	8655	NM_003746	118315	UGGUAUUUGGAAUUUAGGCtg	Non-hit	-0,905	0,150
DYNLL2	140735	NM_080677	35969	AUUGUACUUCUCCAUGGCCtg	Non-hit	-0,099	0,426
DYNLL2	140735	NM_080677	118341	GAUGAAGUGCUUUGUCUCGtg	Non-hit	-0,156	0,930
DYNLRB1	83658	NM_014183	279206	AAGCUCUUGCUCCAAAACCtg	Non-hit	-0,133	0,952
DYNLRB1	83658	NM_014183	279207	CGACAAAGUGAACUGAAGGtc	Non-hit	-0,304	0,506
DYNLRB2	83657	NM_130897	36233	UUGUUCGGAUGGGAAUACCtt	Mild hit	-0,360	0,139
DYNLRB2	83657	NM_130897	118342	CAGUGUCGCUUAAACAGCCtt	Mild hit	-1,031	0,495
DYNLT1	6993	NM_006519	17983	AAUUGCGCUUUCUAUAGCCtc	Non-hit	0,022	0,384
DYNLT1	6993	NM_006519	139625	UUCUGCAUAAUUACACAGGtc	Non-hit	-0,504	0,289

Gene Symbol [1]	Gene ID[1]	RefSeq Accession Number[2]	siRNA ID[3]	Antisense (target) siRNA Sequence[3]	Hit gene[4]	Z-score [5]	P-value [5]
DYNLT3	6990	NM_006520	17984	UACCAGAUUUAAUUUACCCtc	Non-hit	-0,616	0,166
DYNLT3	6990	NM_006520	18077	GAUUCACUUUUUUCCUCCCtt	Non-hit	-0,522	0,609
ECT2	1894	NM_018098	26070	AAAGCCCACUUUAAUGUCCtt	Non-hit	-0,052	0,587
ECT2	1894	NM_018098	146755	AGUUAAUGCUAGACUCUGGtg	Non-hit	0,459	0,297
ENAH	55740	NM_018212	26351	ACUUGGGAAAGAGGUAUCCtc	Non-hit	-0,349	0,513
ENAH	55740	NM_018212	26445	UCACACCAAUAGCAUUCCCtc	Non-hit	-0,026	0,746
ENAH	55740	NM_018212	132358	GUUUAUCACGACCUGAUGGtc	Non-hit	-0,019	0,404
ENAH	55740	NM_018212	132359	GGUGGAAGGUCUGUGUAGCtt	Non-hit	-1,186	0,050
EVL	51466	NM_016337	24121	GAUCACAACCUGCUGAUCCtg	Non-hit	0,013	0,708
EVL	51466	NM_016337	24216	UGAAUAAUUGAUCACAACCtg	Non-hit	-0,282	0,731
EZR	7430	NM_003379	13018	GCCGAUAGUCUUUACCACCtg	Strong hit	-1,513	0,141
EZR	7430	NM_003379	13110	UCAGCCAGGUAGGAAAUCCtt	Strong hit	-0,387	0,382
FAM13B	51306	NM_016603	135118	AUCUAAGAAGGCUAAUAGCtg	Non-hit	-0,587	0,887
FAM13B	51306	NM_016603	135119	GAAUACUGACACACGCUGCtt	Non-hit	0,721	0,097
FARP1	10160	NM_005766	16818	UGAUGGACACGAGUUUUCCtg	Non-hit	-0,201	0,945
FARP1	10160	NM_005766	16914	UGGAACUUCAAAUGCCUCCtg	Non-hit	-0,930	0,212
FARP1	10160	NM_005766	138078	ACAACAACGUGCUUUGGCCtt	Non-hit	-0,357	0,655
FARP1	10160	NM_001001715	215120	UGUCCACGUUCCAAGGUACtg	Non-hit	0,352	0,485

Gene Symbol [1]	Gene ID[1]	RefSeq Accession Number[2]	siRNA ID[3]	Antisense (target) siRNA Sequence[3]	Hit gene[4]	Z-score [5]	P-value [5]
FARP2	9855	NM_014808	22052	CACUUGUGUCAGUAAUACCtg	Mild hit	-1,016	0,004
FARP2	9855	NM_014808	22148	AGCACCACAUUCUUUGGCCtt	Mild hit	-0,003	0,260
FBLIM1	54751	NM_001024216	108962	AGGCACUUUUUAAGGGACCtt	Non-hit	-0,184	0,184
FBLIM1	54751	NM_001024216	279293	CAUUGAAGAGCUGCAUAGGtg	Non-hit	0,020	0,647
FBLIM1	54751	NM_017556	279294	CCAUCCUUCUGGUAGAAGCtc	Non-hit	-0,165	0,775
FBLIM1	54751	NM_001024216	288613	CCACCCUCUUCUCAGGCUUtg	Non-hit	0,103	0,396
FBLIM1	54751	NM_017556	288614	UUCCUCCGCCACGGCCACAtc	Non-hit	-0,869	0,264
FBLIM1	54751	NM_017556	288615	GCCUCACAAACUGCCUGCCtc	Non-hit	-0,750	0,228
FERMT2	10979	NM_006832	136119	AUACCAUACUUAUCUAAGGtc	Mild hit	-0,031	0,167
FERMT2	10979	NM_006832	136120	GAUAGAUUAAUAGUCGUGCtt	Mild hit	-1,076	0,297
FGD1	2245	NM_004463	14738	UUCUCUGUCCUUCUCUUCCtc	Mild hit	-1,355	0,022
FGD1	2245	NM_004463	14826	CAGCUUUAACAGAUAGUCCtt	Mild hit	-0,747	0,192
FGD2	221472	NM_173558	40846	UUCAGGGAGUUCAGGUACCtc	Non-hit	0,248	0,412
FGD2	221472	NM_173558	41034	CAUCCAGGAAAUCAUUUCCtc	Non-hit	-0,018	0,817
FGD3	89846	NM_033086	131558	CUUUAAGCUACCACUCAGCtc	Non-hit	0,398	0,168
FGD3	89846	NM_033086	131559	GACACACCCACAUCUAUCCtg	Non-hit	0,028	0,976
FGD4	121512	NM_139241	129200	GGUUCUAGGAGCAUUUAGGtt	Non-hit	-0,070	0,947
FGD4	121512	NM_139241	129201	GUGGUUGUCAAUCCAUGCCtt	Non-hit	0,100	0,431

Gene Symbol [1]	Gene ID[1]	RefSeq Accession Number[2]	siRNA ID[3]	Antisense (target) siRNA Sequence[3]	Hit gene[4]	Z-score [5]	P-value [5]
FGD6	55785	NM_018351	26648	UAAUCUGUCAGCAACAGCCtg	Non-hit	0,137	0,781
FGD6	55785	NM_018351	26743	GUUUCUGAAAGUUGUCUCCtt	Non-hit	0,052	0,988
ARHGEF25	115557	AK057416	288683	CAGGACAAUUAGGUUUGGUtc	Non-hit	-0,854	0,011
ARHGEF25	115557	AK057416	288684	GUGGGUGGGUUGCAGAACUta	Non-hit	0,460	0,261
FLNA	2316	NM_001456	9963	GCUUCUUCACCAUGUUGCCtg	Non-hit	-0,360	0,643
FLNA	2316	NM_001456	144674	AUUGUCCAAGCACUCGAGCtg	Non-hit	0,044	0,466
FLNB	2317	NM_001457	9964	UUCUUCAGGAGUGAUGACCtg	Mild hit	0,449	0,903
FLNB	2317	NM_001457	10059	CAAACACCAUCACGUCUCCtt	Mild hit	-1,495	0,022
FLNC	2318	NM_001458	9965	ACCAGGUUUGAGCUUGGCCtt	Mild hit	0,015	0,759
FLNC	2318	NM_001458	10060	GUCAUUGUUGGGAACCACCtt	Mild hit	-1,165	0,024
FYN	2534	NM_153048	1442	CUCCAAAGACGGUGAGUCCtt	Mild hit	-0,393	0,188
FYN	2534	NM_153047	1537	GAGACGAAGAGUUCACACCtc	Mild hit	-0,339	0,169
FYN	2534	NM_002037	1627	AGAAAUCCAGUAAACUUCCtt	Mild hit	0,711	0,586
FYN	2534	NM_153048	144827	CCACAAAGAGUGUCACUCCtg	Mild hit	-0,131	0,208
FYN	2534	NM_153048	144828	AAAGGACAAUAGCUGUCGCtc	Mild hit	-0,482	0,815
FYN	2534	NM_153047	144829	CGCGGAUAAGAAAGGUACCtc	Mild hit	-0,268	0,508
GAPD	2597	NM_002046	42838	AAAGUUGUCAUGGAUGACCtt	Mild hit	-1,245	0,463
GAPD	2597	NM_002046	44902	AAGCUUCCCGUUCUCAGCCtt	Mild hit	-0,589	0,712

Gene Symbol [1]	Gene ID[1]	RefSeq Accession Number[2]	siRNA ID[3]	Antisense (target) siRNA Sequence[3]	Hit gene[4]	Z-score [5]	P-value [5]
ARHGEF25	115557	NM_133483	36531	AGCCUUCUUCUUCUGUUCCtc	Non-hit	-0,699	0,029
ARHGEF25	115557	NM_133483	36623	AUAUUCCCAAACACAAUCCtg	Non-hit	-0,123	0,719
GIT1	28964	NM_014030	20497	UAUUGGCACUCAACCAGCCtt	Non-hit	0,224	0,457
GIT1	28964	NM_014030	20586	AUUUUCUCUUCGAUCCACCtc	Non-hit	-0,907	0,820
GIT2	9815	NM_057170	35700	GGUGUGUGUUUCAGAUGCCtc	Non-hit	-0,046	0,858
GIT2	9815	NM_057169	35791	AUUGGGAUGUACUUUAUCCtg	Non-hit	-0,136	0,735
GIT2	9815	NM_057169	35874	UUUUUGUGAUCUGGUUUCCtg	Non-hit	-1,019	0,096
GIT2	9815	NM_057170	138618	GCACCGUUAUUAUACAAGGtc	Non-hit	-0,902	0,055
GIT2	9815	NM_057170	138619	CCAUAUAGAGUUAGCACCGtt	Non-hit	-0,704	0,407
GIT2	9815	NM_057170	138620	ACUCAUAAUAGACGCAGGGtc	Non-hit	-0,254	0,721
GIT2	9815	NM_057170	288632	GAUGGUUUUCAGUAUGAGCtc	Non-hit	-0,521	0,979
GIT2	9815	NM_057170	288631	CACUCAUCACAUAAAAACGtt	Non-hit	-0,779	0,223
GMIP	51291	NM_016573	24794	UUUUUCCUUAUAGGAACCCtc	Non-hit	-0,274	0,024
GMIP	51291	NM_016573	108901	CCCAAAAGGGUUUUAGGCCtc	Non-hit	0,611	0,375
GNB2L1	10399	NM_006098	3664	CCAUAGUUGGUCUCAUCCCtg	Non-hit	-0,567	0,795
GNB2L1	10399	NM_006098	3757	GUUAGCCAGGUUCCAUACCtt	Non-hit	-0,544	0,991
GRB2	2885	NM_203506	4196	ACAUUCUUCGUUCAAAACCtt	Non-hit	-0,814	0,099
GRB2	2885	NM_002086	4292	UUUUCCAUUAAGCUCUGCCtt	Non-hit	-0,753	0,183

Gene Symbol [1]	Gene ID[1]	RefSeq Accession Number[2]	siRNA ID[3]	Antisense (target) siRNA Sequence[3]	Hit gene[4]	Z-score [5]	P-value [5]
GRB2	2885	NM_203506	106680	GCUAGGACUAUACGUGGCCtt	Non-hit	-0,383	0,992
GRB2	2885	NM_203506	144866	CGUCAGCUAGGACUAUACGtg	Non-hit	-1,080	0,238
GRB7	2886	NM_005310	2834	UCCUCCUCUCGAAGUUUCCtg	Non-hit	0,638	0,282
GRB7	2886	NM_001030002	2928	CCCAUCCUCACUGUACACCtt	Non-hit	-0,515	0,056
GRB7	2886	NM_001030002	3020	CACUUCUCCCAUAAUUCCCtg	Non-hit	-0,316	0,926
GRB7	2886	NM_005310	288576	CACGUACACGUUGGACUCGtt	Non-hit	-0,386	0,135
GRLF1	2909	AF159851	288677	GGAGACAAACUUGAGCUGGtc	Non-hit	-0,815	0,052
GRLF1	2909	AF159851	288678	CUUUUUUGUUUUUGCAAGCtg	Non-hit	-0,126	0,620
GSN	2934	NM_000177	8031	AUCCUGAUGCCACACCUCCtt	Non-hit	-0,749	0,171
GSN	2934	NM_000177	8127	UGAAUCCUGAUGCCACACCtc	Non-hit	0,019	0,574
GSN	2934	NM_000177	8218	UUCUUCUUCUUGAGAAUCCtt	Non-hit	0,028	0,871
GSN	2934	NM_198252	242584	UUGAAGUAGCCUAGGAAGGtg	Non-hit	-0,150	0,651
HMHA1	23526	NM_012292	147474	AUCUGGUAGUAGGAGAUCGtg	Mild hit	-1,280	0,232
HMHA1	23526	NM_012292	147475	GAAAGAACCACACGGUGGCtt	Mild hit	-0,662	0,410
ILK	3611	NM_001014794	1461	CACGACAAUGUCAUUGCCCtg	Non-hit	-0,375	0,978
ILK	3611	NM_001014795	1556	CAAAGCAAACUUCACAGCCtg	Non-hit	-1,308	0,034
ILK	3611	NM_004517	145116	GGUUCAUUACAUUGAUCCGtg	Non-hit	2,838	0,016
ILK	3611	NM_001014795	145117	AGAGUGAUUCUCGUUGAGCtt	Non-hit	0,926	0,246

Gene Symbol [1]	Gene ID[1]	RefSeq Accession Number[2]	siRNA ID[3]	Antisense (target) siRNA Sequence[3]	Hit gene[4]	Z-score [5]	P-value [5]
ILK	3611	NM_001014795	145118	CUUCUGUACAAUAUCACGGtg	Non-hit	-1,160	0,000
ILK	3611	NM_001014795	288570	GCACUGAGUGAAAAUGUCGtc	Non-hit	0,205	0,523
INCENP	3619	NM_020238	28431	AAUCUGCUUCUUCUUCUCCTC	Non-hit	-0,041	0,742
IQGAP1	8826	NM_003870	13799	UCUCCUUUCAUCCAUCUCCtc	Non-hit	-0,130	0,610
IQGAP1	8826	NM_003870	13894	UUCUUCUGUGAAGUCAACCtt	Non-hit	-0,372	0,944
ITGB1	3688	NM_133376	35488	GUGCAGAAGUAGGCAUUCCtt	Mild hit	-0,509	0,242
ITGB1	3688	NM_133376	109877	UUGGAUCUGAGUAAUAUCCtc	Mild hit	0,136	0,627
ITGB1	3688	NM_033668	109878	UCACUUGUGCAAGGGUUCCtg	Mild hit	-0,992	0,018
ITGB1	3688	NM_133376	109879	GUUAAAAUAGGAACAUUCCtg	Mild hit	-1,312	0,006
ITGB1	3688	NM_033668	112291	ACCCACAAUUUGGCCCUGCtt	Mild hit	-0,208	0,678
ITGB1	3688	NM_002211	112292	UUGGAUCUGAGUAAUAUCCtc	Mild hit	-1,032	0,284
ITGB1	3688	NM_133376	112293	GUACAUAUUAUUUUCCAGGtg	Mild hit	-0,676	0,104
ITGB1	3688	NM_133376	288621	CAAAUUUCCAGAUAUGCGCtg	Mild hit	-1,328	0,102
ITGB1	3688	NM_133376	288622	CAGAUAAUGUUCCUACUGCtg	Mild hit	-1,133	0,013
ITGB1	3688	NM_033668	288625	UUUAAAGCUGUCAGAAUCCtt	Mild hit	0,033	0,929
ITGB1	3688	NM_033669	35396	AGAAGUAGGCAUUCCUUCCtg	Mild hit	-0,539	0,532
ITGB1	3688	NM_033666	35575	GCUAAUUUCAAAUUGAACCtc	Mild hit	-0,269	0,118
ITGB1BP1	9270	NM_022334	44218	AGGCAACUUUCCAUCUUGCtg	Non-hit	-1,412	0,029

Gene Symbol [1]	Gene ID[1]	RefSeq Accession Number[2]	siRNA ID[3]	Antisense (target) siRNA Sequence[3]	Hit gene[4]	Z-score [5]	P-value [5]
ITGB1BP1	9270	NM_022334	44998	CAUCUCGUCUUCGUGACACtt	Non-hit	0,579	0,339
ITGB1BP1	9270	NM_004763	137692	CGUCUUCGUGACACUUAGGtt	Non-hit	-0,685	0,656
ITGB1BP1	9270	NM_004763	137693	GAGCGGUAAUCUUUUAAGGtt	Non-hit	-0,810	0,024
ITGB3	3690	NM_000212	8055	AUCCUUCAGCAGAUUCUCCtt	Non-hit	-0,139	0,723
ITGB3	3690	NM_000212	106001	CUAAUAGUUCAGCUCUCCCtg	Non-hit	-0,593	0,406
ITGB3BP	23421	NM_014288	21001	UUCAAGCUCUCUACUGCCCtc	Strong hit	-2,114	0,021
ITGB3BP	23421	NM_014288	21093	AUGCUUUGUGAGGAAGUCCtg	Strong hit	0,205	0,488
ITGB4	3691	NM_001005731	2793	GAACAUCUUGGAGGUGACCtc	Non-hit	-0,602	0,959
ITGB4	3691	NM_001005619	2888	AUGUGAAAGGACCCAGUCCtc	Non-hit	-1,882	0,040
ITGB4	3691	NM_001005731	2981	UUUCAGAUGGAUGUUGCCCtt	Non-hit	-1,026	0,148
ITGB4	3691	NM_001005731	288542	AAUAGGUCGGUUGUCAUCGtt	Non-hit	0,217	0,919
ITGB4	3691	NM_001005731	288543	UCGCUGUACAUAAGGAAGCtg	Non-hit	0,877	0,213
ITGB4	3691	NM_001005731	288544	CAGUUGAAAUGGAUCUUCCtg	Non-hit	0,999	0,415
ITGB5	3693	NM_002213	11108	UAGUGCAUAUGUUGAGACCtg	Non-hit	0,537	0,305
ITGB5	3693	NM_002213	11289	AAAGAAGAGAUUAAGAUCCtc	Non-hit	0,376	0,636
ITGB6	3694	NM_000888	8947	CUUCACAGGUUUCUGCACCtc	Non-hit	0,061	0,205
ITGB6	3694	NM_000888	9041	UGGAUGAGUAAAAUUCUCCtg	Non-hit	-0,415	0,690
ITSN1	6453	NM_001001132	12452	CAGAGGGUAGCUGAUAUCCtt	Non-hit	-0,808	0,347

Gene Symbol [1]	Gene ID[1]	RefSeq Accession Number[2]	siRNA ID[3]	Antisense (target) siRNA Sequence[3]	Hit gene[4]	Z-score [5]	P-value [5]
ITSN1	6453	NM_003024	12546	UAGUGUUUAGUUGUGACCCtg	Non-hit	-0,786	0,011
ITSN1	6453	NM_001001132	12635	UGACUAUUGAAUAAUUGCCtg	Non-hit	-0,965	0,110
ITSN1	6453	NM_003024	142608	GUGGAUGUAUCCUUGUCGCtt	Non-hit	-0,846	0,151
ITSN2	50618	NM_019595	17648	UUGAGGUUAUCAAACUGCCtg	Non-hit	1,234	0,017
ITSN2	50618	NM_147152	17743	CACCUGUUAUGUAACCUCCtg	Non-hit	-0,721	0,984
ITSN2	50618	NM_019595	133782	GCCUGUCAUGCUUAGUACGtt	Non-hit	-0,493	0,021
ITSN2	50618	NM_147152	133783	GAUCACCUGUUAUGUAACCtc	Non-hit	-0,985	0,009
ITSN2	50618	NM_019595	133784	AAGUAUCCUUAUCCUUACGtt	Non-hit	-0,523	0,506
KALRN	8997	NM_001024660	845	AGAGGAGGACAUUUCAUCCtg	Non-hit	-0,315	0,992
KALRN	8997	NM_003947	13846	CAUCAUUCCGAAAAGACCCtc	Non-hit	0,477	0,311
KALRN	8997	NM_001024660	13939	CACGAAGGCCACCUUUUCCtt	Non-hit	0,695	0,347
KALRN	8997	NM_001024660	14029	AGUUGAUAUUUGGUGAUCCtt	Non-hit	0,103	0,690
KALRN	8997	NM_001024660	124683	CACUUCUUAAGAGUGUUGGtg	Non-hit	-0,437	0,959
KALRN	8997	NM_001024660	137405	UCCACAGAUACCAUGCUCGtc	Non-hit	0,890	0,123
KIF11	3832	NM_004523	14672	AGCUCUUGUCAGCCAAUCCtc	Non-hit	0,442	0,423
KIF11	3832	NM_004523	14765	CAUUAGGUGACCUUUCACCtt	Non-hit	-0,022	0,583
KIF12	113220	NM_138424	36707	CAAAAGUUCCAUCAGGGCCtc	Non-hit	-0,847	0,384
KIF12	113220	NM_138424	118498	UGACGGCUGAUGUAAAGGGtg	Non-hit	0,746	0,307

Gene Symbol [1]	Gene ID[1]	RefSeq Accession Number[2]	siRNA ID[3]	Antisense (target) siRNA Sequence[3]	Hit gene[4]	Z-score [5]	P-value [5]
KIF13A	63971	NM_022113	29651	GCAGGACCGUUUGAUUCCCtt	Non-hit	-0,523	0,403
KIF13A	63971	NM_022113	29745	AAUACCUUGGGAGGUUUCCtt	Non-hit	-0,193	0,701
KIF13B	23303	NM_015254	22657	UGAAAACAAUAUCUUGACCtg	Non-hit	-0,525	0,051
KIF13B	23303	NM_015254	22848	GUACUUUUCAAUAUAAGCCtc	Non-hit	-0,129	0,770
KIF14	9928	NM_014875	22099	UUAUGUCUCUGACUUUACCtg	Non-hit	-0,435	0,253
KIF14	9928	NM_014875	22195	UUGUUCCUUGUAGUUCUCCtc	Non-hit	0,980	0,276
KIF15	56992	NM_020242	28246	AAACUUUGAUGGCAUCACCtt	Mild hit	-1,265	0,106
KIF15	56992	NM_020242	118474	AGUUCUGCUCUCCAUCAGCtg	Mild hit	0,258	0,456
KIF16B	55614	BX647572	288693	UGUGAAACGUAAUCUGGGCtt	Strong hit	-1,637	0,008
KIF16B	55614	BX647572	288694	UGUUGAUGAUGUUUUUGGCtc	Strong hit	-0,727	0,044
KIF17	57576	NM_020816	118477	UCGUUGUAGAUCUGCUCGGtg	Non-hit	-0,685	0,196
KIF17	57576	NM_020816	118478	GAUCUCGUUGUAGAUCUGCtc	Non-hit	-0,096	0,647
KIF18A	81930	NM_031217	32973	UCAGUGGGAUGUUGUGUCCtg	Strong hit	-1,762	0,026
KIF18A	81930	NM_031217	118492	CUUUAUGAAAUCCAGCUGCtt	Strong hit	-0,925	0,116
KIF18B	146909	XM_085634	251223	GGCUUUUGAUGACUGUGGCtg	Non-hit	-0,533	0,467
KIF18B	146909	XM_085634	251224	UAUGUACAUGCCAAGAAGCtg	Non-hit	-0,471	0,197
KIF19	124602	NM_153209	39789	AGACAGUGGCAUUGUAGCCtg	Mild hit	-1,131	0,027
KIF19	124602	NM_153209	39883	UGUAGGUUUUCCCACAGCCtg	Mild hit	-1,192	0,042

Gene Symbol [1]	Gene ID[1]	RefSeq Accession Number[2]	siRNA ID[3]	Antisense (target) siRNA Sequence[3]	Hit gene[4]	Z-score [5]	P-value [5]
KIF1A	547	NM_004321	14392	GAUGCACACGUUGUAUCCCtc	Non-hit	0,373	0,767
KIF1A	547	NM_004321	147322	GUAUCCCUCAAAGGCAUGCtg	Non-hit	-0,475	0,195
KIF1B	23095	NM_183416	22400	AAUGAUGCAUUUGGAUUCCtt	Strong hit	-0,980	0,262
KIF1B	23095	NM_183416	118460	GAAGGACUUUGGAGCUUCCtt	Strong hit	-1,987	0,017
KIF1C	10749	NM_006612	18210	AGAUGCACACGUUGUAGCCtt	Non-hit	0,588	0,755
KIF1C	10749	NM_006612	18304	GAUCUCCAUAUAGCUCACCtc	Non-hit	-0,249	0,151
KIF2A	3796	NM_004520	14669	CCAGGUCAAUCUCUUUGCCtt	Mild hit	-1,286	0,037
KIF2A	3796	NM_004520	14762	GUCUAUAAUCCAAACUUCCtc	Mild hit	-0,480	0,297
KIF20A	10112	NM_005733	16618	ACUGUCCUCAGAUGGAACCtg	Non-hit	-0,458	0,245
KIF20A	10112	NM_005733	288582	AGGCUUGACGAAGUUUUCCtg	Non-hit	-0,076	0,579
KIF20B	9585	NM_016195	24036	AGAUUCGAAACUGUUUGCCtc	Non-hit	-0,389	0,298
KIF20B	9585	NM_016195	118465	UUCAUGAGACAGAUCAAGCtt	Non-hit	-0,936	0,099
KIF21A	55605	NM_017641	118471	AUGUACAAAUAUGGCAUCCtt	Non-hit	-0,307	0,576
KIF21A	55605	NM_017641	118472	AUCUUUCCCUAGGAAGACCtg	Non-hit	-0,758	0,229
KIF21B	23046	BC078676	288691	AGAGCUGAGGGAAAGAACAta	Non-hit	-0,233	0,676
KIF21B	23046	BC078676	288692	CCGUCAGGUCACUGGAGGCtg	Non-hit	-0,977	0,097
KIF22	3835	NM_007317	19353	CUGGUAUUUGAGAGUCUCCtg	Mild hit	-1,014	0,323
KIF22	3835	NM_007317	118450	CGAGUAGCUCCAAUCUUGCtt	Mild hit	-1,330	0,194

Gene Symbol [1]	Gene ID[1]	RefSeq Accession Number[2]	siRNA ID[3]	Antisense (target) siRNA Sequence[3]	Hit gene[4]	Z-score [5]	P-value [5]
KIF23	9493	NM_138555	36749	AAAUGAAUACUGAGUCUCCtt	Mild hit	-1,261	0,077
KIF23	9493	NM_138555	118501	CUUAUAGUCUCCAUUUCGGtt	Mild hit	-1,279	0,108
KIF24	55265	NM_018278	26683	CUGUGGCAUUCAGAAUUCCtg	Mild hit	-0,884	0,065
KIF24	55265	NM_018278	26777	AAAUAACUUAUUGUCACCCtg	Mild hit	-1,285	0,015
KIF25	3834	NM_030615	32833	GUAUUUUCCAAAAUGAGCCtg	Non-hit	-0,082	0,666
KIF25	3834	NM_030615	118490	AUGGUAUAGCUCUUUCCGCtg	Non-hit	0,675	0,894
KIF26A	26153	XM_050278	263710	CCUAUGCUAUGCACGAUCCtc	Mild hit	-0,893	0,611
KIF26A	26153	XM_050278	263711	AGAAAAGUCCAAAUCAAGGtc	Mild hit	-1,023	0,121
KIF26B	55083	BC035896	288689	GUCUUCUUUUUCUUCAUCCtc	Mild hit	-1,207	0,193
KIF26B	55083	BC035896	288690	CAUGGAUUUUUUCAAAACCtg	Mild hit	-1,026	0,418
KIF27	55582	NM_017576	118468	UUCUCGGAUGUGAAGAUCCtt	Non-hit	-0,652	0,155
KIF27	55582	NM_017576	118469	CAACAAUCACUGUGUUUCCtt	Non-hit	-0,129	0,556
KIF2B	84643	NM_032559	34309	CCAGGUCAAUCUUCUUGCCtt	Non-hit	-0,538	0,101
KIF2B	84643	NM_032559	118495	UUUUCUCUGUUGAUCUCCGtg	Non-hit	-0,429	0,278
KIF2C	11004	NM_006845	18553	UUCUCCAAGUUCACAGUCCtt	Mild hit	-0,381	0,432
KIF2C	11004	NM_006845	18738	CUUCAUUUUUUCCACUUCCtt	Mild hit	-1,016	0,224
KIF3A	11127	NM_007054	19038	AAAUAGUCCCAUUGUAGCCtt	Non-hit	0,739	0,642
KIF3A	11127	NM_007054	118447	AAGUAAAUGUCUUUGGAGGtt	Non-hit	-0,301	0,177

Gene Symbol [1]	Gene ID[1]	RefSeq Accession Number[2]	siRNA ID[3]	Antisense (target) siRNA Sequence[3]	Hit gene[4]	Z-score [5]	P-value [5]
KIF3B	9371	NM_004798	15207	AUACGAAGCAGCCUUUUCCtt	Mild hit	0,414	0,621
KIF3B	9371	NM_004798	118432	UCAUAGACGGCAUCAAAGGtg	Mild hit	-1,366	0,063
KIF3C	3797	NM_002254	11118	CAGGUCUCGAAUCUCUUCCtg	Mild hit	-0,507	0,479
KIF3C	3797	NM_002254	118421	GAUGUGGGUGAAGAUGUGCtc	Mild hit	-1,144	0,021
KIF4A	24137	AF071592	288675	UGUUCUUGAUUUUUCUUGCtc	Non-hit	0,774	0,177
KIF4A	24137	AF071592	288676	UUAGAUGAUUAAGUUCAGCtg	Non-hit	-0,160	0,941
KIF4B	285643	AF241316	288679	UGUAUUACCCUAGGAAUAAtg	Non-hit	-0,009	0,801
KIF4B	285643	AF241316	288680	CUCUUUUGAUCAAUUUCUUtg	Non-hit	-0,914	0,088
KIF5A	3798	NM_004984	15501	CCAUGGUAUGUGUUUUCCCtg	Non-hit	-0,151	0,805
KIF5A	3798	NM_004984	118435	ACGGUCAAAAACAUAUGGCtt	Non-hit	-0,013	0,381
KIF5B	3799	NM_004521	14670	AGAUGCCAAAAGCUCCUCCtg	Non-hit	-0,105	0,438
KIF5B	3799	NM_004521	14763	GGUAGAUGCCAAAAGCUCCtc	Non-hit	-0,213	0,481
KIF5C	3800	NM_004522	14764	CGCACAUGCAUUGUAAACCtg	Non-hit	-0,412	0,210
KIF5C	3800	NM_004522	14850	GAUCUCAAAAUAGGAAACCtt	Non-hit	0,702	0,535
KIF6	221458	NM_145027	37797	UAUACUUUCUCCCAGGGCCtt	Mild hit	-1,016	0,106
KIF6	221458	NM_145027	37893	CCGCUGGGUGAUUUCUUCCtt	Mild hit	-0,928	0,084
KIF7	374654	NM_198525	118513	UUUCUGCGCAGGUGUAAGGtc	Non-hit	-0,460	0,553
KIF7	374654	NM_198525	118514	CAACUCCUCAAGGCAAAGCtc	Non-hit	-0,291	0,459

Gene Symbol [1]	Gene ID[1]	RefSeq Accession Number[2]	siRNA ID[3]	Antisense (target) siRNA Sequence[3]	Hit gene[4]	Z-score [5]	P-value [5]
KIF9	64147	NM_022342	30070	UUGCUCAUUCUUAAACUCCtc	Non-hit	-0,080	0,989
KIF9	64147	NM_182903	118509	UUCGAUCAUCCUAAAAACCtg	Non-hit	-0,150	0,516
KIFAP3	22920	NM_014970	22364	CAUUCUUCAACCACCUUCCtt	Non-hit	0,392	0,583
KIFAP3	22920	NM_014970	118456	CAUAGUGAACAAUGAGUGCtt	Non-hit	-0,596	0,163
KIFC1	3833	NM_002263	43827	UCCUCUUGAGUCUGCUUCCtg	Non-hit	-0,261	0,521
KIFC1	3833	NM_002263	43923	UGUCCGUUUCUUCUCAGGCtc	Non-hit	0,244	0,832
KIFC2	90990	NM_145754	38128	AGAGUCAGAUGCUGAACCCtt	Non-hit	-0,389	0,701
KIFC2	90990	NM_145754	118504	ACCCUUUUCUCUGAGUCCGtc	Non-hit	-0,667	0,062
KIFC3	3801	NM_005550	16324	UCAGCUCUGACAGCAUGCCtt	Non-hit	-0,508	0,871
KIFC3	3801	NM_005550	118438	UCUGACAGCAUGCCUUUGCtt	Non-hit	-0,868	0,175
LASP1	3927	NM_006148	17398	CUUGUUCUUCUCAAACUCCtc	Mild hit	-0,285	0,493
LASP1	3927	NM_006148	17494	UACGCUGAAACCUUUGCCCtt	Mild hit	-1,138	0,075
LIMK1	3984	NM_002314	1413	GAAGUUGAGCCUCUUGUCCtt	Non-hit	-1,073	0,184
LIMK1	3984	NM_016735	1318	UGUCUCACGGUGUGUCACCtt	Non-hit	-0,748	0,026
LIMK1	3984	NM_016735	143455	UGUAUCGUGAGGGUCAUGCtc	Non-hit	0,608	0,760
LIMK1	3984	NM_016735	143456	UUAUUGUUCUGCGUCUGGGtt	Non-hit	-0,959	0,003
LIMK2	3985	NM_016733	1469	GCAGUAGAGCUUCCCAUCCtt	Mild hit	0,003	0,342
LIMK2	3985	NM_001031801	1563	CCCAUCCUCAAUGAUCACCtt	Mild hit	-1,374	0,082

Gene Symbol [1]	Gene ID[1]	RefSeq Accession Number[2]	siRNA ID[3]	Antisense (target) siRNA Sequence[3]	Hit gene[4]	Z-score [5]	P-value [5]
LIMK2	3985	NM_016733	1653	CAGGUUCAGCUUCUUAUCCtt	Mild hit	-0,312	0,550
LIMK2	3985	NM_016733	144048	GAGAUACUGUUACUGCGCCtt	Mild hit	-0,988	0,365
LIMK2	3985	NM_005569	144049	UUCGAGAAUGCUGGUCUGCtc	Mild hit	-0,771	0,008
LIMK2	3985	NM_005569	144050	UAAGUUUGAAAACAUGAGGtg	Mild hit	-1,183	0,260
LIMS1	3987	NM_004987	15503	CAAACUCAUAGAAGAGUCCtt	Strong hit	-1,540	0,240
LIMS1	3987	NM_004987	15596	GUUCACAGUACUUUCUUCCtt	Strong hit	0,211	0,820
LIMS2	55679	NM_017980	25885	AGAGUUGAGGUCUGUGGCCtt	Mild hit	0,348	0,251
LIMS2	55679	NM_017980	132221	AGCCUUCAUUGUGCAAGCGtg	Mild hit	-1,439	0,157
LRP1	4035	NM_002332	11342	CCACAAAGUAGAAGUUGCCtg	Non-hit	-0,341	0,865
LRP1	4035	NM_002332	111141	ACCCAGGCAGUUAUGCUCGtt	Non-hit	-0,473	0,154
MACF1	23499	NM_033044	258846	AUCCUUCAAGUCACUUUGGtt	Non-hit	0,480	0,865
MACF1	23499	NM_033044	258847	UGUUUAUCAUCCAACCAGGtc	Non-hit	-0,321	0,209
MACF1	23499	NM_033044	258848	UUCUAUCCAUGGCACAAGGtc	Non-hit	0,585	0,474
MACF1	23499	NM_033044	288620	CUCUAAAGUUCUGAGGGCCtt	Non-hit	-1,233	0,257
MAP3K1	4214	XM_042066	263692	CCAAAUUGACAUGCAGUGGtg	Non-hit	-0,615	0,161
MAP3K1	4214	XM_042066	263693	UCACAUACUUAGGUAAGGGtt	Non-hit	-0,252	0,629
MAPK1	5594	NM_002745	1449	AUCUGUUUCCAUGAGGUCCtg	Non-hit	-0,529	0,150
MAPK1	5594	NM_138957	1544	CAUAUUCUGUCAGGAACCCtg	Non-hit	-0,417	0,485

Gene Symbol [1]	Gene ID[1]	RefSeq Accession Number[2]	siRNA ID[3]	Antisense (target) siRNA Sequence[3]	Hit gene[4]	Z-score [5]	P-value [5]
MAPK1	5594	NM_138957	1634	UAGUUCUUUGAGCUUUUCCtt	Non-hit	-1,304	0,036
MAPK1	5594	NM_138957	142301	UUUGCUCGAUGGUUGGUGCtc	Non-hit	-0,446	0,449
MAPK3	5595	NM_002746	142304	GUUAAAGGUUAACAUCCGGtc	Mild hit	0,019	0,911
MAPK3	5595	NM_002746	214749	GUUGAUGAUACAAUUCAGGtc	Mild hit	-1,428	0,002
MAPK8IP1	9479	NM_005456	16261	GUCUUCAUCCUCAAACUCCtc	Non-hit	-0,561	0,262
MAPK8IP1	9479	NM_005456	16356	AUUAUUAUUCAGUGUGUCCtg	Non-hit	0,214	0,687
MAPK8IP2	23542	NM_012324	19889	AAACUCCUGGAAGUCAUCCtg	Non-hit	-0,368	0,980
MAPK8IP2	23542	NM_016431	20076	UCAAGGAUGGGAUGAUCCCtt	Non-hit	-0,248	0,721
MAPK8IP3	23162	NM_033392	22516	AUCGGCAUAGUUCUUGGCCtt	Non-hit	-0,081	0,407
MAPK8IP3	23162	NM_033392	136770	CUUGGACCUCUCAAUGUGCtc	Non-hit	-0,690	0,116
MAPRE1	22919	NM_012325	3708	CACCCAUUCUCUUAAAACCtg	Non-hit	-0,013	0,592
MAPRE1	22919	NM_012325	3891	AACGAAUUCAAAAUUGUCCtg	Non-hit	-0,318	0,671
MAPRE2	10982	NM_014268	20987	CUUCUCCACUGGAAUUACCtt	Mild hit	-1,250	0,109
MAPRE2	10982	NM_014268	136574	UUCCGGAAAGGAAUGAUGGtc	Mild hit	-0,622	0,276
MAPRE3	22924	NM_012326	19890	GCCUGGAACUUCACUUUCCtc	Non-hit	-0,257	0,943
MAPRE3	22924	NM_012326	136502	CAGCAGAGGGUUGUAAUCCtt	Non-hit	0,207	0,502
MCF2	4168	NM_005369	2835	UUUAGGCAUAAAAUCCUCCtg	Non-hit	0,169	0,135
MCF2	4168	NM_005369	144005	AGCAAAUCACUAACUGAGCtc	Non-hit	0,031	0,731

Gene Symbol [1]	Gene ID[1]	RefSeq Accession Number[2]	siRNA ID[3]	Antisense (target) siRNA Sequence[3]	Hit gene[4]	Z-score [5]	P-value [5]
MCF2L	23263	NM_024979	32098	CAUGACAUUCUGGAACUCCtt	Non-hit	-0,173	0,569
MCF2L	23263	NM_024979	137007	GUCCUUUGGAAAAAACCCGtc	Non-hit	-0,438	0,647
MCF2L2	23101	NM_015078	22402	UAUUCGUGUCAAGGAUGCCtt	Strong hit	1,534	0,022
MCF2L2	23101	NM_015078	119310	UCCAGUUGAACUAAUAACCtt	Strong hit	-0,237	0,912
MLPH	79083	NM_024101	42410	UCUCUGAGCAGGACUCAUCtg	Non-hit	-0,549	0,153
MLPH	79083	NM_024101	42493	UGUCUGGAAGGUGAGAUGCtg	Non-hit	0,328	0,608
MSN	4478	NM_002444	11593	GCCAAUAGUUUUCACCACCtg	Non-hit	-0,320	0,889
MSN	4478	NM_002444	143572	UCAAAUAGCUGCUUCCCGGtg	Non-hit	-0,463	0,045
MYH1	4619	NM_005963	17114	UGGGCUUCAAUUCGCUCCCtt	Mild hit	-1,081	0,055
MYH1	4619	NM_005963	17208	UGCUUUCACAAAGGACUCCtt	Mild hit	-0,733	0,528
MYH10	4628	NM_005964	147398	UCCACACUAGCUUUUUAGCtg	Mild hit	-1,397	0,162
MYH10	4628	NM_005964	147399	GUUCUUCUUUGAUACUAGCtg	Mild hit	-1,071	0,299
MYH11	4629	NM_022844	43338	UCUCCUCCUUAAUGCUGGCtg	Non-hit	-0,993	0,508
MYH11	4629	NM_002474	118370	AUCUUUCCCAACCGUGACCtt	Non-hit	-0,293	0,722
MYH13	8735	NM_003802	13581	UUGAGCCUCGAUUCUCUCCtt	Non-hit	-0,824	0,323
MYH13	8735	NM_003802	13674	GCCUUUCACAUACAUUUCCtt	Non-hit	-0,731	0,278
MYH15	22989	AB023217	288671	UUGGAAAUCUCUCCUCUGCtt	Non-hit	-0,952	0,078
MYH15	22989	AB023217	288672	AUAGUAGGCUUUGAUUUGCtc	Non-hit	-0,796	0,207

Gene Symbol [1]	Gene ID[1]	RefSeq Accession Number[2]	siRNA ID[3]	Antisense (target) siRNA Sequence[3]	Hit gene[4]	Z-score [5]	P-value [5]
MYH2	4620	NM_017534	24900	UCACCGUCACUUUUCCUCCtt	Non-hit	-0,539	0,566
MYH2	4620	NM_017534	118403	GGGUAAUCAUAUGGGUUCGtg	Non-hit	0,088	0,748
MYH3	4621	NM_002470	11602	CUCAGUUUCCACAGUGACCtt	Mild hit	-0,370	0,385
MYH3	4621	NM_002470	11788	UCCAAUUUCCUUUUGUUCCtt	Mild hit	-1,176	0,150
MYH4	4622	NM_017533	24899	CUGAGCUUCAAUUCGCUCCtt	Non-hit	-0,138	0,552
MYH4	4622	NM_017533	24994	UGCUUUCACGUAGGACUCCtt	Non-hit	-0,744	0,247
MYH6	4624	NM_002471	11603	GGCUUUGACAAACUCUUCCtt	Non-hit	-0,550	0,309
MYH6	4624	NM_002471	11699	UUUCAGCAAUGACCUUGCCtc	Non-hit	-0,326	0,159
MYH7	4625	NM_000257	8079	UUCUUGAGGUCAAAAGGCCtg	Non-hit	-0,392	0,140
MYH7	4625	NM_000257	8172	AUCAGGCACGAAGACAUCCtt	Non-hit	-0,087	0,455
MYH7B	57644	AB040945	288673	GGUCAUCAGCUUGUUGAGGtt	Mild hit	-1,121	0,376
MYH7B	57644	AB040945	288674	CUUCAUCUUGAAAAAGAGCtt	Mild hit	-1,332	0,169
MYH8	4626	NM_002472	11604	AAACGGCUUGUUUUGGGCCtc	Non-hit	-0,719	0,071
MYH8	4626	NM_002472	11700	GCUCUUCACAUAGGAUUCCtt	Non-hit	-0,757	0,098
MYH9	4627	NM_002473	11605	AUCCUUGUUCACCUUCACCtt	Mild hit	-0,102	0,795
MYH9	4627	NM_002473	11701	GAUGUCAUCCUUGUUCACCtt	Mild hit	-1,355	0,120
MYLIP	29116	NM_013262	20179	UCUAUGAUUCCCAGUCGCCtg	Non-hit	-0,421	0,997
MYLIP	29116	NM_013262	118397	GAUAUGCCUAGUCUGCUCCtg	Non-hit	0,203	0,550

Gene Symbol [1]	Gene ID[1]	RefSeq Accession Number[2]	siRNA ID[3]	Antisense (target) siRNA Sequence[3]	Hit gene[4]	Z-score [5]	P-value [5]
MYLK	4638	NM_053032	1510	GACCCUGUUGAGGAUUUCCtg	Non-hit	0,522	0,118
MYLK	4638	NM_053027	1692	UUUUACAUGAGGCUUUUCCtc	Non-hit	-0,389	0,936
MYLK	4638	NM_053026	103376	UAAAGAGCAGUUCCCGUCCtc	Non-hit	-1,240	0,095
MYLK	4638	NM_053031	144402	CAUCGUUUCCACAAUGAGCtc	Non-hit	0,806	0,531
MYLK	4638	NM_053031	288626	GUUGAAAUCUGUUUCAUCGtg	Non-hit	0,480	0,620
MYLK	4638	NM_053031	288627	GCUGCUAGGUAUCAACUGCtg	Non-hit	-0,461	0,859
MYLK	4638	NM_053031	288628	GGAACUCUUAAAAAGUCCCtt	Non-hit	0,378	0,906
MYLK	4638	NM_005965	103460	UCCAAGACUGUUGACAGCCtt	Non-hit	0,115	0,291
MYLK	4638	NM_053030	144401	UUUUCUGCAUUGAGCGGGCtg	Non-hit	-1,237	0,309
MYLK	4638	NM_053030	144403	AGCAUAAUGUCCUUAAUGCtt	Non-hit	-0,877	0,277
MYO10	4651	NM_012334	19898	UAGUGCUUUCGGUUUUACCtg	Non-hit	-0,669	0,299
MYO10	4651	NM_012334	19992	AACACAGGAUGUCUUCUCCtt	Non-hit	-0,421	0,742
MYO15A	51168	NM_016239	24065	AUAAUACUCGCCCAGGUCCtg	Non-hit	-0,360	0,950
MYO15A	51168	NM_016239	118400	UGCGUCAUGAGCUUUGACGtg	Non-hit	-0,474	0,474
MYO15B	80022	BC027875	251256	AAGCCUUCAUUUCACCCGGtg	Non-hit	-0,160	0,441
MYO15B	80022	BC027875	251257	UCUAUCAGGAAGACAGUGGtg	Non-hit	-0,159	0,529
MYO16	23026	AB020672	288669	UCCUCUCACAGAACUGAAGtt	Mild hit	-0,614	0,457
MYO16	23026	AB020672	288670	UUAACUAAAGGGUGCACAAtc	Mild hit	-1,052	0,181

Gene Symbol [1]	Gene ID[1]	RefSeq Accession Number[2]	siRNA ID[3]	Antisense (target) siRNA Sequence[3]	Hit gene[4]	Z-score [5]	P-value [5]
MYO18A	399687	NM_078471	147986	GAGGAUGAUUGACUGAUCCtg	Strong hit	-1,545	0,353
MYO18A	399687	NM_203318	147987	CUUGUAUCUUUCCAACUCCtg	Strong hit	-0,980	0,116
MYO18B	84700	NM_032608	34346	CUUCCUCUGUCUCGCUUCCtt	Mild hit	-1,371	0,371
MYO18B	84700	NM_032608	118407	CUUGUCUUCUCCAUCUGGGtc	Mild hit	-0,503	0,231
MYO1A	4640	NM_005379	16050	AAACGGCUUGUUUUGGGCCtc	Strong hit	-1,484	0,084
MYO1A	4640	NM_005379	144012	GCGAUAAUUCUUUCGGGCCtt	Strong hit	-1,594	0,102
MYO1B	4430	NM_012223	148408	GGGUAAAGACCGGUAUGGGtt	Non-hit	0,482	0,248
MYO1B	4430	NM_012223	148409	CGGGUUGGACUGUAAAAGCtg	Non-hit	-0,687	0,133
MYO1C	4641	NM_033375	35347	UCCAUGUACUUCCCGAACCtg	Non-hit	-0,641	0,170
MYO1C	4641	NM_033375	118410	GAACCUGCUGGAGUUAUCGtt	Non-hit	0,063	0,385
MYO1D	4642	NM_015194	222682	CUGUAAUGCUCAGUUUGCCtt	Strong hit	-0,401	0,783
MYO1D	4642	NM_015194	251683	UCGAUUUACCUUACGGACGtg	Strong hit	-1,699	0,076
MYO1E	4643	NM_004998	15509	UUUCAUACUGUGCCGCUCCtt	Non-hit	-0,182	0,362
MYO1E	4643	NM_004998	15693	GAGAAUAAAAAUGUCAUCCtg	Non-hit	-0,028	0,987
MYO1F	4542	NM_012335	19899	AUCUUUGACGUGCUGGACCtt	Non-hit	-0,945	0,055
MYO1F	4542	NM_012335	118394	AUAGAGGUCGAUCUCACGGtc	Non-hit	-0,333	0,673
MYO1G	64005	NM_033054	221471	ACUGUUGACGGGAAACACCtc	Mild hit	-1,215	0,094
MYO1G	64005	NM_033054	221472	GUUUGCCAUACUCAGGGCCtt	Mild hit	0,340	0,787

Gene Symbol [1]	Gene ID[1]	RefSeq Accession Number[2]	siRNA ID[3]	Antisense (target) siRNA Sequence[3]	Hit gene[4]	Z-score [5]	P-value [5]
MYO3A	53904	NM_017433	1486	UAGCAUCACAUCUUUGCCCtc	Mild hit	-0,078	0,315
MYO3A	53904	NM_017433	131930	AAUCUCUUCGUCAAUAUCGtg	Mild hit	-1,097	0,183
MYO3B	140469	NM_138995	1137	AUCUCUCUUGUUAGUUACCtt	Non-hit	-0,782	0,635
MYO3B	140469	NM_138995	1138	CAAUUGAAGGUAACAUUCCtg	Non-hit	-0,670	0,299
MYO5A	4644	NM_000259	8081	GCAGGAGGACUUUAUCUCCtg	Strong hit	0,072	0,406
MYO5A	4644	NM_000259	8174	UUCCAAAUCCUUUCCUUCCtc	Strong hit	-1,522	0,030
MYO5B	4645	AY274809	288685	CUUCUUUGUAGUCCUUGGUta	Mild hit	-1,012	0,126
MYO5B	4645	AY274809	288686	AUAGAUUGGCAACUGUUCAta	Mild hit	-0,814	0,100
MYO5C	55930	NM_018728	27397	GUCACCAACUCUGUAGUCCtt	Mild hit	0,314	0,456
MYO5C	55930	NM_018728	118404	CACGGCAAAUAUGUGUGGGtc	Mild hit	-1,252	0,548
MYO6	4646	NM_004999	15510	GAGCCAAAAAUGUCUUGCCtt	Non-hit	-0,407	0,806
MYO6	4646	NM_004999	15603	CACAUCUUUUUUACUGUCCtc	Non-hit	-0,875	0,505
MYO7A	4647	NM_000260	8082	GUCUUCAUCAUCCACCACCtg	Non-hit	-0,754	0,165
MYO7A	4647	NM_000260	8175	UAGAACACGUGGUAGUUCCtt	Non-hit	-0,521	0,635
MYO7B	4648	XM_291001	263743	GGCGAAAAUGGACCUCUCCtt	Mild hit	-1,134	0,117
MYO7B	4648	XM_291001	263744	CACAUAUGAGGUCAGCAGGtc	Mild hit	-0,307	0,308
MYO9A	4649	NM_006901	18770	UCGGACAGUAGAUUGUCCCtt	Non-hit	0,136	0,808
MYO9A	4649	NM_006901	18866	UAUAAGAGACUCAAUCACCtc	Non-hit	0,444	0,704

Gene Symbol [1]	Gene ID[1]	RefSeq Accession Number[2]	siRNA ID[3]	Antisense (target) siRNA Sequence[3]	Hit gene[4]	Z-score [5]	P-value [5]
MYO9A	4649	NM_006901	18960	AUUUUUUUCCCGGAAAUCCtt	Non-hit	-0,910	0,355
MYO9A	4649	NM_006901	144275	UCCACCAAAUUCCUUUACCtc	Non-hit	-0,241	0,616
MYO9B	4650	NM_004145	14116	GAAGUAGUAGCCAUCCUCCtg	Non-hit	-0,302	0,883
MYO9B	4650	NM_004145	14207	CAGGAAGUAGUAGCCAUCCtc	Non-hit	0,219	0,655
MYO9B	4650	NM_004145	14293	CUUGAUCUGAUAUUUCACCtt	Non-hit	-1,306	0,019
MYO9B	4650	NM_004145	143862	AUUUCUCGACGACAGCUCCtc	Non-hit	-0,698	0,337
NCK1	4690	NM_006153	17402	AGUUAGAAGGCACAAAACCtg	Non-hit	-0,677	0,891
NCK1	4690	NM_006153	17498	UUCCGAGCACUGUUUUUCCtt	Non-hit	-0,563	0,269
NCK2	8440	NM_003581	13296	CUUCUCGAAGUUGAGCUCCtc	Non-hit	-0,630	0,030
NCK2	8440	NM_003581	13379	UGAAGUGUUUGUUCUUCCCtg	Non-hit	-1,567	0,013
NCK2	8440	NM_003581	13457	AUUGUCCACGAGCUGCACCtt	Non-hit	-1,044	0,228
NCK2	8440	NM_003581	215169	UGUCUUUCUGAGUCACCGGtt	Non-hit	-0,954	0,220
NCK2	8440	NM_001004722	288563	UAAAGUGUUGGUAGCUCCCtt	Non-hit	-0,874	0,694
NCK2	8440	NM_003581	288564	CAAAGAUCAGCUGUUUUCCtt	Non-hit	1,404	0,006
NET1	10276	NM_005863	16886	UCUUUUAUUGCUUGGCUCCtc	Non-hit	-0,195	0,025
NET1	10276	NM_005863	16981	CAUUUCAUAUAUUGCCUCCtg	Non-hit	-0,517	0,287
NEXN	91624	NM_144573	37246	CCUCUUUUCUAACAUAUCCtg	Non-hit	-0,053	0,805
NEXN	91624	NM_144573	37341	UAAGUAGUGAAUCAUCUCCtt	Non-hit	0,174	0,659

Gene Symbol [1]	Gene ID[1]	RefSeq Accession Number[2]	siRNA ID[3]	Antisense (target) siRNA Sequence[3]	Hit gene[4]	Z-score [5]	P-value [5]
NF2	4771	NM_181833	8090	AAUCAAAGAGGUCCUUCCCtt	Mild hit	-1,147	0,019
NF2	4771	NM_016418	8183	CACCAAAUCAAAGAGGUCCtt	Mild hit	-0,217	0,693
NF2	4771	NM_181832	8273	UAAAAUCUGCUUCUUUACCtg	Mild hit	-0,195	0,918
NF2	4771	NM_181825	202366	GGCAGUAGAUCUUUUCAUCta	Mild hit	-1,139	0,110
NF2	4771	NM_181832	202367	AGGAGGGCAGUAGAUCUUUtc	Mild hit	-0,786	0,562
NF2	4771	NM_181828	202368	UCAGGAGGGCAGUAGAUCUtt	Mild hit	0,841	0,063
NF2	4771	NM_181834	288641	CUCUUGAGAGAGCUGAAGCtc	Mild hit	-1,174	0,009
NF2	4771	NM_181834	288642	GCGUCCAUGGUGACGAUCCtc	Mild hit	-0,061	0,914
NGEF	25791	NM_019850	135246	ACUCAGGUUUCACCUUGGCtg	Non-hit	-0,638	0,004
NGEF	25791	NM_019850	135247	CGGAGCUGAGUCAAAUACCtg	Non-hit	-0,472	0,904
ITSN2	50618	NM_006277	17834	CUUUCUAUGUCUUUUCUCCtt	Non-hit	0,281	0,443
NUDT16L1	84309	NM_032349	34040	GGGCAUCAUGUUGAGCACCtt	Strong hit	-0,228	0,923
NUDT16L1	84309	NM_032349	34136	AGAAUAAACAAGAGCAUCCtg	Strong hit	1,726	0,026
OBSCN	84033	NM_052843	131675	GCUUUCGGAGGAGGUUUCCtt	Mild hit	-0,830	0,226
OBSCN	84033	NM_052843	251364	AUUAUGCACUGACUGCUCCtt	Mild hit	-1,171	0,275
OCRL	4952	NM_000276	8189	AUCUUGAACAUGCUGUUCCtt	Non-hit	-0,174	0,574
OCRL	4952	NM_000276	104448	GUACCAGCUAGAUGAGUCCtt	Non-hit	-0,864	0,637
OCRL	4952	NM_001587	114042	GCUAGAUGAGUCCUUUUGCtc	Non-hit	-0,468	0,484

Gene Symbol [1]	Gene ID[1]	RefSeq Accession Number[2]	siRNA ID[3]	Antisense (target) siRNA Sequence[3]	Hit gene[4]	Z-score [5]	P-value [5]
OCRL	4952	NM_001587	104450	GAUAUGUUUGAUGAGACCCtc	Non-hit	0,449	0,813
OPHN1	4983	NM_002547	11646	GAGCAAUUCAGCAAAUUCCtt	Mild hit	-0,825	0,129
OPHN1	4983	NM_002547	143673	GACUCGAAAAAAUUGUGCCtc	Mild hit	-1,111	0,089
PAFAH1B1	5048	NM_000430	8383	CACAUCUAAUUCAGCUUCCtt	Mild hit	-1,241	0,026
PAFAH1B1	5048	NM_000430	8478	CACCUUAAUUGUAGCAUCCtc	Mild hit	-0,702	0,173
PAK1	5058	NM_002576	249	GUCCUUCUUUUUCUUCUCCtc	Non-hit	-0,806	0,273
PAK1	5058	NM_002576	143703	AAUGGAUCGGUAAAAUCGGtc	Non-hit	-0,526	0,372
PAK2	5062	NM_002577	110776	CAGUGAGCUUAACAGAUCCtt	Non-hit	-0,208	0,389
PAK2	5062	NM_002577	110779	UCUAAUUUUAGCUACUACCtg	Non-hit	0,442	0,309
PAK4	10298	NM_001014831	732	UUCUCGUGCUGGUAGUCCCtc	Non-hit	0,231	0,215
PAK4	10298	NM_001014831	733	ACACUCAUACAUGUUCACCtc	Non-hit	-0,326	0,810
PAK4	10298	NM_001014834	288584	CUGGAGUUCAGUAGUAGGGtc	Non-hit	-0,737	0,678
PAK4	10298	NM_001014835	288585	CUGGUUCUUCAGGCAGUGGtt	Non-hit	-0,381	0,827
PAK4	10298	NM_001014834	288586	AAGUCUGACAGCUUCACCCtg	Non-hit	0,379	0,893
PAK4	10298	NM_001014835	288587	GUUCAGUAGUAGGGUCUCAtc	Non-hit	-0,786	0,003
PAK4	10298	NM_001014835	288588	CUUGAUGAAGUUGUCCAGGta	Non-hit	0,465	0,338
PAK4	10298	NM_005884	288589	GUUCUUCAGGCAGUGGUUCtg	Non-hit	0,976	0,087
PAK4	10298	NM_001014834	288590	UUCACCUCUUAGUGUUCUCtc	Non-hit	-0,696	0,005

Gene Symbol [1]	Gene ID[1]	RefSeq Accession Number[2]	siRNA ID[3]	Antisense (target) siRNA Sequence[3]	Hit gene[4]	Z-score [5]	P-value [5]
PAK4	10298	NM_001014835	288591	AAGGCCACUCUUCGGACAUtc	Non-hit	-0,509	0,626
PAK4	10298	NM_005884	288592	UGUCCAGGUGCAGUAGUCAtt	Non-hit	-0,463	0,475
PAK4	10298	NM_001014834	288593	AAAGUCACGAGAUCAAAACtg	Non-hit	-0,309	0,906
PALLD	23022	NM_016081	23784	ACUCUUGUUUAUCUCUUCCtg	Mild hit	-1,384	0,050
PALLD	23022	NM_016081	23879	UUCACCCAAUUUGGUCUCCtt	Mild hit	0,216	0,824
PARVA	55742	NM_018222	26357	ACCUCCUUGGCUUUCUUCCtc	Non-hit	-0,373	0,229
PARVA	55742	NM_018222	26545	GUUUAAAUGAAUGCAUUCCtc	Non-hit	-0,170	0,536
PARVB	29780	NM_001003828	20220	AGUUGAUGGCAUUCUUGCCtt	Non-hit	-0,943	0,211
PARVB	29780	NM_013327	20312	GAGGACCUUGACCAGUUCCtt	Non-hit	-0,855	0,739
PARVB	29780	NM_001003828	134049	AAUCAUCGUGCGCUCCUCGtt	Non-hit	-0,912	0,066
PARVB	29780	NM_001003828	134050	GCACGAGUGUUUAGAAUCCtg	Non-hit	-1,176	0,032
PFN1	5216	NM_005022	15713	UCAAACCACCGUGGACACCtt	Non-hit	-0,377	0,701
PFN1	5216	NM_005022	45010	CGUAAAAACUUGACCGGUCtt	Non-hit	0,358	0,484
PFN2	5217	NM_053024	11684	AACCGUUGGUAAAGAAACCtt	Non-hit	-0,309	0,726
PFN2	5217	NM_002628	11776	CUUUCUUGUUAAGUGUGCCtc	Non-hit	-1,381	0,005
PFN2	5217	NM_053024	11862	UGAUGCAUGCACUUUUUCCtc	Non-hit	-0,606	0,051
PFN2	5217	NM_053024	143784	AUUUCUAUUGGCGUAAUGCtc	Non-hit	-0,744	0,638
PIK3CA	5290	NM_006218	2960	AAUAUUUCUUCGGAAGUCCtg	Strong hit	-1,637	0,038

Gene Symbol [1]	Gene ID[1]	RefSeq Accession Number[2]	siRNA ID[3]	Antisense (target) siRNA Sequence[3]	Hit gene[4]	Z-score [5]	P-value [5]
PIK3CA	5290	NM_006218	144250	CUUCACGGUUGCCUACUGGtt	Strong hit	-0,764	0,163
PIK3CB	5291	NM_006219	17439	UGUUUCAUCUUCAAGCUCCtc	Non-hit	-0,490	0,589
PIK3CB	5291	NM_006219	144253	ACCUCUGAGCUUACGAUGGtt	Non-hit	0,389	0,096
PIK3CG	5294	NM_002649	11879	GAACACACUCUCGUGGUCCtt	Mild hit	-1,076	0,313
PIK3CG	5294	NM_002649	11974	AUGCCUCUGAUCUUGACCCtg	Mild hit	-0,084	0,464
PIK3R1	5295	NM_181524	203811	GUAUUAGAGAUACAGUAGGtt	Non-hit	-1,486	0,031
PIK3R1	5295	NM_181524	118085	UGUUGGCUACAGUAGUAGGtt	Non-hit	-0,658	0,374
PIK3R1	5295	NM_181524	118086	GUAUUCUUUGCUGUACCGCtc	Non-hit	0,210	0,686
PIK3R1	5295	NM_181524	118087	GUUUAAUGCUGUUCAUACGtt	Non-hit	0,576	0,838
PIK3R1	5295	NM_181524	288635	AUCUAUUCAUAUUCAGCCGtt	Non-hit	0,254	0,433
PIK3R1	5295	NM_181523	288636	AGAUUCAUUCCGGUAGUGGtt	Non-hit	-0,758	0,323
PIK3R1	5295	NM_181523	288637	AUCAUAUAUCAGGAGUGCCtc	Non-hit	-0,013	0,689
PIK3R1	5295	NM_181524	288638	CAACCACAUCAAGUAUUGGtc	Non-hit	-0,647	0,315
PIK3R1	5295	NM_181523	288639	UUUAGGAUGCUACACUGGGtg	Non-hit	-0,423	0,411
PIK3R1	5295	NM_181523	288640	UCAUCAUACAGCCUUAGGCtg	Non-hit	-0,794	0,080
PIK3R2	5296	NM_005027	15718	CUGCUCUUCCAAGUGUUCCtg	Mild hit	1,109	0,050
PIK3R2	5296	NM_005027	15906	GAUAGUCUCAUUGAAGGCCtc	Mild hit	-0,098	0,434
PIP5K1C	23396	NM_012398	136520	UAAAACGGCACACACGUGCtt	Non-hit	1,599	0,224

Gene Symbol [1]	Gene ID[1]	RefSeq Accession Number[2]	siRNA ID[3]	Antisense (target) siRNA Sequence[3]	Hit gene[4]	Z-score [5]	P-value [5]
PIP5K1C	23396	NM_012398	136521	GAGGUUUGCACAUUUCUCCtg	Non-hit	-1,112	0,019
PLEKHG2	64857	NM_022835	148850	AUGGUACUUGAGAAUGCGCtg	Non-hit	-0,747	0,734
PLEKHG2	64857	NM_022835	148851	AGCGUGCUUGAAUCCAGGCtt	Non-hit	-0,178	0,718
PLEKHG4	25894	AK024475	288681	UGAUAUUUCUGAUAAAGGGtc	Non-hit	0,357	0,803
PLEKHG4	25894	AK024475	288682	AGGCAAUGUUCCUUGGAGCtg	Non-hit	0,590	0,482
PLEKHG5	57449	NM_020631	123225	AGAGUGAAGCAUUCCUUGCtt	Non-hit	-0,142	0,401
PLEKHG5	57449	NM_020631	217272	ACAAAGUCUUGUAAGGAGGtt	Non-hit	0,938	0,264
PLEKHG5	57449	NM_198681	217273	UUUCAGAGUGAAGCAUUCCtt	Non-hit	-0,673	0,438
PLEKHG5	57449	NM_198681	288617	AAAUACAGGCAGCAGCACCtc	Non-hit	-1,218	0,620
PLEKHG6	55200	NM_018173	26321	AUGGGCCUUGGUGAGUUCCtt	Strong hit	-1,552	0,337
PLEKHG6	55200	NM_018173	140527	CUUUCUCACGUAGAUCAGCtc	Strong hit	-0,443	0,543
PPFIA1	8500	NM_177423	13311	GUAUCAAGAAGGCGGUCCCtt	Non-hit	-0,268	0,913
PPFIA1	8500	NM_177423	13394	AUCUCUUUCAUGACCAACCtc	Non-hit	0,078	0,831
PPFIA1	8500	NM_177423	13472	CUCAUUAAGAGUUUGUACCtt	Non-hit	1,059	0,143
PPFIA1	8500	NM_177423	107195	CUUUCAAGGAGCUGUUCCCtg	Non-hit	0,251	0,026
PPIA	5478	NM_203430	7523	UUCUGCUGUCUUUGGGACCtt	Non-hit	-0,449	0,147
PPIA	5478	NM_203431	103856	ACCCUUAUAACCAAAUCCUtt	Non-hit	-0,096	0,587
PPIA	5478	NM_021130	112126	ACCUCUUAAUUCUGGCUCCtt	Non-hit	-0,711	0,194

Gene Symbol [1]	Gene ID[1]	RefSeq Accession Number[2]	siRNA ID[3]	Antisense (target) siRNA Sequence[3]	Hit gene[4]	Z-score [5]	P-value [5]
PPIA	5478	NM_203431	122514	UGACCCAACCUCUUAAUUCtg	Non-hit	-0,192	0,707
PPIA	5478	NM_203431	122515	UGCAGACUGACCCAACCUCtt	Non-hit	0,075	0,347
PPIA	5478	NM_203430	288645	AUAAUAGCUCACUCUAGGCtc	Non-hit	1,233	0,251
PREX1	57580	NM_020820	28779	GAUGUUCGAGAACAGGACCtt	Non-hit	0,080	0,963
PREX1	57580	NM_020820	121870	AACAUUCCCAAGUUCAUGCtg	Non-hit	-0,415	0,468
PRKCA	5578	NM_002737	300	AAACUUGGCACUGGAAGCCtt	Strong hit	-1,644	0,030
PRKCA	5578	NM_002737	42854	UUGAACUUGUGCUUGCUCCtg	Strong hit	-1,258	0,069
PRKCE	5581	NM_005400	679	CUCCAGAUCAAUCCAGUCCtc	Non-hit	-0,911	0,617
PRKCE	5581	NM_005400	677	GACUUGACACUGGUAUCCCtg	Non-hit	0,218	0,494
PRKD1	5587	NM_002742	103310	ACCCUUCACAUUUAAGACCtt	Non-hit	0,196	0,424
PRKD1	5587	NM_002742	103397	GGUAAUUCAGACCACACCCtt	Non-hit	0,490	0,369
PRR5-ARHGAP8	23779	NM_181334	202491	AUCGUUCUCAACGUAUUGGtc	Non-hit	-0,183	0,961
PRR5-ARHGAP8	23779	NM_181334	213040	CGUGCUCAGCGCAGGAUCCtg	Non-hit	0,842	0,108
PRR5-ARHGAP8	23779	NM_181334	213042	GUCGUCAAAGUUCACGGGCtt	Non-hit	-0,289	0,836
PRR5-ARHGAP8	23779	NM_181334	213201	AGUUUUCAUUAGAAGGUUCtg	Non-hit	-1,206	0,061

Gene Symbol [1]	Gene ID[1]	RefSeq Accession Number[2]	siRNA ID[3]	Antisense (target) siRNA Sequence[3]	Hit gene[4]	Z-score [5]	P-value [5]
PTEN	5728	NM_000314	45927	CAAAGUACAUGAACUUGUCtt	Strong hit	-2,230	0,038
PTEN	5728	NM_000314	142044	CAUUACACCAGUUCGUCCCtt	Strong hit	-1,124	0,174
PTK2	5747	NM_005607	103596	GCAAGCUCAUACUUCUCCCtc	Non-hit	-1,423	0,449
PTK2	5747	NM_153831	103649	CAUAUAAUCGCUCUUCACCtg	Non-hit	-0,923	0,239
PTK2	5747	NM_153831	103698	AGAUCCAAACUGUAUUUCCtt	Non-hit	-0,558	0,602
PTK2	5747	NM_153831	142859	UCUUAGUACUCGAAUUUGGtg	Non-hit	-0,518	0,607
PTPN1	5770	NM_002827	4264	UGGGUAAGAAUGUAACUCCtt	Strong hit	-1,570	0,040
PTPN1	5770	NM_002827	104533	CCAUGAUGAAUUUGGCACCtt	Strong hit	-1,004	0,785
PTPN11	5781	NM_002834	4361	GGGUUACUUUUACUAGGCCtt	Strong hit	-1,863	0,005
PTPN12	5782	NM_002835	4270	AUCAAAUGGCAGUAUGUCCtt	Mild hit	-1,214	0,084
PTPN12	5782	NM_002835	142400	AACCAUAUGCAACACUGGCtt	Mild hit	-0,891	0,005
PTPRA	5786	NM_080840	4271	UGGAUUUGAAGUUUUGGCCtc	Non-hit	-0,687	0,125
PTPRA	5786	NM_080840	4363	CAUUCUCCGGUUAAUUUCCtc	Non-hit	0,107	0,290
PTPRA	5786	NM_080841	104563	AGGGUUACAGGCCUUCACCtt	Non-hit	-1,279	0,085
PTPRA	5786	NM_080841	104566	AUACUGAGGGUUACAGGCCtt	Non-hit	-0,596	0,217
PTPRA	5786	NM_080841	104569	AUAUUAAAGGCAAUCCUCCtg	Non-hit	0,734	0,312
PTPRA	5786	NM_080841	114285	UCUUUAACUGGUUCUGCCGtt	Non-hit	-0,806	0,071
PTPRF	5792	NM_002840	4274	AUCAUCAAACUCAAUGACCtc	Non-hit	0,201	0,261

Gene Symbol [1]	Gene ID[1]	RefSeq Accession Number[2]	siRNA ID[3]	Antisense (target) siRNA Sequence[3]	Hit gene[4]	Z-score [5]	P-value [5]
PTPRF	5792	NM_130440	4366	GUCUACAGGAAGGAAGUCCtt	Non-hit	-0,907	0,039
PTPRF	5792	NM_130440	4454	AAAAAACAUUGAGUUUCCCtg	Non-hit	-0,848	0,100
PTPRF	5792	NM_130440	104588	AUACAUGAUGAUCCGCUCCtg	Non-hit	-0,099	0,803
PXN	5829	NM_002859	12157	GAAGAGGUUGUGGUAGUCCtt	Mild hit	-1,064	0,085
PXN	5829	NM_002859	12253	GAACAUGUCGAAGUAGUCCtt	Mild hit	0,133	0,352
RAC1	5879	NM_006908	27408	UUUUACAGCACCAAUCUCCtt	Non-hit	0,856	0,131
RAC1	5879	NM_018890	45358	AGACAGUAGGGAUAUAUUCtc	Non-hit	-0,132	0,267
RAC1	5879	NM_006908	120600	UGAGCAAAGCGUACAAAGGtt	Non-hit	-0,647	0,356
RAC1	5879	NM_006908	120601	AAUAAGGCUUUAAGAAGGCtt	Non-hit	-0,508	0,321
RAC1	5879	NM_006908	120602	UAAAGAGGGUCAGUAUUGGtc	Non-hit	-0,168	0,861
RAC1	5879	NM_006908	242587	AAGGAAAGCACUUAUUAGCtc	Non-hit	0,012	0,493
RAC2	5880	NM_002872	43342	UGUCCACCAUCACAUUGGCtg	Non-hit	-0,784	0,027
RAC2	5880	NM_002872	43438	UUCUCAUAAGAGGCUGGGCtg	Non-hit	-0,656	0,098
RAC3	5881	NM_005052	41918	CCACUUGGCACGAACAUUCtc	Mild hit	0,737	0,375
RAC3	5881	NM_005052	42005	GUAUUUCACAGAGCCAAUCtc	Mild hit	-1,221	0,033
RACGAP1	29127	NM_013277	20189	ACGGAAAUCCUCAAAGUCCtt	Non-hit	-0,409	0,707
RACGAP1	29127	NM_013277	20283	CCACUUUUUACGGAAAUCCtc	Non-hit	-0,494	0,287
RALBP1	10928	NM_006788	18602	CCUGAAAGGCUGCAUAGCCtt	Mild hit	0,088	0,997

Gene Symbol [1]	Gene ID[1]	RefSeq Accession Number[2]	siRNA ID[3]	Antisense (target) siRNA Sequence[3]	Hit gene[4]	Z-score [5]	P-value [5]
RALBP1	10928	NM_006788	18693	CAUUUUUGUUUCCAGUUCCtt	Mild hit	-1,192	0,004
RASGRF1	5923	NM_002891	12181	GAGAUUCUUAAAUCUGCCCtc	Non-hit	-0,187	0,569
RASGRF1	5923	NM_153815	120291	CUCAUGGAGACUUCUGAGCtc	Non-hit	0,163	0,704
RASGRF2	5924	NM_006909	120492	GGUCGCAUUCGUUCUUUGGtt	Mild hit	-1,016	0,183
RASGRF2	5924	NM_006909	120493	AACCAUCCUCGCAUGAAGCtc	Mild hit	-0,990	0,011
RDX	5962	NM_002906	12193	ACCAACUGUUUUCACCACCtg	Non-hit	-0,247	0,544
RDX	5962	NM_002906	142472	UAUCAUUAGCCAGGUAGCCtg	Non-hit	-0,388	0,223
RGNEF	64283	BC012946	288687	GUUUUGUUUUCAAUCUUAUtt	Mild hit	-0,358	0,332
RGNEF	64283	BC012946	288688	CAUAUAACAGAGUCCUUUCtt	Mild hit	-1,179	0,136
RHOA	387	NM_001664	2808	UACCUGCUUUCCAUCCACCtc	Non-hit	-0,381	0,681
RHOA	387	NM_001664	120211	UUUUCUAAACUAUCAGGGCtg	Non-hit	0,909	0,081
RHOB	388	NM_004040	41889	AAUGUCGGCCACAUAGUUCtc	Non-hit	-0,767	0,495
RHOB	388	NM_004040	120361	CAGACAAGGGAUAUCAAGCtc	Non-hit	-0,436	0,927
RHOBTB1	9886	NM_014836	43848	GCCUGAGAGAAACACUCACtt	Non-hit	-0,159	0,859
RHOBTB1	9886	NM_014836	43944	CAAAGCCUGAGAGAAACACtc	Non-hit	-0,180	0,740
RHOBTB1	9886	NM_001032380	44031	UAAAGGUUUCUGGACUUUCtt	Non-hit	-1,200	0,294
RHOBTB1	9886	NM_001032380	138464	GCCUGGCUCGAUUAACAGCtt	Non-hit	-0,666	0,581
RHOBTB1	9886	NM_198225	138465	CCAAACUGGUCAAACACGCtt	Non-hit	-0,437	0,871

Gene Symbol [1]	Gene ID[1]	RefSeq Accession Number[2]	siRNA ID[3]	Antisense (target) siRNA Sequence[3]	Hit gene[4]	Z-score [5]	P-value [5]
RHOBTB1	9886	NM_198225	138466	GUCCAAUUUAAAUGUCACGtc	Non-hit	-0,151	0,249
RHOBTB2	23221	NM_015178	22631	AUCUUCUGCCAUCUCUUCCtg	Mild hit	-1,251	0,013
RHOBTB2	23221	NM_015178	136812	GCUGACAUCAUCUACCACGtc	Mild hit	-0,667	0,338
RHOC	389	NM_175744	44091	GACCUCCGGAAACUGAUCCtt	Non-hit	-0,017	0,916
RHOC	389	NM_175744	44189	GAUCAUAGUCUUCCUGCCCtg	Non-hit	-0,318	0,607
RHOD	29984	NM_014578	21520	GGUCAUAGUCAUCUUGCCCtg	Non-hit	-0,038	0,644
RHOD	29984	NM_014578	21613	CACGACGAUGAUGGGUACCtt	Non-hit	-0,443	0,101
RHOF	54509	NM_019034	27700	AAAAAAAAUUCCCAGACCCtc	Non-hit	0,005	0,741
RHOF	54509	NM_019034	27796	AUGCUUGUUUUAAAAGUCCtg	Non-hit	0,091	0,694
RHOG	391	NM_001665	10243	CACUUCCUUGACACCAUCCtg	Mild hit	0,600	0,111
RHOG	391	NM_001665	45990	UUAGUCCUUAAGGCACAGCtg	Mild hit	-1,448	0,057
RHOH	399	NM_004310	5062	CUCCUUCUGUUUCGUCUCCtg	Non-hit	-0,102	0,435
RHOH	399	NM_004310	120805	AUUGCUAAGGGCUGAGCACtc	Non-hit	0,217	0,828
RHOJ	57381	NM_020663	28549	CAAAAACCGCUUUGAGACCtt	Mild hit	-0,023	0,552
RHOJ	57381	NM_020663	28644	UCCGUGCAAAGGGAGUUCCtt	Mild hit	-1,089	0,792
RHOQ	23433	NM_012249	19665	CAGACGGUCAUAGUCUUCCtg	Non-hit	0,394	0,064
RHOQ	23433	NM_012249	19755	AUUGGGUAAGAUAAAGGCCtc	Non-hit	-0,304	0,574
RHOU	58480	NM_021205	29108	CAGCUUGUCAAAUUCAUCCtg	Non-hit	-0,067	0,748

Gene Symbol [1]	Gene ID[1]	RefSeq Accession Number[2]	siRNA ID[3]	Antisense (target) siRNA Sequence[3]	Hit gene[4]	Z-score [5]	P-value [5]
RHOU	58480	NM_021205	29197	GAUGGCUGCAUCAAAGACCtc	Non-hit	0,093	0,727
RHOV	171177	NM_133639	36445	AAGUCGGUCAAAAUCCUCCtg	Mild hit	-1,300	0,008
RHOV	171177	NM_133639	120713	AGUACGUUGACAUCGUCCCtc	Mild hit	-0,039	0,450
RND1	27289	NM_014470	21295	GGUCUCUGGAUAGCAAUCCtt	Non-hit	-0,369	0,881
RND1	27289	NM_014470	21389	UAUCGUAGUAGGGAGAUCCtg	Non-hit	0,120	0,590
RND2	8153	NM_005440	16082	UAUCAUAGUAAGAGGAACCtg	Strong hit	-1,686	0,044
RND2	8153	NM_005440	16252	UGUGUAACAGGGAUAAGCCtc	Strong hit	0,541	0,444
RND3	390	NM_005168	15798	AAAAUUCCUGGAUUUCACCtt	Non-hit	0,439	0,317
RND3	390	NM_005168	15891	GGUAUUUGGACAAAAUUCCtg	Non-hit	-0,340	0,779
RNF5	6048	NM_006913	18776	CCCAUAAAGCGGGACAACCtt	Mild hit	-0,835	0,198
RNF5	6048	NM_006913	46173	CUUUACAUACUGGACACUCtt	Mild hit	-1,086	0,394
ROCK1	6093	NM_005406	681	ACCUUUUAAAUUGUCUGCCtc	Mild hit	-1,246	0,024
ROCK1	6093	NM_005406	142844	ACACCAUUUCGCCCUAACCtc	Mild hit	0,669	0,211
ROCK2	9475	NM_004850	595	GCACUUCACCAAAAGCACCtc	Mild hit	-0,796	0,284
ROCK2	9475	NM_004850	110865	UUUCCGUAAGGUAAUCUCCtc	Mild hit	-1,453	0,098
SDC4	6385	NM_002999	12434	CUCAAAGUCAUCAGAUUCCtg	Strong hit	-1,784	0,003
SDC4	6385	NM_002999	12529	CACCUUGUUGGACACAUCCtc	Strong hit	-1,075	0,100
SDCBP	6386	NM_001007067	16556	CUUUAUCAGAGCUCCAUCCtg	Non-hit	-0,524	0,477

Gene Symbol [1]	Gene ID[1]	RefSeq Accession Number[2]	siRNA ID[3]	Antisense (target) siRNA Sequence[3]	Hit gene[4]	Z-score [5]	P-value [5]
SDCBP	6386	NM_001007068	16651	GUGCCGUGAAUUUUAAACCtc	Non-hit	0,139	0,126
SDCBP	6386	NM_001007067	16742	AUGUAAGAUAGAAAGGUCCtc	Non-hit	1,418	0,189
SDCBP	6386	NM_001007070	121549	UGGCUUUUAGUCUAGAUGCtt	Non-hit	-0,604	0,104
SDCBP	6386	NM_001007070	121550	UAAGCAGCUAUGCUAUAGCtc	Non-hit	-0,448	0,918
SDCBP	6386	NM_001007070	121551	GGCUAGUGUACAUUUCAGGtt	Non-hit	0,055	0,736
SDCBP	6386	NM_001007070	288578	GAGGGAUAGGAGCAGAAGCtt	Non-hit	-0,255	0,211
SDCBP	6386	NM_001007070	288579	GGGAGUCAAAAGUUUAUCCtg	Non-hit	-0,572	0,258
SDCBP	6386	NM_005625	288580	AAUUGCUGGAUUGGCAGGGtt	Non-hit	-0,189	0,724
SDCBP	6386	NM_005625	288581	CCAUCCCAAAGUAGCUAGGtt	Non-hit	-1,111	0,115
SH3BP1	23616	NM_018957	27462	GCCUGAAUUCUUGGUUGCCtg	Non-hit	0,201	0,241
SH3BP1	23616	NM_018957	27556	UUUCCUCUUCAGCUCCUCCtc	Non-hit	0,981	0,854
SIRPA	140885	NM_080792	43659	UGACAUUCACCUGGUUCUCtg	Non-hit	-0,544	0,323
SIRPA	140885	NM_080792	112326	CCACAAUAUAGAUGUUCCGtt	Non-hit	-0,307	0,719
SORBS1	10580	NM_006434	22706	AGGUGAGGUGGGUUUUUCCtg	Non-hit	0,292	0,390
SORBS1	10580	NM_001034957	22801	UGCUCUUUUUUCAAUAGCCtt	Non-hit	0,258	0,398
SORBS1	10580	NM_015385	22895	UUCUCCAUAUUCCAAAACCtg	Non-hit	-0,926	0,141
SORBS1	10580	NM_015385	136917	UUGCUUUCGUGUUGCCGGGtt	Non-hit	0,418	0,538
SORBS1	10580	NM_001034957	136918	GGAAACAUCGCUUAAGUCCtg	Non-hit	-0,753	0,044

Gene Symbol [1]	Gene ID[1]	RefSeq Accession Number[2]	siRNA ID[3]	Antisense (target) siRNA Sequence[3]	Hit gene[4]	Z-score [5]	P-value [5]
SORBS1	10580	NM_001034957	136919	GGCUGAUAUUCGUAAAUGCtc	Non-hit	-1,577	0,040
SORBS1	10580	NM_024991	288594	GUUUUUCACCAGUGGUCGCtt	Non-hit	-1,201	0,009
SORBS1	10580	NM_006434	288595	UCUCUUUAUCAUCAUGACGtc	Non-hit	1,264	0,083
SORBS1	10580	NM_024991	288596	GCUACUGAGUCGUUUUUGCtg	Non-hit	0,149	0,263
SORBS1	10580	NM_015385	288597	CUAGCUGUAUUUAAAGAGGtg	Non-hit	-1,167	0,100
SORBS1	10580	NM_015385	288598	AUGUCUGCAUAGGACAUGCtc	Non-hit	-0,252	0,621
SORBS1	10580	NM_006434	288599	GGUUGAGUGAGGGAUUUGGtc	Non-hit	0,488	0,588
SORBS1	10580	NM_006434	288600	GUGAGUUAUUUGGAAUUCCtt	Non-hit	-0,916	0,412
SORBS1	10580	NM_024991	288601	GAAAUUUCCGGAGUAGGGCtg	Non-hit	-0,242	0,807
SORBS3	10174	NM_001018003	16824	GAAGGGUAGACAAAGUCCCtc	Non-hit	-0,711	0,005
SORBS3	10174	NM_001018003	16920	CUCUUCUUCUCUUCCCUCCtg	Non-hit	-0,282	0,850
SORBS3	10174	NM_005775	17014	UUUCUCUUCUUCUCUUCCCtc	Non-hit	-0,696	0,087
SORBS3	10174	NM_001018003	126654	GUCUGGUCUCAAUAAGGCCtg	Non-hit	-0,923	0,304
SOS1	6654	NM_005633	16561	ACUUUUUUGAACACGUUCCtc	Mild hit	-0,491	0,233
SOS1	6654	NM_005633	142883	UUUAUAACCUAGGACCUCCtt	Mild hit	-1,300	0,449
SOS2	6655	NM_006939	143048	UCUUUUCGUAUACAGAAGGtt	Non-hit	-0,524	0,493
SOS2	6655	NM_006939	143049	AAGGACAUAACGAACUGCCtc	Non-hit	-0,619	0,145
SPATA13	221178	NM_153023	39762	CAGAAGAUUGUCCAGUUCCtc	Non-hit	-0,658	0,200

Gene Symbol [1]	Gene ID[1]	RefSeq Accession Number[2]	siRNA ID[3]	Antisense (target) siRNA Sequence[3]	Hit gene[4]	Z-score [5]	P-value [5]
SPATA13	221178	NM_153023	129604	UGUGGUCCUACUGACGAGCtt	Non-hit	0,132	0,595
SRC	6714	NM_198291	103333	CUUGCCAAAAUACCACUCCtc	Non-hit	-0,339	0,828
SRC	6714	NM_198291	103417	CCUCAGCUUCUUCAUGACCtg	Non-hit	0,124	0,836
SRC	6714	NM_198291	142855	GCCUCCGACGAAUUGUUGGtt	Non-hit	-0,871	0,131
SRC	6714	NM_198291	288644	CUAUGUCUGCUUGAUUGCCtc	Non-hit	-1,660	0,210
SRGAP1	57522	NM_020762	148766	AACUCGCAUCUCCGUUUGCtg	Mild hit	-0,244	0,681
SRGAP1	57522	NM_020762	148767	ACCAGAUCUCCCAAUUUGCtt	Mild hit	-1,326	0,061
SRGAP2	23380	NM_015326	261179	UACCGAUUUACCAAUUUGCtt	Non-hit	-0,538	0,276
SRGAP2	23380	NM_015326	261180	CCUUUAAUCUAACUAAGGCtc	Non-hit	0,062	0,512
SRGAP3	9901	NM_001033116	22081	GAAGGCAUCAUCCAUGUCCtg	Strong hit	-0,826	0,014
SRGAP3	9901	NM_001033117	138476	CAAGUAGUCAUUCCGGGCCtt	Strong hit	1,405	0,038
SRGAP3	9901	NM_014850	22273	AAUAGAAACCUUUCAUCCCtt	Strong hit	-0,582	0,660
SRGAP3	9901	NM_001033117	138477	GAGUAAAUCGUGCUUGGCCtg	Strong hit	-0,376	0,331
SRGAP3	9901	NM_014850	138478	UAUAUACACUUAGUAUGCGtg	Strong hit	-1,112	0,042
SRGAP3	9901	NM_014850	288609	UUAUAGCUGCGUUGGUGGCtg	Strong hit	-2,238	0,058
STARD13	90627	NM_052851	288666	UCCAAAAGAUCUCCUGUGCtg	Non-hit	-0,170	0,543
STARD13	90627	NM_178007	288668	GAGAAAGGUCUCACUGAGCtt	Non-hit	-0,494	0,980
STARD13	90627	NM_052851	35407	GUGACCCAUUUCUGUCUCCtc	Non-hit	0,340	0,736

Gene Symbol [1]	Gene ID[1]	RefSeq Accession Number[2]	siRNA ID[3]	Antisense (target) siRNA Sequence[3]	Hit gene[4]	Z-score [5]	P-value [5]
STARD13	90627	NM_178007	35499	AAUGAUUUGGCCCUAGCCCtc	Non-hit	0,200	0,849
STARD13	90627	NM_178007	35584	UUAUGGAUUUACUGCUUCCtt	Non-hit	-0,624	0,524
STARD13	90627	NM_178007	202336	GAUGGGAAAUUGUGAAUCCtc	Non-hit	0,182	0,173
STARD13	90627	NM_052851	202362	UUCAACGUAUUUAGUCGUCtg	Non-hit	0,274	0,811
STARD13	90627	NM_178008	131863	UGUUCAACGUAUUUAGUCGtc	Non-hit	0,439	0,978
STARD8	9754	NM_014725	21799	GAUGGUACACUGCUCUUCCtc	Non-hit	-0,613	0,322
STARD8	9754	NM_014725	138366	UGGCCCUGUAAAAUCCAGCtg	Non-hit	0,266	0,755
STARD9	57519	AK122666	251250	UAUCUCAUUUACUCGUGGCtt	Non-hit	-0,852	0,170
STARD9	57519	AK122666	251251	CUGAUUUCCAGUCUUCUGCtc	Non-hit	-0,743	0,110
SYDE1	85360	NM_033025	34994	AGCAAGCGCGAGAACUACCtt	Non-hit	0,196	0,309
SYDE1	85360	NM_033025	125786	CUAAAGAGGUGUCCUCAGCtg	Non-hit	-0,876	0,906
TENC1	23371	NM_198316	22677	AGGUUUCUUCCGGAAAACCtt	Non-hit	-0,640	0,127
TENC1	23371	NM_198316	22773	UGUCCCAUCGAUGGUCACCtt	Non-hit	-0,842	0,090
TENC1	23371	NM_170754	22868	AUGUUACCAUGACAUCGCCtt	Non-hit	-0,568	0,436
TENC1	23371	NM_198316	136884	UUUUCUGUGCGUCGCCACCtt	Non-hit	-0,280	0,291
TENC1	23371	NM_170754	136885	CAUUCCUAAGGGAGGGUGCtt	Non-hit	0,253	0,429
TENC1	23371	NM_198316	136886	GCAGUAUAGUACGACCACGtg	Non-hit	-1,244	0,096
TES	26136	NM_152829	23211	AGAAGUGCAGUUCGAAUCCtt	Non-hit	-0,116	0,559

Gene Symbol [1]	Gene ID[1]	RefSeq Accession Number[2]	siRNA ID[3]	Antisense (target) siRNA Sequence[3]	Hit gene[4]	Z-score [5]	P-value [5]
TES	26136	NM_152829	23307	UUUUCCCACUUUUCGAUCCtc	Non-hit	-1,557	0,002
TES	26136	NM_152829	134609	UUUCGAUCCUCUUCAUUGCtc	Non-hit	0,160	0,209
TES	26136	NM_152829	134610	CACUUUGGAUAGCUAUGGCtc	Non-hit	-0,751	0,583
TGFB1I1	7041	NM_015927	23481	CUGAGUGGCAUUAAGUUCCtg	Non-hit	-0,927	0,003
TGFB1I1	7041	NM_015927	23577	AUCUUCAGACUGGUCCUCCtt	Non-hit	-0,434	0,032
TIAM1	7074	NM_003253	4716	AAUGUCAUCAAAUAUUCCCtc	Non-hit	-0,909	0,761
TIAM1	7074	NM_003253	138877	AGUCAGUGUAAGACACAGGtc	Non-hit	0,684	0,623
TIAM2	26230	NM_012454	20229	UGGGUCAGUGACAGUGUCCtt	Non-hit	-0,017	0,341
TIAM2	26230	NM_012454	258554	UACUAUGAUUUUCCGUGGCtc	Non-hit	-0,748	0,555
TIAM2	26230	NM_001010927	258555	AAACACGGUCCCAUAAUCCtc	Non-hit	0,884	0,228
TIAM2	26230	NM_001010927	258556	AGAUGGUUUCUGGCCGUCCtt	Non-hit	0,470	0,088
TLN1	7094	NM_006289	5379	AGCCUCCAGCCAUAUACCCtt	Non-hit	-0,982	0,174
TLN1	7094	NM_006289	5467	GGUCCCUGUUAUUUCCUCCtt	Non-hit	-0,940	0,322
TLN2	83660	NM_015059	5622	UCCAGCCAAAUCCCUUUCCtc	Non-hit	0,937	0,048
TLN2	83660	NM_015059	5717	UUUUGAGUGUGCCCGUUCCtt	Non-hit	-0,869	0,006
TNS1	7145	NM_022648	30149	UGAACAGCAGGUAGUUGCCtc	Non-hit	0,071	0,864
TNS1	7145	NM_022648	30244	CCAGCCAAAUUCCAGUACCtt	Non-hit	-0,639	0,430
TPM1	7168	NM_001018004	8333	CAGUUCAUCUUCGGUGCCCtt	Non-hit	-0,983	0,255

Gene Symbol [1]	Gene ID[1]	RefSeq Accession Number[2]	siRNA ID[3]	Antisense (target) siRNA Sequence[3]	Hit gene[4]	Z-score [5]	P-value [5]
TPM1	7168	NM_001018020	8429	CUCACUCUCAUCUGCUGCCtt	Non-hit	0,237	0,944
TPM1	7168	NM_001018004	8523	UUCCUCAUAUCUGUCUUCCtt	Non-hit	-0,711	0,902
TPM1	7168	NM_001018004	118352	UCAGAGAAGCUACGUCGGCtt	Non-hit	-0,608	0,088
TPM1	7168	NM_001018008	118353	UCCAAUUUAGUUACUGACCtc	Non-hit	-0,919	0,130
TPM1	7168	NM_001018005	118354	UUACAUGGAAGUCAUAUCGtt	Non-hit	0,064	0,658
TPM1	7168	NM_001018008	288545	UCUCAAUGACUUUCAUGCCtc	Non-hit	-0,640	0,955
TPM1	7168	NM_001018008	288546	CUCUUUCAGUUGGAUCUCCtg	Non-hit	-0,621	0,387
TPM2	7169	NM_003289	12962	AUACUUUUCCACCUCAUCCtc	Non-hit	-1,428	0,592
TPM2	7169	NM_003289	13058	UUCAGAAUACUUUUCCACCtc	Non-hit	-0,960	0,007
TPM2	7169	NM_213674	13149	UUUCGAUGACCUUCAUUCCtc	Non-hit	-0,468	0,413
TPM2	7169	NM_213674	118375	CAGCUUGCUUCUUGUCGGCtt	Non-hit	-0,110	0,707
TPM3	7170	NM_153649	43886	UUUCAAUAACCUUCAUACCtc	Non-hit	-0,645	0,089
TPM3	7170	NM_153649	43982	GGCCCGGUUUUCAAUAACCtt	Non-hit	-0,604	0,003
TPM3	7170	NM_152263	46535	UUUUUCAGCUUCUUCCAGCtt	Non-hit	-0,380	0,519
TPM3	7170	NM_153649	288634	AAGAAUCUUGAUUUCUUCCtc	Non-hit	-0,632	0,930
TPM4	7171	NM_003290	12963	UUUCUAUCACCUUCAUUCCtc	Non-hit	-0,295	0,654
TPM4	7171	NM_003290	13059	GGCCCGGUUUUCUAUCACCtt	Non-hit	-0,444	0,730
PTPN11	5781	NM_080601	4449	GAAAACUACCAUGUUUUCCtt	Strong hit	-1,781	0,001

Gene Symbol [1]	Gene ID[1]	RefSeq Accession Number[2]	siRNA ID[3]	Antisense (target) siRNA Sequence[3]	Hit gene[4]	Z-score [5]	P-value [5]
TRIO	7204	NM_007118	849	GAUAUGUUCAUAUAUUCCCtg	Non-hit	0,066	0,930
TRIO	7204	NM_007118	103343	AAUGAGUCUCCUGAGAUCCtc	Non-hit	0,578	0,948
TRIP6	7205	NM_003302	12968	AAACUUCCUGUGAAAGUCCtc	Non-hit	-0,875	0,212
TRIP6	7205	NM_003302	13155	AACAAUUCUCACAGUCUCCtc	Non-hit	-0,686	0,048
TRPM7	54822	NM_017672	1490	AAGGCAUCUGUGAGGGUCCtt	Strong hit	-1,565	0,001
TRPM7	54822	NM_017672	212797	AGUAAAACAAGCAUGUUGCtt	Strong hit	-1,608	0,115
TSPAN4	7106	NM_001025234	12769	CAGGAGGCACUUGUUCUCCtt	Non-hit	0,158	0,424
TSPAN4	7106	NM_003271	12860	GUUCUCCUGAAGCCACACCtt	Non-hit	0,013	0,537
TSPAN4	7106	NM_003271	46050	GAAAGUGAGCAGGAGGCACtt	Non-hit	-0,178	0,679
TSPAN4	7106	NM_003271	138895	ACCACUUGGCAGUACAUGGtc	Non-hit	-0,508	0,111
TSPAN4	7106	NM_003271	138896	GCCCACUAUGGAAUGUAGGtg	Non-hit	-0,619	0,788
TSPAN4	7106	NM_001025239	288553	GCCUUUCUUCAGGUCUUGCtg	Non-hit	-0,234	0,849
TSPAN4	7106	NM_003271	288554	UUUUUUUCAAGGUUGCUGCtc	Non-hit	0,237	0,232
TSPAN4	7106	NM_001025238	288555	UACCUGUCAAUCUUGUCCGtg	Non-hit	-1,093	0,112
TSPAN4	7106	NM_001025238	288556	UACAUGGUCAUGGCGAAGGtc	Non-hit	0,983	0,329
TSPAN4	7106	NM_001025235	288557	AACCUGUUUUCCAGGAGGCtg	Non-hit	-0,356	0,425
TSPAN4	7106	NM_001025239	288558	UCGAACCAGUCAGUGUAGUtg	Non-hit	-1,064	0,214
TSPAN4	7106	NM_001025239	288559	ACGGGCCCACUAUGGAAUGta	Non-hit	-0,540	0,415

Gene Symbol [1]	Gene ID[1]	RefSeq Accession Number[2]	siRNA ID[3]	Antisense (target) siRNA Sequence[3]	Hit gene[4]	Z-score [5]	P-value [5]
TSPAN4	7106	NM_003271	288560	CCUGUCAAUCUUGUCCGUGta	Non-hit	-0,889	0,243
TSPAN4	7106	NM_003271	288561	UGCUCACACUUUAUUAAGAtg	Non-hit	-0,798	0,042
TSPAN6	7105	NM_003270	12768	GUAAUUCUCCAGGCUCACCtt	Non-hit	-0,222	0,543
TSPAN6	7105	NM_003270	138892	AUCUUGUCUACUGCAUGGCtt	Non-hit	0,257	0,251
TUBA1B	10376	NM_006082	42130	UCUCAAGGGCAGCCAUAUCtt	Non-hit	0,628	0,015
TUBA1B	10376	NM_006082	42217	UGGAUAAUUAGUAUUCCUCtc	Non-hit	-0,311	0,618
TUBB	203068	NM_178014	120764	GACUCCUCCAGAGUAGAGCtt	Mild hit	-1,083	0,015
TUBB	203068	NM_178014	120844	GUUGGUUCUAAAUGGGAUCtg	Mild hit	-1,028	0,182
LOC441930	441930	XM_497745	271492	UAGGAAAACCUGGUGGUCCtc	Non-hit	0,136	0,738
LOC441930	441930	XM_497745	271493	AGGACACCAUCCUUAUCCCtt	Non-hit	-0,921	0,343
VASP	7408	NM_003370	13013	UCCUGCUUGCUGACUUUCCtg	Non-hit	0,034	0,902
VASP	7408	NM_003370	13105	CCAACUUGCGUGGCUUUCCtt	Non-hit	-0,830	0,108
VASP	7408	NM_003370	13195	GUUACAGCAUCUUAUUUCCtc	Non-hit	-0,565	0,384
VASP	7408	NM_003370	288562	ACUUUGAAGGCAUUAAGCGtt	Non-hit	0,700	0,147
VAV1	7409	NM_005428	2839	GAUGACCUUGCCAAAAUCCtg	Non-hit	-0,898	0,006
VAV1	7409	NM_005428	2933	AGACAGGGUGUAGAUGACCtt	Non-hit	0,310	0,789
VAV2	7410	NM_003371	13014	UCAAACAGCUCGCUGUUCCtt	Mild hit	-1,259	0,006
VAV2	7410	NM_003371	138981	CCUUAAUCCAAAUUUAUCGtg	Mild hit	-0,225	0,700

Gene Symbol [1]	Gene ID[1]	RefSeq Accession Number[2]	siRNA ID[3]	Antisense (target) siRNA Sequence[3]	Hit gene[4]	Z-score [5]	P-value [5]
VAV3	10451	NM_006113	17378	CAGGCCGUGAGAAAUGUCCtt	Mild hit	-0,396	0,677
VAV3	10451	NM_006113	107954	CACAUAUUGUGCCAAGUCCtt	Mild hit	-1,121	0,345
VCL	7414	NM_003373	20480	UCUCUUCAAAAUCUGAUCCtc	Mild hit	-1,187	0,008
VCL	7414	NM_014000	20570	GGUGCAAGCAUUCUCAACCtt	Mild hit	-0,772	0,144
VCL	7414	NM_014000	108453	AAUUUUACGGACCUCAGCCtc	Mild hit	-0,590	0,235
VCL	7414	NM_014000	108454	UGGCCAUCUUAGUCAUUCCtg	Mild hit	-1,012	0,364
VIM	7431	NM_003380	13019	AAAUCCUGCUCUCCUCGCCtt	Non-hit	-0,362	0,433
VIM	7431	NM_003380	13111	CAGAGAAAUCCUGCUCUCCtc	Non-hit	-0,506	0,106
YES1	7525	NM_005433	690	UUAAAAAAUCAAUGCAACCtc	Non-hit	0,511	0,121
YES1	7525	NM_005433	691	GAAAUUAACUGCUGUUCCCtt	Non-hit	0,437	0,564
ZYX	7791	NM_003461	13054	AUACUGCUCACCUUCUCCCtg	Non-hit	-0,597	0,099
ZYX	7791	NM_003461	13145	CAAAUCAAUACUGCUCACCtt	Non-hit	0,091	0,655
ZYX	7791	NM_003461	115435	CAUAGGUGAAGCUGGGAGGtt	Non-hit	0,159	0,379
ZYX	7791	NM_003461	139068	AUCCCUAGACCAUGUUGGGtc	Non-hit	-0,605	0,968

Appendix III. Expression of kinesins in HeLa cells

Gene ID and gene information is given according to http://www.ncbi.nlm.nih.gov/gene/

Gene Symbol	Gene ID	Expression in HeLa	Forward primer Sequence (5'->3')	Reverse primer Sequence (5'->3')	Expected fragment length, b.p.
KIFC1	3833	+	GAGTGGGTGGTGGCCGTTGG	GCACCCAGGCCTCTGTCCG	334
KIFC2	90990	+	GAGACGGAGCAGAACTGCAGGCG	AGGTCTTCCCGGTGCCTGTCTGG	526
KIFC3	3801	+	GTCGGCTCTGGGGGACGTCAT	ACTTCCCCGAGGGCTGCAGCTTC	373
KIF1A	547	-	CAGTGAGGACCAGCAGGCTATGCTC	AGAGCCGAGTGTCACCCCTCACCC	1000
			GCTGGAGGCCCCGGAGTGACA	GGGGCAAGTGGAGGGAGGGGGTGAG	440
			TCCCAACTTGTTCCACCAGAGCAC	GACGAGTCCTGGACAGATCTGTGGCCTAT	1275
KIF1B	23095	+	CCTGCAACTTCTCACCCACACTT	AGGCCGACGGACGACAACAAAAT	407
KIF1C	10749	+	ATGGCGTCACCAGGGTCGGC	GCTGGGCAGACCACAGCGTT	586
KIF2A	3796	+	GGGGTGTGGGGAGTTCCCCT	GGCACGGGGTCTCTTCGGGT	373
KIF2C	11004	+	AGTTGGGCCTGGAAGTCTATGTGA	ACGGGGTGTGAGCCTTGTTCTG	440
KIF3A	11127	+	AACTGGAGCTACTGGACAGCGCC	CGAAGCTCCCGGCTAAGTTGCCG	981
KIF3B	9371	+	GAGCCGTCTGAGGGCCTTCATGC	GCGCCCTTGGTCATGGAGGTGTG	322
KIF3C	3797	+	CCCGCCGGAGGaGAAGAACAAGAT	GGAAGGTGGAGGCCGCTGAGGACT	405
KIF4A	24137	+	GAACCGCCAGCAAGGCAAGGATAG	TCTGGACCTGGAGGCTAAGGCCCA	526
KIF5A	3798	-	TCTGGAGGAGACAGTTGCCCGG	AGAATGGCCCCGTTTGCCCG	399
			AGAAATGGAGCCCGAAGACAGTGG	TAGGGGTTGGTGGGTGAGGATGCT	345

KIF5B	3799	+	CGGTCGTGATCGCGTCCAAGC	ACAAAACGCTCTGTGCACCCC	405
KIF5C	3800	+	CATTCAGCCCAGATCGCCAAGCC	TCTGCCTCCACGGCACTTGGTTG	506
KIF6	221458	-	TGGAAGACAGCATCCCCAAGAGGC	AACCAGAGCACGGGCCAAGG	581
			GCCGTGCCTCTGATGCCAGAC	TGGCCTCTTGGGGATGCTGTC	458
KIF9	64147	-	TTCAAAGAGCCACTCAGGCCCGAC	GCAGGCGGTGGCGACACTGATC	403
			GGCCCATTCCCGGACCTTATCA	CCTCAAGAAGCAGTACCGCAGCGA	356
KIF11	3832	+	TCCCAACAGGTACGACACCACAG	TGGGCTCGCAGAGGTAATCTGC	397
KIF13A	63971	+	GTACACTCGAGGCGTGCTGCAGG	GGCATGCTCTCCTGGCTTAGAAGAGG	449
KIF15	56992	+	CTCCATGCGGGCGTCAACGT	CCTGAGCCAGTCTGTCCATATGCA	483
KIF16B	55614	+	AGGAACCACCACAGCAGTG	AATATAGCCAGCCACATGG	429
KIF17	57576	+	CTGGCCCGTCTGCAGCTGTTGG	AGGCTGGTTTTTGTGATGACGGGATG	491
KIF18A	81930	+	CCTTGTTGCTCATCTTCAGGTGGAA	TGGCACCATGCTTGGTACAGGC	512
KIF19	124602	-	GCGGGAGGACTCTAAGGGGGTGAT	TGAGCTTGCTGTCGCGATAGTTGA	397
			CATCGCCCAGTACACCAGCATCAT	CCCTGTCCCCTAAACCCACTCTCC	554
KIF20A	10112	+	GGAGTTGGCTGCTGAAGCCTCAAG	GGGCAGCCAGGTCCGAAGACG	407
KIF22	3835	+	TGCTCCGGCCCCTTTCACAT	CTCCCGCCAGCCCACGATTAG	337
KIF23	9493	+	TCTCCATCACCTGTGCCTCTTTCT	CGGAGACGAATTGGTGGTGCGT	374
KIF24	347240	+	GAGCACAGGGGGCCCAGTTGTG	ATGACCACCTGCTGCGCTTGCTC	636
KIF26B	55083	-	TGCTGCGGGAGTCTCTGGGGAACA	GCAGGGCTGGCACGATAGGGACAA	387
			GGG GCT GGG CAA GGT GAA AGT	GAG GTA CAC GCC CGG GGA CT	549
			CGCCCTACAGCAAGATCACGCCC	CACATGGCCTCCTTGCTGGCACC	493

Appendix IV. Results of the validation experiments

1 Gene name and Gene ID according to http://www.ncbi.nlm.nih.gov/gene/

2 Manufacturer's SiRNA ID. The IDs starting with SI... belong to siRNAs purchased from Qiagen. The numeric siRNA IDs belong to siRNAs purchased from Ambion.

3 Target mRNA accession number according to http://www.ncbi.nlm.nih.gov/nuccore/

4 ND = „No Data“

Gene Symbol [1]	Gene ID[1]	siRNA_ID[2]	Target sequence [2]	Target transcript [3]	Mean integrin endocytosis, % of control	Integrin endocytosis, SEM	Mean integrin expression, % of control	Integrin expression, SEM	Mean cell count, % of control	Cell count, SEM
Negative control siRNA		251283	ACGUGACACGUUCGGAGAAtt		100		100		100	
CAV1	857	SI00299635	AAGCATCAACTTGCAGAAAGA	NM_001172895 NM_001172896 NM_001172897 NM_001753	31,68	13,03	95,86	10,14	105,46	16,8
CAV1	857	SI00299642	AAGCAAGTGTACGACGCGCAC	NM_001172895 NM_001172896 NM_001172897 NM_001753	28,78	15,9	79,83	1,33	65,79	12,04
CLTC	1213	SI00299880	TAATCCAATTCGAAGACCAAT	NM_004859	26,16	0,72	ND[4]	ND	ND	ND

Gene Symbol [1]	Gene ID[1]	siRNA_ID[2]	Target sequence [2]	Target transcript [3]	Mean integrin endocytosis, % of control	Integrin endocytosis, SEM	Mean integrin expression, % of control	Integrin expression, SEM	Mean cell count, % of control	Cell count, SEM
DNM2	1785	SI02654687	CTGCAGCTCATCTTCTCAAAA	NM_001005360 NM_001005361 NM_001005362 NM_004945	27,2	6,63	82,45	13,77	98,56	6,88
DNM2	1785	SI04224591	CTCATACGTGGCCATCATCAA	NM_001005360 NM_001005361 NM_001005362 NM_001190716 NM_004945	21,14	6,2	95,58	10,07	99,15	10,83
ABL2	27	SI02634499	CCCAAGTGTAATAAGCCTACA	NM_001100108 NM_001136000 NM_001136001 NM_001168236 NM_001168237 NM_001168238 NM_001168239 NM_005158 NM_007314	88,09	26,92	96,83	0,59	49,15	14,98
ABL2	27	SI02660287	AACCCTGTCCTTAATAACTTA	NM_001100108 NM_001136000 NM_001168236 NM_001168237 NM_001168238 NM_001168239 NM_005158 NM_007314	52,78	9,94	56,84	4,49	72,05	18,60

Gene Symbol [1]	Gene ID[1]	siRNA_ID[2]	Target sequence [2]	Target transcript [3]	Mean integrin endocytosis, % of control	Integrin endocytosis, SEM	Mean integrin expression, % of control	Integrin expression, SEM	Mean cell count, % of control	Cell count, SEM
ABR	29	SI00290388	AAGCGTTTGTCGATAACTATA	NM_001092 NM_001159746 NM_021962	13,16	2,19	60,22	1,30	83,70	2,79
ABR	29	SI04334841	CACCAGCAATAAAGACGACGA	NM_001092 NM_001159746 NM_021962	203,25	41,01	124,51	2,55	71,65	16,27
ARF1	375	SI00299250	ACGTGGAAACCGTGGAGTACA	NM_001024226 NM_001024227 NM_001024228 NM_001658	35,77	3,32	68,00	13,80	186,80	55,70
ARF1	375	SI02654470	CACCATAGGCTTCAACGTGGA	NM_001024226 NM_001024227 NM_001024228 NM_001658	49,17	7,43	99,11	17,67	99,16	37,85
ArhGAP18	93663	SI00302169	CAGGGAGTGATTCGAGTGCAA	NM_033515	20,64	228,66	89,45	4,98	57,93	5,46
ArhGAP18	93663	SI03238522	TGGCTTAAAGAGGCCGGTTTA	NM_033515	43,52	11,40	96,35	4,02	76,57	7,99
ARHGAP6	395	SI04173302	CAGGGCCTATAAACTCAAGCA	NM_006125 NM_013423 NM_013427	42,03	6,35	43,14	4,33	75,59	7,24
ARHGAP6	395	SI04283888	CAGAAACACCGAATGAGTCAA	NM_006125 NM_013423 NM_013427	81,09	22,14	ND 4	ND	99,68	5,92

Gene Symbol [1]	Gene ID[1]	siRNA_ID[2]	Target sequence [2]	Target transcript [3]	Mean integrin endocytosis, % of control	Integrin endocytosis, SEM	Mean integrin expression, % of control	Integrin expression, SEM	Mean cell count, % of control	Cell count, SEM
ArhGEF 1	9138	SI00302680	CAGCAGCTCTGAGAACGGCAA	NM_004706 NM_198977 NM_199002	110,75	29,06	87,84	8,40	76,58	5,66
ArhGEF 1	9138	SI04266171	CCCAATGAGCCTGGAGTCCTT	NM_004706 NM_198977 NM_199002	109,26	19,10	61,61	0,04	57,37	6,88
CHN1	1123	SI04145456	ATCCTCGAAGAATTACCTGTA	NM_001025201 NM_001822	22,33	4,00	71,46	0,35	ND	ND
CHN1	1123	SI04248531	TTGGGCATATAACCAGATTAA	NM_001025201 NM_001822	163,74	18,39	122,51	7,03	ND	ND
CRK	1398	146743	GAGGCAAGAUACCUAUCCCtt	NM_016823	149,34	27,24	88,29	14,33	77,42	12,50
CRK	1398	146745	UCGCCAUUUGAUAGUAUGGtt	NM_005206	208,24	14,32	132,02	25,79	104,42	13,39
CRK	1398	SI00073787	CAGCAGCTAACTAGAGTCCTA	NM_005206 NM_016823	107,84	8,14	95,99	39,81	74,26	5,69
CRK	1398	SI00299929	AATCCGGGACAAGCCTGAAGA	NM_005206 NM_016823	106,10	12,61	78,83	6,35	94,01	10,46
ITGB1	3688	SI00300573	AAAAGTCTTGGAACAGATCTG	NM_002211 NM_033666 NM_033667 NM_033668 NM_033669 NM_133376	7,38	3,40	54,12	7,10	ND	ND

Gene Symbol [1]	Gene ID[1]	siRNA_ID[2]	Target sequence [2]	Target transcript [3]	Mean integrin endocytosis, % of control	Integrin endocytosis, SEM	Mean integrin expression, % of control	Integrin expression, SEM	Mean cell count, % of control	Cell count, SEM
ITGB1	3688	SI02662590	ACAGATGAAGTTAACAGTGAA	NM_002211 NM_033666 NM_033667 NM_033668 NM_033669 NM_133376	0,67	0,67	50,76	7,44	ND	ND
KIF11	3832	SI02653693	ACGGAGGAGATAGAACGTTTA	NM_004523	101,80	11,85	ND	ND	50,89	14,78
KIF11	3832	SI02653770	GCCGATAAGATAGAAGATCAA	NM_004523	101,02	15,56	ND	ND	41,46	6,48
KIF13a	63971	29651	GCAGGACCGUUUGAUUCCCtt	NM_022113	125,23	0,80	155,04	23,06	102,02	21,26
KIF13a	63971	29745	AAUACCUUGGGAGGUUUCCtt	NM_022113	79,48	21,32	81,32	11,12	99,14	48,11
KIF13a	63971	SI00462322	AACCTATGAAATAGTATCCAA	NM_001105566 NM_001105567 NM_001105568 NM_022113	59,84	10,30	73,65	1,58	106,45	38,18
KIF13a	63971	SI03019800	CTGGCGGGTAGCGAAAGAGTA	NM_001105566 NM_001105567 NM_001105568 NM_022113	55,56	9,29	68,60	11,87	84,40	4,12
KIF15	56992	118474	AGUUCUGCUCUCCAUCAGCtg	NM_020242	86,31	6,06	88,59	8,34	125,79	2,11
KIF15	56992	28246	AAACUUUGAUGGCAUCACCtt	NM_020242	27,80	4,45	96,50	2,30	106,44	7,75

Gene Symbol [1]	Gene ID[1]	siRNA_ID[2]	Target sequence [2]	Target transcript [3]	Mean integrin endocytosis, % of control	Integrin endocytosis, SEM	Mean integrin expression, % of control	Integrin expression, SEM	Mean cell count, % of control	Cell count, SEM
KIF15	56992	SI02643914	TTGAGATTGACCAACTTTCAA	NM_020242	129,74	18,17	116,20	8,96	74,13	3,99
KIF15	56992	SI03029390	AACGAGCAGATATATGATCTA	NM_020242	47,85	0,25	76,53	4,62	87,27	6,49
KIF16b	55614	288693	UGUGAAACGUAAUCUGGGCtt	BX647572	101,58	3,79	110,16	17,06	ND	ND
KIF16b	55614	288694	UGUUGAUGAUGUUUUUGGCtc	BX647572	125,12	12,31	107,39	18,49	96,00	12,03
KIF16b	55614	SI00287280	AACGAACGTGTGAGAGATCTA	NM_001199865 NM_001199866 NM_024704	78,23	5,27	ND	ND	100,34	4,62
KIF16b	55614	SI00287301	TTGCATCGTGTGATTAGTGAA	NM_001199865 NM_001199866 NM_024704	97,09	12,00	100,43	5,72	82,43	4,12
KIF17	57576	SI00462364	CAGCAACTACTTCCGATCTAA	NM_001122819 NM_020816 NM_020816 NM_020816	83,80	10,06	ND	ND	92,39	6,73
KIF17	57576	SI03099243	CTGGGTGCTGCTTAACGTCTA	NM_001122819 NM_020816 NM_020816 NM_020816	78,47	4,37	ND	ND	122,96	24,44
KIF18a	81930	118492	CUUUAUGAAAUCCAGCUGCtt	NM_031217	51,12	9,54	97,64	16,74	98,64	31,44
KIF18a	81930	32973	UCAGUGGGAUGUUGUGUCCtg	NM_031217	43,54	12,65	75,91	8,52	72,72	11,26

Gene Symbol [1]	Gene ID[1]	siRNA_ID[2]	Target sequence [2]	Target transcript [3]	Mean integrin endocytosis, % of control	Integrin endocytosis, SEM	Mean integrin expression, % of control	Integrin expression, SEM	Mean cell count, % of control	Cell count, SEM
KIF18a	81930	SI00140238	CAGGTGGAACTAATCTGGTTA	NM_031217	196,97	27,07	109,63	18,38	71,58	13,37
KIF18a	81930	SI03090941	CTCGAAGTGTAAATTACCCGA	NM_031217	145,65	36,36	90,72	1,60	52,54	21,05
KIF1b	23095	118460	GAAGGACUUUGGAGCUUCCtt	NM_183416	99,67	21,32	112,96	4,75	114,10	16,39
KIF1b	23095	22400	AAUGAUGCAUUUGGAUUCCtt	NM_183416	55,78	7,70	85,19	14,08	93,70	3,23
KIF1b	23095	SI03078040	CCCGCGGATATCAACTACGAT	NM_015074 NM_183416	69,03	7,80	75,15	4,01	83,24	7,80
KIF1b	23095	SI03103345	GAGGAAGCTATTGAACGTTTA	NM_015074 NM_183416	79,65	7,92	82,83	7,05	80,32	4,39
KIF1c	10749	SI02655401	AAGAAGCGAAAGTCGGATTTT	NM_006612	93,32	12,95	ND	ND	81,27	17,25
KIF1c	10749	SI02781331	CTGGAGAATCAGTACCGGAAA	NM_006612	132,85	9,95	ND	ND	111,27	10,80
KIF20a	10112	SI00300601	AAGGCCAGGTTTCTGCCAAAA	NM_005733	102,97	13,36	ND	ND	102,84	47,17
KIF20a	10112	SI02654064	AACGAACTGCTTTATGACCTA	NM_005733	101,51	0,16	ND	ND	65,63	15,29
KIF22	3835	118450	CGAGUAGCUCCAAUCUUGCtt	NM_007317 AB017430.2 BC004352.1 BT007259.1 AK223431.1 DC370294.1 AK312234.1	141,74	2,68	110,58	1,13	46,90	7,25

Gene Symbol [1]	Gene ID[1]	siRNA_ID[2]	Target sequence [2]	Target transcript [3]	Mean integrin endocytosis, % of control	Integrin endocytosis, SEM	Mean integrin expression, % of control	Integrin expression, SEM	Mean cell count, % of control	Cell count, SEM
				AK294380.1 AK316050.1						
KIF22	3835	19353	CUGGUAUUUGAGAGUCUCCtg	NM_007317 AB017430.2 BC004352.1 BT007259.1 AK223431.1 DC370294.1 AK312234.1 AK294380.1 AK316050.1	211,43	52,25	109,23	19,10	19,65	4,34
KIF22	3835	SI02638713	CAGGACATCTATGCAGGTTCA	NM_007317	82,69	13,68	82,69	13,68	84,31	20,34
KIF22	3835	SI03019856	ACAGATGGAGTCCTTCCTGAA	NM_007317	87,55	3,65	87,55	3,65	107,64	4,30
KIF23	9493	118501	CUUAUAGUCUCCAUUUCGGtt	NM_138555	25,40	6,36	92,69	33,23	49,11	22,74
KIF23	9493	36749	AAAUGAAUACUGAGUCUCCtt	NM_138555	50,89	6,86	79,80	5,06	81,46	28,84
KIF23	9493	SI02653483	AAGGCTGAAGATTATGAAGAA	NM_004856 NM_138555	107,33	17,74	79,72	11,24	73,41	5,47
KIF23	9493	SI02653910	CAGAAGTTGAAGTGAAATCTA	NM_004856 NM_138555	168,49	28,47	81,22	30,62	61,16	12,62
KIF24	55265	26683	CUGUGGCAUUCAGAAUUCCtg	NM_018278	212,10	13,90	66,58	8,24	ND	ND
KIF24	55265	26777	AAAUAACUUAUUGUCACCCtg	NM_018278	83,99	16,67	100,12	28,11	ND	ND

Gene Symbol [1]	Gene ID[1]	siRNA_ID[2]	Target sequence [2]	Target transcript [3]	Mean integrin endocytosis, % of control	Integrin endocytosis, SEM	Mean integrin expression, % of control	Integrin expression, SEM	Mean cell count, % of control	Cell count, SEM
KIF24	55265	SI03019926	ACCCTATTCTATCATCATATA	NM_194313	72,35	11,01	60,11	2,94	86,77	7,82
KIF24	55265	SI04714192	TACGTCGTGGAGAAATTAATA	NM_194313	100,54	7,45	88,49	21,51	96,49	10,05
KIF2a	3796	14669	CCAGGUCAAUCUCUUUGCCtt	NM_004520	352,91	41,60	163,11	5,33	ND	ND
KIF2a	3796	14762	GUCUAUAAUCCAAACUUCCtc	NM_004520	59,52	22,00	57,50	6,59	108,71	9,22
KIF2a	3796	SI02781310	CAGCAAGCAAATCAACCCGAA	NM_001098511 NM_001243952 NM_001243953 NM_004520	119,74	19,07	82,63	8,97	90,76	10,59
KIF2a	3796	SI03019751	AAGAACCAAGATTGTTCTAAA	NM_001098511 NM_001243952 NM_001243953 NM_004520	49,07	7,06	66,53	13,13	84,94	2,73
KIF2a	3796	SI04435613	AAGCGCAGCGATGGCCGAATA	NM_001098511 NM_004520 NM_004520 NM_004520	105,93	9,71	84,81	11,05	74,84	6,95
KIF3a	11127	SI02655415	AAGACCTGATGTGGGAGTTTA	NM_007054	77,48	7,77	ND	ND	147,18	9,58
KIF3a	11127	SI04438847	CAAGAACGCTTGGATATTGAA	NM_007054	79,25	6,72	ND	ND	95,85	24,00
KIF3b	9371	SI02655303	AATCCGTGGTGACCCTGAAAA	NM_004798	104,20	5,31	ND	ND	93,09	24,22

Gene Symbol [1]	Gene ID[1]	siRNA_ID[2]	Target sequence [2]	Target transcript [3]	Mean integrin endocytosis, % of control	Integrin endocytosis, SEM	Mean integrin expression, % of control	Integrin expression, SEM	Mean cell count, % of control	Cell count, SEM
KIF3b	9371	SI03019772	CAGAAATGCATGGGTAAGGTA	NM_004798	122,71	8,94	ND	ND	105,80	18,48
KIF4a	24137	288675	UGUUCUUGAUUUUUCUUGCtc	AF071592	87,74	22,89	103,93	20,87	105,81	10,65
KIF4a	24137	288676	UUAGAUGAUUAAGUUCAGCtg	AF071592	102,58	28,96	143,48	29,66	84,09	8,55
KIF4a	24137	SI00099232	CAGGTCCAGACTACTACTCTA	NM_012310	87,97	11,14	68,54	2,96	ND	ND
KIF4a	24137	SI03030699	AACTGTGGAACCATCAGAGAA	NM_012310	60,63	0,68	ND	ND	ND	ND
KIF5b	3799	SI02654848	AAACCGAGTTCCCTATGTAAA	NM_004521	88,96	20,66	ND	ND	111,34	14,24
KIF5b	3799	SI02781317	AACGTTGCAAGCAGTTAGAAA	NM_004521	72,77	1,53	ND	ND	72,81	14,13
KIF5c	3800	SI04916394	TCCCACGAATTGCCCATGATA	NM_004522	128,43	2,08	ND	ND	101,41	24,92
KIF5c	3800	SI04916401	CCGACACGTGGCTGTGACAAA	NM_004522	85,04	7,82	ND	ND	116,13	33,27
KIFC1	3833	43827	UCCUCUUGAGUCUGCUUCCtg	NM_002263	153,12	14,88	104,06	17,18	89,11	5,46
KIFC1	3833	43923	UGUCCGUUUCUUCUCAGGCtc	NM_002263	114,42	12,99	84,57	15,25	ND	ND
KIFC1	3833	SI02653210	TGGGACTTAAAGGGTCAGTTA	NM_002263	102,34	25,41	83,57	83,57	74,67	20,29
KIFC1	3833	SI02653336	TCGGGAAACACAGGCCATTAA	NM_002263	49,10	2,59	95,42	14,80	87,80	8,64
KIFC2	90990	SI03019884	CCAGATGGATCCACATCCCAA	NM_145754	113,19	0,44	ND	ND	84,09	1,54

Gene Symbol [1]	Gene ID[1]	siRNA_ID[2]	Target sequence [2]	Target transcript [3]	Mean integrin endocytosis, % of control	Integrin endocytosis, SEM	Mean integrin expression, % of control	Integrin expression, SEM	Mean cell count, % of control	Cell count, SEM
KIFC2	90990	SI03092250	CTCGTTGCTCATCTACATCTT	NM_145754	70,39	13,93	ND	ND	77,34	7,83
KIFC3	3801	SI00078722	CAGCGCTGCGGAGATCTACAA	NM_001130099 NM_001130100 NM_005550 NM_001130100 NM_005550 NM_001130100 NM_005550	93,62	9,99	ND	ND	88,60	17,75
KIFC3	3801	SI03082583	CCGGGCGCAGATTGCCATGTA	NM_001130099 NM_001130100 NM_005550 NM_001130100 NM_005550 NM_001130100 NM_005550	124,21	7,18	ND	ND	89,98	14,40
LIMS1	3987	SI00071043	TAGGAAATAGAGGCTTTCAAA	NM_004987	122,97	6,52	109,72	19,67	ND	ND
LIMS1	3987	SI03031609	AAGACTTAAGAAACTAGCTGA	NM_004987	74,54	2,53	96,57	2,08	ND	ND
Myo1a	4640	SI00653268	CTGGATAGTGAATCGAATCAA	NM_005379	165,23	8,59	95,64	12,65	85,23	8,92
Myo1a	4640	SI04242917	GCCCGAAAGAATTATCGCAAA	NM_005379	72,02	13,87	81,00	4,18	91,59	9,90
Myo1a	4640	16050	AAACGGCUUGUUUUGGGCCtc	NM_005379	36,43	12,58	67,95	4,19	126,42	46,71
Myo1a	4640	144012	GCGAUAAUUCUUUCGGGCCtt	NM_005379	42,19	37,93	74,17	15,61	116,50	32,84

Gene Symbol [1]	Gene ID[1]	siRNA_ID[2]	Target sequence [2]	Target transcript [3]	Mean integrin endocytosis, % of control	Integrin endocytosis, SEM	Mean integrin expression, % of control	Integrin expression, SEM	Mean cell count, % of control	Cell count, SEM
NF2	4771	202366	GGCAGUAGAUCUUUUCAUCta	NM_181825	41,67	7,87	79,04	9,90	136,65	0,51
NF2	4771	288641	CUCUUGAGAGAGCUGAAGCtc	NM_181834	35,59	3,10	95,89	13,64	85,77	3,19
NF2	4771	SI02664137	CACCGTGAGGATCGTCACCAT	NM_000268 NM_016418 NM_181825 NM_181828 NM_181829 NM_181830 NM_181831 NM_181832 NM_181833	129,73	18,86	87,57	2,92	74,82	7,62
NF2	4771	SI02664452	CCGGGTCGCGCCTGCACCGAA	NM_000268 NM_016418 NM_181825 NM_181828 NM_181829 NM_181830 NM_181831 NM_181832 NM_181833	86,42	7,07	93,48	18,76	90,87	9,88
PRKCA	5578	SI00301308	AACCATCCGCTCCACACTAAA	NM_002737	101,02	23,33	73,18	4,75	62,52	11,79
PRKCA	5578	SI00605934	TACAAGTTGCTTAACCAAGAA	NM_002737	65,43	7,28	102,95	4,25	99,24	32,08
PTEN	5728	SI00301504	AAGGCGTATACAGGAACAATA	NM_000314	88,20	9,65	89,61	3,21	123,54	56,29

Gene Symbol [1]	Gene ID[1]	siRNA_ID[2]	Target sequence [2]	Target transcript [3]	Mean integrin endocytosis, % of control	Integrin endocytosis, SEM	Mean integrin expression, % of control	Integrin expression, SEM	Mean cell count, % of control	Cell count, SEM
PTEN	5728	SI03116092	TCGACTTAGACTTGACCTATA	NM_000314	118,43	13,79	123,71	4,74	67,57	20,36
PTPN11	5781	SI02225902	CAGAAGCACAGTACCGATTTA	NM_002834	132,87	7,40	99,67	16,31	84,74	3,62
PTPN11	5781	SI02225909	CCGCTCATGACTATACGCTAA	NM_002834	39,15	5,19	76,83	3,72	66,07	28,10
TRPM7	54822	SI03048465	ATCGGAGGTCTGGCCGAAATA	NM_017672	79,52	8,29	61,59	3,63	108,13	13,59
TRPM7	54822	SI03079468	CCCTGACGGTAGATACATTAA	NM_017672	179,54	58,91	70,97	3,62	51,40	5,43